Dissertation

Modelling, Simulation and Energy-Exergy Assessment of a Local District Heating Network in Vienna

ausgeführt zum Zwecke der Erlangung des akademischen Grades eines

Doktors der technischen Wissenschaften unter der Leitung von

ao. Univ.-Prof. Dipl.-Ing. Dr. techn. Karl Ponweiser

Institut für Energietechnik und Thermodynamik / E302

eingereicht an der Technischen Universität Wien

Fakultät für Maschinenwesen und Betriebswissenschaften

von

Dipl.-Ing. Mario Potente Prieto

Matrikelnummer 01329754

Porzellangasse 47/2/6, 1090 Wien

Wien, am 12. December 2019   eigenhändige Unterschrift

EIDESSTATTLICHE ERKLÄRUNG: Ich erkläre hiermit an Eides statt, dass ich die vorliegende Arbeit selbstständig verfasst, andere als die angegebenen Quellen/Hilfsmittel nicht benutzt, und die den benutzten Quellen wörtlich und inhaltlich entnommenen Stellen als solche kenntlich gemacht habe.

STATUTORY DECLARATION: I hereby declare that I have authored this thesis independently, that I have not used other than the declared sources/resources, and that I have explicitly marked all material which has been quoted either literally or by content from the used sources

Kurzfassung

Fernwärmenetze sind in Städten und Stadtgebieten auf der ganzen Welt weit verbreitet. Diese dienen dem Transport und der Verteilung von thermischer Energie an die im Versorgungsgebiet angeschlossenen Haushalte. Derzeit werden mehrere Projekte durchgeführt, um bestehende Netzwerke auszubauen, zu verbessern und zu optimieren, um die Wassertemperatur im Umlauf zu senken und somit die Energieeffizienz zu erhöhen.

Neben Temperatur und Energie wird die Exergie als weitere wichtige thermodynamische Größe behandelt, welche die Umwandelbarkeit des im thermodynamischen System transportierten Energiestroms kennzeichnet. Sie kennzeichnet damit die "Qualität" der Energie in einem thermodynamischen System und sollte daher in die Analyse von Fernwärmenetzen einbezogen werden.

Das Ziel dieses Projektes ist die Modellierung, Simulation, Berechnung und Analyse einer realen Fallstudie, bestehend aus einem Nahwärmenetz in der Stadt Wien (Österreich). Dabei wird nicht nur die aktuelle Leistung des Netzwerks, sondern auch dessen Verhalten nach Umsetzung von verschiedenen Modifikationen, dargestellt in Szenarien, analysiert. Diese Szenarien betreffen mögliche Änderungen und Verbesserungen, wie den Austausch von Heizkörpern durch Fußbodenheizungen, die Einführung von Wärmepumpen zur Unterstützung des Netzwerks oder die direkte Verringerung der Wassertemperatur im Fernwärmekreislauf.

Die Analyse der aktuellen Situation durch die beiden definierten thermodynamischen Systeme (Gebäude und Fernwärmenetz) zeigt, dass bei niedrigerem Wärmebedarf der Massenstrom im Netzwerk reduziert wird. Die damit verbundenen Wärmeverluste und der Energieertrag sind während der wärmeren Perioden des Jahres größer als während der kälteren.

In Bezug auf die Exergie, verhält sich jedes Subsystem auf andere Art und Weise: Für Gebäude ist der Haupteinflussfaktor die Temperaturdifferenz zwischen dem städtischen Netz und dem internen Netzwerk des Gebäudes. Diese führt zu einer progressiven Erhöhung der Exergie-Ausbeute, beim Übergang von der kälteren zur wärmeren Periode. Das Netzwerk-Subsystem verhält sich genau umgekehrt: Der Exergie-Ertrag ist hauptsächlich mit dem Wärmestrom verbunden, der wiederum eng mit dem Massenstrom des zirkulierenden Wassers zusammenhängt und dieser ist in der kälteren Periode höher.

Was die übrigen Szenarien anbelangt, verbessert sich die Energie-Exergie-Effizienz des Netzwerks bei jenen Konfigurationen, bei denen die größte Temperaturabsenkung stattfindet. Bei diesen und anderen Verbesserungen können aber mehrere sich gegenseitig und auch gegensätzlich beeinflussende Phänomene auftreten. Zum Beispiel bewirkt das Ersetzen von Heizkörpern durch eine Fußbodenheizung oder der Einsatz einer Wärmepumpe im Fernwärmenetz einen erhöhten Verbrauch an elektrischer Energie, welcher den exergetischen Vorteil des Niedertemperaturheizsystems relativiert.

Abstract

District heating networks (DHN) are widely used systems in cities and urban areas around the world, designed for the transport and distribution of thermal energy to all households. Currently, multiple projects are carried out, in order to extend, improve and optimize existing networks, with the aim of reducing circulating water temperature and therefore, increasing energy efficiency.

In addition to temperature and energy, exergy is revealed as another important thermodynamic magnitude that determines the amount of energy that can be truly used in a thermodynamic system. It measures the quality of the energy compromised, and therefore, it should be introduced in the analysis of district heating networks.

The objective of this project is the modelling, simulation and calculation of a real case study consisting of a local district heating network located in the city of Vienna (Austria), analysing not only the current performance of the network but also its behaviour after new hypotheses raised. These hypotheses are based on possible changes and improvements, such as the replacement of radiators by radiant floors, the introduction of heat pumps supporting the network or the direct reduction of DH water temperature.

The analysis of the current situation through the two defined thermodynamic systems, buildings and network reveal that the lower the heat demand, the lower the flow rate that circulates through the network. The related heat losses, and therefore, the energy yield, are greater during the warmer periods of the year than during the colder ones.

Regarding the exergy performance, each subsystem evolves in a different way: for buildings, the main factor is the temperature difference between the urban network and the internal network of the buildings, leading to a progressive increase of the exergy yield as we move from cold to warm periods. The network subsystem behaves exactly in the opposite way: the exergy yield is mainly associated with the heat flow, which in turn is closely linked to the mass flow of circulating water, higher during the cold periods.

Concerning the rest of the hypotheses raised, the energy-exergy efficiency of the network improves in those configurations where the reduction of temperature is greatest. These and other improvements involve several counterparts, like replacing radiators by radiant floors or installing heat pumps connected to the district heating network, leading to an increase of power consumption.

4

Acknowledgements

"La grandeza de los hombres no consiste en alcanzar la victoria,
sino en saber levantarse ante la derrota"

Chinese proverb.

In the loving memory of Georgios Kazas, engineer, researcher, colleague and friend.
May his soul rest in peace. We will never forget you.

Contents

Nomenclature

Abbreviations

Abbreviation	Text
4GDHN	4th Generation District Heating Networks
Ad.	Adimensional
ASAHP	Air Source Absorption Heat Pump
B	Boiler
C	Cooling mode
CCHPP	Combyned Cycle Heat and Power Plant
CE	Cogeneration Engine
CHP	Combined Heat and Power
CHPP	Combined Heat and Power Plant
COP	Coefficient of Performance
CV	Control Valve
DH	District Heating
DHC	District Heating and Cooling
DHN	District Heating Network
DHW/DHWC	Domestic Hot Water for Consumption
DWC	Domestic Water for Consumption
EDF	Europäisches Institut für Energieforschung
EeB	Energy Efficient Buildings
EES	Engineering Equation Solver
EU	European Union
EW	Extreme Winter
GHG	Greenhouse Gas Emissions
GTPP	Gas-Turbine Power Plant
GUFO	Gebietsumformerstation (General DH Substation)
H	Heating
HE	Heat Exchanger
HP	Heat Pump
HSC	High Stage Compressor
LSC	Low Stage Compressor
HW	Hot Water
IES	Institute of Energy Systems
IN	Intercooler
ITN	Initial Training Network

Abbreviation	Text
IWH	Industrial Waste Heat
LTDHCN	Low Temperature District Heating and Cooling Networks
LTDHN	Low Temperature District Heating Networks
M	Mid-season
MILP	Mixed Integer Linear Programming
MWIP	Municipal Waste Incineration Plant
NRV	Non-Return Valve
NW	Normal Winter
PLDH	Peak Load District Heating Plant
RD	Return-Demand
RF	Return-Forward
S	Summer
SBPP	Steam-Based Power Plant
SD	Source-Demand
SF	Source-Forward
SHE	Solution Heat Exchanger
SR	Source-Return
TI	Temperature indicator
TC	Temperature controller
WWTP	Waste Water Treatment Plant

Latin Symbols

Symbol	Unit	Definition
A_j	m^2	Sectional area of the branch j
$A_{ext\ j}$	m^2	External area of the branch j
A_{LMHT}	m^2	Logarithmic mean heat transmission area
$\dot{B}_{AN}$	kW	Anergy flow extracted from the anergy network
e	m	Pipe's wall thickness
C_f	$J/(kg \cdot K)$	Specific calorific capacity of the fluid
C_{s1}	$J/(kg \cdot K)$	Specific calorific capacity of the soil, material 1
C_{s2}	$J/(kg \cdot K)$	Specific calorific capacity of the soil, material 2
C_{sn}	$J/(kg \cdot K)$	Specific calorific capacity of the soil, material n
Cp	$J/(kg \cdot K)$	Specific calorific capacity at constant pressure
d_b	m	Cylinder diameter
$D_{ext\ j}$	m	External diameter for the branch j
d_j	m	Pipe diameter
$D_{N\ j}$	m	Nominal pipe diameter for the branch j
$D_{N\ AC\ j}$	m	Nominal diameter of the pipe accessory, branch j
ex_{in}	J/kg	Specific exergy value relative to P and T for the input stream
ex_{out}	J/kg	Specific exergy value relative to P and T for the output stream
Ex	J	Exergy of the system
Ex_1	J	Exergy of the system, initial state
Ex_2	J	Exergy of the system, final state

Symbol	Unit	Definition
Ex_D	J	Destroyed exergy term
$\dot{E}x$	kW	Exergy flow
$\dot{E}x_{CS}$	kW	Exergy flow supplied to the customer
$\dot{E}x_{DH1}$	kW	Exergy flow supplied from the primary network
$\dot{E}x_{DH2}$	kW	Exergy flow supplied from the secondary network
$\dot{E}x_{DHS}$	kW	Exergy flow supplied from the network to the building
$\dot{E}x_Q$	kW	Maximum usable theoretical work that could be obtained from the stated heat when it is exchanged with the environment
$\dot{E}x_W$	kW	Maximum usable theoretical work associated to $\dot{W}$
f	Ad.	Multiplication factor for EW, NW, M and S
f_D	Ad.	Darcy friction factor
g	m/s^2	Gravitational acceleration value
Gr	Ad.	Grashof number
h	kJ/kg	Specific enthalpy
H	m	Height
h_{CN}	W/(m^{2}K)	Heat transmission coefficient by natural convection
HS	m^2	Heated Surface
HP_{DH2}	m	Impulse charge for the secondary network
I	A	Electric current
I_{ij}		Incidence Matrix
i_{ij}	Ad.	Factor ij located inside the incidence matrix
k	W/(mK)	Thermal conductivity
k (factor)	Ad.	Load factor of the DH system
k_j	kg/m^7	Characteristic parameters factor of the pipe (branch j)
L	m	Length
L_j	m	Pipe Length associated to the branch j
$L_{EQ\ AC\ j}$	m	Equivalent pipe length for accesory of the branch j
m	Ad.	Represents the total number of nodes in the network
m (radiators)	Ad.	Radiator's experimental coefficient/correction factor
m (heated floors)	Ad.	correction factor for heated floors
m_{cv}	kg	Mass inside the control volume
$\dot{m}$	kg/s	Mass flow
$\dot{m}_{cv}$	kg/s	Mass flow crossing the control volume
$\dot{m}_{AN}$	kg/s	Mass flow of the anergy network
$\dot{m}_{CS}$	kg/s	Mass flow of hot water, customer side
$\dot{m}_{DH}$	kg/s	Mass flow of hot water circulating through a DHN
$\dot{m}_{DH1}$	kg/s	Mass flow circulating through the primary network
$\dot{m}_{DH2}$	kg/s	Mass flow circulating through the secondary network
$\dot{m}_{DHS}$	kg/s	Mass flow of hot water, district heating network side
$\dot{m}_{rf}$	kg/s	Mass flow of hot water circulating through the radiators
$\dot{m}_r$	kg/s	Return mass flow of the DH water
$\frac{\dot{m}_W}{\dot{m}_{W\ N}}$	Ad.	Relationship between the circulating mass flow for design and normal conditions
n	Ad.	Represents the total number of branches in the network
n (radiators)	Ad.	Radiator's coefficient

Symbol	Unit	Definition
Ne	kW	Installed power capacity
Nu	Ad.	Nusselt number
P	Pa	Pressure
P (Power)	kW	Power
P_{BOILER}	Pa	Boiler's pressure
$P_{CONDENSER}$	Pa	Condenser's pressure
$P_{DISCHARGE}$	Pa	Discharge pressure after the hydraulic pump
$P_{initial}$	Pa	Initial system pressure
P_{final}	Pa	Final system pressure
P_N	Pa	Nominal pressure
P_r	Pa	Return pressure of the DH water
P_{rad}	kW	Radiator power
P_{SP}	Pa	Set point pressure (minimum pressure of the system)
Pr	Ad.	Prandtl number
Q	J	Heat
$\dot{Q}$	W	Heat flow
$\dot{Q}_C$	kW	Heat flow extracted from the heat source
$\dot{Q}_{CS}$	kW	Heat flow supplied to the customer side
$\dot{Q}_{CHP}$	kW	Heat flow generated by the combined cycle
$\dot{Q}_{CHP/HE}$	kW	Heat flow obtained from a combined cycle or HE
$\dot{Q}_{COND,HP}$	kW	Heat flow supplied by the heat pump
$\dot{Q}_{DH1}$	kW	Heat flow supplied by the primary network
$\dot{q}_{DH2}$	m^3/s	Volumetric flow of DH water, secondary network
$\dot{Q}_{DH2}$	kW	Heat flow supplied by the secondary network
$\dot{Q}_{DHS}$	kW	Heat flow supplied from the district heating side
$\dot{Q}_e$	kW	Heat flow in x = e
$\dot{Q}_H$	kW	Heat flow supplied to the heat sink
$\dot{q}_{rad}$	m^3/s	volumetric flow of the water circulating through the radiators
$\dot{Q}_{th}$	kW	Installed thermal capacity
$\dot{Q}_w$	kW	Heat flow in x = w
$\dot{Q}_x$	W	heat conduction term in the x direction
R_{bc}	-	Resistance to the heat flow (boundary condition value)
R_{bs}	-	Resistance of the heat transmission of the external DH pipe wall
R_{fg}	-	Resistance of the heat transmission of the feed/return internal tube wall
R_{gb}	-	Resistance of the heat transmission of the internal insulation material of the DH pipe
r_{HG}	Ad.	Fraction of energy transformed into heat
r_{Nj}	m	Nominal radius for the branch j
r_{PG}	Ad.	Fraction of energy transformed into power
$R_{s1,s2}$	-	Resistance of the heat transmission of the external insulation material of the DH pipe, s1-s2
$R_{si,1i}$	-	Resistance of the heat transmission of the external insulation material of the DH pipe, si-1i
$R_{sn,1n}$	-	Resistance of the heat transmission of the external insulation material of the DH pipe, sn-1n

Symbol	Unit	Definition
Ra	Ad.	Rayleigh number
Re	Ad.	Reynolds number
s	$J/(kg \cdot K)$	Specific entropy of the mass in the system
S	-	Represents the energy incomes or losses for a pipe
SC	kW/m^2	Cooling demand ratio
S_{HT}/HTS	m^2	Heat transfer surface
t	s	Time/time instant
T	K	Temperature
T_0	K	Reference temperature
$T_{1,i}$	K	Fluid temperature inside the feed tube
$T_{2,i}$	K	Fluid temperature inside the return tube
T_A	K	Ambient temperature inside the room
T_{amb}	K	Ambient temperature for a buried pipe
T_{AN}	K	Temperature of the anergy network
$T_{AN\,post\,HP}$	K	Temperature of the anergy network after crossing the HP
$T_{AN\,pre\,HP}$	K	Temperature of the anergy network before the HP
T_b	K	Temperature of the cylinder
$T_{b,i}$	K	Temperature of the internal wall of the DH pipe
T_c/T_{com}	K	Comfort temperature inside the room
T_C	K	Temperature of the heat source
T_{COND}	K	Condenser's temperature
T_{CS}	K	Temperature of the customer side
T_{DH1}	°C	Temperature of the primary network
T_{DH2}	°C	Temperature of the secondary network
T_{DHS}	°C	Temperature from the district heating side
$T_{DHS\,post\,HP}$	°C	Temperature after the heat pump, district heating side
$T_{DH,feed}$	K	Feed temperature of the DHN
T_{DHW}	K	Domestic Hot Water temperature
T_{DWC}	K	Domestic Water for Consumption temperature
T_e	K	Temperature in x = e
T_{ext}	°C	External temperature
T_{EV}	K	Evaporator's temperature
T_F	K	T at the external boundary of the thermodynamic system.
$T_{g1,i}$	K	T of the external wall of the feed tube
$T_{g2,i}$	K	T of the external wall of the return tube
T_H	K	T of the heat sink
$T_{DH,return}$	K	Return temperature of the DHN
T_r	°C	Return temperature of the DH water
T_{rAN}	°C	Return temperature, anergy flow
T_{rCS}	°C	Return temperature, customer side
T_{rDH1}	°C	Return temperature, primary network
T_{rDH2}	°C	Return temperature, secondary network
T_{rDHS}	°C	Return temperature, district heating side
$T_{rad,feed}$	K	Inlet T of the water circulating through the radiators
$T_{rad,return}$	K	Return T of the water circulating through the radiators

Symbol	Unit	Definition
$\bar{T}_{rf}$	K	Average T of the radiant floors
$T_{rf,feed}$	K	Inlet T of the water circulating through the radiant floors
$T_{rf,return}$	K	Inlet T of the water circulating through the radiant floors
T_s	K	Supposed T of the external pipe surface
$T_{s1,2,...n,i}$	K	T of the insulation layer 1,2,n
T_w	K	T in x = w
U (heat transfer)	$W/(m^2\,K)$	Global Heat transmission coefficient
U (thermodynamics)	J/kg	Specific internal energy of the mass in the system
u	m/s	Fluid velocity
V	m^3/kg	Specific volume
$\dot{V}_{fluid,j}$	m^3/kg	Volumetric flow of the fluid circulating through the branch j
$\dot{W}$	kW	Electric work flow
$\dot{W}_{CHP}$	kW	Electric work flow generated by the combined cycle
$\dot{W}_{DH2}$	kW	Power consumed by the hydraulic pump
$\dot{W}_{HP}$	kW	Electric work flow consumed by the heat pump
W_{irr}	J	Irreversible work transported into the system
W_{rev}	J	Reversible work transported into the system
Z_{in}	m	Height of the first pipe endpoint (+ or -)
Z_{out}	m	Height of the second pipe endpoint (+ or -)

Greek Symbols

Symbol	Unit	Definition
α	-	relation between the pressure losses and the length
α (factor)	-	factor gathering together several terms, equations (2.58)
β	K^{-1}	Thermal expansion coefficient
β (factor)	-	factor gathering together several terms, equations (2.58)
γ	Ad.	Coefficient associated to the irreversibilities of the heat pump
Δ	-	Increment
η	Ad.	Efficiency
λ_f	-	Heat transfer term
μ	$kg/(m\,s)$	Viscosity
π	Ad.	Physical constant Pi
ρ	kg/m^3	fluid density circulating through the the branch j
σ	-	Internal entropy generation term
ϕ	Ad.	Darcy-Weisbach friction factor

Subscripts

Symbol	Definition
0	Reference P and T conditions
1	Initial state of the thermodynamic system
2	Final state of the thermodynamic system
AC	Accesory
AIR	Air
AN	Anergy Network
$calc.$	Calculated
CHP	Combined Heat and Power
CM	Cooling Machine
CN	Natural Convection
com	Comfort
$COND$	Condenser
cs	Cold side of the heat exchanger
CS	Customer Side
cv	Control volume
DHS	District Heating Side
EN	Energy
env	Environment
EQ	Equivalent
EX	Exergy
ext	External
EV	Evaporator
EW	Extreme Winter
f	Fluid
FL	Feed Line
FW	Fresh Water
g	Represents the insulation material
$H2O$	Liquid water
H	Heating branch
HD	Heat Demand
HE	Heat Exchanger
$HE - LB$	Last building Heat Exchanger
$HE - S$	Substation Heat Exchanger
hf	Heated floors
HP	Heat Pump
hs	Hot side of the heat exchanger
HT	Heat Transfer
HW	Hot Water branch
i	Identifier for nodes/buildings
in	Input to the system
INS	Insulation
irr	Irreversible
j	Represents a branch inside I_{ij}

Symbol	Definition
M	Mid-season
n	Manufacturer's testing conditions of radiators
N	Design conditions / Nominal
NW	Normal Winter
NWD	Non Working Day
out	Output from the system
PVC	Polyvinyl chloride
r	Return
R	Recirculation
rad	Radiators
rev	Reversible
rf	Radiant floors
RL	Regulation Line / Return Line
S	Summer
SP	Set Point
SUB/S	Substation
t	Actual value
WD	Working Day
x	X axis direction
y	Y axis direction

Chapter 1

Introduction

1.1   About the CI-NERGY Project

The CI-NERGY Marie Curie Initial Training Network (ITN) aims to train young scientists to develop urban decision making and operational optimisation software tools to minimise non renewable energy use in cities. The ITN will be a highly multidisciplinary coordinated PhD programme focused on urban energy modelling aimed at addressing one of the most challenging and critical urban sustainability problems. The training will be structured to provide a balanced combination of theory and practical application.

Figure 1.1: Ci-NERGY logo and European programs involved.

The training was carried out by a close collaboration of six of the best academic research centres and four leading industrial companies from the energy and software technology sector (Siemens, TU Wien, Wien Energie, EDF/EIFER, and IES). The research fellows apply their results in two case study cities (Geneva and Vienna), which were chosen for their very ambitious sustainability goals. The CI-NERGY network is a highly multi-disciplinary coordinated PhD programme on urban energy sustainability, covering the key challenges in cities related to a low carbon future. It is expected that European cities will be able to reduce their emissions by up to 40 % by 2020 through the development and implementation of urban energy system tools [1].

There is a gap in high level integrated training in the urban energy research field, which is due to the wide range of fragmented disciplines from building physics and energy supply technologies with electrical and thermal engineering up to software engineering and information technology. The CI-NERGY network provided training and knowledge by excellent academic and industry partners from all areas of smart cities, closing this gap. The impact of the network training activities will be highly noticeable for energy supply utilities, IT companies, policy makers, urban planners, researchers on sustainable urban energy systems and finally the inhabitants of cities themselves.

This doctoral thesis constitutes the research carried out by Mario Potente Prieto, member of the

CI-NERGY project as early stage researcher number 6 (ESR 6) and hired as project assistant in the Department of Energy and Thermodynamics in the Technical University of Vienna (TU WIEN).

1.2 Motivation

The main objective of the CI-NERGY project is the development of a general methodology for urban energy planning, in order to maximize energy efficiency and minimize the use of fossil fuels. The introduction of renewable energies in the different strategies is one of the cornerstones for achieving this goals, involving the modernization and adaptation of buildings and distribution networks.

This energy planning encompasses all the elements related to the energy supply chain for an urban area, from the energy production, through transport and distribution systems, until the final consumer.

Likewise, the aforementioned general methodology covers four fundamental tasks, namely: Decision Support and Integrated Energy Planning, Urban Energy and Network Modelling, 3D Geospatial Data Server Optimization Methods and Model Integration. This approach combines various strategies used to address the energy management challenge.
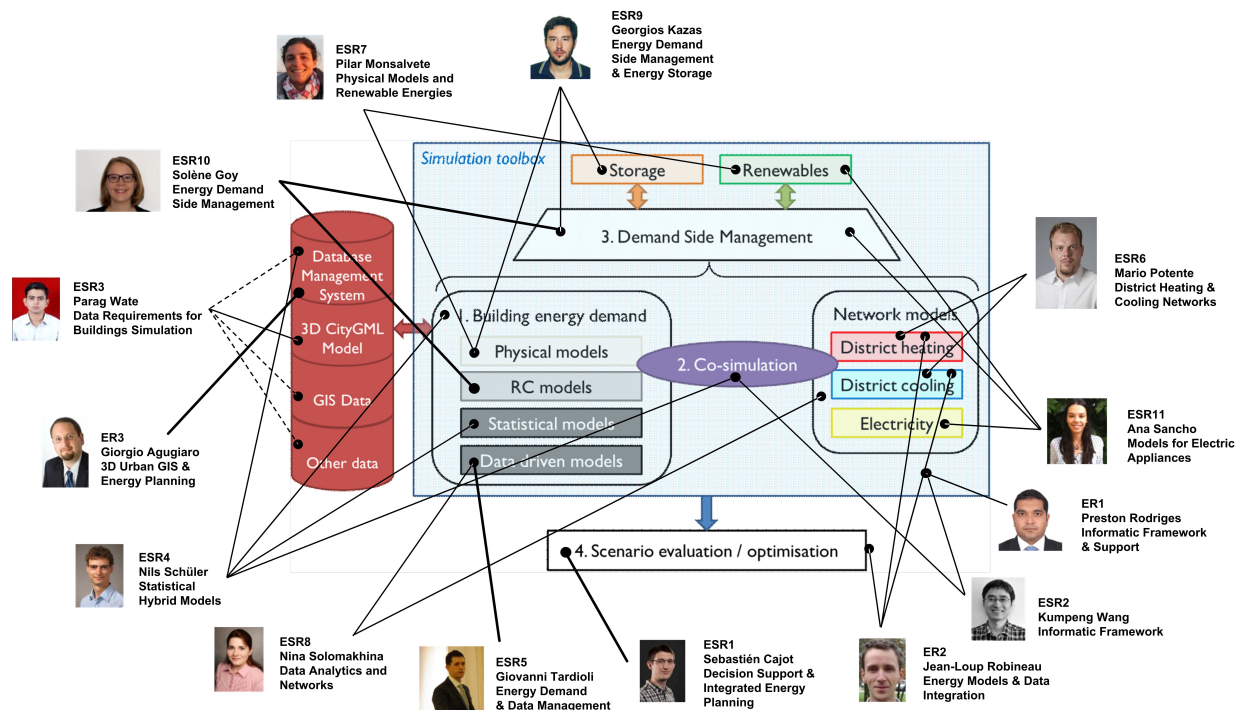
Figure 1.2: Work areas and Researchers of the CI-NERGY project

As shown in Figure 1.2 the part of the CI-NERGY project that concerns this doctoral thesis corresponds to the area of Urban Energy and Network Modelling applied to urban energy systems, more specifically to District Heating and Cooling (DHC) networks.

Consequently, the present work brings together two main motivations. Firstly, elaborating a modelling and simulation methodology of district heating and cooling networks applicable to the case

studies of Vienna and Geneva. It can be integrated with the other models of the other areas of the CI-NERGY project. For example, the model for the district heating network must be able to perform the calculations based on the energy demand values calculated from other models within the CI-NERGY framework.

Secondly, this methodology is used to simulate different scenarios within the same case study, based on the gradual improvement of the current Viennese district heating network (DHN), in order to study its possible evolution towards the fourth generation of district heating networks [2]. These scenarios contemplate the modification of the network at different levels, including the replacement of heating systems in buildings, the introduction of centralized and decentralized heat pumps to support the DHN, and the direct temperature reduction of the water circulating through the network.

1.3   Goals

For the project covered by this PhD thesis; and based on the previous explanation, the following goals are defined:

1. Obtaining and classifying the relative information for the specific case study.

2. Elaborating all physical and numeric models for all the elements that operate in a DHN.

3. Including the exergetic method in the DH models. The exergy will be used to analyse the efficiency of the system.

4. Building, validating and operating a simulation from the generated models, in order to determine the behaviour of the system, calculating all operating variables as well as pressure, mass, energy and exergy balances.

5. Building other simulations following the same case study, representing new scenarios in which the network has been improved.

6. Analysis of all results and preparation of a conclusive report.

Chapter 2

State of the art

2.1   Urban Energy Systems

Urban energy systems are defined as all those facilities and devices which objective is the energy supply to the consumers, either in the form of heat or electricity. In short, Urban energy systems thus serve the following purposes:

- Satisfying electricity demand

- Covering heat and cooling demands

- Providing domestic hot water.

In turn, an urban energy system consists of two fundamental stages: generation and distribution. Depending on which energy source is used, the generation process will be conducted in one or another way. Non-renewable energies and biomass are fuels available to be stored and further used depending on the demand. In this case, those fuels have to be processed for its further transformation and their chemical energy has to be transformed into heat and subsequently into power.

On the other hand, the volatility of renewable energy sources (except biomass) requires the installation of efficient capture systems in combination with energy storage devices, in order to couple the fluctuations between availability and demand.

Both forms of energy, thermal and electrical, are susceptible to be transported, distributed and stored. For electric power, the appropriate way of transport is the electric flow circulating through the cables, and the driving force that generates this intensity is the potential difference or voltage. In the case of thermal or heating energy, the most efficient form of heat transport is the DHN [3], in which a heat transfer fluid circulates through the pipeline installed under the pavement of the streets. Therefore, the fluid movement is possible by hydraulic pressure difference.

Of course, distribution systems do not work ideally. In power grids, electrical energy gets lost by conversion into heat caused by the Joule effect due to the resistance of the cables [4]. In DH networks there are two different kinds of losses: pumping power (Loss of mecanical Power or pure exergy) and heat losses due to the temperature difference between the heat transfer fluid and the environment [5].

2.1.1 Centralized and Decentralized Energy Systems

As mentioned above, using non-renewable energies gives rise to a kind of energy strategy in which the fuel (natural gas, fuel, coal ... etc.) is exploited in a certain reservoir and transported to thermal power plants. Thus, it will be a rigid energy strategy in which the reservoir from which the fuel comes is far away from the urban areas where the consumers live. It is even possible that a specific country or region does not have those resources and needs to import them from other countries, leading to a high dependence and increasing the importance of an effective energy policy which includes the transformation of the energy system and the search for new energy markets. This is the case of the European Union and the Energy Roadmap 2050 [1].
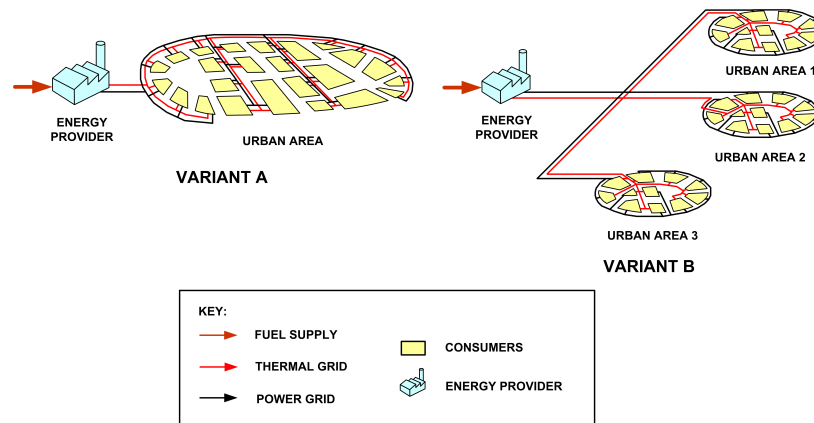
Figure 2.1: Various configurations for centralized energy systems

In a centralized system, fuels are received at specific points and transformed into various forms of distributable energy to the end users, who will find their energy needs covered by a single option. Combined Heat and Power plant (CHP) plants produce power and heat distributed along power grids and pipe networks covering one or several urban areas, reaching all the end users (see Figure 2.1). The ratio of heat to power generation depends on the efficiency and flexibility of the power cycles, as it will be explained later. Generally, there is a certain proximity between generation point and consumers, with all the elements located generally in the same country or region. This is the most common option and followed by most of the current power and thermal grid systems.

A typical example of figure 2.1 (variant A) is the Spanish city of Ceuta, which has a Diesel power plant as the only electricity source [6],[7]. This plant is the one and only energy source that feeds the whole city.

Regarding mode 2, the thermal power plant of Velilla, located in the town of Velilla del Río Carrión (Palencia, Spain), is a good example since it supplies electricity to several urban areas spread along the provinces of Palencia, Burgos, León, Cantabria, and Asturias. In principle, this plant exploited the coal obtained from the surrounding coal mines, although later it had to import it from foreign countries [8].

Concerning DH networks, Russia is an example of a country in which the energy strategy is strongly centralized [9].
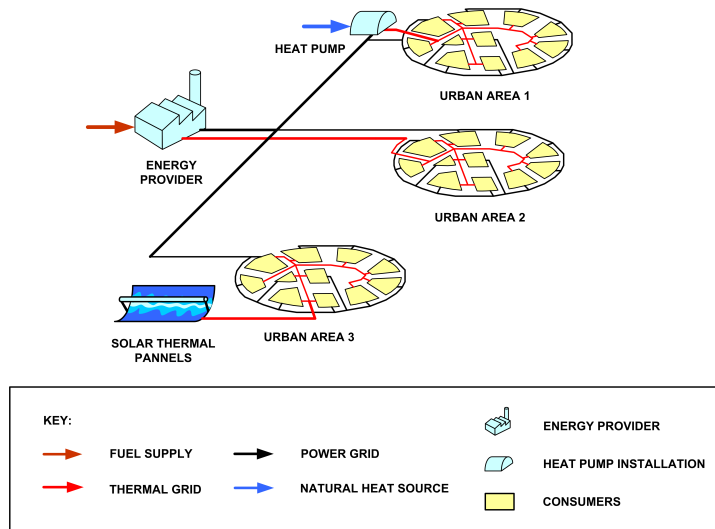
Figure 2.2: Various configurations for partial decentralized energy systems

From here, and due to the increase of the diversity of available urban energy systems, configurations can be varied according to the needs and the availability of resources around cities environment. Regarding partially decentralized systems, the main energy generating center - in this case the CHP plant - is still present and supplies a type of energy, in this case electricity, to all consumers (Figure 2.2). However, due to the long distances between the CHP plant and populations 2 and 3, it is easier to extend the electrical network to those areas, which will be able to "create" their own thermal networks at local level and feed them with the natural energy sources available in the environment, since large distances make not worth thermal network extension. Both the solar thermal panels and heat pumps are ready to obtain thermal energy from the environment, either by concentrating solar rays (thermal solar panels) or from ambient air, surface water, underground water or even the subsoil itself (ground heat pumps).

This configuration allows many different possibilities, giving rise to a great variety of projects and examples, like Fichera's work [10], which consists of a cost-based mathematical study for a centralized energy supply in a network of distributed energy systems. Likewise, M. Rämä [11] studies the effect of introducing a new heat pump and sollar collector capacity in an existing DH system. Other examples can be found along this section and section 2.2).
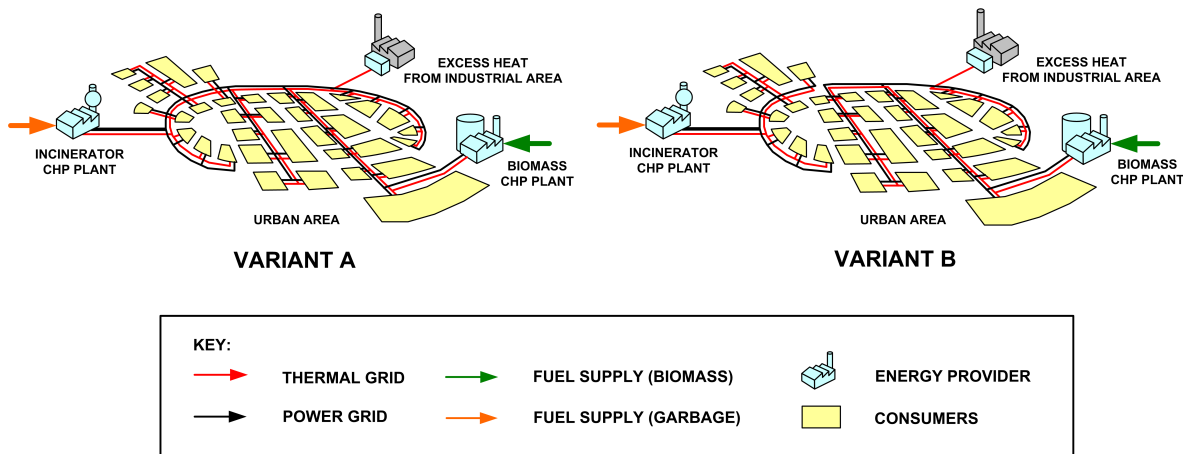
Figure 2.3: Several configurations for decentralized energy systems

Another possibility within the decentralized strategy is using a unique grid covering the whole urban area, and fed from several power and heat generators which are close enough (Figure 2.3, Variant a). The Viennese Network follows this configuration, as it will be explained in chapter 3.1. Moreover, there are interesting studies like Vesterlund's [12], in which a real case study of a multi-source complex DHN is optimized, or Ostergaard's [13], whose paper describes a renewable energy scenario for Aalborg municipality based on low-temperature geothermal heat, wind power and biomass

The second main variant deals with several zones within the same urban area, covered from different energy sources and grids (Figure 2.3 Variante b). This is the typical case for large cities served by different energy generation and distribution companies, giving rise to a much more complex energy strategy in which there are more partners at stake. The clear example is the city of New York [14].
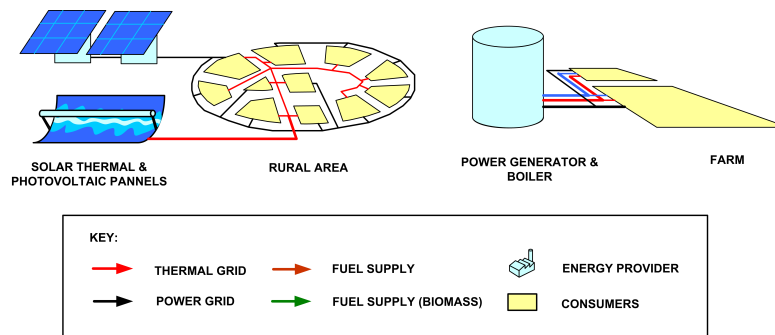
Figure 2.4: Various configurations for total decentralized energy systems

Finally, the last case regards to low population density areas, like small towns and villages, in which consumers are not only far away from the city center but also widely dispersed throughout a large part of the territory. Here, each consumer procures individually his own energy, either from fossil or renewable fuels (Figure 2.4 RURAL AREA and FARM).

There are multiple examples for this type of configuration, both for rural thermal grids, fed by renewable energy sources [15], [16], [17] and other surrounding resources of the environment [18] and for electricity grids powered by renewable energies in rural isolated areas or desert areas [19], [20], and there are even other types of projects in which renewable energies are used for other purposes, such as water desalination [21].

2.1.2   Main Urban Energy Systems

In general, the possibilities for feeding thermal energy into the distribution networks are hereby mentioned:

- Heating plants, fired with coal, oil, or natural gas, biomass (wood), waste

- Production of electrical and thermal energy by cogeneration (A higher quality of the primary energy is required, e.g. oil or natural gas. Lower quality of primary energy need higher effort on waste gas cleaning (e.g. waste, biomass) and is therefore not so attractive.)

- Waste heat from industry

- Solar thermal fields (not so common yet, but coming up)

- Heat from environment with increased quality by use of heat pumps

- Power two heat (just useful if the electrical energy cannot be used in a better way (shaving of peaks in production, e.g. PV surplus)

Among all the existing mentioned urban energy systems, this thesis focuses on the following ones:

- Cogeneration, as the origin of the thermal energy supplied to networks

- Heat pumps to support these networks

- Domestic heat technologies, such as radiators and heated floors.

2.1.2.1   Cogeneration and its adaptation to DH Networks

Cogeneration (also known as combined heat and power, CHP) is defined as the simultaneous generation of mechanical energy (power) and useful thermal energy from a single energy stream such as oil, coal, natural or liquified gas (non-renewables), or biomass and solar energies (renewables) [22].

Cogeneration begins to extend from the 1880s, when the need for power generation is higher due to the electrification of industries and cities. More and more steam-moved industrial machinery is replaced by electrical devices (power engined systems). During the 20th century, coal fired boilers and steam turbine generators produced most of the power needs, using the latent heat from exhausted steam for several industrial applications [23].

Cogeneration's development becomes more prominent especially since the first oil crisis in 1973. During this period, prices rised dramatically, triggering the technological development in a different direction. The improvements in technology made the cogeneration an interesting and economically attractive alternative, allowing the heat plants to sell the whole heat of the Rankine cycle, instead of wasting it, and reducing costs because of the lower consumption of primary energy.

In addition, due to stricter environmental laws, the emission of pollutants has been reduced as well. Since then until today, the use of cogeneration in Europe is actively promoted through the Energy Efficiency Directive of the European Union [24].

This directive establishes a set of binding measures to help the EU to reach the 20 % energy efficiency target by 2020. Under the directive, all EU countries are required to use energy in a more efficient way at all stages of the energy chain from production to final consumption. One of those specific measures and policies mentions explicitly "monitoring efficiency levels in new energy generation capacities", which is clearly related with cogeneration installations in thermal power plants [25].

Likewise, that regulation requires each EU country to carry out a comprehensive assessment of national cogeneration potential and DHC by december 2015 [26], with Austria as one of the countries plenty involved in this energy strategy [27].

Cogeneration is also described as an evolution respect to classic thermal power plants which are totally dedicated to power generation. Basically, in a regular power plant, a small amount of heat is lost with the flue gas in the chimney, but a larger amount heat is lost in the condenser after the turbine. With cogeneration the heat exchanged in the condenser is not lost anymore because it will be sent to buildings or other facilities as useful heat. Moreover, cogeneration plants are able to achieve energy efficiency levels closer to 90 %, lowering greenhouse emissions by up to 250 million tons by 2020. Small cogeneration systems are a good option as well, specially for isolated or remote areas which are not capable to build a grid infrastructure for theirselves [26].

In conventional power generation, part of consumed heat is released to the environment, obeying the Second Principle of Thermodynamics [28]. Thermodynamic cycles are optimized to maximize power generation, releasing heat at the lowest possible temperature, limited by the environment. This heat is released due to the cooling needs of the circulating fluid (usually liquid water transformed into steam and then liquefied again) within the cycle.

However, in cogeneration plants, electric current production is lower, since the heat is supplied to consumers at higher temperature, and not wasted by releasing it to the outside at environmental temperature.
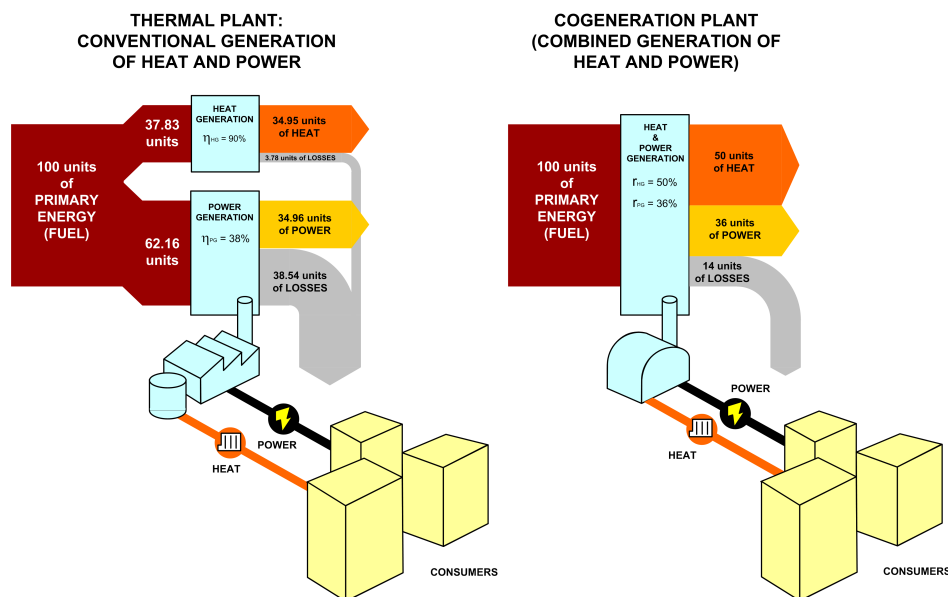
Figure 2.5: Comparison between conventional generation and cogeneration systems [29], where η_{HG} = heat generation efficiency for boilers (heat production only), η_{PG} = power generation efficiency for power plants (power generation only) r_{HG} = fraction of energy transformed into heat, r_{PG} = fraction of energy transformed into power

As it is explained in Figure 2.5, combining heat and electricity generation together instead of both systems separately generates lower energy losses (14 units vs 42). Therefore, in a combined cycle the heat is managed in a better way, consuming the fuel more efficiently and reducing the environmental damage related to the heat released to the environment.

Furthermore, it is also important to note that cogeneration implies not only greater energy use but also exergy, since the internal energy of the fuel is used to generate a greater electricity flow (pure exergy), while in the conventional option, the boiler is simply burning a resource and producing heat without any power generation.

In the longer therm, the increase of energy efficiency with cogeneration implies lower costs and lower greenhouse emissions [30], as well as other pollutants like NOx or SOx. This entails another associated advantage, allowing to use other cleaner fuels such as natural gas or biomass. Another great advantage of this type of plants is the easier assembly in the places where it is needed, leading to lower energy losses and lower expenses associated with transport and distribution. In addition, cogeneration can be used not only to supply energy to urban areas, but also as a heat or electricity source in the industry itself (chemical plants, sewage treatment plants [31], paper industries ... etc).

The main disadvantages derive from the high investment and maintenance that this type of facilities need, as well as other problems linked to localized pollution where those facilities are installed, specially if they are close to rural or natural areas, crops ... etc.

There are 4 fundamental types of cogeneration plants (CHPP): Steam-based Power Plants (SBPP), Gas-Turbine Power Plants (GTPP), Combined Cycle Heat and Power Plants (CCHPP) and Cogeneration Engines (CE).

2.1.2.1.1   Steam Power Plants

Steam power plants are primarily designed to produce power from fuel's chemical energy. Due to the Second Principle of Thermodynamics this conversion is limited, generating heat which has to be transferred to the environment.

The basic thermodynamic cycle of a steam power plant is the Rankine cycle, in which the thermal fluid is water circulating through the circuit, changing its phase as it passes through the different stages. High pressure steam is generated from water, using fossil resources, like natural gas, fuel oil, or even gasified coal as fuels. Renewable fuels like biomass are also possible here.
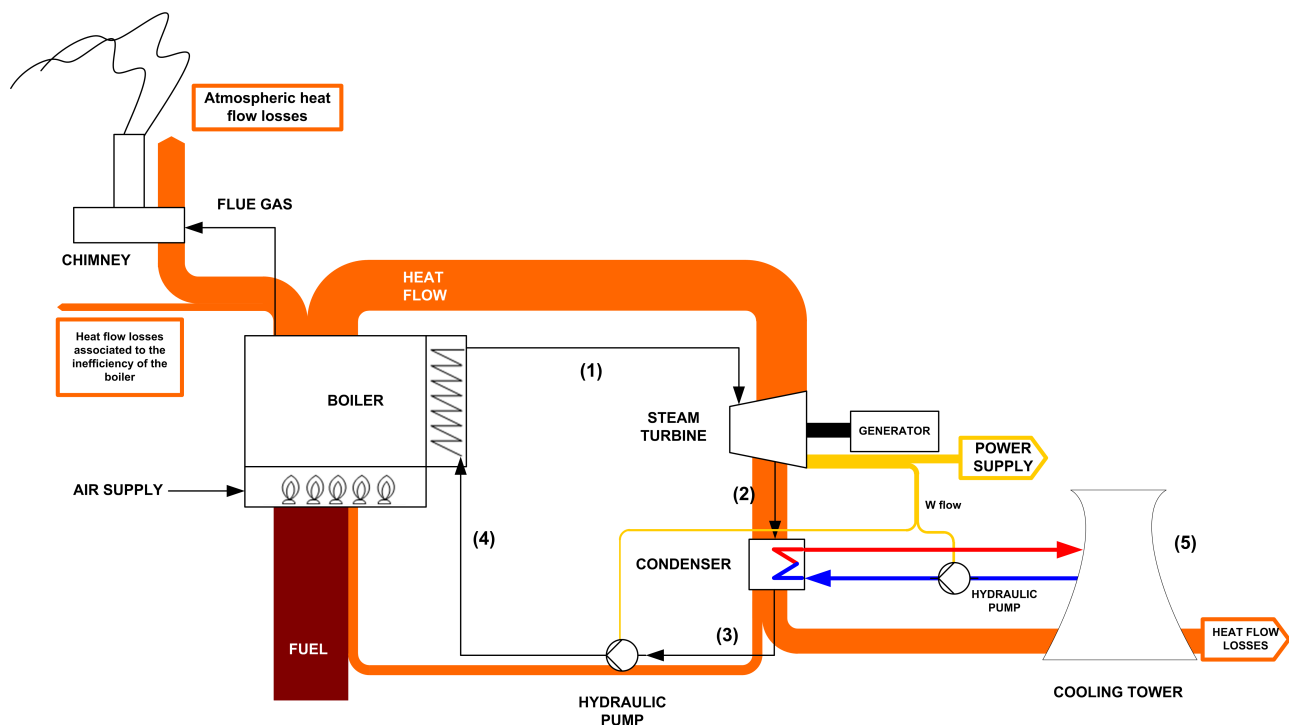
Figure 2.6: Steam power plant with classic Rankine cycle

The superheated steam generated at high pressure in the boiler (Figure 2.6, point 1) is adiabatically expanded in the turbine by changing its pressure from boiler's pressure (P_{BOILER}) to condenser's pressure ($P_{CONDENSER}$), generating power. The result of this process is a saturated steam after the turbine (Figure 2.6, point 2) with all its latent heat available to be transferred at the condenser, obtaining saturated liquid water (Figure 2.6, point 3). Then the liquid water is pumped by a hydraulic pump, implying power consumption. The fluid pressure is increased to P_{BOILER} value (Figure 2.6, point 4). Firstly, the turbine generates mechanical energy. Secondly, there is a generator installed after the turbine that generates power (Figure 2.6, step 1-2). Finally, the heat is transferred from the outlet stream from the turbine to the condenser. (Figure 2.6, step 2-3).

Under ideal conditions, both the steam expansion process in the turbine (Figure 2.6, stage 1-2) and the impulsion in the hydraulic pump (Figure 2.6, stage 3-4) would be considered isentropic, and the condenser and the boiler would not have pressure losses. In reality, in either of theses cases, those statements are not true.

Classic thermal power plants are optimized to produce as much electrical energy as possible. This requires the lowest possible heat release temperature in the thermodynamic cycle. Most efficient (at the lowest temperature) is cooling the condenser with water from any natural source, like a well or a river. If not enough water is available (the temperature of the cooling water would rise too high) cooling towers are used. The purpose of these devices was to disperse the water in the cooling circuit to make it contact with the external air, reducing its temperature. Cooling towers work the better the more water can be evaporated. If absolutely no water for cooling is available, dry re-cooling units are in operation [32].
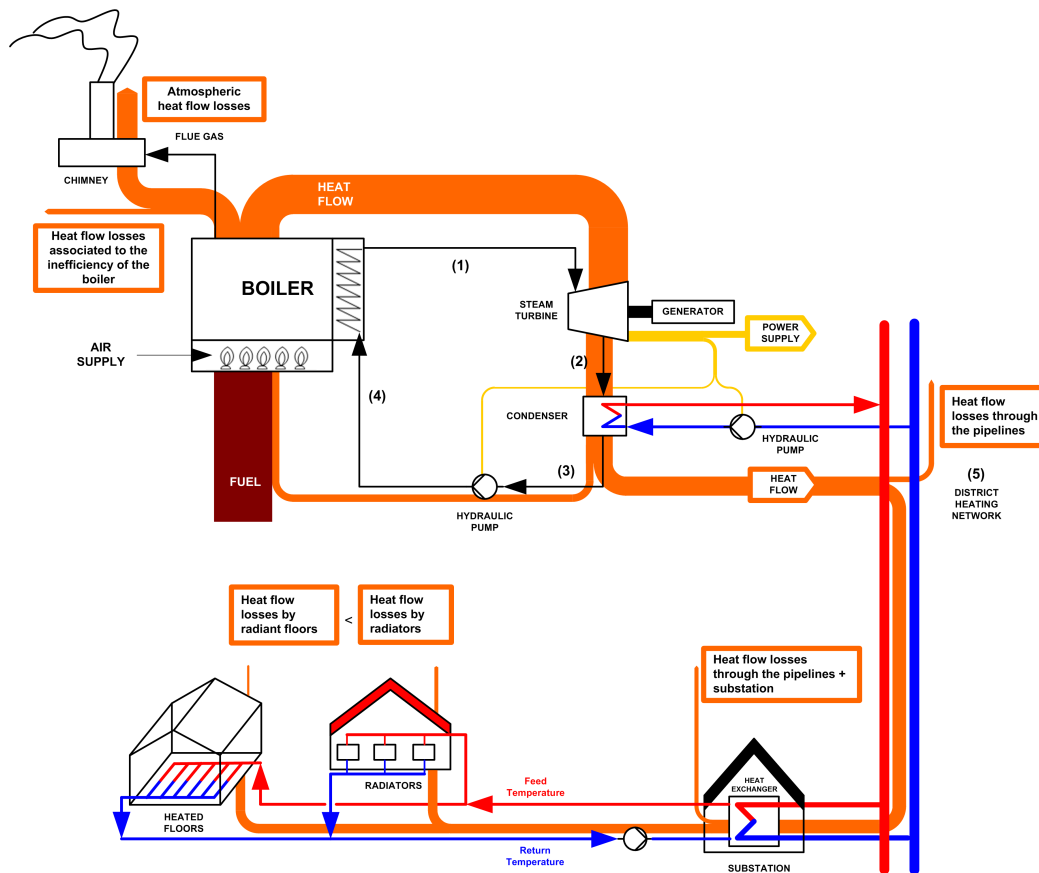
Figure 2.7: Steam power plant with classic Rankine cycle adapted for DH

While the condensing temperature in the condenser is a few degrees above the river temperature in case of river cooling, in dry re-cooling units the condensing temperature is a several degrees above the environmental air temperature. This situation happens due to physical heat transfer limits, leading to significant less thermal efficiencies.

If the heat is needed in the nearer surroundings of the power plant, the condensation is produced deliberately at higher temperatures. Therefore, the power generation is reduced but the heat is not wasted anymore. The cooling tower can be removed (2.6, point 5) and substituted by the heat consumers in the city, resulting in the district heating network (figure 2.7) [32].

As a summary, some general features of steam power plants are described:

- No high quality fuel needed. It can proceed from a fossil source (coal, gasoil) or renewable (biomass).

- The heat release (due to the 2nd law of thermodynamics) happens at constant temperature. That can be the temperature of the environment (if electricity is produced, as much as possible), or at higher temperature for running processes e.g. drying, or heating. In this case less electrical energy can be produced.

- Typical steam inlet values: P = 40-250 bar and T = 400-500 °C

- More frequent in conventional generators

- High powers are possible (> 10 MW)

- Large facilities - Investments raised but with low ratio €/kW

- High duration (> 20 years)

- High degree of reliability of electrical supply

2.1.2.1.2   Gas-Turbine Power Plants

Similar to steam power plants, gas turbine power stations are designed to transform the chemical energy of the fuel into electrical energy as well. The conversion is limited too, which means that a part of the energy is unused and transferred as lost heat to the environment.

The basic thermodynamic cycle of a gas turbine power station is the Brayton cycle. In this case, no water steam circulates through the cycle, and the work fluid is kept in gas phase during all the process.

The open Brayton cycle is formed by a gas turbine whose shaft is solidly attached to a compressor. The turbine generates mechanical work for two uses: one part moves the compressor, and the other is converted into power.
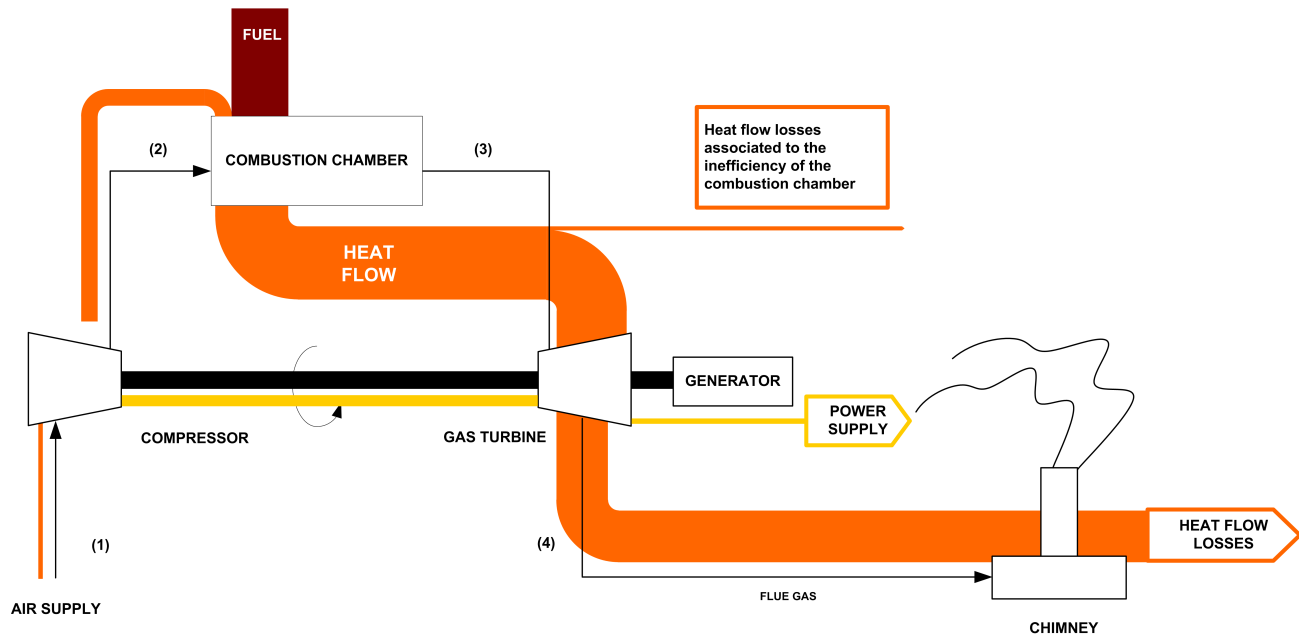
Figure 2.8: Open gas turbine unit based on the Brayton cycle

The flow of fresh air at ambient temperature (Figure 2.8, point 1) is adiabatically compressed in the compressor, giving the required combustion pressure to the air and increasing its temperature, until it reaches the combustion chamber (Figure 2.8, Point 2). In this enclosure, the fuel is burned at constant pressure producing high temperature flue gases (Figure 2.8, point 3). Those are conducted to the turbine, where they are adiabatic expanded, generating power. Since it is an open cycle, the flue gases are evacuated at constant pressure from the turbine and are directly expelled to the atmosphere without any recirculation.

Main features of gas-turbine units [32]:

- The most used in medium to large cogeneration

- Fuel: mainly natural gas or similar

- Possibility of direct use of the flue gas in a heat recovery boiler

- Possibility of post-combustion before using the flue gas in the recovery boiler

- Average power: 50-250 MW

- Possibility of post-combustion: Noise and emission problems (NOx, ..)

- Bad behaviour in partial load or stop conditions

The advantage of this cycle is that the mean temperature of energy feed to the working fluid is much higher compared to the Rankine cycle and therefore this cycle has the potential for higher thermal efficiencies.

On the other side, heat release of the cycle is at higher temperatures compared to the Rankine cycle too, which would reduce the high thermal efficiency if the high temperature exhaust gas would not

be used. Another disadvantage of the gas turbine cycle is the necessity of high quality fuel, like gas or oil. The fuel can be of fossil nature but regenerative (biogas, or more theoretically solar produced hydrogen) as well [32].
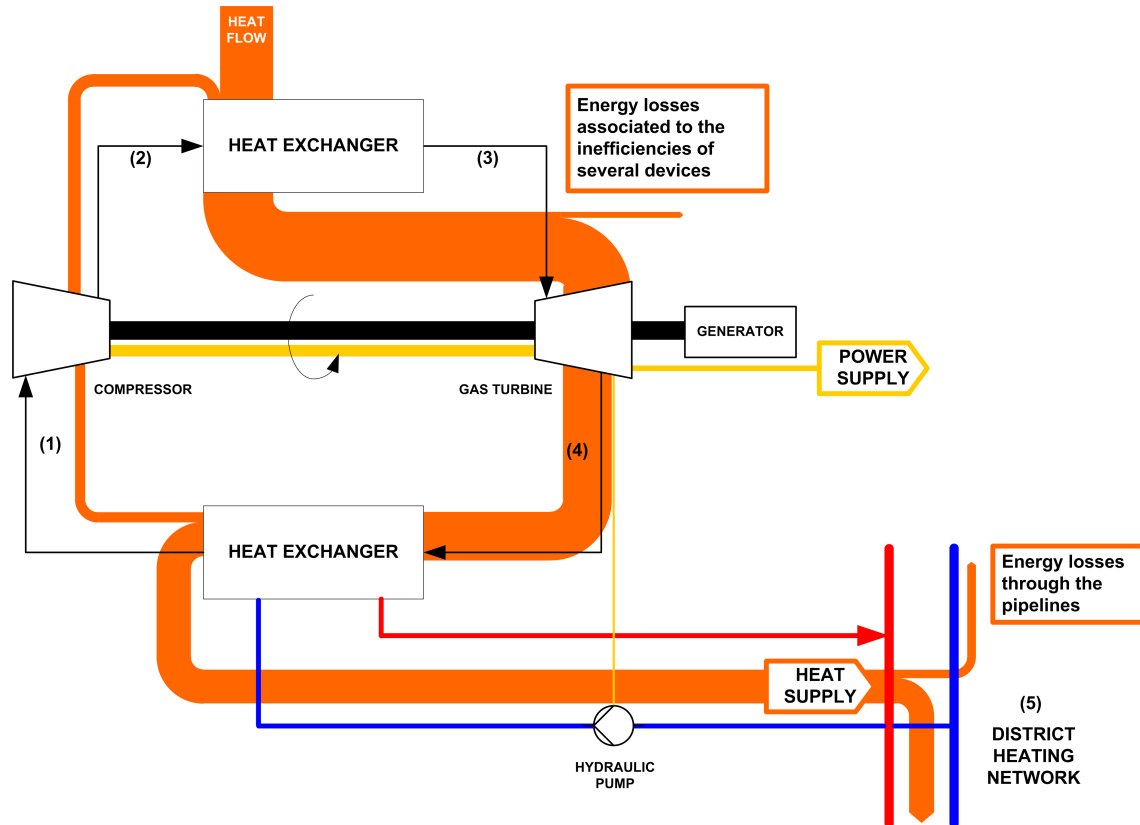
Figure 2.9: Closed gas turbine unit based on the Brayton cycle

In the case of the closed Brayton cycle shown in Figure 2.9, the combustion chamber is replaced by a heat exchanger and the working fluid receives its energy from an external source. The gas leaving the turbine passes through a second heat exchanger (Figure 2.9, point 4), where it is cooled to return to the compressor. Once again, the system can be adapted to serve a urban thermal network, introducing district heating water as a coolant to the mentioned heat exchanger (Figure 2.9, point 5).

2.1.2.1.3 Combined Cycles

Two thermodynamic cycles are joined together in such a way that the heat generated by one of the cycles is partially or totally used as heat which is absorbed by the other cycle. The most common way is coupling a Brayton cycle with a Rankine cycle, as shown in Figure 2.10.

Both power cycles are coupled in such a way that the heat absorption occurs at high temperature in the gas turbine cycle and the heat release occurs at low temperature in the steam cycle. Therefore, thermal efficiency is higher than having a single cycle in operation (may exceed 55%, considering that a gas turbine rarely exceeds 40%, and the most common values are around 35% [33]).
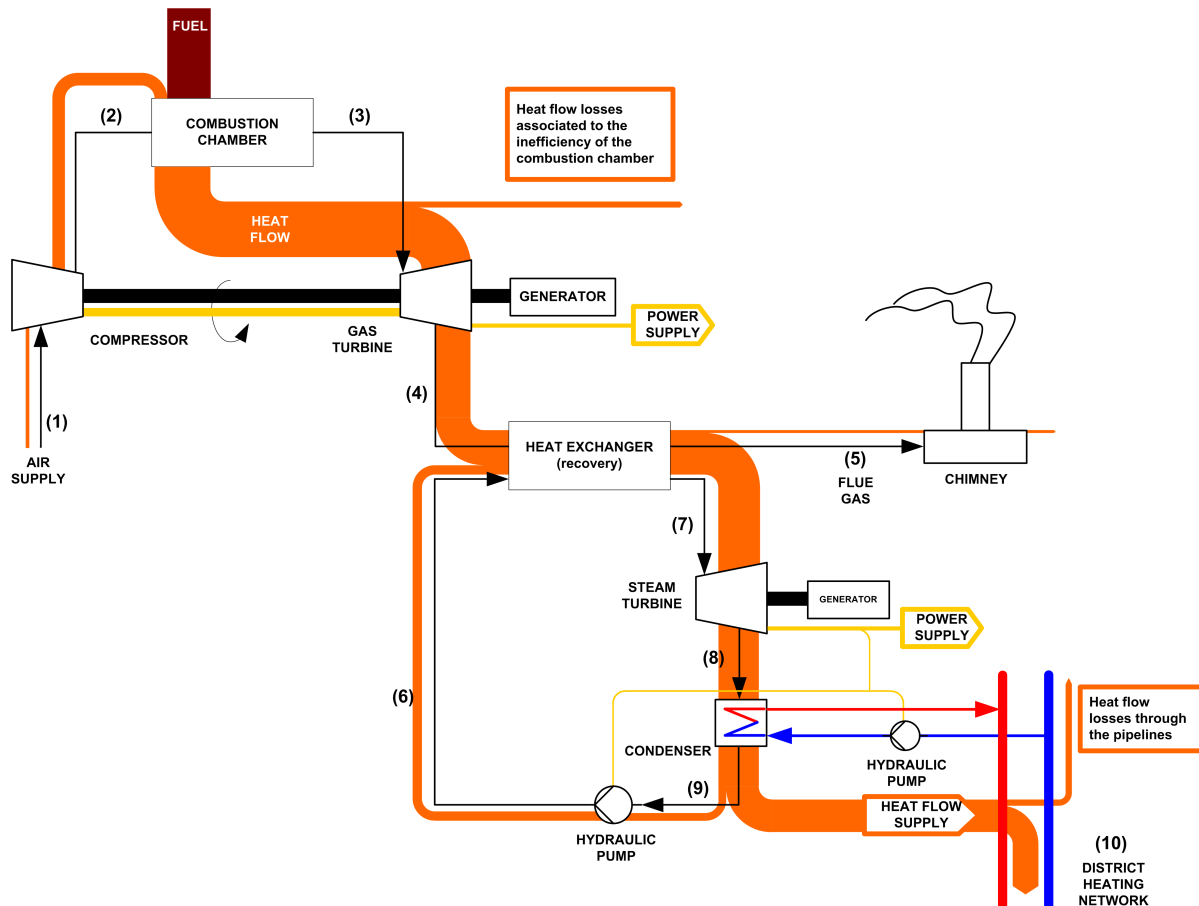
Figure 2.10: Typical combined heat and power cycle

The key is the recovery boiler, in which both cycles are communicated. In this device, hot exhaust gases from the Brayton cycle and high-pressure water of the Rankine cycle are exchanging heat (Figure 2.10, points 4-5), that is to say, the heat from the exhaust gases is totally utilized, decreasing their temperature to the lowest possible value. The cooled gases are discharged to the atmosphere through the chimney (Figure 2.10, point 5)[32].

2.1.2.1.4   Cogeneration Engines

These are small, functional and compact units that can be used in areas with low electricity demand, and even as a complement to certain locations where a rapid conversion from fuel into power is needed, such as hospitals, water treatment plants , biogas plants... etc.

The use of biogas as fuel for this type of engines is a special research topic for the scientific community. There are several projects adapted to each installation collecting all usable biogas [34] and using microturbine technology [31]. Other studies are focused on technological developments to increase the efficiency of heat and power generation [35], [36] and decrease NO_X emissions [37].
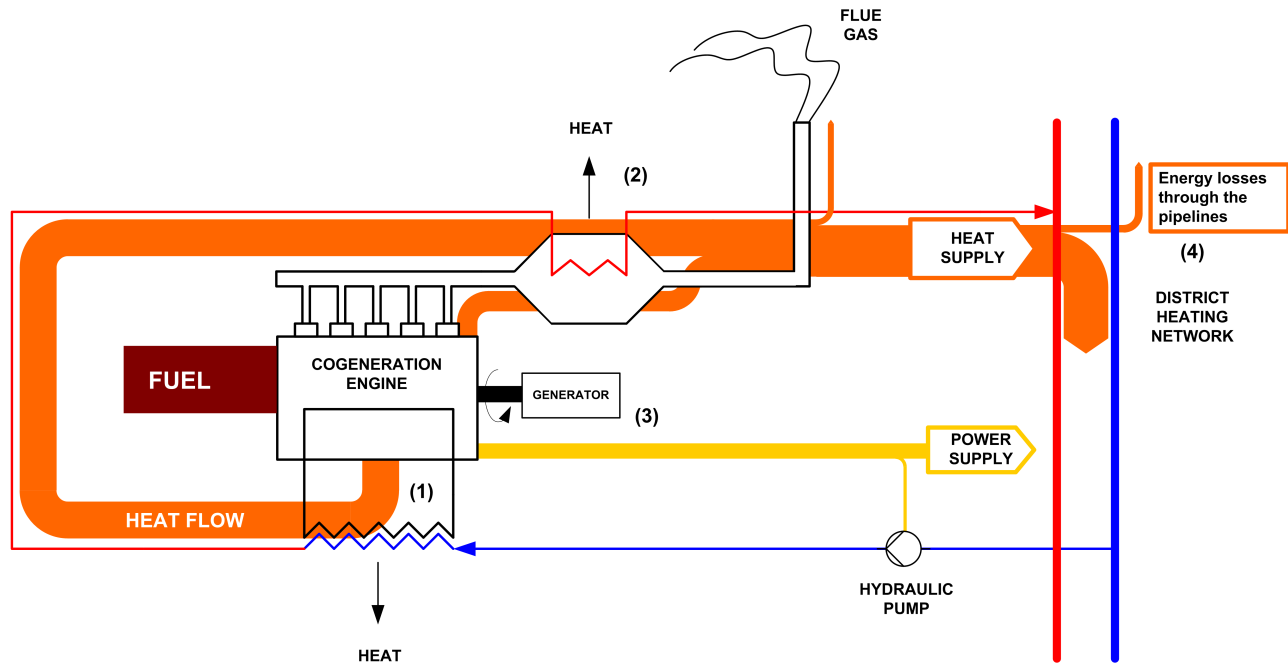
Figure 2.11: Basic schema of a cogeneration engine

In this kind of systems, the thermal engine behaves like any other standard engine receiving fuel, producing mechanical energy in the transmission and hence electrical energy in the alternator (Figure 2.11, point 3). It is a highly versatile device and relatively easy to install. It is able to use different kinds of fuels, both at gaseous and liquid phase.

The heat is mainly extracted from the flue gases at two different points: inside the engine (Figure 2.11, point 1) and in the exhaust gas oultet points (Figure 2.11, point 2). Cooling the engine is not only useful to feed a possible urban heating network [38], but also to improve the efficiency of the mentioned device.

2.1.2.2   Heat Pumps

The heat pump is one of the practical applications of the Carnot cycle, whereby it is possible to extract heat flow from the outside (low temperature heat source), and supply it to the desired place (heat sink). The heat is transferred in the opposite way of the spontaneous processes that occur in the nature, which are ruled by the Second Principle of Thermodynamics, whereby it is impossible for a self-acting machine, unaided by any external agency, to convey heat from one body at a low temperature to another body at a higher temperature [39].
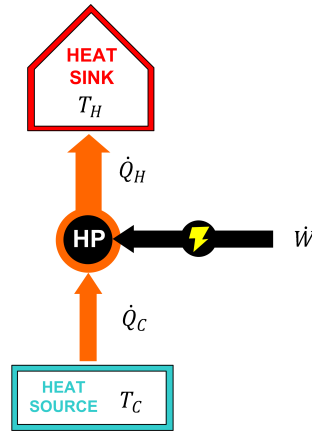
Figure 2.12: Basic heat pump operation

Since T_H is the temperature of the heat sink (the place to be heated), T_C is the temperature of the heat source (from where the heat is extracted), $\dot{Q}_H$ is the heat flow supplied to the heat sink, $\dot{Q}_C$ is the heat flow extracted from the heat source (generally a natural source like water from a river or lake, surrounding air, etc), and $\dot{W}$ is the electric work flow required for the heat pump operation.

According to this principle; the heat transferred from a cold source to a hot sink can be only possible by supplying work (in the form of electric power) to the process, by means of a refrigerant flow undergoing pressure, temperature and phase transformations (liquid and gas). The refrigerant absorbs heat from the source and transfers it to the heat sink, fulfilling the First Principle of Thermodynamics [39] [40]:

$$\dot{Q}_H = \dot{W} + \dot{Q}_C \tag{2.1}$$

Consequently, the use of a heat pump will always be more advantageous than using simple heating using Joule-effect electric resistances [4], since this kind of systems are built to obtain heat only from the electric current as expressed in the following equation:

$$Q = I^2 \cdot R \cdot t \tag{2.2}$$

Since Q is the thermal energy, I is the electricity flow across an electrical resistance R, and t is the time elapsed.

While the heat pump obtains energy flows from two sources: $\dot{W}$ and $\dot{Q}_C$. In addition, and as it will be explained later, converting power into heat through electrical resistances is exergetically inefficient, since using electricity for heat generation is, in some way, a waste of exergy in its purest form.
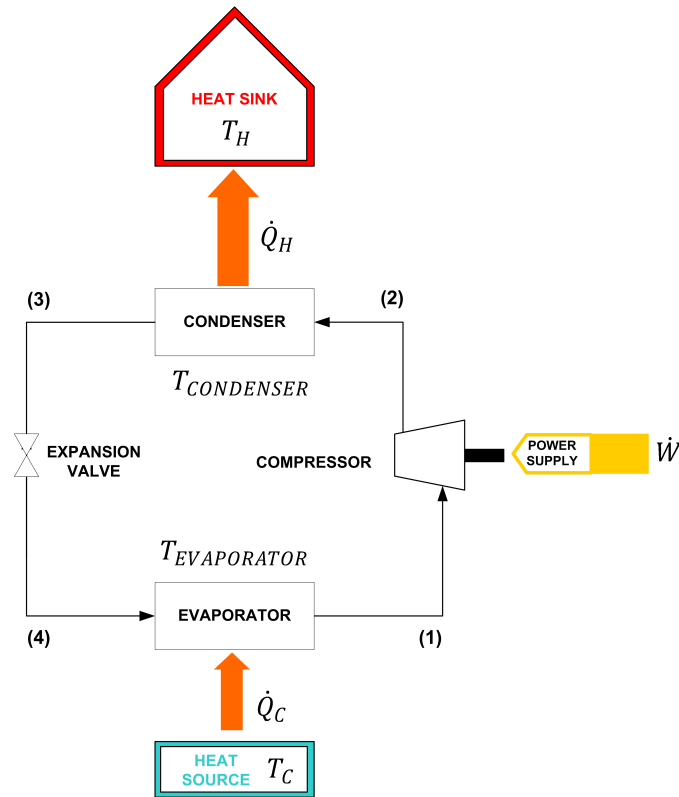
Figure 2.13: Heat pump operation

Stages of the refrigerant inside the Heat Pump (Figure 2.13):

- Stage 1-2. adiabatic compression, steam enters at low pressure and saturation temperature or even slightly oversaturated (point 1) the compressor, raising its pressure and temperature (point 2), and consuming work.

- Stage 2-3. Condensation stage: the heat carried by the cooling fluid is extracted from the condenser and transferred to the heat sink (the stream or air to be heated) at constant temperature ($T_{CONDENSER}$).

- Stage 3-4. Adiabatic expansion: the fluid is expanded in saturation conditions and ready to boil in the evaporator. Some steam may be formed at this stage.

- Stage 4-1. Evaporation stage, isothermal expansion. The fluid passes from saturated liquid to full steam by taking up latent heat at constant temperature ($T_{EVAPORATOR}$) from the heat source.

By a 4-way valve it is possible to change the direction of the refrigerant flow, converting the heat pump into a cooling unit (air conditioning) in the summer months. This kind of device is defined as a reversible heat pump, as shown in the following figure:
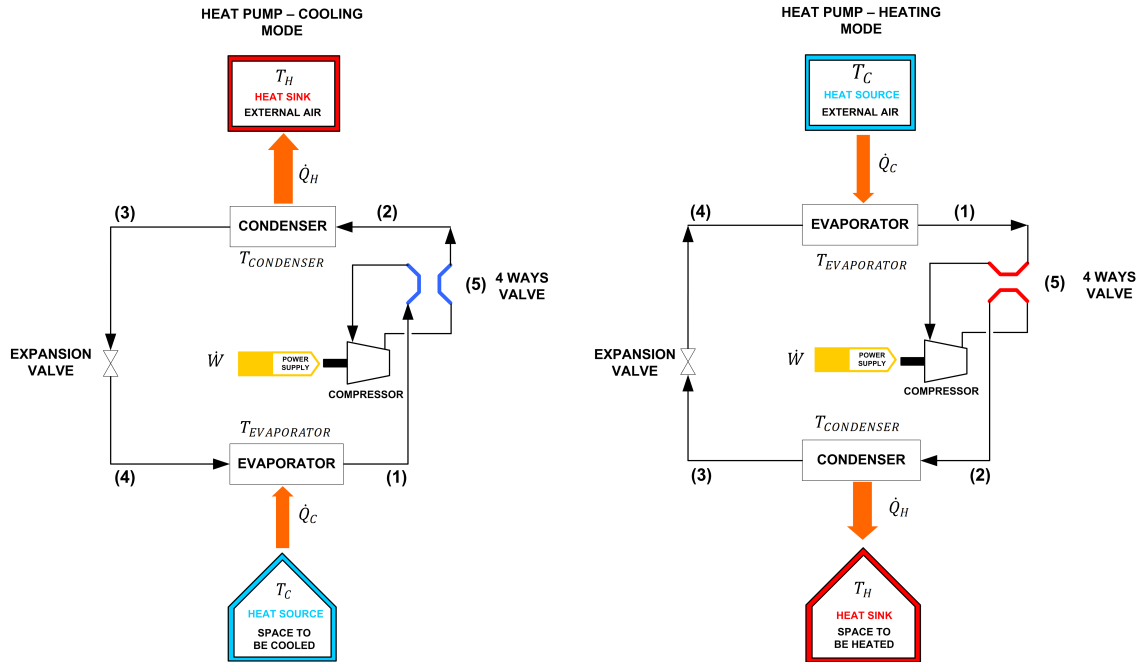
Figure 2.14: Reversible heat pump operation: Cooling-Heating mode

The direct and best-known application of this technology is the domestic air conditioning-heating appliances, whereby the heat extracted from the heat source is the indoor air of the house to be cooled. During winter months, the device can be switched to heat pump mode, so that the heat source is the external ambient air from which the heat is extracted.

The efficiency of the heat pumps is described by the COP (Coefficient of Performance), which measures the performance of the Carnot machine in both modes, either as a refrigerating machine or as a heat pump. In cooling mode it is calculated as the quotient of the heat extracted from the source and the electric work that must be provided.

If considered as an ideal process, the equations are the following:

$$COP_{CARNOT\,CM} = \frac{\dot{Q}_C}{\dot{W}} = \frac{T_C}{T_H - T_C} \tag{2.3}$$

Therefore, in order to increase the efficiency of a refrigerating machine, it is important that the difference between the two temperature levels ($T_H - T_C$) must be as low as possible. This means that the efficiency of the refrigerating machine decreases when low cooling temperatures are required (T_C), or when the heat sink temperatures such as the indoor ambient air is high (T_H).

$$COP_{CARNOT\,HP} = \frac{\dot{Q}_H}{\dot{W}} = \frac{T_H}{T_H - T_C} \tag{2.4}$$

Also for the heat pump the efficiency increases when the temperature difference between the heat source and sink (here the useful heat) is low, i.e. when the ambient temperature is relatively high.

Considering the irreversibilities, the performance of a real heat pump is obtained from the following expression:

$$COP_{HP} = \gamma \cdot COP_{CARNOT\ HP} \tag{2.5}$$

Since γ is the coefficient associated to the irreversibilities of the heat pump [41][42].

COP values usually range between 3 and 5. A COP value lower than 3 implies low energy efficiency. For values equal or greater than 5, the device is considered efficient.

The use of heat pumps involves the deployment of accessible heat sources (anergy sources) such as water from rivers, lakes, aquifers, or the ambient air itself. Therefore, heat pumps are well suited options for rural areas and low population densities (see Figure 2.2), where the installation of larger thermal power plants is not easily possible.

The great advantage of combining heat pumps with CHP plants or DH networks entails the introduction of a new degree of freedom that basically allows changing the heat to electricity ratio generated in the system. When a heat pump is operating, it is possible to reduce the heat and electricity generation of the CHP plant, allowing the use of renewable energies and extracting heat from the surroundings. In addition, the district heating network (DHN) next to the CHP plant can be adapted just decreasing temperature, leading to a Low Temperature District Heating Network (LTDHN).

Hence, the heat needs of the users can be covered by two different ways:

1. Heat from thermal power plants

2. Electricity from various sources, not only from cogeneration, but also from other renewable energy sources such as solar photovoltaic panels coupled with heat pumps.
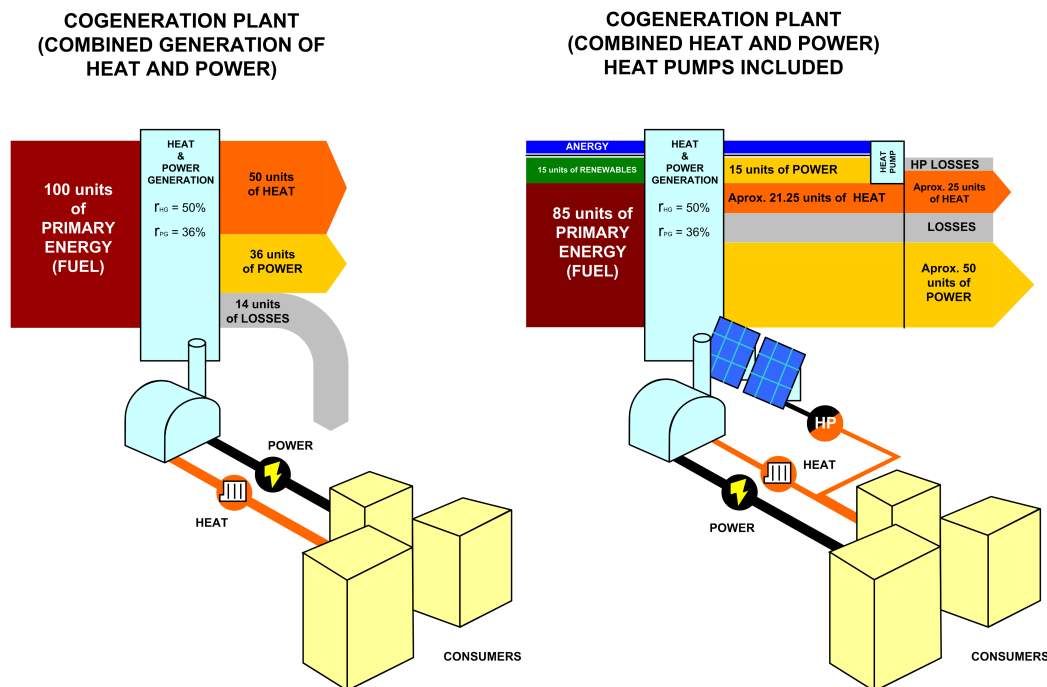
Figure 2.15: Introducing heat pumps connected to CHP plants in combination with DH systems

In essence, this means diversifying the energy sources that feed the district heating network, which will lead to some advantages and disadvantages that will be analysed throughout section 2.2.

According to [43], the sizing and subsequent selection of a heat pump associated with a CHP system and a DHN depends mainly on the maximum capacity of the mentioned network and the COP of the heat pump. It can be done through the following expression:

$$Ne = COP_{HP} \cdot k \cdot \dot{Q}_{th} \tag{2.6}$$

Since Ne is the installed power capacity, k is the coefficient of load of the district heating system (between 0.5 and 0.7, depending on the characteristics of the DH system), and $\dot{Q}_{th}$ is the installed thermal capacity (more information can be found in D. Lauka's article: [43])

Additionally, as explained by Ommen [44], the heat pump can be directly associated to a CHP plant through the post-turbine condenser, giving rise to a CHP-HP system from which the DHN begins, as shown in the following figure:
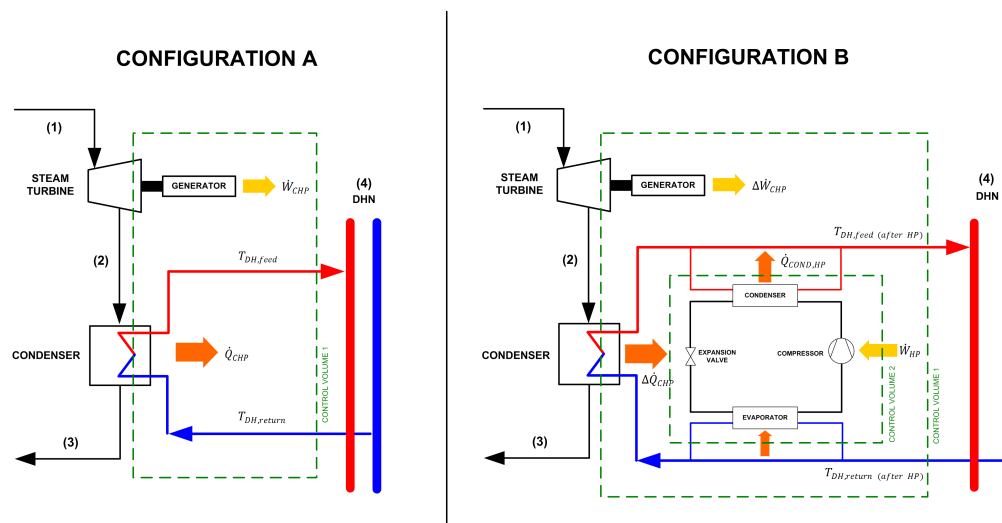
Figure 2.16: CHP-HP system [44]: Configuration A represents the subsequent part of the combined cycle after the turbine, with no heat pump installed (see Figure 2.10). Configuration B represents the same cycle with a heat pump installed

Where $T_{DH,feed}$ is the feed temperature of the DHN, $T_{DH,return}$ is the return temperature, $\dot{Q}_{COND,HP}$ is the heat flow supplied by the heat pump, $\dot{W}_{HP}$ is the electric work flow consumed by the heat pump, $\dot{Q}_{CHP}$ is the heat flow generated by the combined cycle, $\Delta\dot{Q}_{CHP}$ is the heat flow generated by the combined cycle after installing the heat pump, $\dot{W}_{CHP}$ is the electric work flow generated by the combined cycle, $\Delta\dot{W}_{CHP}$ is the electric work flow generated by the combined cycle after installing the heat pump.

Out of the many configurations studied by Ommen, the figure 2.16 only shows the RF2 (return-forward), which consists of using the return DH stream as the energy source for the evaporator of the heat pump, and in turn use the energy of the condenser to raise the temperature of the feed stream ($T_{DH,feed}$), giving rise to electrical consumption ($\dot{W}_{HP}$). This article will serve as inspiration to classify the different combinations of heat pump - district heating, as it will be explained in further section 2.2.1.

Taking as a reference control volume 2, the theoretical efficiency of the heat pump alone (Configuration B) is calculated in the same way as a normal heat pump, following the expression:

$$COP_{CARNOT\ HP} = \frac{\dot{Q}_{COND,HP}}{\dot{W}_{HP}} \tag{2.7}$$

Instead, if control volume 1 is considered, the global system CHP-HP follows the equation:

$$COP_{CHP-HP} = \frac{\dot{Q}_{COND,HP} + \Delta\dot{Q}_{CHP}}{\dot{W}_{HP} - \Delta\dot{W}_{CHP}} \tag{2.8}$$

With COP_{CHP-HP} as the coefficient of performance for the combined system CHP plant - Heat Pump.

2.1.2.3 Radiators and Heated Floors

A radiator is a type of heat emitter, and one of the elements of the conventional heating systems, whose function is to exchange heat from the heating system to the ambient air of a room, home ... etc. This device has no moving parts, it is usually fixed in a certain place and does not generate heat by itself.

The heat exchange process is carried out by two mechanisms: convection and radiation. In order to encourage the renewal of air near the radiator walls and avoid the film effect produced by the saturation of the hot air around the radiator's wall, there are modalities with forced convection, called specifically "convectors". In addition, the heat transferred depends on the temperature difference between the radiator and the ambient air, and the heat exchange surface. The greater the exchange surface, the greater the heat transfer.

In addition to the surface, the radiator's power depends on the following factors:

- Thermal Leap

  Defined as the average temperature difference between the water in the radiators and the ambient air. It is related to the following expressions [46]:

$$P_{rad} = P_{rad,n} \left[\frac{(T_{rad,feed} - T_A)(T_{rad,return} - T_A)}{(T_{rad,n,feed} - T_A)(T_{rad,n,return} - T_A)} \right]^{\frac{n}{2}} \left[\frac{T_{rad,feed} - T_{A,n} - \Delta T}{T_{rad,n,feed} - T_{A,n} - \Delta T n} \right]^{m} \tag{2.9}$$

$$\Delta T_{rad} = T_{rad,feed} - T_{rad,return} \tag{2.10}$$

$$\Delta T_n = T_{rad,n,feed} - T_{rad,n,return} \tag{2.11}$$

  Since P_{rad} is the radiator power, $T_{rad,feed}$ is the inlet water temperature to radiators, $T_{rad,return}$ is the return water temperature from radiators, T_A is the ambient temperature inside the room (all of them in °C), ΔT_{rad} is the thermal leap or temperature difference between the inlet and

outlet flow, n as subindex represents manufacturer's testing conditions ($\Delta T_n = 50K$), n is a radiator's coefficient (typical value is 1.3), and m is a experimental coefficient between 0.1 and 0.4, which can be calculated using the following expression:

$$m = 0.55 \cdot \frac{L}{H} - 0.11 \cdot L \tag{2.12}$$

With L as the radiator length, and H as the height.

In practice, taking into consideration that operation temperatures will not be so high, in most cases Recknagel expression is used [47]:

$$P_{rad} = P_{rad,n} \cdot \left(\frac{\Delta T}{\Delta Tn} \right)^n \tag{2.13}$$

the general trend recommends the feed water temperature to the radiators $T_{rad,n,feed}$ not higher than 70 °C [48].

- Volumetric flow

$$P_{rad} = \frac{\dot{q}_{rad} \cdot \Delta T_{rad}}{0.86} \tag{2.14}$$

With $\dot{q}_{rad}$ as the volumetric flow, in m^3/s.

Therefore, following the equation (2.14), an increase of the volumetric flow leads to a subsequent increase of radiator's power. However, if Inlet temperature ($T_{rad,feed}$) is kept constant, return temperature will be increased ($T_{rad,return}$) as well, which means a rise of the thermal leap.

The main radiators types used in the actual buildings and facilities are the following:

(a) Tubular radiator   (b) Tubular fin radiators   (c) Flat pannels   (d) Unit-composed radiators
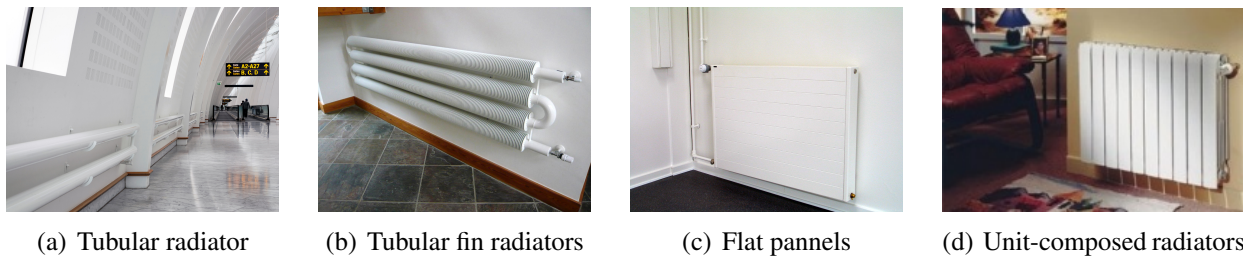
Figure 2.17: Types of Radiators. Pictures a, b and c are courtesy of MEINERTZ [49], picture d is courtesy of Materiales Calefacción [50]

a) Tubular radiators

They are built by smooth steel tubes arranged both vertically and horizontally, showing high resistance to pressure variations and very appropriate for steam or superheated water. This kind of devices are suitable for large installations and high-rise buildings.

b) Tubular fin radiators

Similar to the previous ones, but including fins attached around the tubes. The purpose is increasing heat exchange surface between the tube and the surrounding air.

c) Flat pannels

Several pannels are welded each other in different points, leaving a small space between them (between 2 and 4 mm), and improving the heat emission. They require a very small installation space and are the cheapest due to their price/power ratio.

d) Unit-composed radiators, also called aluminium radiators

The most used and widely extended. Several elements equal each other are joined together until obtaining the desired power. In former times they were made by melt iron, but actually Aluminium is the best option due to its chemical corrosion resistance.

Installation configurations:

- Monotubular
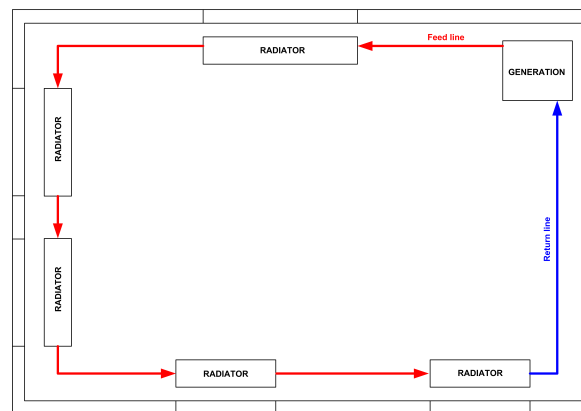
Figure 2.18: Monotubular configuration

The radiators are connected one after the other, in serie, creating a ring that starts from the generator (central boiler, heat exchanger ... etc), connects each radiator and returns to the boiler, closing the circuit. Throughout the process, the flow remains practically constant. The user can control the flow of the incoming water to each radiator by means of a monotube valve installed in a bypass system. In this way, the water can continue circulating even if the radiator is switched off or inoperable.

Advantages:

- Tubes length is reduced
- Simpler installation. One loop covers the entire place
- recommended for small houses and appartments.

Disadvantages:

    – Last radiators have to be dimensioned and prepared for a lower temperature, thus, they will be larger than the corresponding ones in bitubular configuration

    – pressure losses are higher than a bitubular system, leading to greater power used to feed the hydraulic pump

- Bitubular
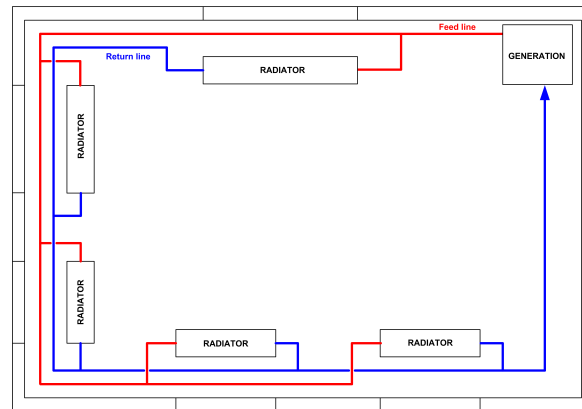
Figure 2.19: Bitubular configuration

In this case, the radiators are installed in parallel, with an inlet pipe feeding the system which is ramified arriving to each radiator, and a return pipe collecting the water from each device. Each radiator has to receive a volumetric flow equal to its power divided by its thermal leap. The total flow of the system is obtained after summing up all the flows from all the radiators. This is the most common and extended configuration.

The second system referred to this section is the radiant floor technology. A radiant floor is a kind of heating system that provides heat using a part or the total surface of the room's floor. There are three heat transmission mechanisms occurred; conduction, radiation, and in a certain way, natural convection.

The basic principle of these systems consists of supplying hot water at medium temperature through circuits of pipes made of a thermoplastic material, generally cross-linked polyethylene.

Unlike radiators, which only have utility in winter but in summer are switched off, radiant floor installations can provide service also in the warm seasons of the year, cooling the air of the room. That is called "cooling mode".

In the same way as in other heat exchange devices, in radiant floors it is true that the greater the exchange surface, the lower the necessary temperature difference between the emitter and the environment, as stated in the fundamental heat transmission equation [51]:

$$\dot{Q} = U \cdot S_{HT} \cdot \left(\bar{T}_{rf} - T_c \right) \tag{2.15}$$

Since $\dot{Q}$ is the heat flow transmitted (W), which it should be equal the heat flow demand of the room, U is the heat transfer coefficient $\left(\mathrm{W}/(\mathrm{m}^2\,\mathrm{K}) \right)$, S_{HT} is the heat transfer surface, T_c is the comfort temperature of the air inside the room, and $\bar{T}_{rf}$ is the average radiant floor temperature, which follows the expression below:

$$\bar{T}_{rf} = \frac{T_{rf,feed} + T_{rf,return}}{2} \tag{2.16}$$

This is the reason why in the guidelines consulted [52],[53],[54] and in the regulations [55], [56] , a $T_{rf,feed}$ of 35-45 °C is recommended. This regulation also indicates that the maximum temperature of the external surface of the pavement should not exceed 29 °C. It is not allowed to exceed this maximum value, due to the risk of deterioration of certain materials.

Working at these low temperatures, together with the heat transmission by radiation, makes the radiant floors's thermal leap (difference between the supply and return temperature) much lower than radiator's:

$$\Delta T_{rad} = T_{rad,feed} - T_{rad,return} = 15K - 20K \tag{2.17}$$

$$\Delta T_{rf} = T_{rf,feed} - T_{rf,return} = 5K - 10K \tag{2.18}$$

The flow of circulating water depends on the thermal demand of the place to be heated, and it is calculated by the well-known expression [51]:

$$\dot{Q} = \dot{m}_{rf} \cdot Cp \cdot \Delta T_{rf} \tag{2.19}$$

Since $\dot{m}_{rf}$ is the mass flow of hot water circulating through the radiators and Cp is the thermal capacity of the thermal flow at constant pressure.

Therefore, installing radiant floors means reducing the thermal leap by a half, doubling the mass flow of circulating water [57].

Under cooling conditions in summer, the norm specifies a pavement contact temperature not lower than 18 °C, in order to avoid the condensation point of the water present in the ambient air.

The low temperature of the thermal fluid allows the possibility of introducing new energy systems to obtain the heat, such as heat pump systems, solar thermal energy, geothermal energy, heat recovered in industrial processes...etc. Those possibilities will be explained later, in section 2.2
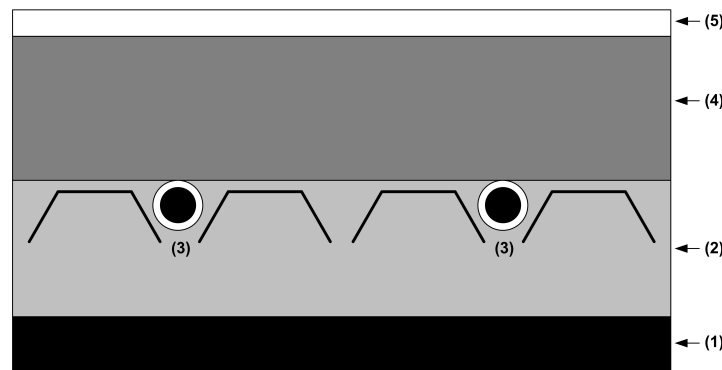
Figure 2.20: Radiant floor section, with the following parts: (1) structural base, (2) thermal insulation / tubes fixation structure, (3) tubes, (4) cement layer, (5) pavement

There are several configurations, but generally the tube circuits are supported on a thermal insulation layer, made of a plastic material (2), which in turn is supported on the structural base (1). This layer prevents the heat coming from the pipes circuit (3) to be transferred to the floor below. It also works as a sound insulator and as an structural fixation for the pipes. Likewise, a peripheral insulation is also usually installed, in order to protect from possible heat leakages to the sides, and the corresponding expansion joint, which is necessary to prevent possible dilatation of the pavement due to temperature changes. Both the tube circuit with the base and the insulation are covered by a cement mortar layer (4), providing homogeneity and stability. The final pavement is then placed (5), which may be made of ceramic, stone, wood, linoleum ...etc.

Figure 2.21: Radiant floor installation, courtesy of Novelec [58]. Tubes circuit and insulation surfaces are visible under the cement layer

The typical radiant floor circuit design starts from the heat generator (see Figure 2.22, point 1), which heats the water to the desired temperature. To regulate it, a mixing valve is required, defining the following control loop [59]:
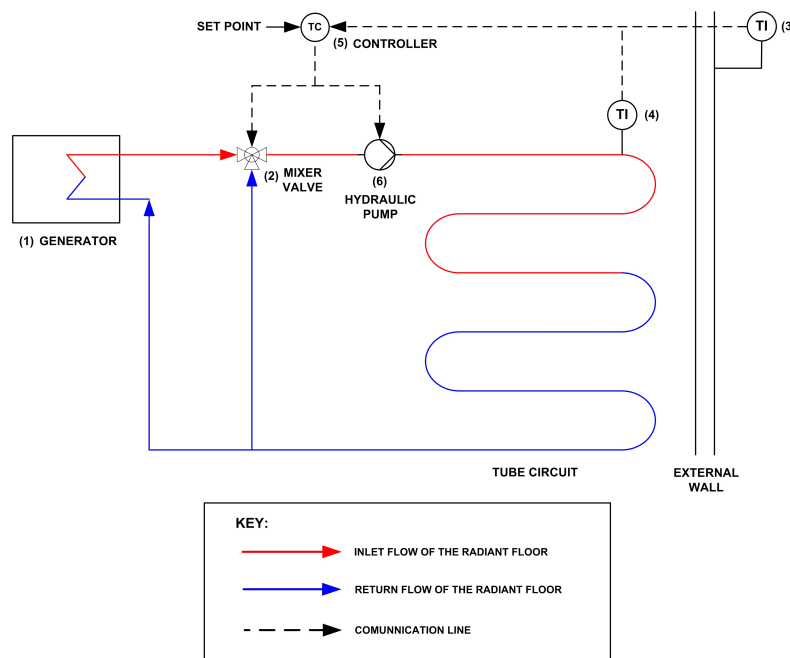
Figure 2.22: Radiant floor regulation system [59]. Acronyms used: TI = Temperature Indicator, TC = Temperature Controller

The three-way mixing valve (2) receives a part of the return water. The temperature regulation is carried out by means of a valve controller (5) that constantly receives the external temperature values from the external probe (3), as well as the values of the circulating fluid (4) and the desired comfort temperature value (SET POINT). Based on all this information, the controller calculates the inlet temperature ($T_{rf,feed}$) and opens or closes the mixing valve, reducing or increasing the water temperature. This loop is also a security system that stops the impulsion pump (6) when $T_{rf,feed}$ is equal to or greater than 60°C [60]

Installation configurations [61]:

- Spiral Configuration
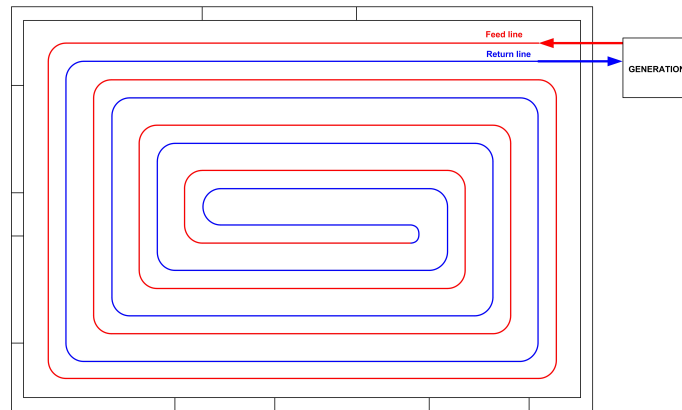
Figure 2.23: Radiant floors, spiral configuration

The most common is the spiral configuration, since allows a better and homogeneous temperature distribution. As the figure 2.23 shows, the input pipe, with the water at the highest temperature is located closer to the walls and windows, which are the coldest areas where more heat flow is lost to the outside.

- Longitudinal Configuration
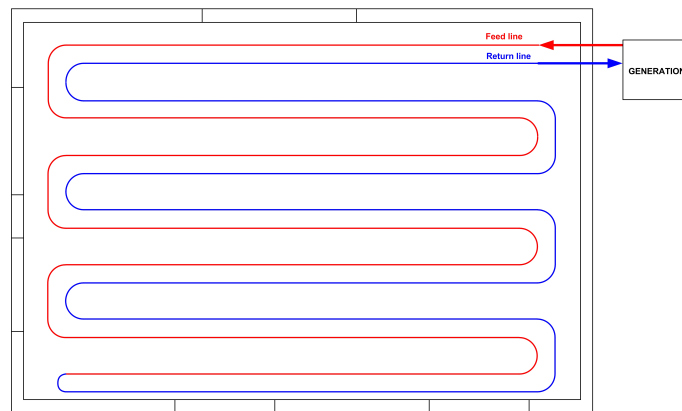
Figure 2.24: Radiant floors, longitudinal configuration

The other most commonly used configuration is called longitudinal or double coil, in which the tubes are placed in parallel, keeping always the same distance between each other. This

arrangement is recommended for small areas and rooms, since it takes longer to reach the required temperature.

The main advantages of the radiant floors respect to conventional systems are the following:

- Homogeneous heat distribution among the living area

- The temperature of the thermal fluid is much lower compared to radiator systems, saving energy and fuel consumption

- Due to installation characteristics, radiant floors are clean and silent systems that do not occupy useful space in the rooms

- If the pavement is made of the right material, it acts as a heat accumulator, allowing the system to be turned off at certain periods of the day

In the same way, radiant floors also offer the following disadvantages:

- Construction works are needed, leading to higher costs and installation time

- Difficult access for reparations

- The control system is more complex than conventional installations. Requires calibration and maintenance and, in general, the access is difficult for the users

- longer waiting time until reaching the desired temperature

2.2   Evolution of the District Heating Networks

Since the first district heating network installation was built in Lockport (New York, USA) [62] at the end of the 19th century, more cities have progressively started to install and operate various kinds of thermal grids according to their needs. These systems are widely extended in the majority of cold climate countries, especially Scandinavia, Central and Eastern Europe and constitute one of the main strengths for the fulfillment of EU goals expected for 2050. According to them, the European energy systems must be decarbonized to at least 80 % below 1990 levels by 2050 [1].

The extended generational classification (Figure 2.25) shows the four stages of the DHN evolution. The first generation was based on high temperature steam produced in thermal power stations and distributed through the city in reinforced ducts, delivering the latent heat by condensation of the steam in the radiators. New York is the best example, although it is currently undergoing an important transformation and improvement process [14].

The second generation was mainly developed between 1930 and 1970, by the Eastern European countries and the Soviet Union. Here, the heat transfer fluid is pressurised liquid water, pumped through insulated pipes and concrete ducts installed under street pavements. Feed temperatures never exceeded 100 °C , avoiding steam formation.
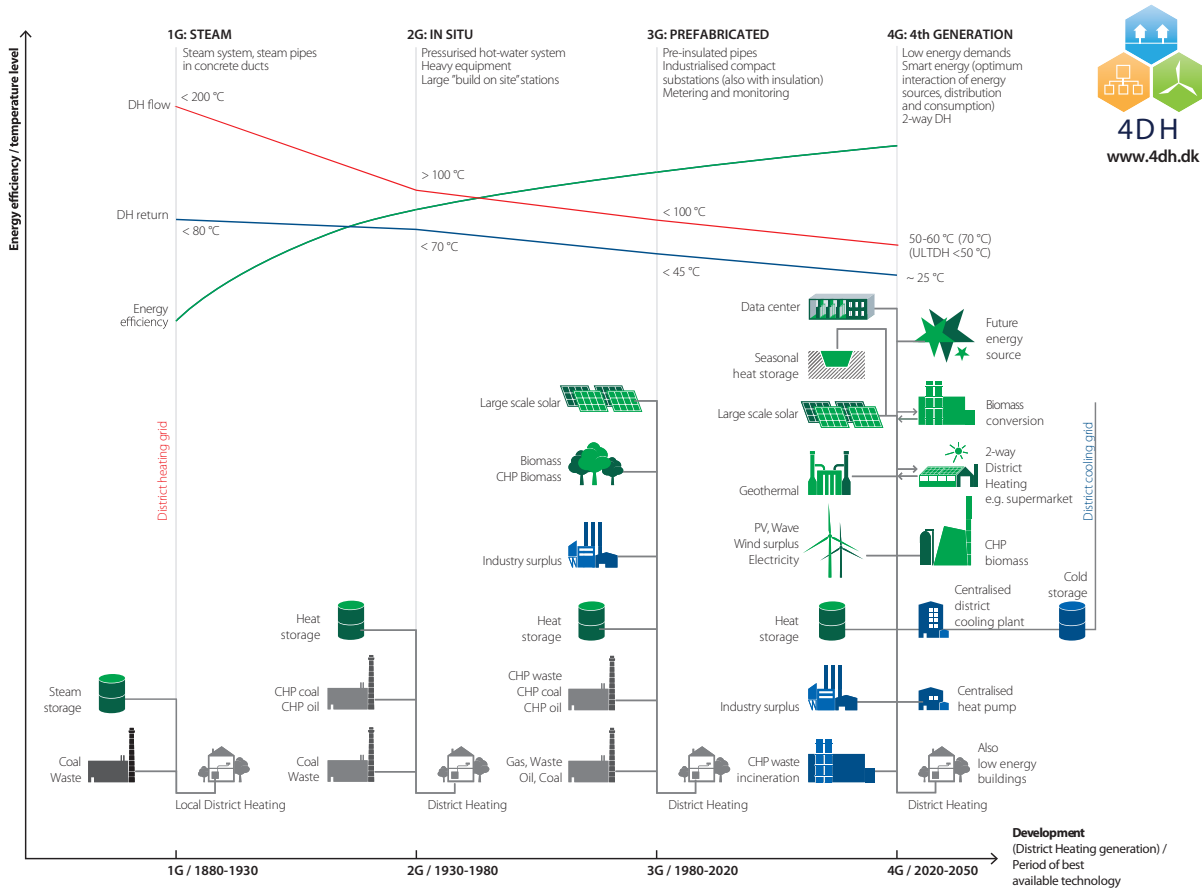
Figure 2.25: Evolution of DH networks. Courtesy of Prof. Henrik Lund [2].

In the decade of 1960-1970 there was an evolutionary leap generated mainly by northern and central European countries, with the Scandinavian countries as the main actors [63] [64] [65]. This is known as the Third Generation of DH Networks. The main developments were based on the introduction of instrumentation and control systems and the use of new energy sources to feed the network, such as renewable energies (Mainly biomass and solar thermal [66]) as well as the use of other possible heat sources existing in the environment, such as industrial effluents [67] or waste incineration.

There is a broad and controversial discussion, with many articles, books and studies about how the general strategy should be conducted, in order to carry on the evolution of actual installed networks to the fourth generation [68] [69] [70] [71] [3] [72] [73].

There are also several projects and studies in different directions focused on developing and extending thermal grids in combination with other technologies, such as renewable energies [74], thermal storages [75], heat pumps [44], refurbishments [76] or combinations of several devices [77].

In addition, the fourth generation of DH networks is somehow related to the Smart Grids concept [78][79], since both ideas agree with certain areas, such as adaptation and flexibilization of CHP plants, electrification of district heating networks, penetration of renewable energies and the use of energy storage systems to meet the demand. It is possible now to consider the 4th generation of district heating networks (4GDHN) as a part of the Smart Grid project, and not as a unique goal itself [2] [80] [81] [82].
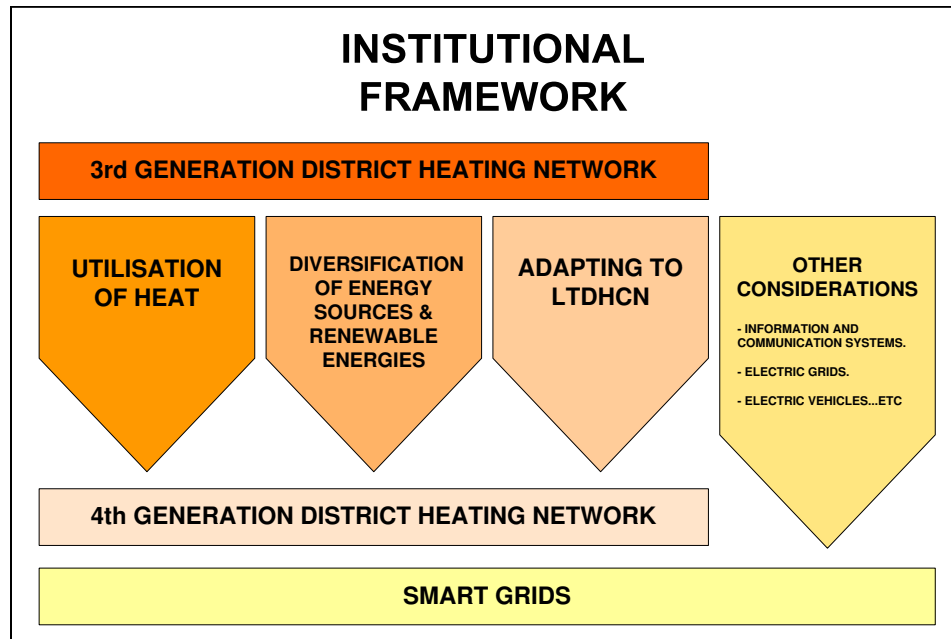
Figure 2.26: Development from 3rd to 4th generation of DH networks inside the smart grid framework. LTDHCN = Low temperature district heating and cooling networks

The different phases within the next DHN evolution integrated inside the Smart Grids concept shown in Figure 2.26 are described below:

1. Institutional framework

   A global strategy is required, integrating all actions and bureaucratic regulations working in the same direction:

   a) Suitable planning.

   b) Promoting energy-efficient buildings (EeB) [83] already prepared and designed for Smart Grids and low temperature heating networks.

   c) Encouraging strategic and political actions to motivate and adapt present facilities into future energy systems.

   d) Defining new operation and maintenance procedures, increasing efficiency and reducing costs.

2. Utilisation of available heat

   Basically, a DHN performs as a sink if it receives heat from thermal plants or other heat sources and as a source when the heat is transferred to the consumption points. It is also possible that consumers are heat producers and therefore donors to the network, in which case they are called "prosumers", increasing the complexity of the grid. Establishing temperature levels (high, medium, low and return temperatures) and considering three-pipe technologies, it is possible to define a hierarchy of temperatures and satisfy the particular needs for each kind of building.

   In order to follow this strategy, and using the annual energz demand as the main characteristic, a classification of the buildings will be required, in order to make groups of elements with similar features, defining archetypes.
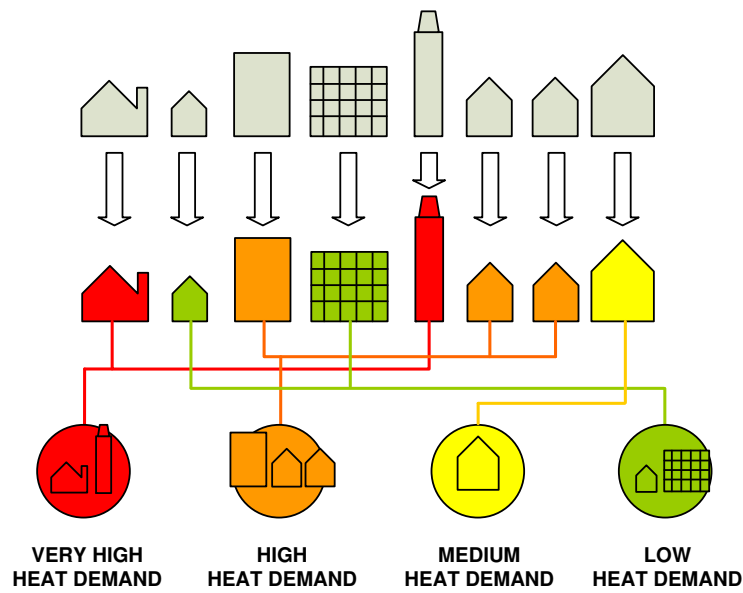
Figure 2.27: Defining arquetypes of buildings

Therefore, it is possible to recycle low-medium temperature effluents from potential residual energy donors, such as industries [67] [84] [85], with the consequent reduction of greenhouse emissions [86]. Urban waste waters are also a possible heat source to be recovered, since their temperature level stays between 25-35 °C, [87] (Figure 2.28).
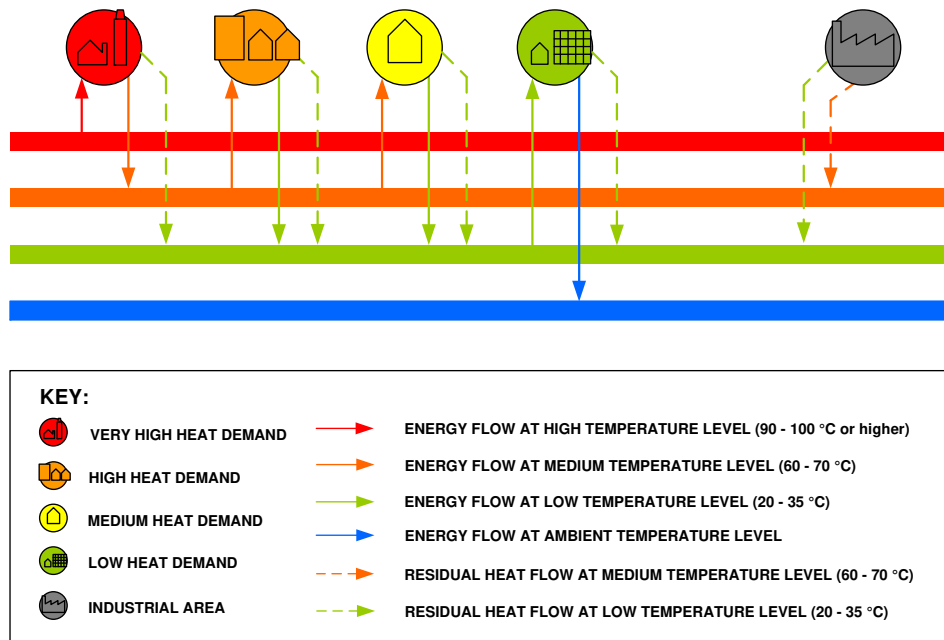
Figure 2.28: Defining prosumers and industrial heat using four temperature levels.

As the figure shows, dotted lines represent all the heat that can be recovered from the different waste effluents generated in buildings or industries. Higher heat-demand buildings obtain

heat from high-temperature networks and send residual effluents at usable temperature level to medium or low-temperature networks. Low heat-demand buildings are then able to use this residual energy and send effluents to a lower temperature level. This process is known as energy cascade, and heat pump technology is frequently involved in order to make it possible [88].

Since factories and industrial areas cover several production processes involving different temperature levels, they can also be considered as potential energy suppliers.

3. Diversification and use of new energy sources. Integration with fourth generation DH networks [89]

This action involves the conversion from basic thermal plants to CHP/CC plants, as well as the integration of renewables with DH networks, as observed in Figure 2.29.
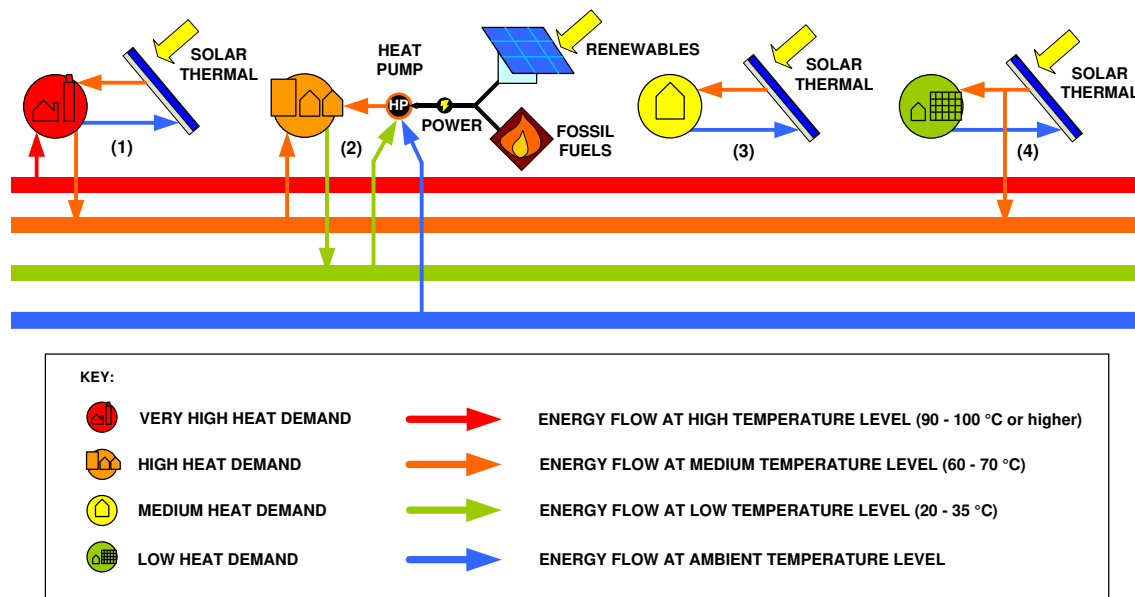
Figure 2.29: Several theoretical ways to combine local renewables with thermal networks: (1) Solar thermal in combination with DHN (consumer), (2) Heat pumps in combination with DHN: heat pumps are power consumers from fossil origins, but they also allow the use of power from renewables (e.g. solar photovoltaic), to locally increase the temperature of water coming from a LTDHN, (3) Individual solar thermal, self-sufficient buildings, (4) Solar thermal in combination with DHN (prosumer): The customer is able to provide an energy surplus to the network.

There are important projects planned or operating all over the world, each with characteristics dependent on meteorological conditions and resources available. For example, for a warm winter area it will be convenient to use a local air-water heat pump to produce hot water below 50 °C [90], since the external air temperature will be high enough and hot water temperature will be low enough to operate the device with high performance. However, users in colder regions should use water-water systems, making use of diverse potential anergy sources present in the surroundings of the house, such as sewage water [91], geothermal energy [92], or mixed systems such as geothermal and solar assisted heat pumps [93].

Although these actions are interesting individually, global energy strategy should be the main issue in which DH networks play a fundamental role.

4. Adaptation to LTDHN

   The general trend faced by the current DH systems is the reduction of the circulating water temperature in the network to values between 30 and 70 °C, with the consequent decrease of the return temperature, leading to an increase of energy efficiency of the plant and decreasing fuel consumption and carbon footprint, [94]

   In order to achieve this goal, one of the main tasks will be the replacement of current heating systems, such as radiators, to low temperature devices such as radiant floors. The main peculiarity of this kind of device is the large heat exchange surface it offers compared to radiators, allowing a lower temperature of the circulating water.

   In order to maintain the desired comfort temperature, it will be necessary to supply a constant heat flow that is able to overcome the heat losses from the building, which are higher the colder the outside air. If the heat flow coming from the radiant floors is not enough to keep this temperature, it is possible to reduce those heat losses by renovation [95].

   As indicated above (Figure 2.29, point 2), the use of heat pumps exploiting the anergy of natural systems is a huge opportunity for the evolution of the current thermal networks into low temperature systems. Special heat pump devices will be able to combine the heating systems in the buildings with the LTDHN [96] [97], or connect the heat pumps immediately after the CHP plants, modifying feeding and return temperatures and influencing the overall performance of the system [44]. In addition, there are interesting projects in which the heat pump is fed directly with seawater and performs as a thermal plant itself, providing heat to the DHN attached [45] or, following the idea explained in Figure 3, using available anergy from low temperature sources, such as sewage water [87] or residual industrial heat [98].

   All these projects, as well as the various combinations between thermal grids and heat pumps and their implications in relation to the LTDHN, will be explained in more detail in section 2.2.1

In summary, the fundamental requirements to carry out this evolutionary leap are the following:

1. Reduction of DHN water temperature, improving to low temperature systems [97][99][88][100], and decreasing heat losses as much as possible.

2. Replacement of fossil fuels by new alternative energy sources

3. Establishment of new energy politics

2.2.1   Combining DH Networks and Heat Pumps. LTDH Networks

As shown in Figure 2.29, point 2, combining thermal networks with heat pumps is one of the most interesting possibilities, since it allows the use of electricity from various sources, including renewables. The heat pumps can increase the temperature of DH water in local points, taking advantage of the surrounding energy sources and avoiding the use of Power to Heat technologies based on electrical resistances. Therefore, It is important to focus on this point, since the electrification of DH networks constitutes one of the essential pillars for the evolution of the current systems towards the 4GDHN, as well as a fundamental topic for this thesis.

Given the large number and diversity of existing projects, both in the design phase or in operation, the different configurations established by T. Ommen [44], are very useful to establish a classification of these projects, as well as understand how heat pumps can be connected to DH networks and what kind of service are they able to provide.

There are five possible configurations identified. All temperature values are orientative.

2.2.1.1 Source - Forward (SF)
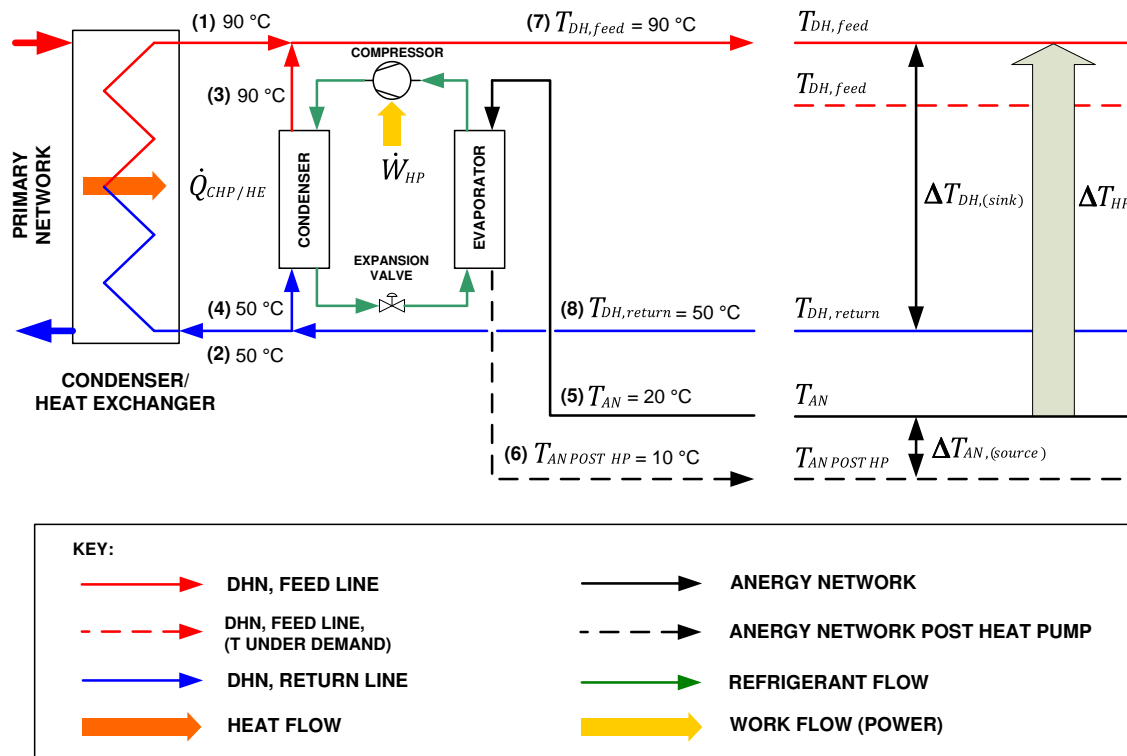
Figure 2.30: Source-Forward Configuration. With $T_{DH,feed}$ as the feed temperature of the DHN, $T_{DH,feed\,(under\,demand)}$ as the feed temperature of the DHN, which is used for a certain purpose, mainly domestic DHW preparation or low temperature heating, $T_{DH,return}$ as the return temperature, T_{AN} as the temperature of the anergy network (AN), $T_{AN\,POST\,HP}$ as the temperature of the anergy network after crossing the heat pump, $\Delta T_{DH,(sink)}$ as the temperature difference contributed by the condenser of the heat pump, $\Delta T_{AN,(source)}$ as the temperature difference extracted from the anergy network, ΔT_{HP} as the global temperature difference generated by the heat pump, $\dot{W}_{HP}$ as the electric work flow supplied to the heat pump, and $\dot{Q}_{CHP/HE}$ as the heat flow supplied from any heat source to the DHN through a heat exchanger, either from a thermodynamic cycle (condenser post-turbine, CHP plant), boiler intermediate substation...etc.

In this configuration, as shown in figure 2.30, the heat pump is connected to the two branches, input and output, of the district heating network (streams 1 and 2) through the condenser. This element receives part of the return stream (stream 4) raising its temperature, generating current 3, which is subsequently joined to stream 1, giving rise to the DH feed line (stream 7).

Meanwhile, the evaporator extracts the necessary energy for the evaporation of the refrigerant

through stream 5. This flow is used as an anergy source for the heat pump. It has different origins, from water coming from a river or a lake, underground water or even the external air.

Therefore, temperature is increased by the heat pump following the expressions:

$$\Delta T_{DH,(sink)} = T_{DH,feed} - T_{DH,return} \tag{2.20}$$

$$\Delta T_{AN,(source)} = T_{AN} - T_{AN\,POST\,HP} \tag{2.21}$$

$$\Delta T_{HP} = T_{DH,feed} - T_{AN} \tag{2.22}$$

The main characteristic of this configuration is that the heat pump does not increase DHN temperature, it simply heats the return water in another way, using electrical energy and the aforementioned anergy source. Therefore, if streams 1 and 2 of the heat exchanger were disconnected, the heat pump would be the only way to heat the DH water.

A clear example of this type of system is the project of Drammen [45], consisting of a district heating network which thermal energy is supplied by a heat pump in the town of Drammen (Norway):

- General Information:

  - Place: Drammen (Norway)
  - Served Population: 60878 habitants.
  - Thermal Capacity: 14 MW
  - Annual generation: 67 GWh
  - Owner: Drammen Fjernvarme

- System characteristics:

  - 3 systems supplying a combined capacity of 14 MW providing 85 % of the hot water needs for the city.
  - Refrigerant R717 (Ammonia). Under steam - compression refrigeration cycle
  - Heat source (AN): Sea water taken from 40 m depth, at 8-9 °C temperature.
  - $COP_{HP} = 3.0$
  - Single screw compressor, High pressure version, compressing simultaneously on opposite sides. Possibility to varying the volume ratio. ΔP supplied = 26 bar for each compressor.
  - Shell and Tube heat exchangers. ΔT between water outlet and refrigerant = 2 °C.
  - Condenser stage is split into 3 stage systems working in series (see Figure 2.31). Subcooling range = 25 C.
  - Intercoolers, subcoolers and oil coolers: All are single pass shell and tube heat exchangers operating in countercurrent flow.
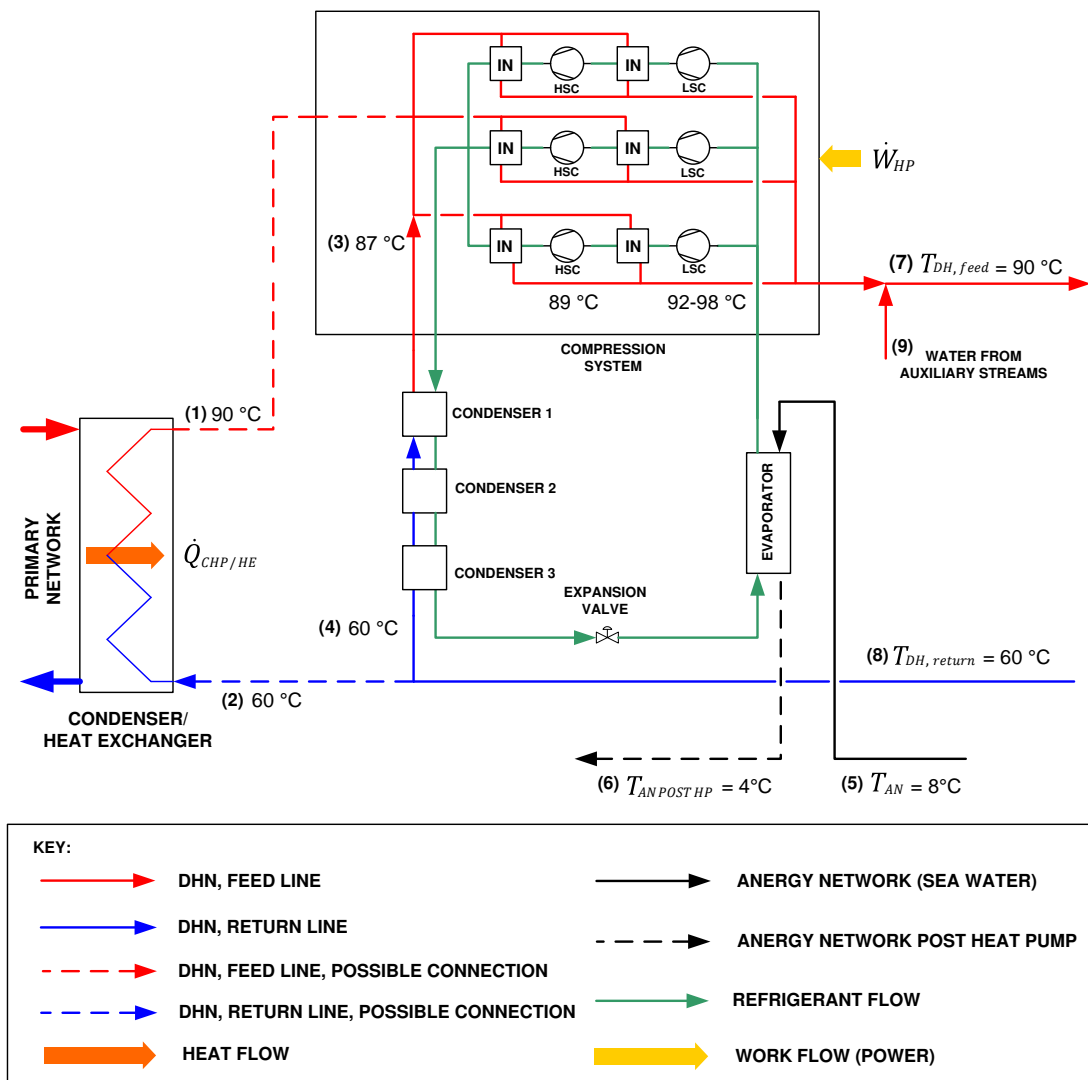
Figure 2.31: Possible configuration of Drammen heat pump, not specified in the article [45]. Acronyms used: IN = Intercooler, HSC = High Stage Compressor, LSC = Low Stage Compressor

As shown in the previous figure (2.31) The system heats return district heating water flow (4) from 60 to 90 °C through 3 stages: 60 °C to 69 °C, 69 °C to 78 °C and 78 °C to 87 °C.

After the main flow has been heated to 87 °C (3), it is split into three streams going through the high stage desuperheated for each of the systems. Temperature is raised to 89 °C. Besides the main DH water flow there are separate streams crossing subcoolers, high stage and low stage oil coolers and intercoolers, which are used to cool the superheated gas from the low stage compressors before entering the high stage compressors.

After compression system, the main DH stream at 92-98 °C is mixed with the water from all auxiliary streams obtaining the final DH feed stream at 90 °C.

In this installation, the heat pump is the only device in operation and it is not connected to any other thermal energy source, such as a CHP plant or other process. That is why streams 1 and 2 are represented as discontinuous lines.

2.2.1.2 Source - Demand (SD)

Figure 2.32: Source-Demand Configuration. With $T_{DH,feed(under\,demand)}$ as the DHN water temperature = 60 °C, used for hot water production.

In this kind of system 2.32, in contrast with the previous configuration, the heat pump has no connection with the DNH, although both systems usually operate together. Therefore, it is possible to utilize the heat pump as a heat source to produce domestic hot water for consumption (DHW) (stream 3, $T_{DH,feed\,(under\,demand)}$), and leave the DHN as a high temperature thermal source used only for heating service (stream 1). Furthermore, there are several cases in which this configuration is used for direct room heating, so that the air inside the room is directly heated by the heat pump, whose AN is the external air (stream 5).

Temperature is increased by the heat pump following the expressions:

$$\Delta T_{DH,(sink)} = T_{DH,feed\,(under\,demand)} - T_{AN} \tag{2.23}$$

$$\Delta T_{AN,(source)} = T_{AN} - T_{AN\,POST\,HP} \tag{2.24}$$

$$\Delta T_{HP} = T_{DH,feed\,(under\,demand)} - T_{AN} \tag{2.25}$$

This is the typical configuration for individual commercially available heat pump installations in dwellings. Air source heat pumps are commonly used here. Those are simple structure devices with low initial installation costs, so that users can buy them easily and do their own individual heating installation. They are so popular in the market, but only worthwhile for $COP_{HEAT\,PUMP} \geq$ 3. This is only worthwhile for places with mild winters, where external air temperature is not too low and more or less constant during the year.

There are several projects following this configuration. The first one to be referred here is the Air Source Absorption Heat Pump (ASAHP) of Beijing, described below [90]:

- General Information:

    - Four Cities considered: Shenyang, Beijing, Shangai and Guangzhou.
    - Served Population: 60878 habitants.
    - Thermal Capacity: 14 MW
    - Annual generation: 67 GWh
    - Project of Tsinghua University, Beijing, China.

- System Characteristics:

    - In this study an ASAHP is implemented linked to a DHN to produce heating/hot water to the users. As the paper shows, colder cities like Shenyang and Beijing use the system for heating, while warmer cities like Shanghai or Guangzhou, for domestic hot water.
    - Several refrigerants used depending on the metheorology of each city and their outside temperature. Shenyang, Beijing and Shanghai use $NH_3/LiNO_3$. Guangzhou require $LiBr/H_2O$
    - Heat source (AN): ambient air, with different average temperatures and variations depending on the city and the period of the year
    - Different efficiencies depending on the city:
        * $COP_{HP\,Shenyang} = 1.42$
        * $COP_{HP\,Beijing} = 1.49$
        * $COP_{HP\,Shangai} = 1.62$
        * $COP_{HP\,Guangzhou} = 1.77$
    - Operating conditions:
        * Generator stage: $T_{DH,feed} = 130$ °C, T difference in generator = 10 °C, Heat load = 331.5 kW
        * Condenser stage: $T_{DH,feed\,(under\,demand)} = 45$ °C, T difference in condenser = 5 °C, Heat load = 146.7 kW
        * Absorber stage: $T_{DH,return} = 35$ °C, T difference in absorber = 5 °C, Heat load = 353.3 kW
        * Evaporator stage: T_{AN} (external air) = Differs in different regions, T difference in evaporator = 10 °C, Heat load = 165.3 kW
        * Solution Heat Exchanger (SHE): Efficiency = 80 %, Heat load = 359.1 kW

∗ Mechanical work: Hydraulic pump = 3.2 kW, fan = 3.5 kW
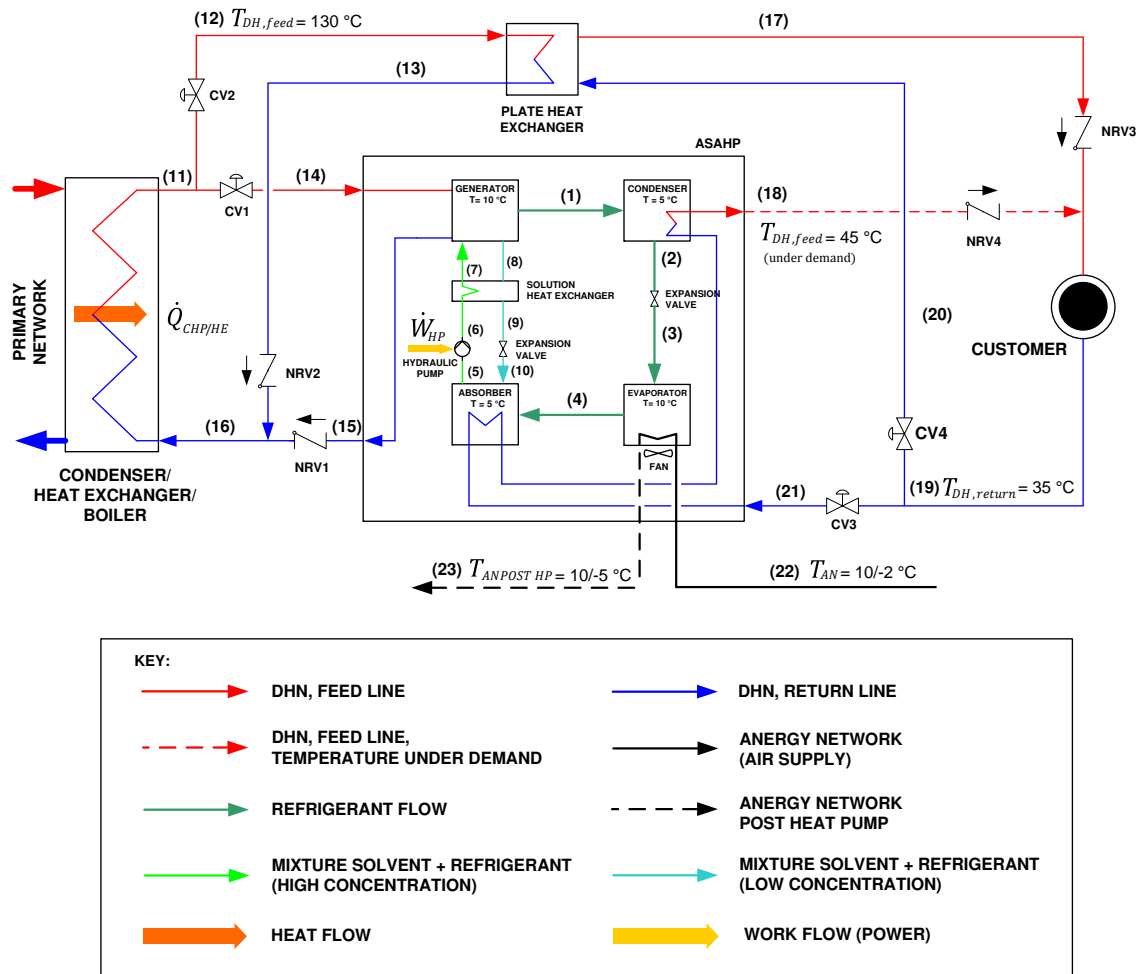
Figure 2.33: Diagram of the ASAHP integrated with a DHN, as explained in article [90]. Acronyms used: ASAHP = Air source absorption heat pump, CV = Control valve, NRV = Non-return valve.

The main motivation of this project is the use of a heat pump that makes the role of the substation, although there is still a parallel connection with the main DHN through a plate heat exchanger. This design ensures the supply of heat to consumers against possible failures in the main system.

The study tries to find out the reliability of the ASAHP system as a substitute for the DHN in different cities as well as the possible alternation in the use of both systems.

In this case, as shown in Figure (2.33), the heat provided to the DHN ($Q_{CHP/HE}$ comes from a coal-fired boiler (which is the most common technology used in China), leading to stream 16 (return DH) and 11 (feed DH). Stream 11 continues as stream 14 and it is sent to the heat pump, as the thermal energy source for the generator. Thus, this technology will not be totally independent from the DHN. Stream 21 comes stream 19 (return DH stream) exchanging heat with the absorber and the condenser, and therefore, increasing its temperature from 35 to 45 °C ($T_{DH,feed\,(under\,demand)}$) and sent to the customer, either for heating or for hot water production.

The refrigerant cycle inside the absorption heat pump works in the same way as a standard heat pump (streams 1, 2, 3 and 4, where the refrigerant circulates in vapour phase). In the absorber, the refrigerant in steam phase is mixed with the mixture solvent - refrigerant (stream 5) and driven by an hydraulic heat pump (stream 7), whose power consumption is lower than a compressor. However, the generator stage needs heat to evaporate the refrigerant, leading to a dependence on the district heating network, as mentioned before.

The conclusions of this project can be summed up by the following statements:

- In Shenyang, the temperature level is very low, so the change between ASAHP and DH is relatively frequent and the utilization ratio is low. Heat pumps work intermittently in this case

- In Beijing, the external air temperature is greater, so switching from one system to the other is not frequent. There is a high improvement of the energy saving rate

- In Shangai, the ASAHP mode operates to produce domestic hot water during all the year, leading to a greater COP and increasing the energy savings rate to a 37 %.

The second one talks about the connection between a heat pump and a DHN, using a sewage water stream as anergy network [87]:

- General Information:

    - Place: Project of Tianjin University, Qin Huangdao (China)
    - Heating period = 152 days
    - T outdoor = -12 °C in winter
    - Total building area = 3038.78 m^2
    - heating area = 2698.42 m^2
    - cooling area = 1604.23 m^2
    - Total heating load = 337.8 kW
    - Total cooling load = 260.6 kW

- System Characteristics:

    - Heat source (AN): treated sewage water (secondary effluent)

        * $T_{AN,winter\,season)} = 10\,°C$
        * $T_{AN,rest\,of\,the\,year)} = 20 - 22\,°C$
        * Concentration of suspended solids = 30 mg/l
        * Mass flow of the secondary effluent = 5000 t/h.

    - $T_{DH,feed(under\,demand)} = 50\,°C$
    - $T_{DH,return)} = 40\,°C$
    - Heat Pump unit:

∗ Number of heat pumps: 3 units

∗ Model: RHSBW140HM, (semi-hermetic screw modular chiller)

∗ Cooling capacity = 141 kW each

∗ Heating capacity = 161 kW

∗ Motor power = 30.1 kW

∗ COP_{HP} = between 3.5 - 4.5 in winter

∗ Compressor: high powered semi hermetic compressors

∗ Heat exchangers: brazed welding plate heat exchangers made of stainless steel
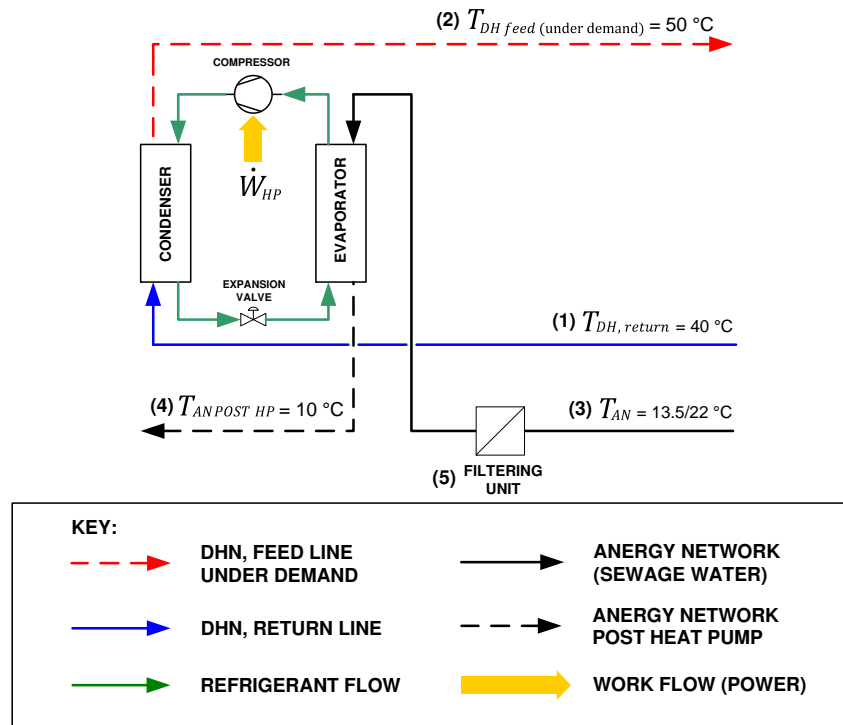
Figure 2.34: Simple diagram for Quin Huangdao's Heat Pump, as explained in article [87].

As shown in Figure 2.34, this kind of heat pump generates a LTDHN (streams 1 and 2), further used only for DHW production . There are two kinds of sewage heat source pump systems:

1. Untreated sewage water: This is an interesting option since an accessible, stable and totally available heat source, like sewage water is used for local heat pumps. The biggest problem with this technique is the high concentration of suspended solids in this kind of water, which could clog the heat exchanger.

2. Treated sewage water: This is the actual case for this project, in which the treated water from a WWTP (Waste Water Treatment Plant) is used at constant temperature and a large supply is guaranteed. However, WWTP facilities are usually located so far away from the users, which means long pipeline installations to transport the water.

Anyway, in order to avoid possible inconveniences with suspended solids inside the equipment, there are 2 filters around the submersible pump (5), the first one has a 40 item filter frame, the second one is even narrower, with a 60 item filter frame.

It is assumed that the secondary effluent (streams 3 and 4) enters directly into the heat pump's evaporator, rather than trough another intermediate heat exchanger for two reasons; first one, the temperature of the secondary effluent is relatively low in winter, and it will be even lower if crosses another heat exchanger, leading to a possible freeze of the evaporator; second one, the mentioned filters ensure that no suspended solids can cross through the heat pump device.

The heat pump consists on 3 semi-hermetic screw modular chillers divided into a main unit and two sub-units. They can operate together or independently. The running time of three units is balanced, guaranteeing the same running time.

The paper refers to a control system to change heating/cooling operation modes through a system of valves that switch depending on the season (for more information see section 2.1.2.2)

The third example is similar to the previous one, but in this case, there is a special type of heat exchanger adapted to obtain heat from sewage water streams [91]:
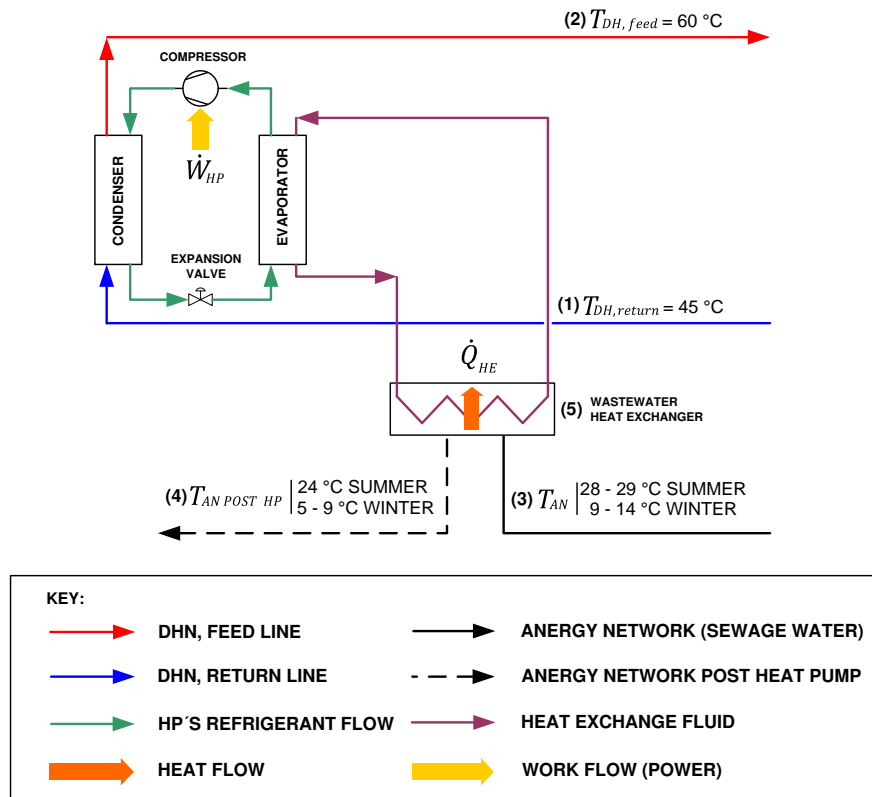
Figure 2.35: Simple diagram for Izmir's Heat Pump [91].

- General Information:

    The article focuses on a special kind of heat exchanger, which can locally use sewage water as a heat source for heat pumps installed next to individual buildings, providing heat for heating and DHW. The waste water has the following characteristics:

$T_{WASTE\,WATER,winter}$ = 9-14 °C

$T_{WASTE\,WATER,summer}$ = 28-29 °C

Based on the diagram (2.35), The system constituted by the heat pump and the domestic hot water network follows three configurations:

1. Monovalent: The heat pump system works alone without any supplementary heating

2. Bivalent: Although the heat pump continues as the main system in operation, a supplementary heating equipment (boiler) is added. It will operate only for extreme cold days or if the heat pump is under maintenance.

3. Multivalent: Installation in tandem (Parallel) with the support boiler and a cogeneration engine system (see 2.1.2.1.4, which will provide power to heat pump and to the building users. It is recommendable for large buildings. Also for isolated places or difficult areas, where a DHN or electrical network connection is not possible (see 2.1.1).

In the last example the complexicity grows due to the introduction of a solar thermal system complementing the anergy flow to the heat pump [93]:

- General Information:

    - Place: Experimental set-up system designed and constructed in an efficient building located in the Solar Energy Institute of Ege University, Izmir, Turkey

    - The use of solar energy has considerable interest for 2 reasons; first, it leads to decrease of fossil fuel consumption, second, solar energy is a non-polluting source of energy.

    - The building is positioned towards the south along a south - north orientation.

- System characteristics:

    - Ground coupling circuit:

        * Vertical-single U-bend type heat exchanger; material: poliethylene, drilling depth = 50 m

        * Brine circulating pump; Type: KPM 50; range of volumetric flow rate: 0.36-2.4 m^3/h ; pressure head: 41-8 m of water column, power: 0.37 kW; speed: 2800 rpm

        * Expansion tank; Type: 541 l; capacity: 12 l; precharge: 1 bar

    - Heat Pump:

        * Heat exchanger - condenser (heating mode): model: CB 26-24; capacity: 6.66 kW

        * Heat exchanger - evaporator (heating mode): model: CB 26-34; capacity: 8.2 kW

        * Compressor: Type: hermetic; reciprocating; model: TFH 4524 F; volumetric flow rate: 7.5 m^3/h; speed: 2900 rpm; the rated power of electric motor driving: 2 HP (1.4 kW); refrigerant: R-22; capacity: 4.134 kW; evaporating/condensing temperatures of 0-45 °C

- Water circulating pump: Type: KPM 50; range of volumetric flow rate: 0.36-2.4 m³/h; pressure head: 41-8 m of water column, power: 0.37 kW; speed: 2800 rpm

- Solar Colector: 1.82 m^2, flat-type
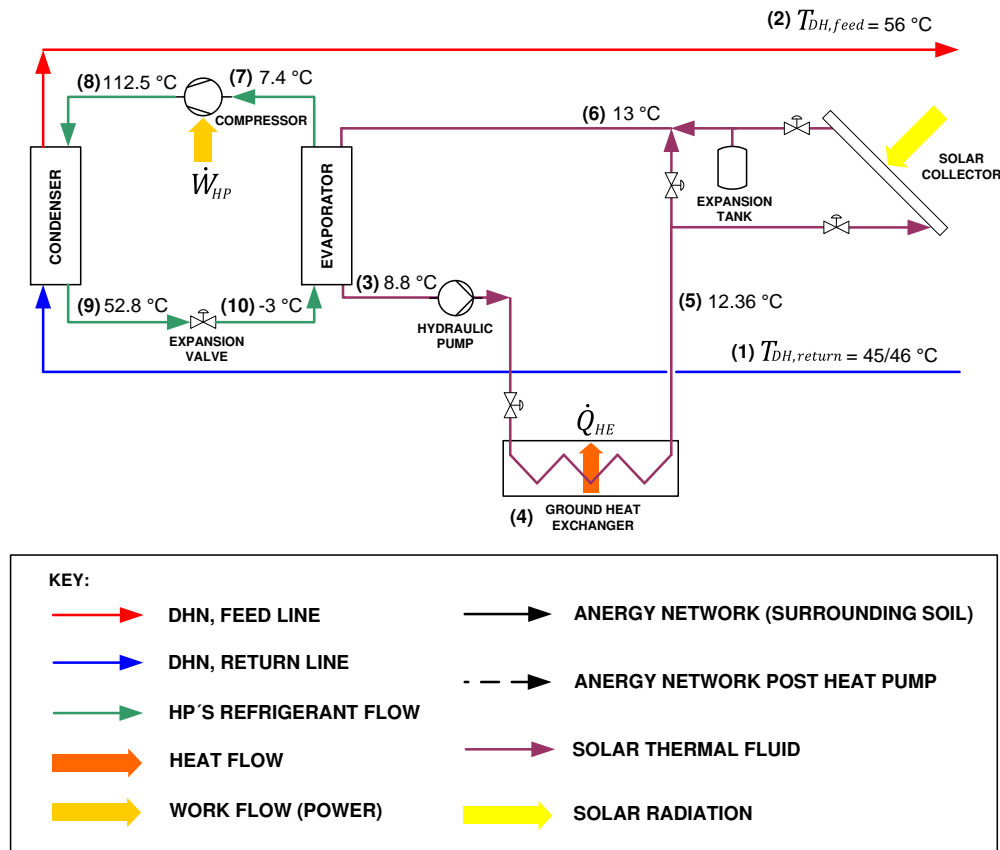
Figure 2.36: Diagram of the solar assisted ground-source heat pump, explained in the article [93]

Looking at the process shown in the previous figure (2.36), there are three visible cycles: The first one is the solar thermal cycle, in which the thermal fluid (stream 3) circulates extracting heat from the ground (4) and from the thermal solar collector (6), increasing its temperature from 8.8 to 13 °C (stream 6). Brine fluid is the liquid flowing through this circuit. The second one is the refrigerant cycle of the heat pump, which is able to increase DH water from 45 to 55 °C. The temperature increase is not so high, but enough to provide a DHW for comsumption in a self-sufficient system moved entirely by renewable sources.

Before closing this section, Hepbasli's work has to be mentioned [92]. It shows a very similar design, but without the solar collector.

2.2.1.3   Source - Return (SR)
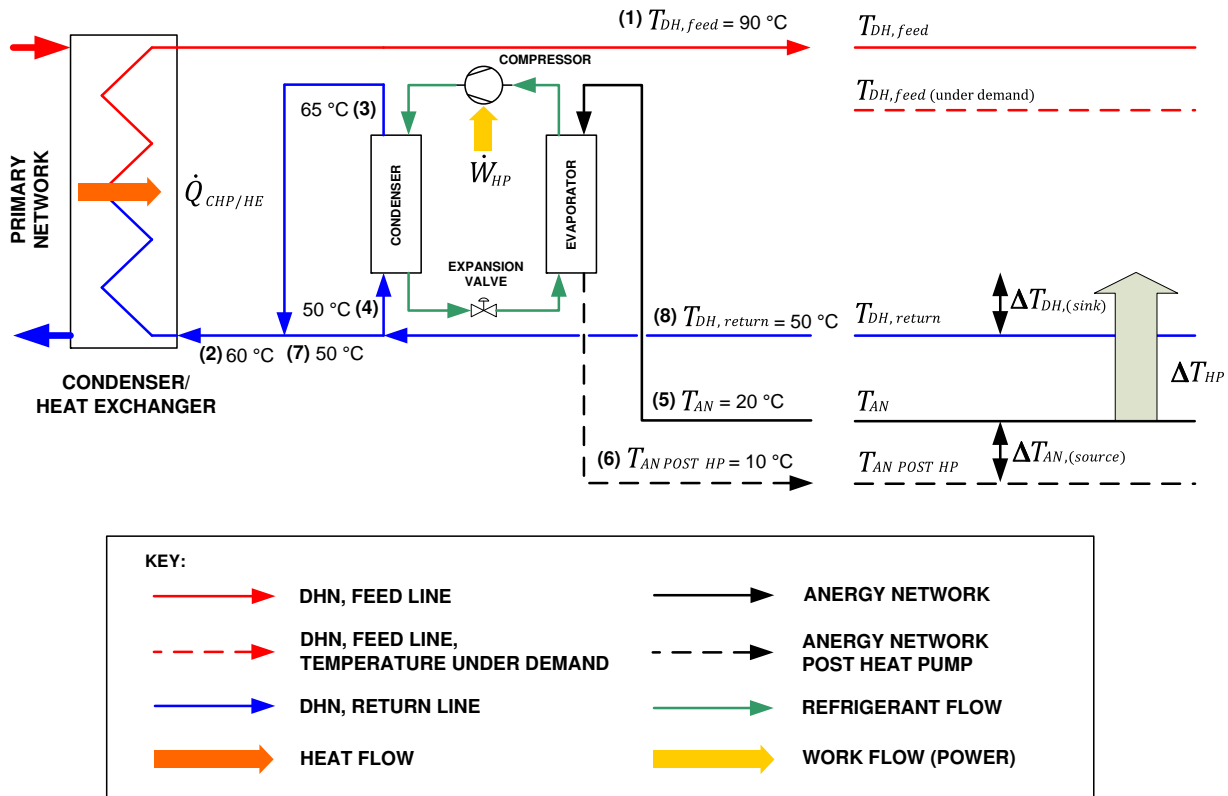
Figure 2.37: Source-Return Configuration

As it appears in the scheme 2.37, the heat pump can be used to preheat the return line of the DHN (stream 8, ramified into stream 4 and 7 afterwards) before entering the CHP plant or the GUFO sub-station (stream 2), thus, ΔT_{HP} is significantly lower compared to SF configuration, which increases heat pump's COP. This will reduce condenser's heat flow ($\dot{Q}_{CHP/HE}$) and therefore, the efficiency of a theoretical CHP plant connected to the DHN due to the increasing condensing temperature. Thus, SR is the best modality to generate a LTDHN with a good COP, but not the best idea for power generation in the CHP plant.

The following expressions are defined:

$$\Delta T_{DH,(sink)} = T_{DH,return\ after\ HP} - T_{DH,return} \tag{2.26}$$

$$\Delta T_{AN,(source)} = T_{AN} - T_{AN\ POST\ HP} \tag{2.27}$$

$$\Delta T_{HP} = T_{DH,return\ after\ HP} - T_{AN} \tag{2.28}$$

Therefore, it can be affirmed that this configuration requires the use of another generation technology, in order to increase $T_{DH,feed}$.

Only one example of this type of system has been found. It is the project of Chungnam [98], consisting of a experimental setup consisted of a two-stage compression heat pump system linked to a DHN:
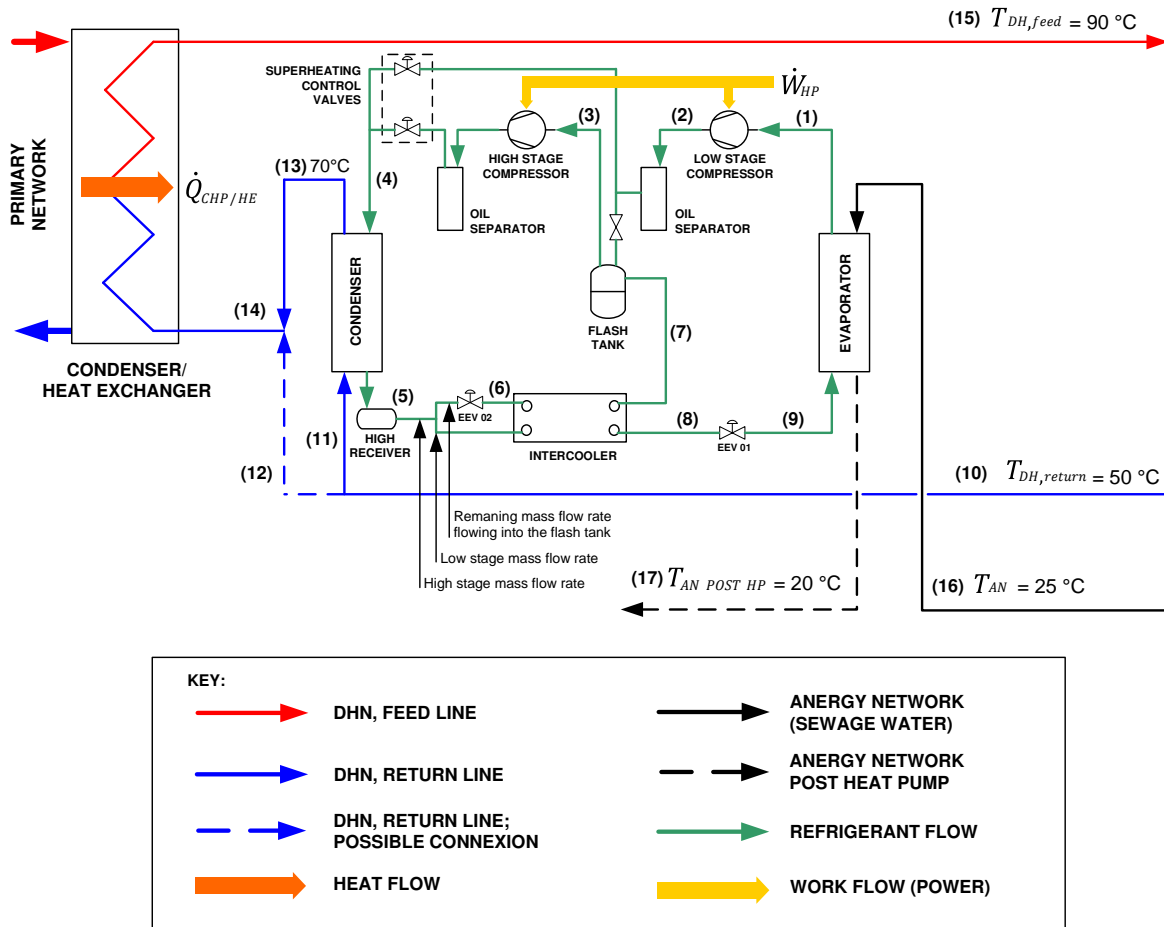
Figure 2.38: Experimental setup of the two-stage compression heat pump system of Chungnam [98]. Acronyms used: EEV = Expansion Valve

- General Information:

  - Place: Not specified. Probably Chungnam (Republic of Korea)
  - Project supported by The Korea Institute of Energy Technology Evaluation and Planning (KETER)

- System characteristics:

  - Heat source (AN): Heat comes from several sources, like WWTP, industrial waste heat, subway waste heat, etc. In general, $T_{AN} = 25\,^{\circ}\mathrm{C}$
  - $T_{DH,feed} = 70\,^{\circ}\mathrm{C}$
  - $T_{DH,return)} = 50\,^{\circ}\mathrm{C}$
  - Heat Pump:
    * Refrigerant used: R-134a

* Heat exchanger - condenser: plate type, 41 kW
* Heat exchanger - evaporator: plate type, 30 kW
* Heat exchanger - intercooler: plate type, 8 kW
* Two-stage compression system; Compressor: one-stage, scroll type, 25 kW; Compressor: two-stage, scroll type, 17 kW
* Flash tank: Material SUS 304
* Expansion device: Low stage expansion valve, EEV type, 34kW ; High stage expansion valve, EEV type, 10kW

Basically, the system utilizes waste energy as a heat source for the heat pump's evaporator, receiving the anergy flow (Figure 2.38, streams 16 and 17), increasing refrigerant's temperature (stream 1). Just after that, the refrigerant flow passes through the low stage compressor (stream 2) and it is discharged to the flash tank, forming two phases. The two phase refrigerant coming from the intercooler is mixed with the superheated refrigerant in the flash tank and enters the high stage compressor in a saturated vapour state (stream 3). Following this way, the overheating of the refrigerant is reduced, which is positive from the efficiency point of view.

After crossing the high stage compressor (stream 4), the superheated refrigerant is enters the condenser, exchanging heat and providing temperature to the return DHN stream (stream 13 and subsequently 14). Therefore, $T_{DH,return}$ is increased, reaching approx. 70 °C. The main heat exchanger, which thermally supplies heat to the DHN through another superior heat source on the other side (A CHP plant, boiler, or simply a high temperature network) makes possible the temperature increase of the DHN feed stream ($T_{DH,feed} = 90$ °C, stream 15).

Finally, the condensed refrigerant (stream 5) passes through the intercooler in a subcooled state, diverting a part of the flow into a high stage expansion device (EEV 2, stream 6), while the rest (streams 8) enters a low stage expansion device (EEV 01).

Once fully converted to liquid phase and reduced its pressure, the refrigerant arrives to the evaporator again, closing the cycle.

The system described is a good alternative to utilize efficiently the waste heat, gathering the different residual streams into one anergy flow. The higher the temperature of this flow, the greater the efficiency of the system.

2.2.1.4 Return - Forward (RF)

Figure 2.39: Return-Feed Configuration A. Acronyms used: CV = Control Valve

In this configuration, the heat pump uses the return line of the district heating network as a heat source, and the feed stream as a sink. Therefore, the return line is used directly as the anergy network.

There are two modalities for this configuration. In the first one (configuration A, Figure 2.39), the return DH line (stream 8) is divided in two branches. The first branch (stream 4) is heated in the condenser (stream 3) and joins the feed DH line (stream 1) afterwards, resulting in stream 7. The second branch continues its way entering the evaporator (stream 5). Stream 9 is only open if the heat pump is not operating (valves CV1 and CV2 are used control the direction of the flow). Therefore, the following expressions are defined:

$$\Delta T_{DH,(sink)} = T_{DH,feed} - T_{DH,return} \tag{2.29}$$

$$\Delta T_{AN,(source)} = T_{DH,return} - T_{DH,return\ post\ HP} \tag{2.30}$$

$$\Delta T_{HP} = T_{DH,feed} - T_{DH,return} \tag{2.31}$$

In the same way as in the SF configuration 2.2.1.1, the heat pump does not increase DHN temperature, it simply heats a part of the return DH line in another way, using electrical energy and the

aforementioned anergy source. In the end, some power is introduced in the system and used to heat a part of the DHN flow.
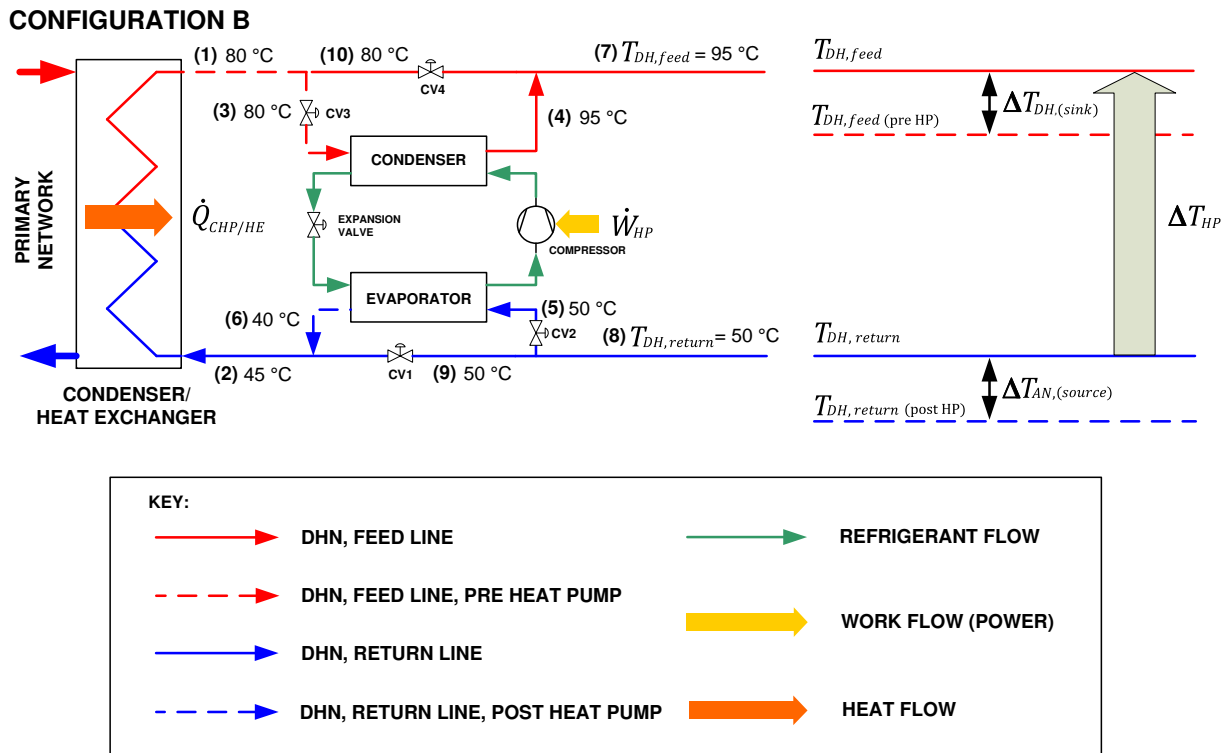
Figure 2.40: Return-Feed Configuration B

The second one 2.40 lies in, again, using the return DH flow (stream 8) as the anergy source for the evaporator of the heat pump (stream 5), decreasing $T_{DH,return}$, and in turn using the energy of the condenser to raise the temperature of the feed DH flow (from stream 1 to stream 7)

In the same way as before, if the heat pump is not operating (due to maintenance, reparations or other reasons), control valves CV 1, CV 2, CV 3, and CV 4 are in charge of deviate the flow in the right direction avoiding the flow to enter the evaporator and the condenser.

As described in the temperature diagram in the figure 2.40 with this configuration, small temperature jumps are achieved in both condenser and the evaporator devices, which makes the overall heat pump efficiency greater. In addition, in the case of a CHPP-DHN-HP system, the reduction of $T_{DH,return}$ caused by both configurations is considered a positive for the condensation process in the condenser of the CHP plant.

The following expressions are obtained:

$$\Delta T_{DH,(sink)} = T_{DH,feed\,pre\,HP} - T_{DH,feed} \qquad (2.32)$$

$$\Delta T_{AN,(source)} = T_{DH,return} - T_{DH,return\,post\,HP} \qquad (2.33)$$

$$\Delta T_{AN,(source)} = T_{DH,feed} - T_{DH,return} \tag{2.34}$$

No clear examples following this configuration were found, however, some scenarios proposed in section 3.3 will be based on configuration B.

2.2.1.5 Return - Demand (RD)
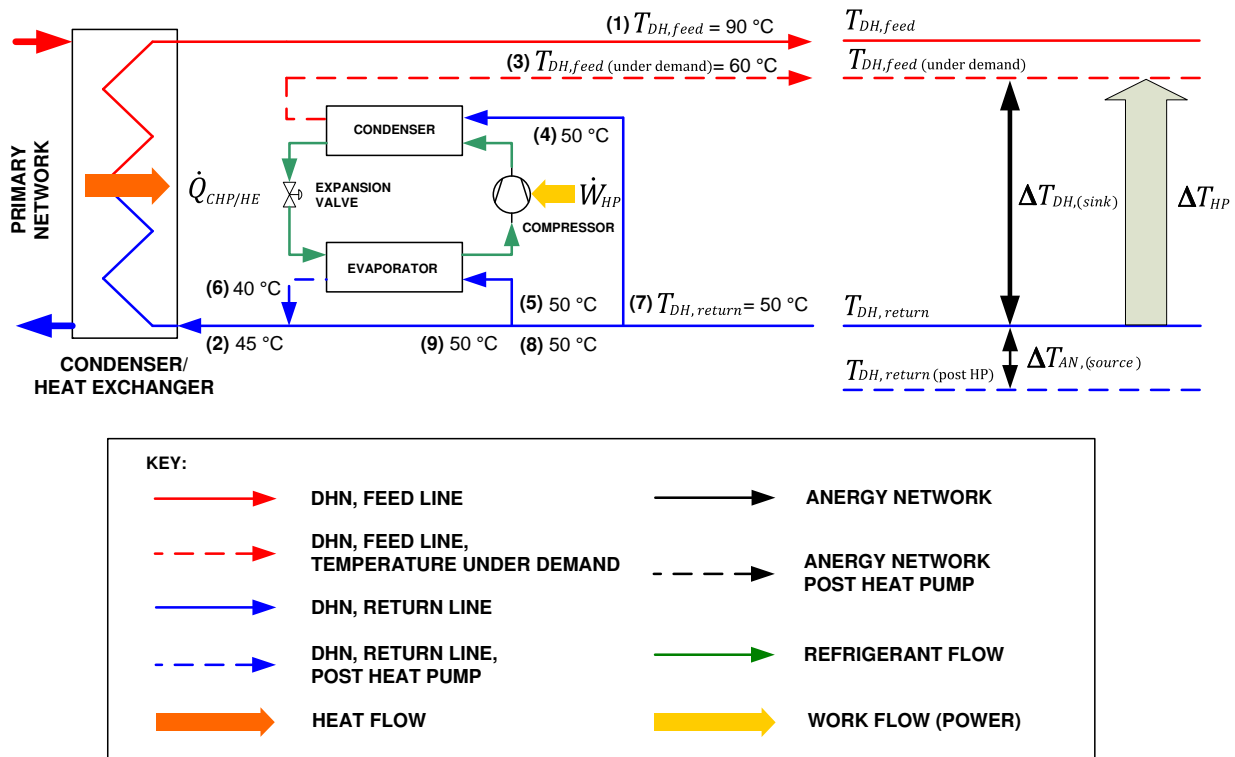
Figure 2.41: Return-Demand Configuration. With $T_{DH,feed(under\,demand)}$ as the DHN water temperature = 60 °C, usually used for hot water production

The kind of installation is very similar to SD (see 2.2.1.2), and also widely used inside residential buildings and large neighborhood communities. In fact, the example that will be described later [97] analyzes different schemes of this configuration. The main difference comes from the anergy network, which is not a flow coming from outside, but the DHN itself.

The article describes the different possible combinations between a LTDHN at 40 °C and the heat pumps, in order to increase locally the temperature to 55 °C or even more only where it is necessary.

- General Information:
    - The simulation, as well as the energy demand calculation, is based on the Danish Building Regulations for low energy buildings. Engineering Equation Solver (EES) is used.

- – The analysed single family house has a heated area of 159 m², thus the energy frame is 36.3 kWh/m².

- – Space heating demand = 2570 kWh/year

- – DHW demand: 2083 kWh/year

- – Power consumption: 525 kWh/year

- – Total energy consumption: 5178 kWh/year

- System characteristics:

  - – LTDHN:

    * $T_{LTDHN,feed}$ = 40 °C
    * $T_{LTDHN,return}$ = 25 °C
    * $DHW\ flow_{VARIANT\ A)}$ = 85 l/h
    * $DHW\ flow_{VARIANT\ B)}$ = 50 l/h
    * $DHW\ flow_{VARIANT\ C)}$ = 75 l/h

  - – Heat Pump:

    * Heat source (AN): return branch of the LTDHN
    * Refrigerant used: R-600a
    * Heat exchanger - condenser: pinch temperature = 2.5 K
    * Heat exchanger - evaporator: pinch temperature = 2.5 K
    * Heat exchanger for DHW: pinch temperature = 2.5 K
    * Compressor: Isoentropic efficiency = 50 %
    * $COP_{HP\ VARIANT\ A}$ = 5.3
    * $COP_{HP\ VARIANT\ B}$ = 3.5
    * $COP_{HP\ VARIANT\ B}$ = 5
    * $W_{HP\ VARIANT\ A}$ = 142 W
    * $W_{HP\ VARIANT\ B}$ = 214 W
    * $W_{HP\ VARIANT\ C}$ = 155 W

  - – Storage tank: Stratified tank, used as a reservoir able to provide domestic hot water all the time at constant temperature, covering peak consumption loads.

    * Peak consumption load = 32.3 kW
    * $V_{STORAGE\ VARIANT\ A}$ = 128 l
    * $V_{STORAGE\ VARIANT\ A}$ = 128 l
    * $V_{STORAGE\ VARIANT\ A}$ = 100 l
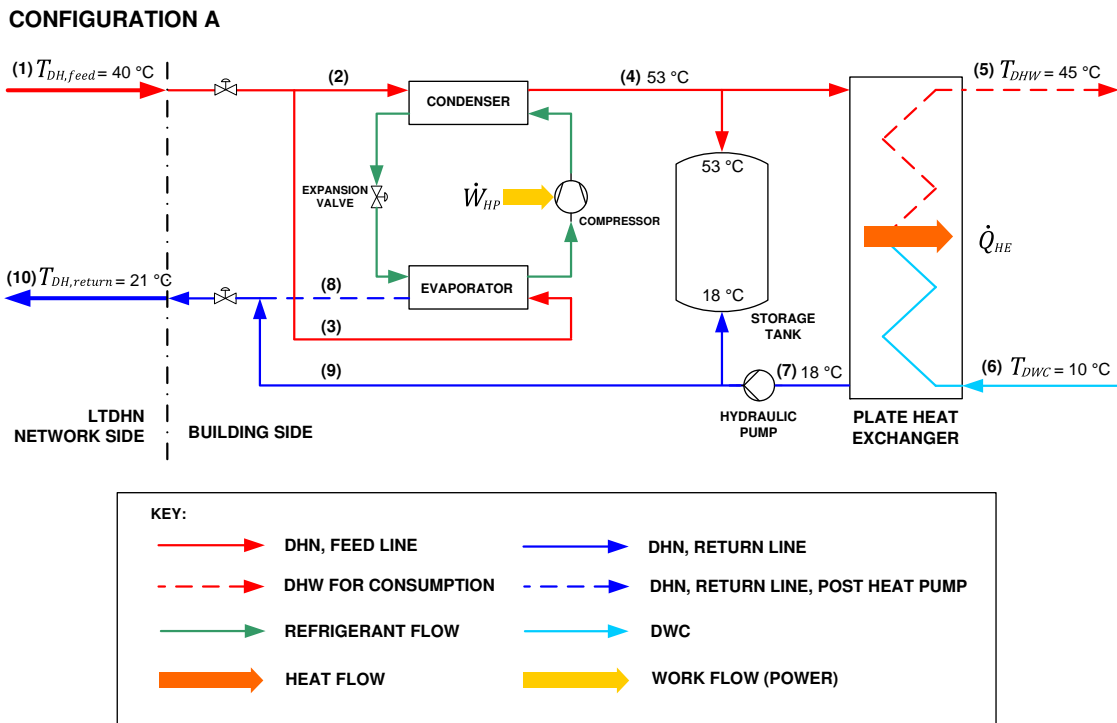
CONFIGURATION A

Figure 2.42: Microbooster heat pump in combination with the DHN, Configuration A [97]. With DWC = Domestic Water for Consumption and T_{DWC} as the DWC temperature = 55 °C
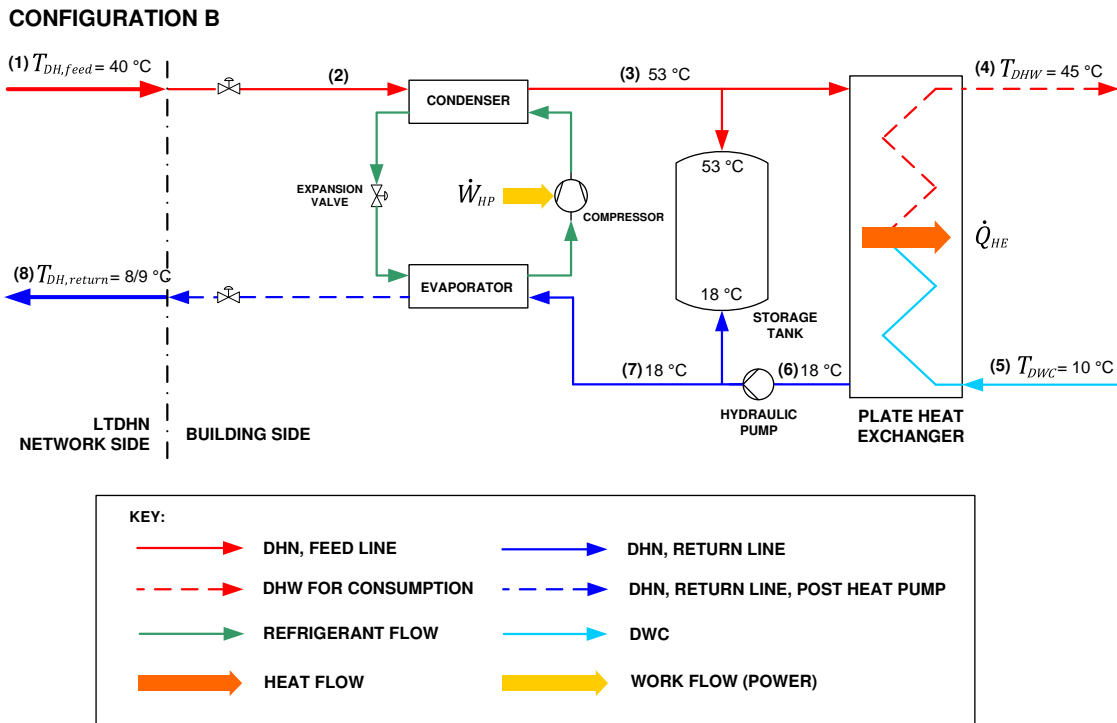
CONFIGURATION B

Figure 2.43: Microbooster heat pump in combination with the DHN, Configuration B [97]
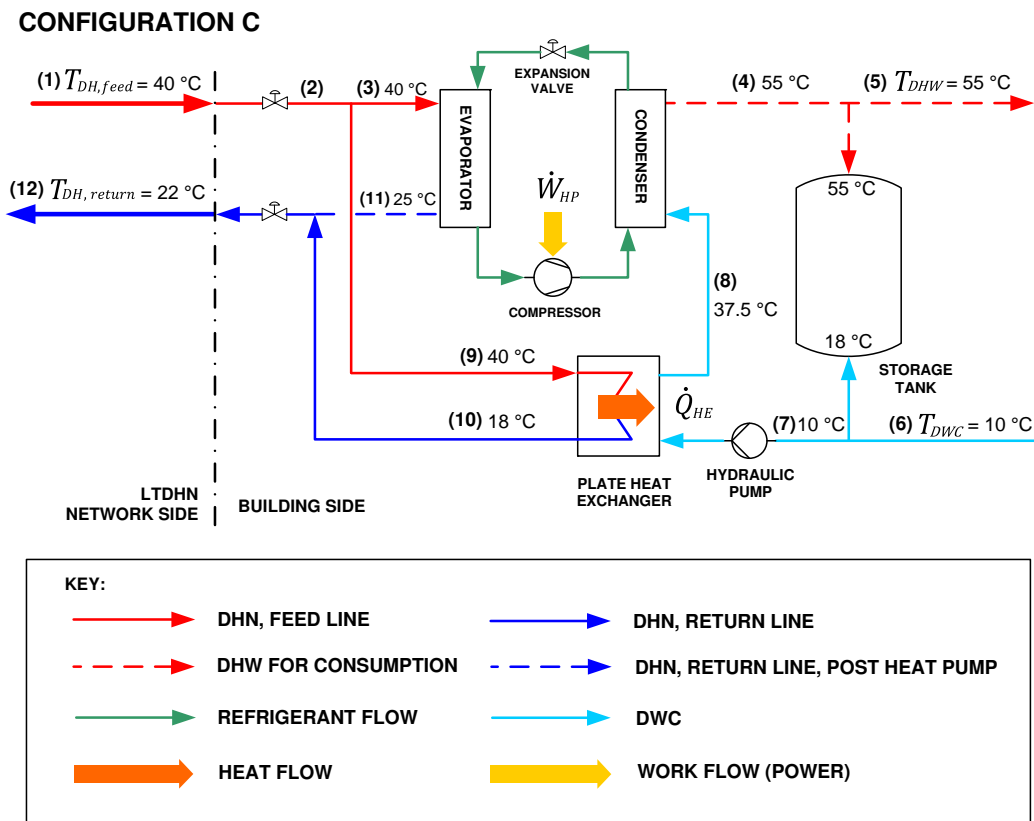
CONFIGURATION C

Figure 2.44: Microbooster heat pump in combination with the DHN, Configuration C [97]

The objective of this work is to simulate the behavior of a microbooster heat pump for DHW production in combination with an external LTDHN. The problem is, that $T_{LTDHN,feed} = 40\,°C$, which is not enough to comply with the European Legionella regulation, which establishes a minimum DHW temperature of 55 °C [101] [102]. The function of the heat pump consists of heating the water rapidly, raising its temperature to the required 55 °C. This work brings several innovations, like configurations A and B (Figures 2.42 and 2.43), where the drinking water is not stored but is directly heated, crossing the heat exchanger and avoiding the risk of Legionella. There is a third configuration (Figure 2.44), in which the DWC is heated through the heat pump's condenser and stored later. Whatever the configuration used, the heat pump is switched on from the start of the tapping sequence until the refilling of the stratified tank. Therefore, the system needs a special type of heat pump, called "Microbooster" which is adapted for this intermittent operation mode.

Design A is the most efficient option for further development. It represents the best way to combine and integrate a heat pump with a LTDHN.

All contents explained during this sub-section were an inspiration source to define the working scenarios reported in this PhD thesis, located in section 3.3.

2.3 Modeling of District Heating Networks and Exergy analysis

Throughout this section the most common methodologies for modelling thermohydraulic networks and carry out exergy analysis are explained. Several methods used in previous projects carried out at the Institute of Energy Systems and Thermodynamics of TU Wien are emphasized, from where this doctoral thesis is being developed. Likewise, there is a compendium of well-known softwares which are commonly used for this purpose in general projects and studies. Subsequently, a summary of other works, articles and projects is described. All this information constitutes a basis from which a work methodology will be further described in section 5.

2.3.1 About the models

Before going deep into the topic and understanding the different methods for modelling DH networks, an introduction is needed, in order to understand what is a model, what is it used for, and the different types of existing models.

A mathematical model is an approximation of a certain process (physical, chemical, thermodynamic, economic ... etc) through one or several equation systems that relates all the process variables. A model helps to understand the process behaviour and respond to certain questions, no need of the process to be in operation.

In general, a mathematical model allows to predict the output values depending on the changes produced in the process or in the input variables.

There are different types of models depending on the process to be analysed and the objectives of this analysis:
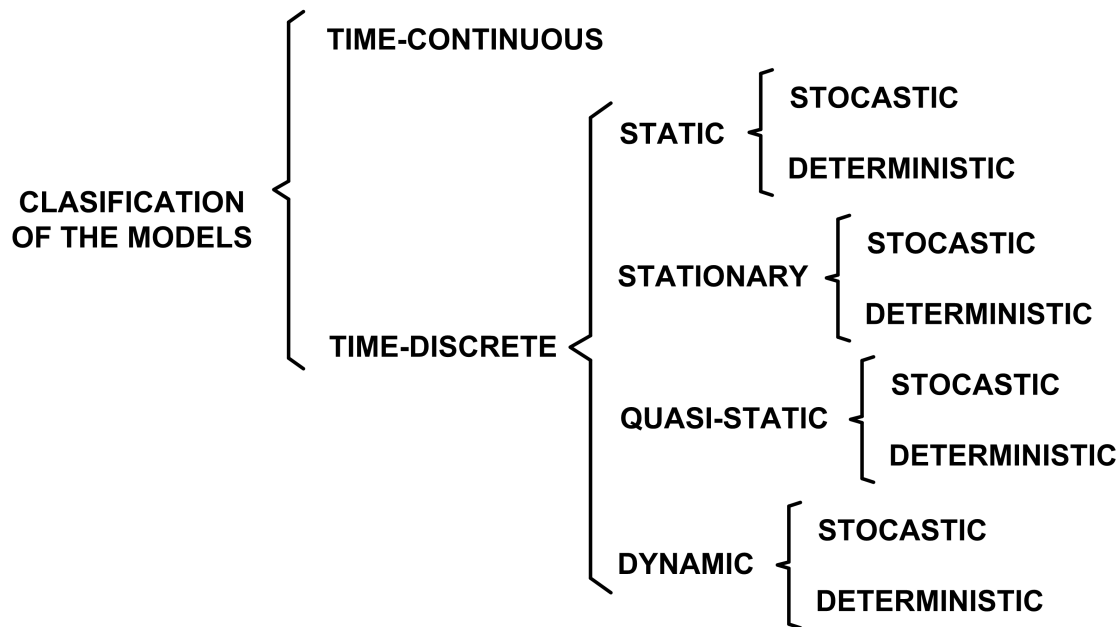
Figure 2.45: Classification of the models

- Time-continuous models

Output variable (E)

System output = E = f(t)

t
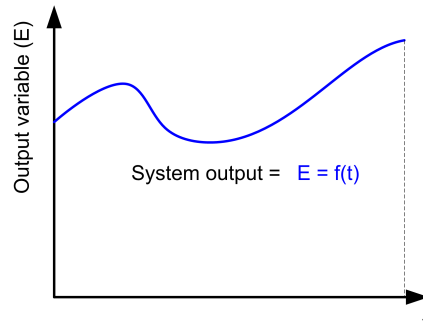
Figure 2.46: System output in a time-continuous model

In this kind of models, the state of the output variables changes continually as a function of time. Those output variables constitute the system response, and can be obtained using a deductive mathematical method. Therefore, the system's response will be a function of time.

- Time-discrete models

Output variable (E)

System output = E = f(nt)

ΔT

t
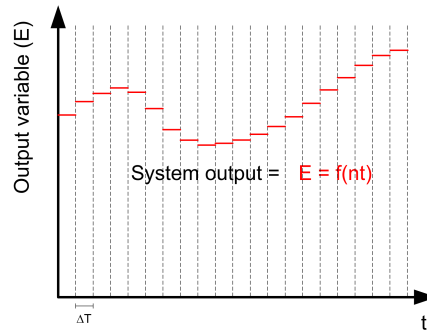
Figure 2.47: System output in a time-discrete model

The state of the output variables of the system changes discreetly along the time. The response of the system is not a continuous function, which delivers a value for any instant of time, but for each defined time interval Δt, a value of the output variable is generated.

In this case, a numerical method is used to obtain the system response, that is, by means of computational procedures to solve the mathematical model.

- Static models

Output variable (E)

System output = E = f [t] (single value)

t
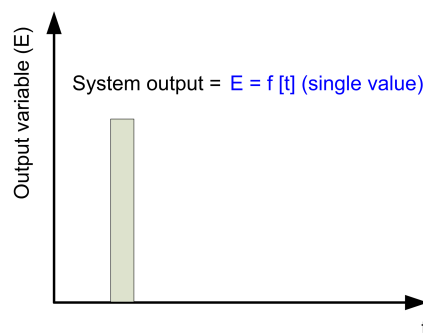
Figure 2.48: System output in a static model

The static model defines the state of the system at a specific time instant, in which the system is in equilibrium and the state of the variables does not change, therefore the time variable does not play a relevant role.

Example: Calculation of the height of the water level in a tank that receives a continuous flow of water from a tap, for a certain instant in the time.

- Stationary flow models
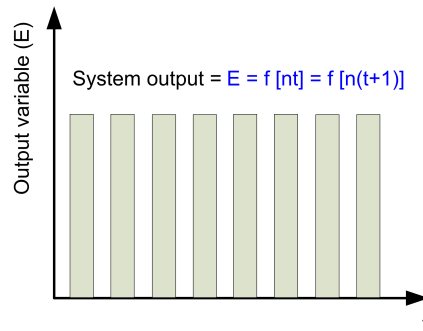
Figure 2.49: System output in a stationary model

The state variables at every point in the system remain constant with the time. There is no variation or modification of the initial values, neither any kind of accumulation (mass, heat) inside the system

Example: A steam turbine model working in steady-state conditions.

- Quasi-static models

In Quasi-static models, the output variables are changing along the time, so that the system output is not a single value but a family of values as a function of time. The model generates an output which is a response based on the received input value. This output is immediate, in such a way that there is no heat or mass accumulation in the system.

- Dynamic models
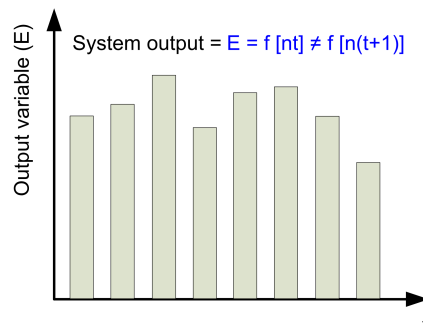
Figure 2.50: System output in a quasi-static and dynamic model

Again, the output variables are changing along the time, generating a family of values. Unlike Quasi-static models, the model reflects the possibility of mass or energy accumulation in the considered system, giving rise to complex resolution methods to solve the proposed equations system (usually differential equations as a function of time).

Example: evolution of the water level in the same tank along the time. In this case, the input flow of water changes during the time, generating a mass accumulation inside the recipient.

- Stochastic models
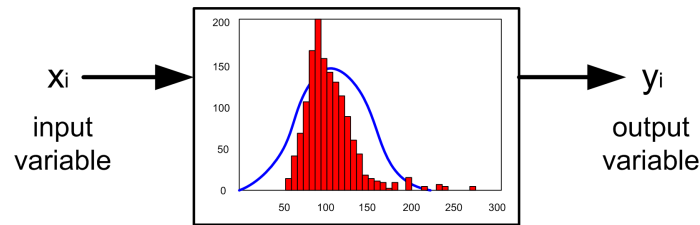
Figure 2.51: Stocastic model

In stochastic models, the value or state of the variable in the next time instant can not be determined from data of the current time instant and the initial conditions established. To solve this type of models and calculate the output variable, statistical and probability studies are used to predict the system response.

Example: predict the tendency of the stock market.

- Deterministic models
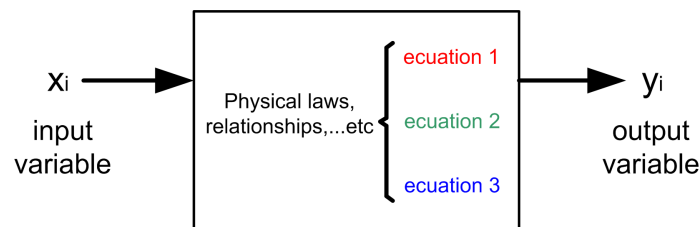
Figure 2.52: Deterministic model

In deterministic models, the value of the variable in the next time instant can be determined from previous data and the initial conditions. In this case, a numeric method is possible in order to calculate the output variable.

Example: Determination of the manufacturing time of a vehicle in an assembly line. All variables affecting the industrial process are known (input of raw materials, manpower involved in the process, production time, robotics, maintenance ... etc)

2.3.2   Modelling a hydraulic network

In this section, a general summary about the main existing methods for the modelling and simulation of thermohydraulic networks is exposed, including the equations to be presented and their subsequent resolution.

As already mentioned before, a district heating network is basically a hydraulic system in which the water is the heat transfer fluid that circulates through a general supply pipe which is divided in different ways towards each of the buildings. Once the heat is delivered, the district heating water

from the buildings is collected and returns to the substation or heat generation point. Once there, the water is reheated and pumped again, closing the cycle.

The three typical topologies in DH networks are the following:

(a) Tree Network   (b) Ring Network   (c) Meshed Network
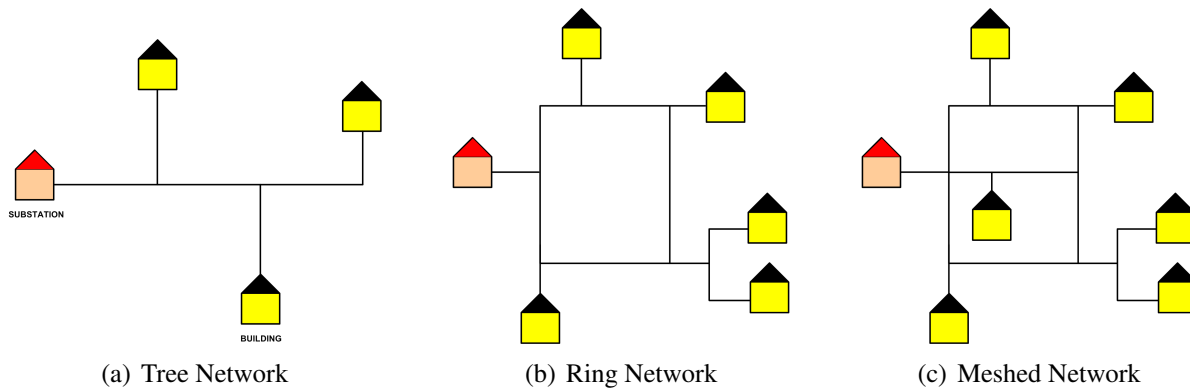
Figure 2.53: Topologies of DH networks

The most common topology is (c), especially in large networks, in which as the main pipes ramify, the complexity of the system increases. In the case of large networks, what usually happens is that a primary network is formed, usually with a ring shape, from which arise various sub-networks with a tree structure covering the different areas and neighbourhoods.

The hydraulic behaviour for a DH network is not so different to that one for any other conventional network. The main difference is based on the second branch which is necessary for the DH networks, in order to bring back the return DH water from the buildings to the substation.
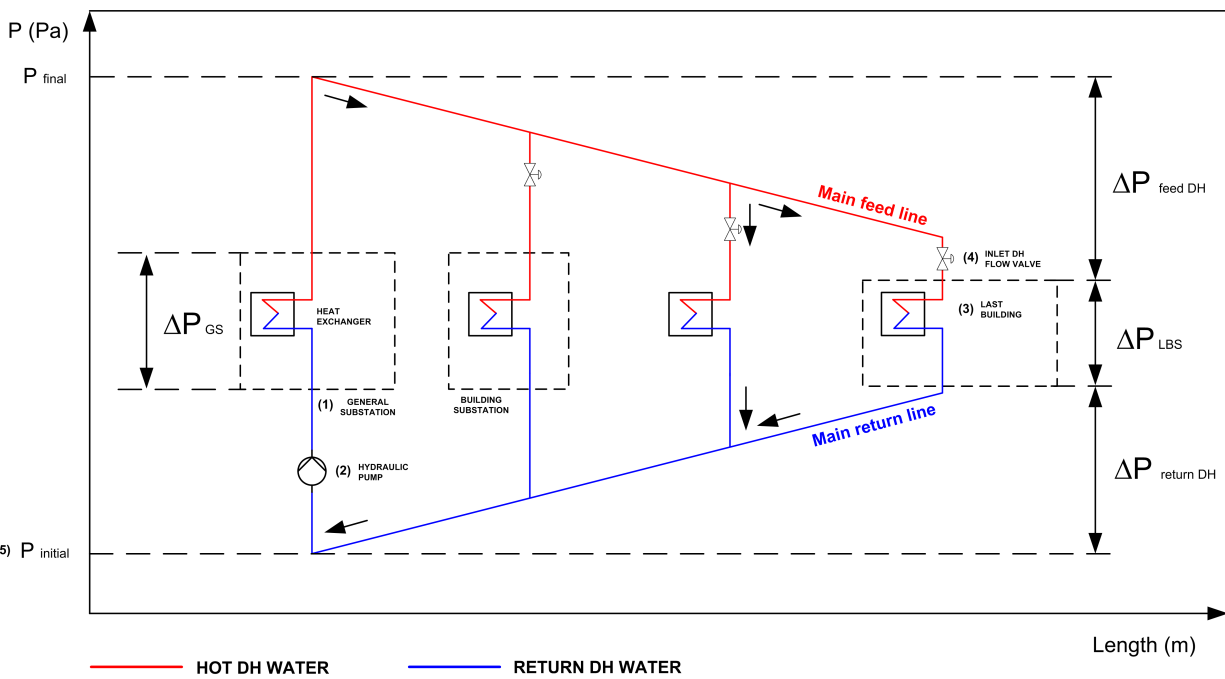
Figure 2.54: Pressure control in conventional DH Networks. Since P_{final} is the final pressure of the system, $P_{initial}$ is the initial pressure, ΔP_{GS} is the pressure losses of the general substation, ΔP_{feedDH} is the pressure losses of the DH feed line, $\Delta P_{returnDH}$ is the pressure losses of the DH return line, and ΔP_{LBS} as the pressure losses of the last building

In conventional DH networks the water pressure is controlled by a hydraulic pump placed just before the general heat exchanger located in the substation. In fact, it is common for both elements to be installed together within this place. As shown in figure 2.54, the hydraulic network is composed of two main branches, main feed line and main return line. They cover all the space from the substation (1) to the furthest building. Therefore, the hydraulic pump (2) has to supply enough pressure to overcome the charge losses for both lines, plus the pressure drop generated by both the general substation and the substation of the farthest building (3). In this way, the DH water enters each building just opening the control valve (4), and each building receives the necessary flow of DH water, therefore , the pressure drop generated by each building makes the return flow of DH water to exit the building and circulate in the right direction. The initial absolute pressure before the pump is fixed by a surge tank (5), which guarantees that the lowest pressure of the system is above the evaporation pressure of the DH water, avoiding cavitation. In addition, a surge tank is also used to remove the surplus of water from the system.

The calculation of the hydraulic network refers to the state of the network for each time step. The main variables are the following:

- Pressure

- Mass flow

- Temperature

In the next step, the hydraulic network should be organized into nodes and branches, in order to locate and estimate the variables correctly.
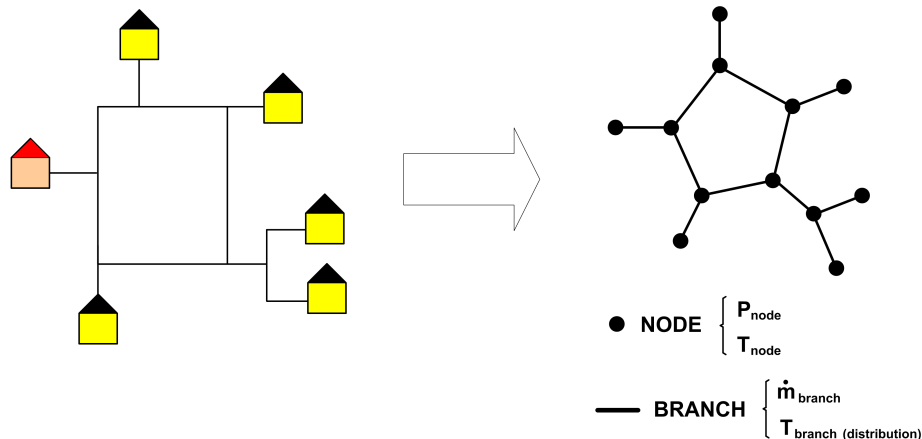
Figure 2.55: Node-Branch distribution, with the correspondent indicated variables

There are basically two types of methodology through which it is possible to model and simulate district heating networks, and in general all kind of hydraulic networks.

- General model:

    It is the main methodology based on the calculation of hydraulic networks and works well for any kind of network, without regard to the size. Determines the values of pressure, temperature and mass flow in all nodes (intersections) and branches of the network. It is

the most used procedure and constitutes the basis of the majority of commercial softwares available. On the other hand, it has a high complexity and requires significant computing resources to work properly.

This system is based on a mathematical representation of network's topology, called incidence matrix. Based on this instrument, it is possible to determine the relationships between the different flows circulating in the network, and based on these relationships, raise all pressure and mass balances, defining a equations system. After that, it is possible to obtain the energy balances in order to calculate temperatures, temperature losses and subsequently, the energy-exergy losses.

- Block-based model

  In this methodology, each of the elements of the network is represented by a block that receives the input variables and the necessary calculation parameters, and generates the output variables.

  For example, in case of a pipe, the corresponding block would look like this:
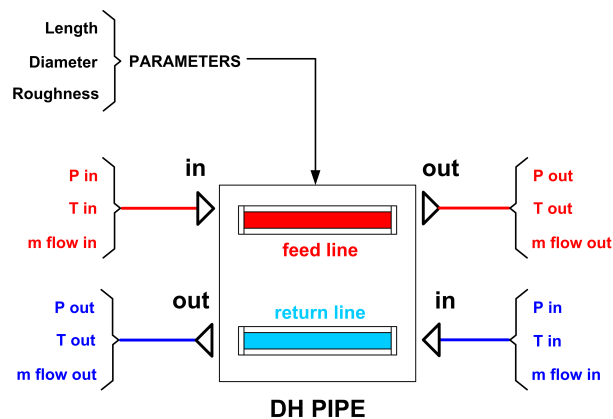
Figure 2.56: Block structure based on inputs, outputs and parameters

This methodology is more visual, understandable and easier to use for all kind of users, specially for those who do not have a deep knowledge about the DH networks, since all the constituent elements of the network are represented and linked in the same way like they would be in the real grid. In turn, each block is constituted by other blocks allowing the user to see the elements working inside. This is the case of a building and its internal hydraulic network, which may include other possibilities, such as connections to other elements like solar panels, heat pumps, auxiliary electrical networks, etc.

This methodology is recommended for small-size networks or simple grids when an exhaustive analysis is needed. This situation coincides with the case study analysed in this doctoral thesis. Therefore, this will be the methodology chosen (see chapter 5).

Following the classification referred previously in section 2.3.1, both methodologies are included into time-discrete, dynamic and deterministic models.

A brief description of the general methodology used for the calculation of hydraulic networks is described below. Much of the information and methods described comes from the works of

Bothe [103] and Nagler [104], previously developed in the department of Energy Systems and Thermodynamic in the TU Wien, where this thesis has been carried out as well.

To solve the problem and determine all these variables, a system of equations that covers both the hydraulic, mass and energy balances has to be proposed. The variables are calculated for each time interval consecutively.

Once all pressure and mass flows are calculated for all nodes and branches, then it is possible to raise and resolve the energy balance and determine the temperatures and therefore, the heat losses. The results of the pressure and mass balances are the boundary conditions for the energy balance, defining all the conditions to calculate the next time step.

The method used is based on the graph theory [105], in such a way that a network is represented by n nodes and m branches arranged in the incidence matrix.
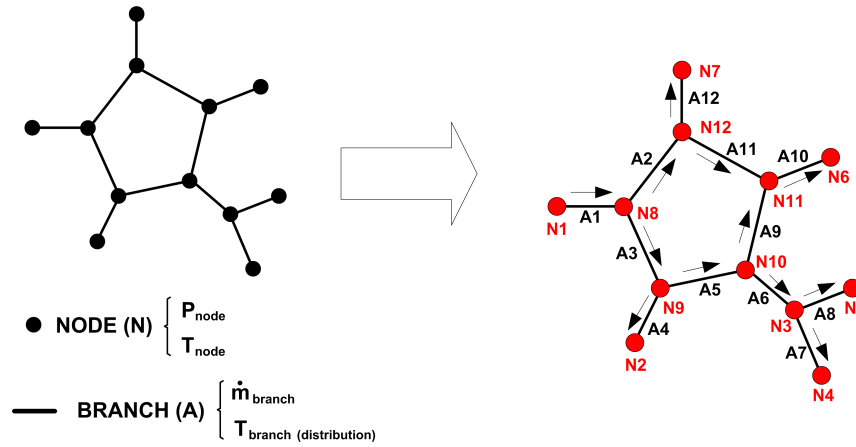
Figure 2.57: Node-Branch distribution prepared to define the Incidence Matrix

Following the example shown in the figure 2.57, considering the network topology and the fluid direction, it is possible to build the Incidence Matrix I_{ij}:

branches (j): from 1 to n

nodes (i): from 1 to m

	A1	A2	A3	A4	A5	A6	A7	A8	A9	A10	A11	A12
N1	1	0	0	0	0	0	0	0	0	0	0	0
N2	0	0	0	-1	0	0	0	0	0	0	0	0
N3	0	0	0	0	0	-1	1	1	0	0	0	0
N4	0	0	0	0	0	0	-1	0	0	0	0	0
N5	0	0	0	0	0	0	0	-1	0	0	0	0
N6	0	0	0	0	0	0	0	0	0	-1	0	0
N7	0	0	0	0	0	0	0	0	0	0	0	-1
N8	-1	1	1	0	0	0	0	0	0	0	0	0
N9	0	0	-1	1	1	0	0	0	0	0	0	0
N10	0	0	0	0	-1	1	0	0	1	0	0	0
N11	0	0	0	0	0	0	0	0	-1	1	-1	0
N12	0	-1	0	0	0	0	0	0	0	0	1	1
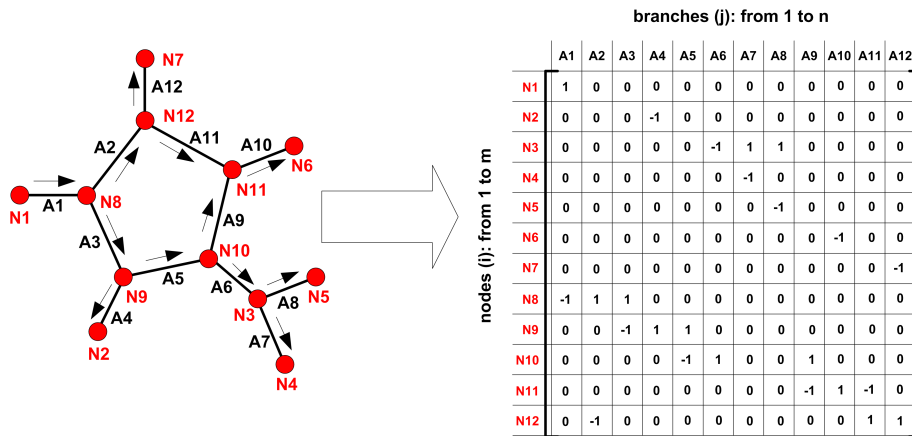
Figure 2.58: Building the incidence matrix

The branches are represented by j, counted from 1 to n. The nodes are represented by i, and are counted from 1 to m. The matrix is filled by the i_{ij} factors, which get the values of 1, -1 or 0,

depending on the following criteria:

- $i_{ij} = 0$ if there is no relation between a node i and a branch j

- $i_{ij} = 1$ if there is a relation between a node i and a branch j, the fluid leaves the node

- $i_{ij} = -1$ if there is a relation between a node i and a branch j, the fluid enters the node

In the next step, mass and pressure balances are raised. The general expressions are the following:

- Mass balance for a node i:

$$\sum_{j=1}^{n\,inputs} \dot{m}_{in,i} = \sum_{j=1}^{n\,outputs} \dot{m}_{out,i} \tag{2.35}$$

The equation 2.35 can be extended, generating the following expression:

$$\sum_{j=1}^{n\,inputs} \left(\frac{\rho_{fluid,j} \cdot d_j^2 \cdot \pi \cdot u_{fluid,j}}{4} \right)_i = \sum_{j=1}^{n\,outputs} \left(\frac{\rho_{fluid,j} \cdot d_j^2 \cdot \pi \cdot u_{fluid,j}}{4} \right)_i \tag{2.36}$$

- General mass balance:

$$\sum_{j=1}^{n\,inputs} \dot{m}_{in,grid} = \sum_{j=1}^{n\,outputs} \dot{m}_{out,grid} \tag{2.37}$$

$$\sum_{j=1}^{n\,inputs} \left(\frac{\rho_{fluid,j} \cdot d_j^2 \cdot \pi \cdot u_{fluid,j}}{4} \right)_{grid} = \sum_{j=1}^{n\,outputs} \left(\frac{\rho_{fluid,j} \cdot d_j^2 \cdot \pi \cdot u_{fluid,j}}{4} \right)_{grid} \tag{2.38}$$

- Pressure balance for a branch j:

$$P_{out,i} = P_{in,i} - k_j \cdot u_j^{(t-1)} \cdot u_j^{(t)} \tag{2.39}$$

Since $u_j^{(t-1)}$ is the previous value of the fluid velocity during the iterative calculation for the branch j, $u_j^{(t)}$ is the actual value of the fluid velocity during the iterative calculation for the branch j, k_j is the factor that meets the characteristic parameters of the pipe corresponding to the branch j, according to the Darcy-Weisbach equation:

$$\Delta P = \frac{8 \cdot f_D \cdot L_j \cdot \rho_{fluid,j}}{d_j^5 \cdot \pi^2} \cdot \dot{V}_{fluid,j}^2 \tag{2.40}$$

With f_D as the Darcy friction factor, L as the length of the correspondent pipe associated to the branch, $\rho_{fluid,j}$ as the fluid density circulating through the pipe, $\dot{V}_{fluid,j}$ as the volumetric flow and d_j the diameter of the pipe.

Thus, the value of k is extracted:

$$k = \frac{8 \cdot \cdot f_D \cdot L \cdot \cdot \rho_{fluid,j}}{d_j^5 \cdot \pi^2} \tag{2.41}$$

It is considered that the entire network is installed in the horizontal plane, therefore, Nagler [104] does not consider the heights of the different nodes in the pressure balance, however, Bothe [103] considers them in his methodology.

- Boundary conditions:

  The problem will not be possible to solve without first defining certain known boundary conditions. From this information it will be possible to match the number of unknowns with the number of equations, giving rise to a solvable system.

  In this type of problems, what is usually done is to establish a minimum admissible pressure value $P_{out,i}$ for the furthest building from the substation . Afterwards, the flow velocities $u_{fluid,j}$ for each consumer are defined as well.

Concerning temperature calculation, the starting point are the mass and energy conservation equations applied for incompressible fluids

- Mass conservation equation:

  It is considered steady state regime, which means that all the input mass flows that are crossing the control volume are also leaving it, Therefore there is no accumulation, creation or destruction of mass inside. The fluid is also considered incompressible, so the density does not vary over the time.

$$\frac{\partial}{\partial x}(\rho\, u) = 0 \tag{2.42}$$

- Energy conservation equation:

  The pressure variation is small and there is no change of phase. Therefore, the heat capacity at constant pressure C_p is used.

$$C_p\frac{\partial}{\partial x}(\rho\, T\, u) + C_p\frac{\partial}{\partial t}(\rho\, T) = \frac{\partial}{\partial x}\dot{Q}_x + S \tag{2.43}$$

The terms of equation (2.43) are hereunder explained:

  - $C_p\frac{\partial}{\partial x}(\rho\, T\, u)$ as the convective term for the energy transport
  - $C_p\frac{\partial}{\partial t}(\rho\, T)$ as the transient term
  - $\frac{\partial}{\partial x}\dot{Q}_x$ as the heat conduction term in x direction
  - S as the energy incomes or losses (energy sources supplying energy to the system or energy sinks extracting energy from the system)

In order to solve both equations, it is necessary to apply the finite-volumes discretization method. It consists of divide the pipes into several control volumes. The volume is calculated following the expression for a cylinder:

$$\Delta V = A_j \, \Delta x = \frac{d_j^2 \, \pi}{4} \, \Delta x \tag{2.44}$$

Since A_j is the sectional area of the considered pipe for the branch j.

The discretization is carried out by the following scheme:
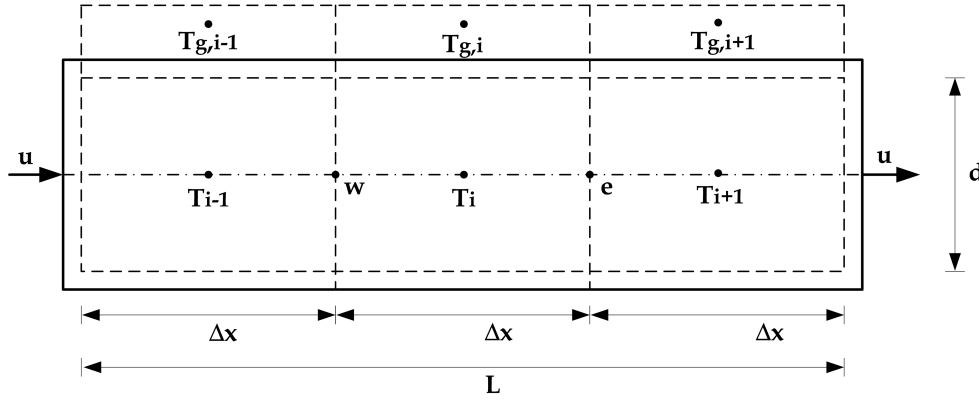
Figure 2.59: Spatial pipe discretization with n = 3 elements, Δx = L/3, T_i = Temperature for each volume element i, $T_{g,i}$ = Ambient temperature related to each T_i
, u = fluid velocity, d = pipe diameter

In the next step the discretization method is applied, integrating over the control volume ΔV, which in turn means using the equation (2.44). The mass balance expression is finally obtained:

$$\dot{m}_w = \dot{m}_e = \rho_{fluid} \, (T_i, P_i) \, \frac{d^2 \, \pi}{4} \, u_{fluid} \tag{2.45}$$

Applying discretization to the energy conservation equation ((2.43)), the following expression is obtained:

$$C_p \, \rho_{fluid} \, u_{fluid} \, (T_e - T_w) + \left(C_p \, \rho_{fluid} \, \frac{\partial T}{\partial t} \right)_i \, \Delta x = \dot{Q}_w - \dot{Q}_e + S \, \Delta V \tag{2.46}$$

With T_w = Temperature in x = w, T_e = Temperature in x = e, $\dot{Q}_w$= Heat flow in x = w, $\dot{Q}_e$ = Heat flow in x = e

Applying Fourier law, the equation (2.46) can be transformed:

$$C_p \, \rho_{fluid} \, u_{fluid} \, (T_i - T_{i-1}) + \left(C_p \, \rho_{fluid} \, \frac{\partial T}{\partial t} \right)_i \, \Delta x = \frac{\lambda_f}{\Delta x} \, (T_{i-1} + T_{i+1} - 2 \, T_i) + S \, \Delta x \tag{2.47}$$

In this case, λ_f is the heat transfer term and S represents the heat losses of the pipe, which is defined by the expression:

$$S = \frac{T_{g,i} - T_i}{A_j \, R_{fg}} \tag{2.48}$$

With R_{fg} as the resistance to heat flow, composed by three terms [106]:

$$R_{fg} = \frac{1}{\pi \, Nu \, \lambda_f} + \frac{1}{2 \, \pi \, \lambda_p} \, Ln\left(\frac{d_a}{d_i}\right) + x_{sg} \, R_g \tag{2.49}$$

The terms of equation (2.49) are hereunder explained:

- $\frac{1}{\pi \, Nu \, \lambda_f}$ as the heat transfer from the fluid to the pipe

- $\frac{1}{2 \, \pi \, \lambda_p} \, Ln\left(\frac{d_a}{d_i}\right)$ as the heat transfer by conduction in the pipe wall

- $x_{sg} \, R_g$ as the heat transfer from the pipe wall through the insulation material or the surrounding material of the pipe

Substituting equations (2.49) and (2.48) inside the equation (2.47), making certain operations and isolating the term $\frac{\partial T}{\partial t}$, the expression results:

$$\left(\frac{\partial T}{\partial t}\right)_i = \frac{1}{C_f}\left[\frac{C_p \, \dot{m} \, (T_{i-1} - T_i)}{\Delta x} + \frac{A_f \, \lambda_f \, (T_{i-1} + T_{i+1} - 2\,T_i)}{\Delta x^2} + \frac{T_{g,i} - T_i}{R_{fg}}\right] \tag{2.50}$$

This is the equation for the temperature calculation T_i of a fluid circulating through the horizontal direction (x axis), crossing the element of volume i, with dimension Δ_x and section A_f.

Applying this equation for both, feed and return DH pipes, the first two equations of the model are obtained:

For the supply line (1):

$$\left(\frac{\partial T_1}{\partial t}\right)_i = \frac{1}{C_f}\left[\frac{C_p \, \dot{m}_{feed\,DH} \, (T_{1,(i-1)} - T_{1,i})}{\Delta x} + \frac{A_f \, \lambda_f \, (T_{1,(i-1)} + T_{1,(i+1)} - 2\,T_{1,i})}{\Delta x^2} + \frac{T_{g1,i} - T_{1,i}}{R_{fg}}\right] \tag{2.51}$$

For the return line (2):

$$\left(\frac{\partial T_2}{\partial t}\right)_i = \frac{1}{C_f}\left[\frac{C_p \, \dot{m}_{feed\,DH} \, (T_{2,(i-1)} - T_{2,i})}{\Delta x} + \frac{A_f \, \lambda_f \, (T_{2,(i-1)} + T_{2,(i+1)} - 2\,T_{2,i})}{\Delta x^2} + \frac{T_{g2,i} - T_{2,i}}{R_{fg}}\right] \tag{2.52}$$

With $C_f = C_p \, \rho_{fluid,j} \, A_f$ and $\dot{m}_{feed-return\,DH} = \rho_{fluid,j} \, u_{fluid,j} \, A_f$

To understand how the different heat flows are transmitted in a DH pipe, Nagler establishes the following scheme based on the analogy between the thermal resistances of this type of systems and the resistances of electrical circuits:
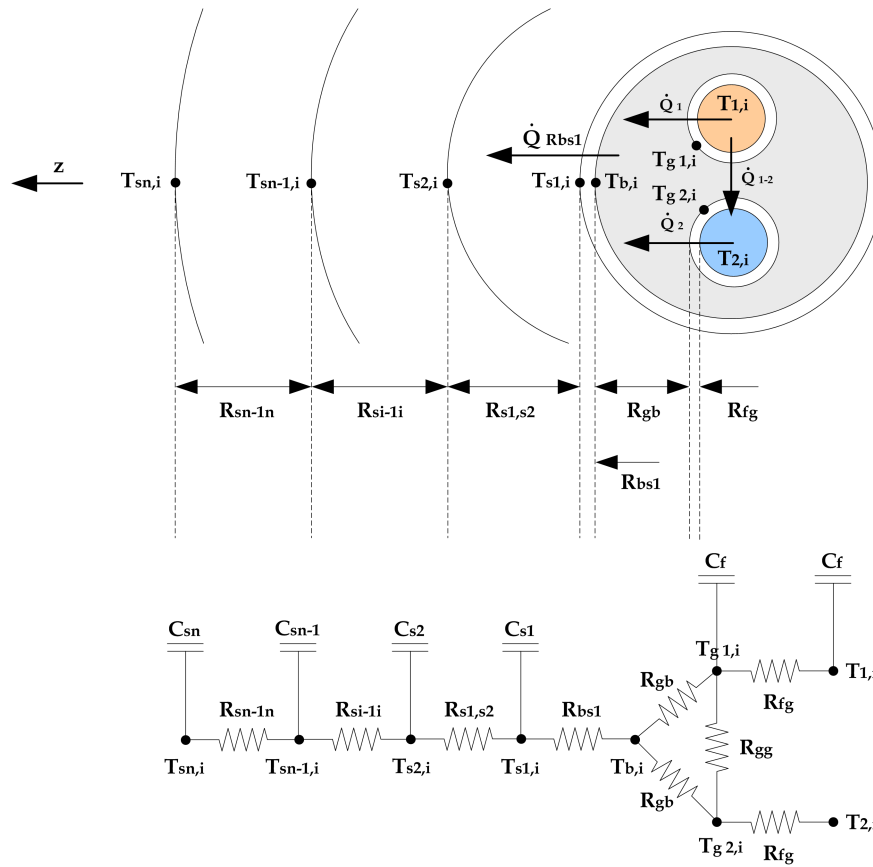
Figure 2.60: Resistance Capacity model for a single horizontal layer i. Every volume element with the capacity symbol is also coupled with the adjacent cells in z direction.

The terms of the figure 2.60 are hereunder explained:

- C_f as the calorific capacity of the fluid

- C_{s1} as the calorific capacity of the soil, material 1

- C_{s2} as the calorific capacity of the soil, material 2

- C_{sn} as the calorific capacity of the soil, material n

- R_{fg} resistance of the heat transmission of the feed/return internal tube wall

- R_{gb} resistance of the heat transmission of the internal insulation material of the DH pipe

- R_{bs} resistance of the heat transmission of the external DH pipe wall

- $R_{s1,s2}$ resistance of the heat transmission of the external insulation material of the DH pipe, s1-s2

- $R_{si,1i}$ resistance of the heat transmission of the external insulation material of the DH pipe, si-1i

- $R_{sn,1n}$ resistance of the heat transmission of the external insulation material of the DH pipe, sn-1n

- $T_{1,i}$ Fluid temperature inside the feed tube

- $T_{2,i}$ Fluid temperature inside the return tube

- $T_{g1,i}$ Temperature of the external wall of the feed tube

- $T_{g2,i}$ Temperature of the external wall of the return tube

- $T_{b,i}$ Temperature of the internal wall of the DH pipe

- $T_{s1,2,...n,i}$ Temperature of the insulation layer 1,2,n

According to the figure, the heat is always transmitted from the inner of the tube to the outside and from the hottest tube to the coldest one, both contained inside the DH pipe and surrounded by the insulation material. Therefore, 2 new equations are obtained $T_{g1,i}$ for the feed tube and $T_{g2,i}$ for the return tube :

$$\left(\frac{\partial T_{g1,i}}{\partial t}\right)_i = \frac{1}{C_g}\left[\frac{T_{g2,i}-T_{g1,i}}{R_{gg}} + \frac{T_{b,i}-T_{g1,i}}{R_{gb}} + \frac{T_{1,i}-T_{g1,i}}{R_{fg}} + \frac{A_g\,\lambda_g\,\left(T_{g1,(i-1)}+T_{g1,(i+1)}-2\,T_{g1,i}\right)}{\Delta x^2}\right] \quad (2.53)$$

$$\left(\frac{\partial T_{g2,i}}{\partial t}\right)_i = \frac{1}{C_g}\left[\frac{T_{g1,i}-T_{g2,i}}{R_{gg}} + \frac{T_{b,i}-T_{g2,i}}{R_{gb}} + \frac{T_{2,i}-T_{g2,i}}{R_{fg}} + \frac{A_g\,\lambda_g\,\left(T_{g2,(i-1)}+T_{g2,(i+1)}-2\,T_{g2,i}\right)}{\Delta x^2}\right] \quad (2.54)$$

In this case, all terms with subscript g represents the insulation material.

The heat balance generates the fifth equation:

$$\dot{Q}_{Rbs1} = \dot{Q}_1 + \dot{Q}_2 \quad (2.55)$$

Or, in other words,

$$\frac{T_{b,i}-T_{s1,i}}{R_{bs1}} + \frac{T_{b,i}-T_{g1,i}}{R_{gb}} + \frac{T_{b,i}-T_{g2,i}}{R_{gb}} \quad (2.56)$$

The last equation is obtained by considering the boundary condition of the heat flow that would be accumulated if a cylinder of diameter d_b and uniform temperature T_b was buried in the ground at the temperature T_{amb}.

$$\frac{T_{b,i}-T_{s1,i}}{R_{bs1}} + \frac{T_{b,i}-T_{amb}}{R_{bc}} \quad (2.57)$$

With R_{bc} as the heat flow resistance (boundary condition value).

Combining the equations (2.51), (2.52), (2.53), (2.54), (2.55), (2.57), integrating the temperature along the time and grouping terms a system with 6 ecuations and 6 unknown variables T_1, T_2, T_{g1}, T_{g2}, T_b, T_{s1} is finally defined. :

$$\alpha_1^{(1)}\, T_{1,(i-1)} + \alpha_2^{(1)}\, T_{1,i} + \alpha_3^{(1)}\, T_{1,(i+1)} + \alpha_4^{(1)}\, T_{g1,i} = \beta_1 \tag{2.58}$$

$$\alpha_1^{(1)}\, T_{2,(i-1)} + \alpha_2^{(1)}\, T_{2,i} + \alpha_3^{(1)}\, T_{2,(i+1)} + \alpha_4^{(1)}\, T_{g2,i} = \beta_2 \tag{2.59}$$

$$\alpha_1^{(2)}\, T_{1,i} + \alpha_2^{(2)}\, T_{g1,(i-1)} + \alpha_3^{(2)}\, T_{g1,i} + \alpha_2^{(2)}\, T_{g1,(i+1)} + \alpha_4^{(2)}\, T_{g2,i} + \alpha_5^{(2)}\, T_{b,i} = \beta_3 \tag{2.60}$$

$$\alpha_1^{(2)}\, T_{2,i} + \alpha_2^{(2)}\, T_{g2,(i-1)} + \alpha_3^{(2)}\, T_{g2,i} + \alpha_2^{(2)}\, T_{g2,(i+1)} + \alpha_4^{(2)}\, T_{g1,i} + \alpha_5^{(2)}\, T_{b,i} = \beta_4 \tag{2.61}$$

$$\alpha_1^{(3)}\, T_{g1,i} + \alpha_1^{(3)}\, T_{g2,i} + \alpha_2^{(3)}\, T_{b,i} + \alpha_3^{(3)}\, T_{s1,i} = 0 \tag{2.62}$$

$$\alpha_1^{(4)}\, T_{b,i} + \alpha_2^{(4)}\, T_{s1,i} = \beta_6 \tag{2.63}$$

The factors α and β are generated by gathering together different known terms, such as some physical properties of the fluid, as well as several pipe characteristics.

Through the incidence matrix I referred to above 2.58 and the methodology explained by Nagler [104], it is possible to calculate the temperature values in every point of the network and the their evolution with respect to the time.

2.3.3 Other related projects

From here, there are many projects dedicated to the modeling and simulation of district heating networks. In a first approximation, I. del Hoyo Arce and M. Rämä [107] developed a simplified model for the thermal energy transport in DH networks using a library integrated in Modelica software and applicable for Simulink. The library comprises detailed models of all the distribution and consumption components commonly found in DH systems.

M. Vesterlund [108] faced the modelling of a real case study in Kiruna (Sweden), developing a new integration method for complex DH systems containing loops and bottlenecks and analysing how those situations affect the behaviour and the distribution path of the thermal energy of the network. The article focuses on the use of a model that solves the problem without simplifying the existing loops, without altering the original structure of the grid.

Subsequently, the same author also uses the MATLAB-Simulink environment in his article [109]. Using the same case study, the methodology detects those pipes in which the circulating heat flow exceeds the levels recommended by the pipe manufacturers, as well as pressure and temperature losses.

Previously, P. Jie [110] studied the dynamic characteristics of DH networks as a prerequisite for the control strategy, distinguishing between a primary and a secondary network, like the Viennese DHN. The study focuses on the determination of the lag time and the relative attenuation degree of DH systems in heat exchange substations, which are parameters that characterize the dynamic behaviour of a thermal network. Lag time is described as the time it takes for the water temperature to change from the inlet to the outlet constant temperature. The Relative attenuation degree refers to the temperature change in the inlet, corresponding to 1 °C in the outlet.

The peak-valley method was introduced to find the actual lag time, and the correspondent analysis method was used to obtain the actual relative attenuation degree in the resolution process of the dynamic models. Both parameters are important for the management and operation of DH networks,

and they will be further used for other authors like J. Zheng [111]. In this article, the thermal dynamic operation of a DHN was analysed with an emphasis on simulating the dynamic temperature distribution. Zheng carries out a new physical method for dynamic temperature simulation, in which the function method takes into account various factors, such as flow time, heat capacity of the pipe and heat losses. The method uses Fourier series expansion as the mathematical basis to solve the transient energy equation. Further, the mentioned factors delay time and relative attenuation degree were described to represent the time delay and heat losses, and were used to obtain the temperature distribution of the network.

Going deep into the analysis of the dynamic behaviour of DH networks, H. V. Larsen [112] studies their dynamic properties focusing on the water flow and heat propagation from the production plants to the customers. In the line of Del Hoyo Arce's work [107], Larsen develops a method in which a fully described DH model is replaced by a simplified one, with the purpose of reducing the simulation time. The problem is simplified by reducing the topological complexity of the original network.

In recent years, new software tools are being used for the modelling and simulation of DH networks. G. Schweiger [113] presents a novel framework for representing and simplifying on-grid energy systems as well as for dynamic thermo-hydraulic simulation of DHC systems. In this work, robust models for simulation and continuous optimization are described, including a new method to decompose a Mixed Integer Optimal Control (MILP) problem into two sub-problems, separating the discrete part from the continuous. The comercial software Modelica is used in this project.

In the same line, B. Van Der Heijde [114] presents a thermo-hydraulic model for thermal grids also implemented in Modelica. This project develops realistic models of the individual network, representing the heat losses, gains, temperature propagation and pressure drops, and compares the calculated values with real experimental data. Results are positive, and a good correspondence between both environments is obtained.

The same author carries out a further job related with the topic [115], in which he describes an accurate and simple model for fast simulation of DH networks. The author models the steady-state thermal behaviour of twin DH pipes, presenting the mathematical derivations and assumptions made in detail, focusing on calculate heat transfers, heat losses and dynamic temperature profiles. The article reaches interesting conclusions, concerning how heat losses are nearly independent of the mass flow rate in the range usually encountered in DH pipes.

More specifically, A. Dénarié [116] presents a new numerical approach to model the heat transmission over long pipes of DH networks, This model splits the thermal capacity of the water between the turbulent core and the boundary layer, leading to a greater accuracy in comparison with the finite-volume method and the node method.

Concerning the connection between thermal networks and thermal plants, V.D. Stevanovic [117] develops a mathematical model for the prediction of thermal transients in DH systems, in order to adjust the loads of CHP plants and pump stations with dynamic consumption needs during changes of the outside temperature and other meteorological conditions.

Stevanovic's model calculates the propagation of the temperature front, which meets well with the real measured data at three consumer substations located at different distances from the thermal plant.

Finally, D. Olsthoorn [74] and M. Leśko [118] elaborate about the modelling and optimization of

DH networks in connection with thermal energy storage. Also S. Falkner [119] makes an important contribution defining the complete model for a thermal storage stratified tank in connection with the DHN.

2.3.4 Main Software Tools

There is a variety of commercial tools available to perform calculations and simulate thermo-hydraulic grids and DH networks. These software tools are widely used for network planning and off-design calculations, as well as for the determination of load flows in DH systems whose characteristics and boundary conditions are given. The following table provides an overview of the common software packages and their abilities.

software	sewage	DH	gas	hydraulic calculation	thermal calculation
PSS ®SINCAL	yes	yes	yes	yes	yes
STANET	yes	yes	yes	yes	yes
Simplex	no	yes	no	yes	yes
Bentley ®sisHYD	yes	yes	yes	yes	yes
EPANET	yes	no	no	yes	no
TERMIS	no	yes	no	yes	no
SIR-3S	yes	yes	yes	yes	yes

Table 2.1: Table of available softwares

2.3.5 Exergy analysis

Although both the concept of exergy and its application in thermal networks will be explained in detail in the sections 4.2.4 and 4.2.5, a reference of the main studies concerning exergy and its use is done here.

Previously in his article, Rezaie [3], revises several DH systems in combination with CHP plants and includes the exergy analysis as an effective method to analyse the efficiency of thermal networks.

Concerning real case studies, Ozgener [120] presents a geothermal DH model with energy/exergy assessment for a real installation in Izmir (Turkey). The study is carried out using actual system data, in order to obtain energy and exergy efficiencies and quantify the exergy destruction in the system by means of the exergy flow diagram.

Another work based on a pilot-project plant is Li's project [121], which is consistent with the 4GDHN concept. In this paper, an energy-exergy analysis for a LTDHN is done. The supply/return temperature is set at 55/25 °C, which agrees with a pilot plant constituted by 30 low energy residential houses located in Denmark. The system uses radiant floors and Low temperature radiators to supply heating and domestic hot water to the consumers. Through a simulation, the overall energy and exergy efficiencies are calculated and the exergy losses for the major DH components are identified. Based on the results, the author suggests to reduce those losses and increase the quality match between consumers heating demand and DH supply.

The temperature level has a great influence in the exergy value, as it is demonstrated in M. Gong's work [122]. In this paper, Gong shows how the exergy concept is applied in DH systems with different temperature levels, with the aim of extend and simplify the use of the exergy concept when comparing current and future temperature levels. The authors are based on the exergy utilisation rate factor, which is defined as the quotient between the final exergy flow supplied to the consumers and the exergy contained in the heat supply feed line. This concept will be also used along the sections 4.2.4 and 4.2.5. The results of this work show that current temperature levels can be reduced, and almost 2/3 of the exergy content in the heat supply input are lost in the heat distribution chain.

Finally, Çomakli in his article [123] elaborates a simplified method to calculate exergy losses and was applied in a real DHN case study in Atatürk University in Izmir (Turkey).

Several parts the text, pictures and tables described in this chapter; mainly sections 2.1 and 2.2, are also included in the book "Urban Energy Systems for Low-Carbon Cities" [32], being Mario Potente Prieto the author of these texts, images and other materials both in the aforementioned book and in this doctoral thesis.

Chapter 3

Case Study

3.1 The Viennese District Heating Network
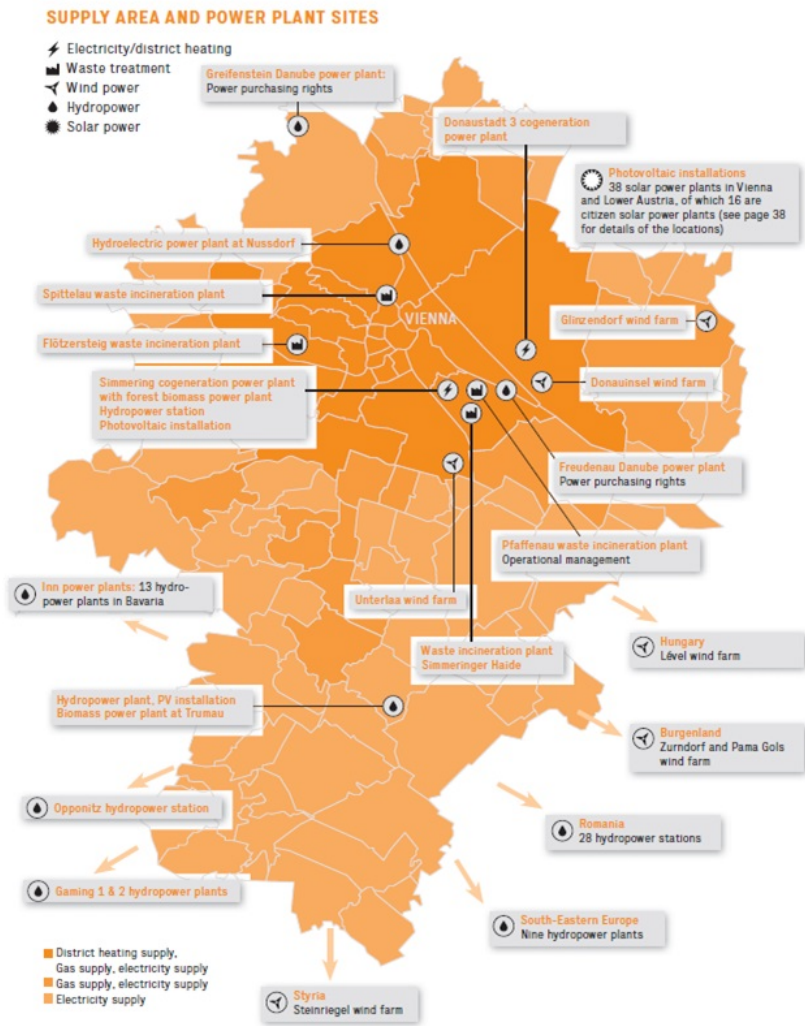
Figure 3.1: General Supply area and power plant sites around the federal district of Vienna [124] [32].

The Viennese energy system is based on centralized generation with several energy plants (generally CHP) feeding the main ring of the thermal network, defined as primary network. As shown in Figure 3.1, in the federal district of Vienna and surroundings there are several energy sources, ranging from thermal and cogeneration plants, eolic and photovoltaic parks and hydroelectric power plants. The latter are very popular in Austria and are located in the federal state of Niederösterreich, which is rich in forest areas and receives strong winds along the year. The diversification of energy allows an efficient utilization of the resources depending on location and season of the year. With an active energy efficiency policy in Vienna, there are currently 21.000 energy consultations per year, 3 million tonnes of CO_2 saved every year and green electricity guaranteed for 660.000 people [124].

(a) Year 1969

(b) Year 1981

(c) Year 1989

(d) Year 2003
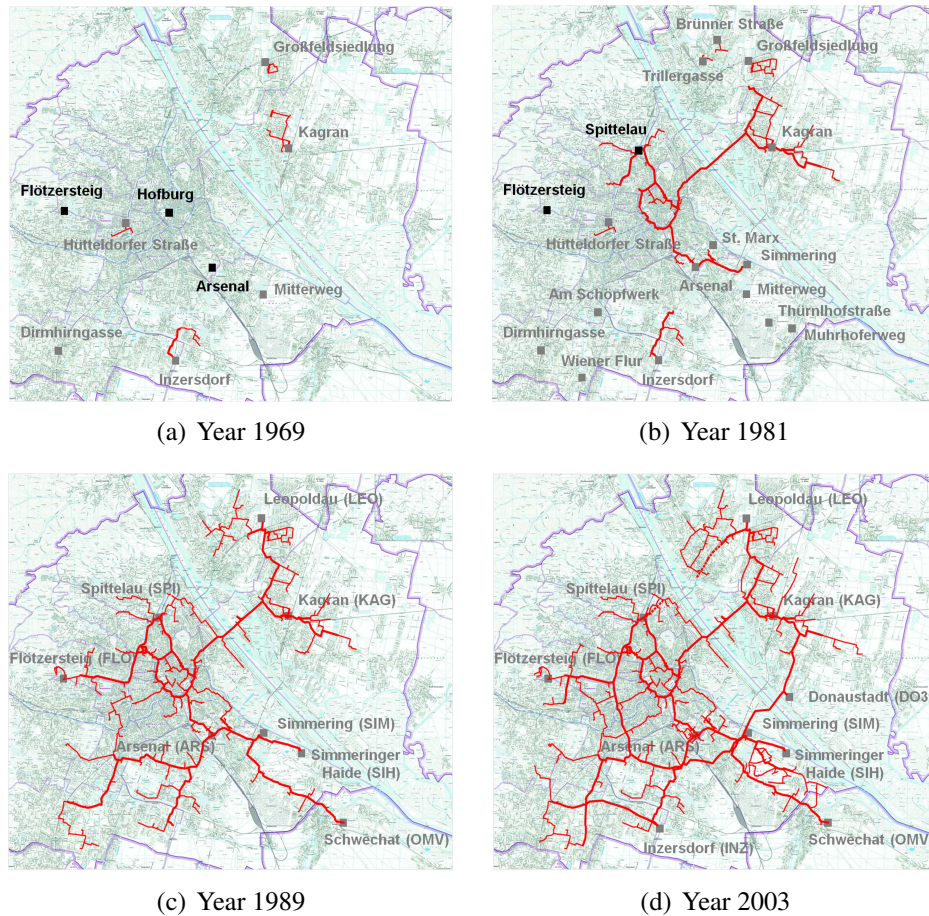
Figure 3.2: Evolution of the district heating network in Vienna [124] [32].

Initially, in 1969 no proper network existed. Only some decentralized heating plants were built providing small local networks in Hütteldorferstraße, Inzersdorf, Kagran and Großfeldsiedlung. In addition, two thermal plants (Arsenal, Hofburg) and the first waste incineration plant (Flötzersteig) were built.

In 1981 the second incineration plant started (Spittelau), creating the central branch of the eastern side of the Danube. The built network around the Kagran thermal plant extends along the western margin, connecting both sides of the river. 8 years later, many of the decentralized plants are dismantled, some of them reconfigured as combined cycles, constituting 8 heat and power plants totally integrated with the district heating network. In addition, the third waste incineration plant is

created, and a heat recovery plant located in Schwechat is built to utilize the excess heat from the OMW refinery, situated 15 km apart from Vienna.

In 2003, two more plants were built: Inzersdorf and Donaustadt, allowing the extension of the DHN on both sides of the south-western Danube and covering a length of 509 km for the primary network and 475 km for the local secondary networks.
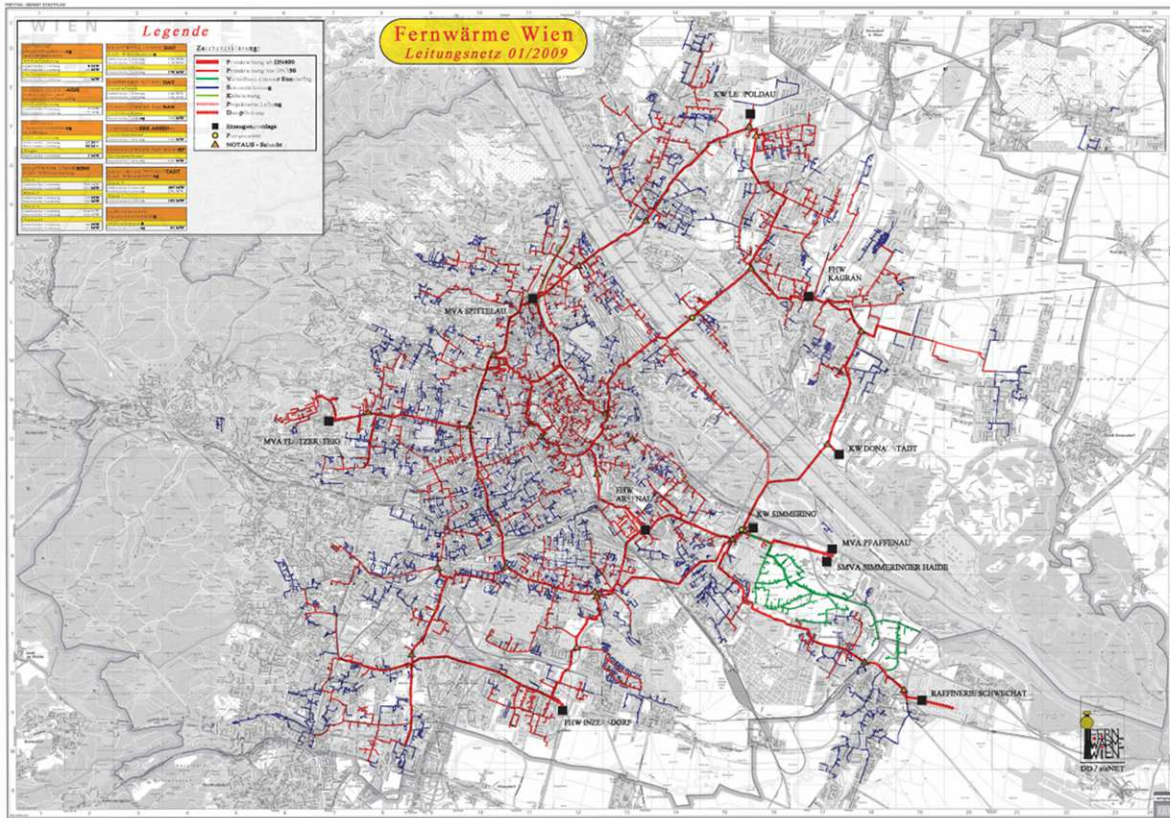
Figure 3.3: Actual DHN of Vienna [124] [32].

Currently, there are 11 operating thermal plants interconnected along a network covering 1192 km. It serves 336,902 users and 6602 major customers through 3758 substations and 5261 transfer stations. The total installed capacity is 3285 MW, reaching a 36 % share in the heat market [124]. Hereby, some of the most important thermal power plants installed in Vienna are described. All of them are actually working, linked to the DHN.

(a) CHP plant Donaustadt 3   (b) CHP-Biomass plant Simmering

Figure 3.4: Two of the CHP plants serving the DHN of Vienna [124] [32].

The CHP plants are the most advanced since their technology is based on Rankine cycles, which are able to generate simultaneously power and heat. The ratio between both forms of energy can be modified according to consumer needs.

(a) MWIP & PL DH plant Spittelau

(b) MWIP Flötzersteig

(c) MWIP Pfaffenau

Figure 3.5: MWIP plants serving the DHN of Vienna [124] [32].

MWIP (Municipal Waste Incineration Plant): Garbage is collected and stored to be burnt mostly for heat production. They use boiler technology and require a combustion gas treatment system, in order to avoid the expulsion of harmful particles into the atmosphere.

(a) PL DH plant Arsenal

(b) PL DH plant Inzersdorf
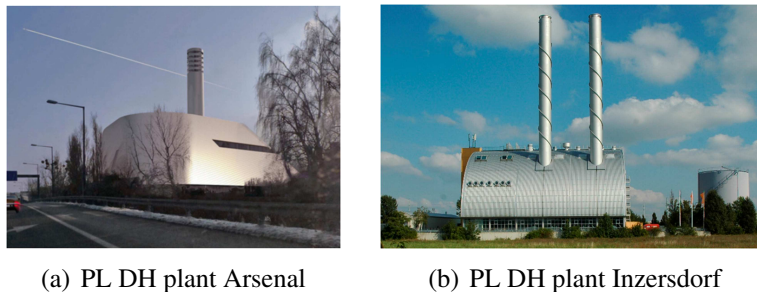
Figure 3.6: PL DH plants serving the DHN of Vienna [124] [32].

PL DH (Peak Load District Heating plants), or simply B (Boilers): These are exclusively dedicated to meet heat consumption peaks appearing at certain times of the year, increasing high temperature water flow. They operate using fossil fuels, especially natural gas or fuel. They are relatively small and their operation is not very complex.

Table 3.1 shows total installed capacity as well as the total power generated (MW) for each of the operating plants and energy source used. As it can be observed in both Table 3.1 and Figure 3.7, most of the installed power corresponds to CHP plants and Peak load DH plants (44.7 % and 44.6 % respectively), which means that the thermal energy generated from fossil fuels still represents almost a 90 % of the total amount.

In addition, in Figure 3.7 the right column represents the installed capacity; which is the maximum amount of heat which could be obtained from the thermal plants operating at full load, while the left column shows the actual percentages of utilization of the thermal plants for the year 2012 / 2013.

Table 3.1: Breakdown of heat generation: Installed capacity.

Energy source	Plant	Power (MW)	
Waste treatment	MWIP Spittelau	58	
	MWIP Flötzersteig	51	
	MWIP Pfaffenau	75	240
	Simmeringer Haide	54	
	Biogas	2	
Biomass	CHP Biomass Simmering	37	37
Industrial Waste Heat	CHP OMV Reffinery	168	173
	IWH Henkel	5	
Combined Heat and Power	CHP Donaustadt	250	
	CHP Leopoldau	170	
	CHP Simmering 1	450	1370
	CHP Simmering 2	150	
	CHP Simmering 3	350	
Peak Load DH Plants	B Leopoldau	230	
	B Spittelau	340	
	B Arsenal	340	1464
	B Kagran	200	
	B Inzersdorf	340	
	B Wilhelminenspital	14	
Total installed capacity =			3284
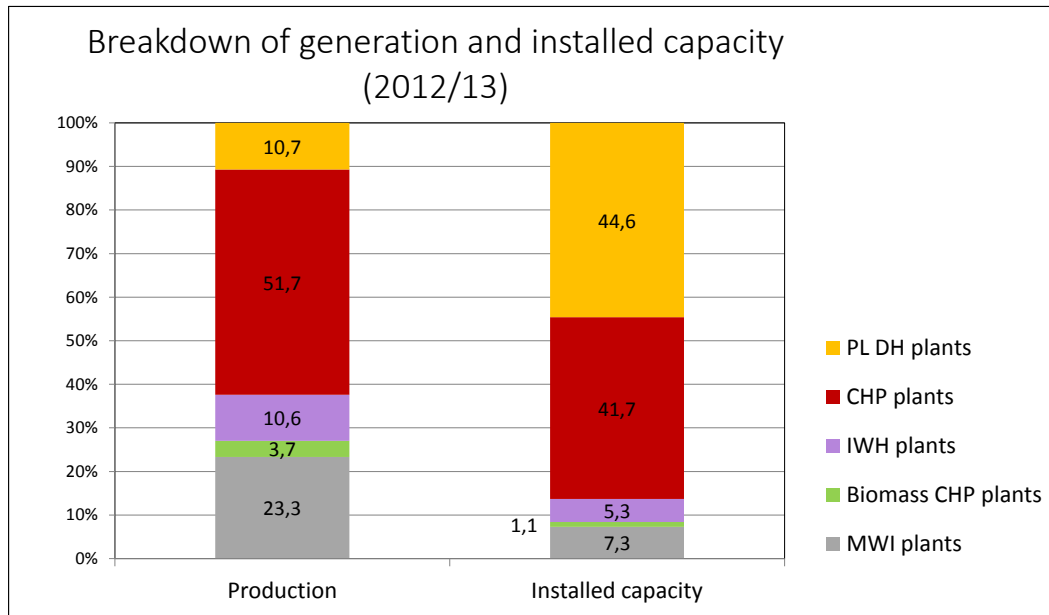
Figure 3.7: Breakdown of the heat generation [124] [32].
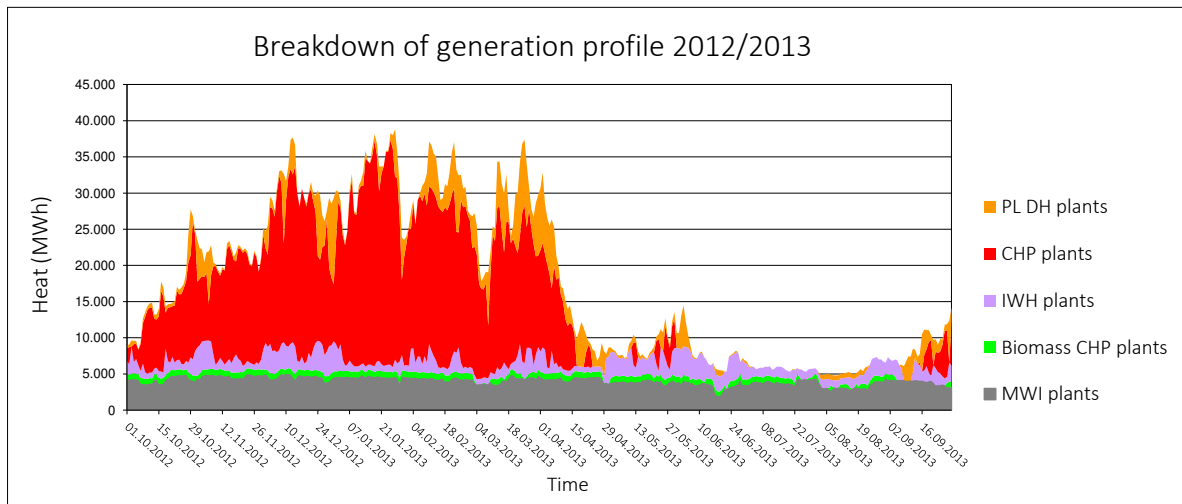
Figure 3.8: Breakdown of the heat generation, Profile for the years 2012/2013 [124] [32].

The maximum consumption values during the months of January, February, March and April, partially satisfied by the Peak Load district heating plants. At certain times, resorting to boilers is better since their start-up and operation is faster and more flexible than CHP plants.

Once the water is heated in the thermal power plants, it is sent to the main piping network, called primary network, whose temperature varies between 90 and 150 °C at pressures levels higher than atmospheric pressure.

The hydraulic pumps are located after the thermal plants keeping the water pressure at least at 5 bar. Depending on the geodetic situation of several buildings, it could reach up to 15 bar or even more. At the same time, control and security systems avoid steam production or cavitation anywhere in the network.

The pipes are isolated and made of steel, which is the right material to withstand the high pressures. The primary network works as an energy source and sink at the same time, and it is connected to the different substations which are partially linked to the secondary networks: Consequently, the mentioned primary network will have a high mass flow, leading to a strong thermal inertia.

From the ecological point of view, there are benefits obtained when choosing a thermal network instead of individual installations:

- Comparing network connected and non-connected buildings, approximately 1.9 Millions of tons of CO_2 emissions are avoided every year by district heating in Vienna

- District heating in Vienna is $\sim 75\,\%$ more efficient than comparable heating systems.

- Without district heating the primary energy demand would be 42 % higher. Greenhouse gas emissions (GHG) would increase by 52 %.

On the other hand, DH systems have several weak points, especially considering the economic point of view:

- High gas prices and low electricity prices make gas fired CHPs uneconomic

- DHN expansions have to be focused on areas with high heat demand density. Extending the network to low population areas is not economically affordable.

- Existing trends towards decentralized heat production, for example gas fired boiler houses combined with solar heat.

Several actions are considered, in order to improve the operation and increase thermal network efficiency:

- Upgrading from boiler to CHP technologies, improving internal Rankine cycles, trying to increase versatility and energy efficiency. In short, the idea is introducing new heat production ratios versus electricity and vice versa, depending on the energy prices and consumer needs.

- Network's operation:

  Considering the well-known expression 3.1:

  $$\dot{Q} = \dot{m}_{DH} \cdot Cp \cdot (T_{DH\ feed} - T_{DH\ return}) \qquad (3.1)$$

  Since $\dot{m}_{DH}$ is the mass flow of DH water (kg/s), Cp is the thermal capacity of the thermal flow at constant pressure (J/(kg K)), $T_{DH\ feed}$ and $T_{DH\ return}$ are the feed and return temperatures of the DHN.

  If the heat flow is required to be increased, there are two possible operation strategies:

  – Keep the $\dot{m}_{DH}$ constant, and modify ΔT, either increasing $T_{DH\ feed}$ or decreasing $T_{DH\ return}$, the aim is increasing the temperature difference, raising in turn the supplied heat flow. This option is unrealistic from the operational point of view, because it is easier to satisfy peak heat demands by increasing mass flows than manipulating temperatures.

  – Using the $\dot{m}_{DH}$ as a manipulable variable, and reducing $T_{DH\ return}$ as much as possible. Therefore, ΔT increases and $\dot{m}_{DH}$ can be reduced as well, saving electricity for the hydraulic pumps.

    In order to reduce the return temperature, replacing radiators by radiant floors is a possible option to be considered. However, it could be possible that the building has to be improved in order to reduce its heat demand, due to the limited maximum heat flow supplied by the radiant floors. Other possibilities, like heat pumps in combination with DHN are also available (see section 3.3).

- Combining the actual district heating network with other technologies, like decentralized heat pump systems, generating a temperature increase in certain chosen points of the district heating network (see section 2.2)

- Inclusion of energy storage tanks, to meet the heat demand peaks at certain times of the year

- There are actual projects related to geothermal energy, using the available heat contained in the underground water (see section 2.2.1)

3.2   The case study

3.2.1   General description (System substation-pipeline-buildings):
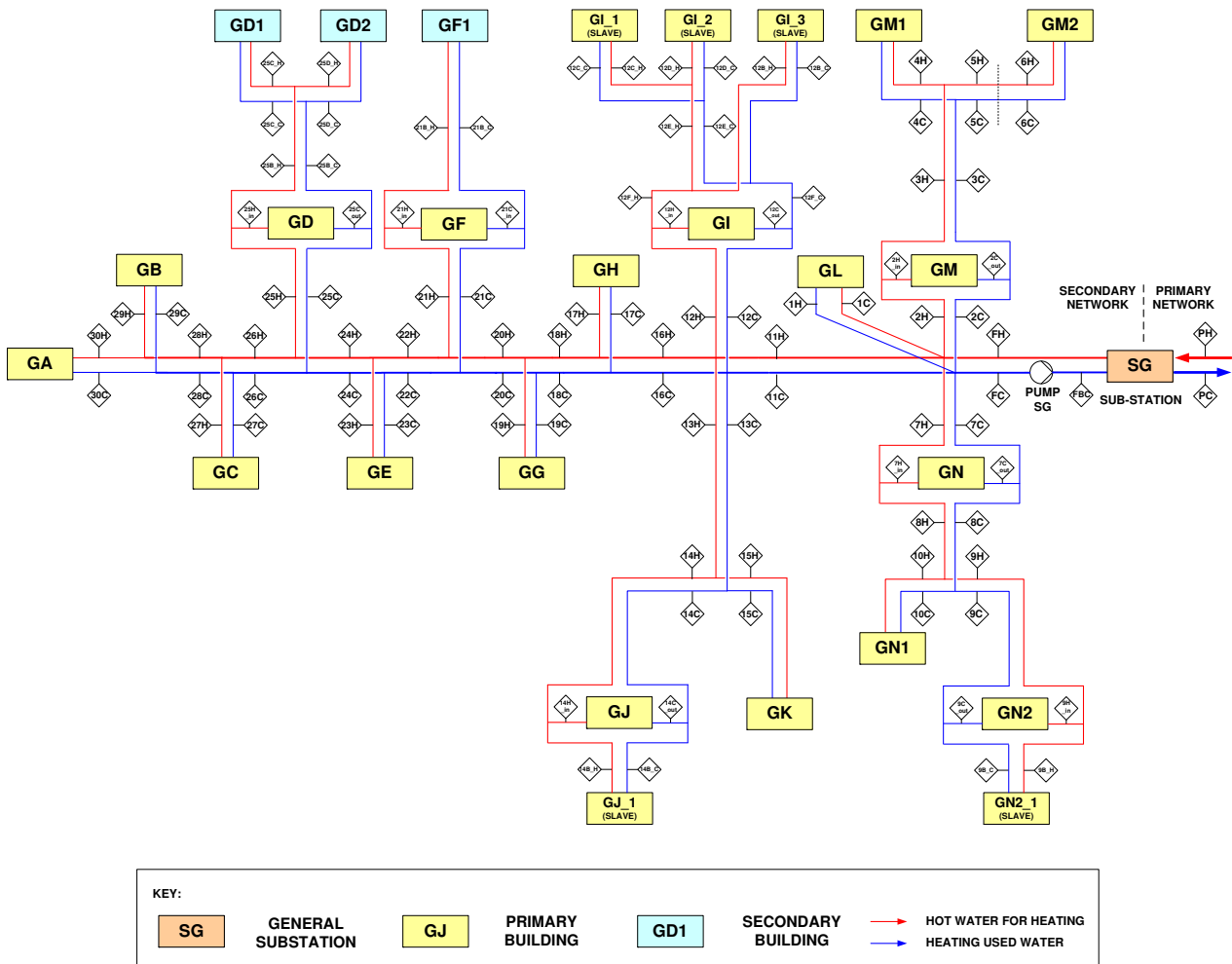
Figure 3.9: General diagram of Girasolstrasse's DHN. [32]

In global terms, the Viennese district heating network is composed of two parts. Firstly, the primary network, which transports a large mass flow of high temperature water (between 90 and 150 °C) from the thermal plants to the district general substations (in technical terms of Wien Energie called GUFO, by their name "Gebietsumformerstation" in German).

Secondly, the local networks (also known as secondary networks, see 3.3), which connect each general substation with the buildings. The temperature of the local networks is regulated in the above-mentioned substations using the hot water flow coming from the primary network. The pressure is also regulated there.

The case study considered here concerns a local network located in the district of Meidling, in south Vienna. There are 21 buildings with 18 substations as the point of heat exchange (not mass) between the secondary local heating network and the thermohydraulic network inside the dwellings.

Mainly plate heat exchangers are used in the substations: they are compact reduced size devices, recommended for water as heat carrier with temperatures below 100 °C. Total heating surface = 61957,52 m^2

The number of buildings and the number of substations are not coincident; this is because there are classified three types of buildings:

- primary buildings: they have their own substation, that is to say, a heat exchanger thermally linked to the local network

- secondary buildings: they have their own substation, but do not receive the DH water directly from the network, but from the primary buildings

- slave buildings: they do not have any substation and are connected to the primary buildings. During the calculation they are considered as part of the primary buildings.

Most of the buildings studied are residential family dwellings which include heating and domestic hot water services. There is a building with special features that is only equipped with a heating service. This distinction is important since not all buildings have the same purpose.

Taking into account all those considerations, the buildings have been classified defining the table A.1. In the other hand, all pipes present in the local grid must be classified as well. Basically there are two principal pipes, feed (H) and return (C), appearing from the general substation and ramifying, shaping a typical tree configuration (see section 2.3.2). Obeying this classification, the tables A.2, A.3 and A.4 are built.

3.2.2 Internal configuration of the buildings

The buildings are the consumption points where all district heating branches end. Their hydraulic networks and internal facilities are important sources of energy and exergy losses. This is why this study is not only limited to calculating and analysing the pipeline of the network but also entering the buildings and studying their energetic and exergetic performance, as it will analysed in the next chapters.

Not all flats sharing the same building are connected to the network, as appears in the figure 3.10.
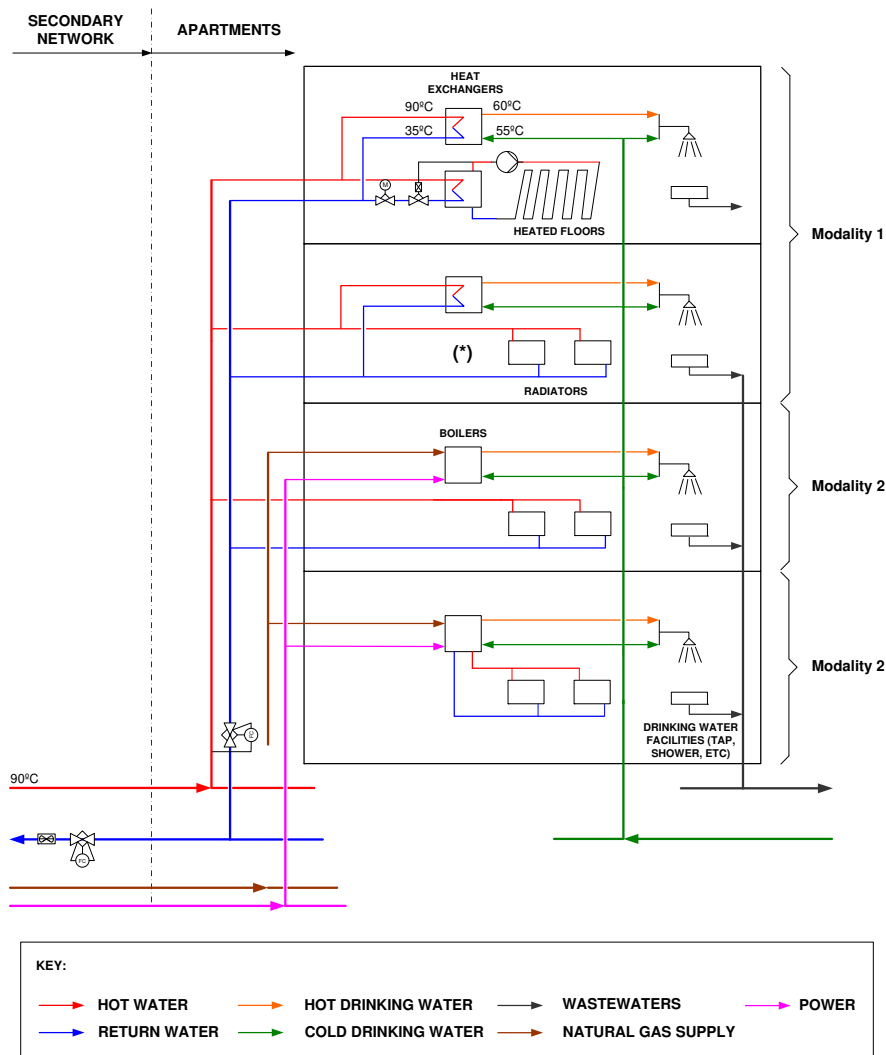
Figure 3.10: General diagram for standard residential buildings. (∗) Only in some cases, a heat exchanger is installed between the DH network and radiator's pipeline system. [32].

There are three different possibilities or combinations to meet the needs of heating and hot water depending on the energy source used. Namely:

- 1st modality : consumers using DHN for both services, having either radiators or radiant floors installed

- 2nd modality : consumers using DHN only for heating. Domestic hot water is produced by electric/gas boilers.

- 3rd modality: these consumers are not connected to the DHN.

In practice, only those users connected to the district heating network will be taken into account, so that the apartments are not simulated as isolated elements, but the building as a whole object or unit.
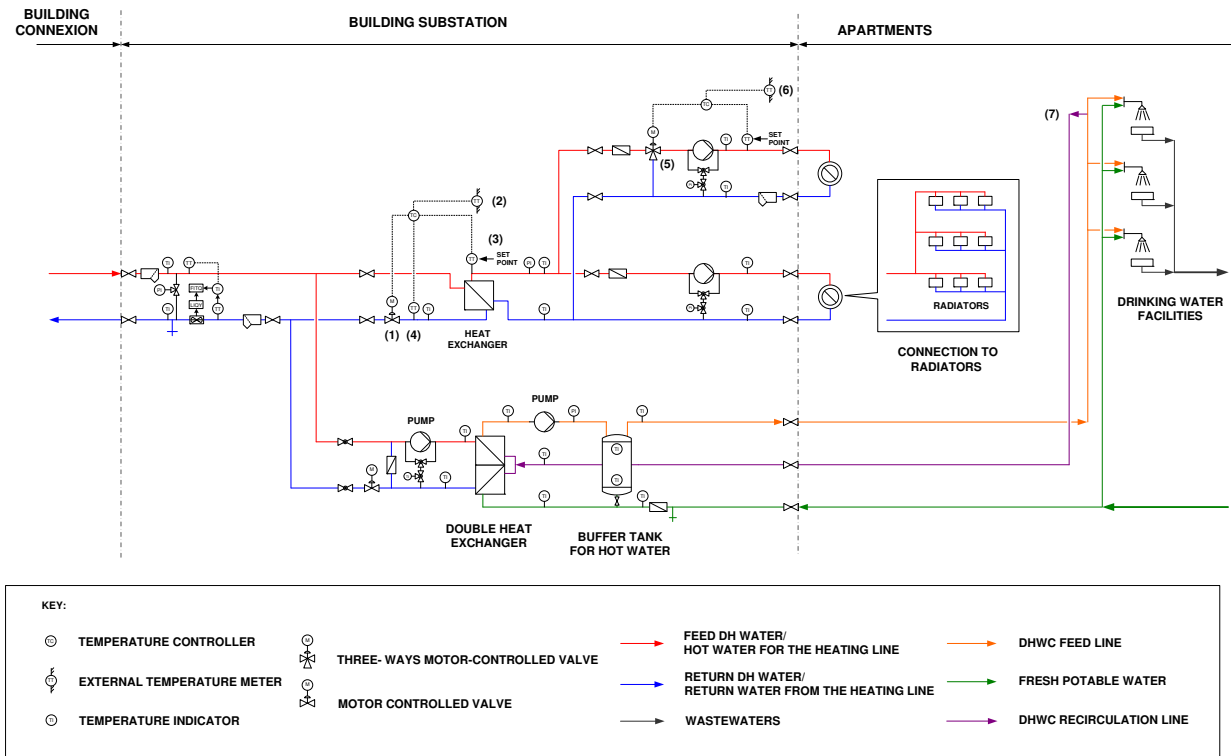
Figure 3.11: Simplified diagram of a residential building (heat exchanger considered in the heating branch) [32], Source: FERNWÄRME WIEN GmbH, Wien Energie [125]. With DHWC = Domestic Hot Water for Consumption. The diagram shows the following control and instrumentation loops: (1) Control system of the returning flow of water to the DHN depending on the three temperatures measured: outside the building (2 and 6), in the radiator's feed (3) and in the returning flow (4). (5) A higher precision temperature control system is possible, by mixing part of the return water with the supply water in the radiator circuit. (7) Recirculation system for instant consumption of hot water.

Figure 3.11 shows the hydraulic network installed in most of the buildings, in which two branches are distinguished; one for heating and another for domestic hot water. Each branch has its own heat exchanger. The main function of the heat exchangers is preparing the water for the service temperature by exchanging heat with the water coming from the DHN, which is necessary for the hot water branch since it is potable water. Of course, it cannot have any contact with the water coming from the network.

3.2.3 Internal configuration and operation of the substation
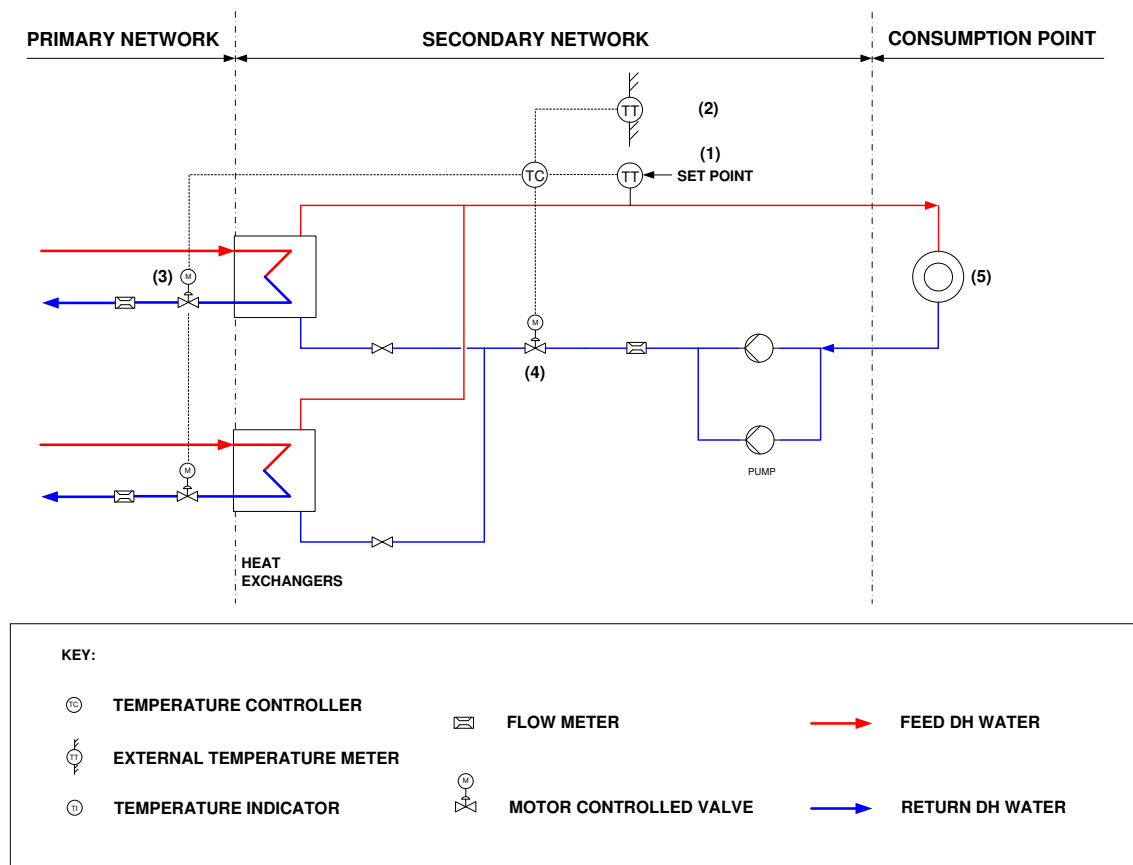
Figure 3.12: Simplified diagram of the GUFO substation [32], Source: FERNWÄRME WIEN GmbH, Wien Energie. The diagram shows the following control and instrumentation loops: (1) Temperature set point dependant from the external temperature (2), ruled by the heating curve. (3) Principal control system, regulating the mass flow of return DH water from the primary and secondary network.

The substation is where all necessary devices for energy exchange between primary and secondary networks are installed. The objective is to produce heating and hot water to cover the consumers needs. Each substation normally contains two heat exchangers installed in parallel, as appears in the above picture (Figure 3.12).

Regarding temperature regulation, a linear mathematical function is used, through which it is possible to calculate the temperature of the feed stream DH water depending on the external temperature.
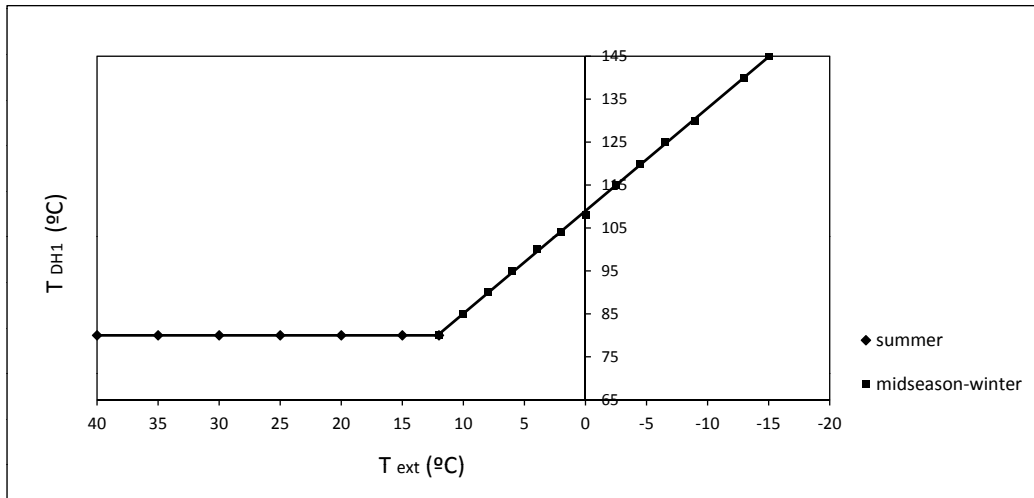
Figure 3.13: Heating curve for the primary network. [32], Source: FERNWÄRME WIEN GmbH, Wien Energie [126].

- Highest value = 145 °C , corresponding to the coldest external temperature condition: -15°C.

- Lowest value = 80 °C, corresponding to 12°C of ambient temperature. Above this ambient temperature the value 80°C keeps constant.

For local networks, the heating curve described is the following:
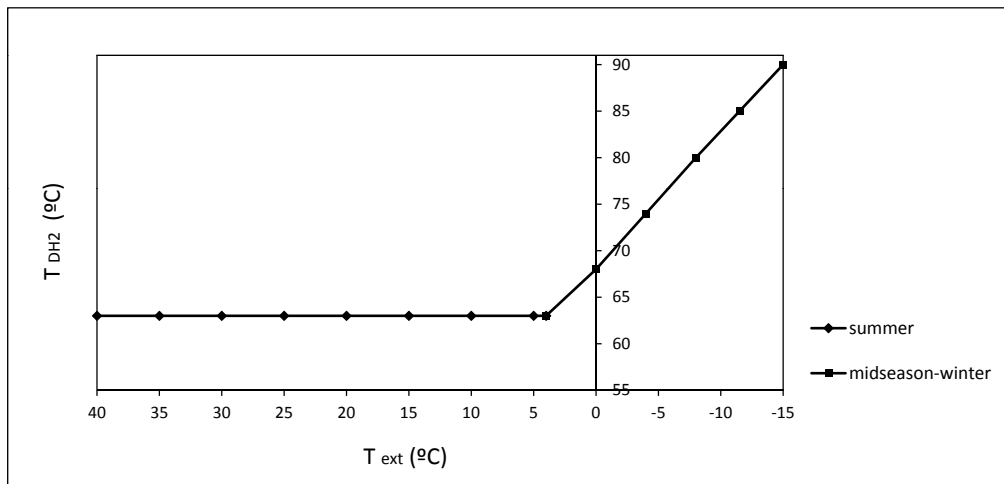
Figure 3.14: Heating curve for the secondary network. [32], Source: FERNWÄRME WIEN GmbH, Wien Energie [126].

- Highest value = 90°C, corresponding to -15 °C ambient temperature.

- Lowest value = 63°C, corresponding to an external temperature of 4 °C. From there onward the value of 63 °C remains constant.

Other important considerations at operation level, related with temperature management [126]:

- Flow Temperatures: The minimum flow temperatures specified in the heating curves are guaranteed by the district heating and must be used for dimensioning. The maximum flow temperatures at the secondary side can temporarily happen and must always be managed by the customer. On the primary side, very small volume flows can happen, leading to temperature fluctuations in the secondary flow.

- Design temperatures from radiators: For newly constructed objects with a specific heating demand $\leqslant 50\,\mathrm{kWh}/(\mathrm{m}^2\,\mathrm{a})$ (energy certificate class B or better), feed temperature to radiators is limited to $60°\mathrm{C}$ flow temperature. Respect to distribution losses for energy efficient heating systems, this results in a standard design of 60/40. Similar values are also a pre-requisite for the economic operation of condensing boilers and heat pumps, corresponding to the state-of-the-art technologies.

- Return temperatures from radiators: The return temperatures to be adhered depend on the building substance. Generally, the lowest possible design temperature is desirable. Higher temperatures are only permitted for existing properties with poor thermal insulation (historical buildings, old residential public dwellings, etc). The used characteristics are the transfer coefficient "U-value" as an average value of the building envelope and the annual heating demand according to the energy certificate (as a measure of the quality of the thermal insulation).

- Return temperatures from domestic hot water branch: The specified maximum return temperature does not apply to the pure recirculation operation. For this time without hot water extraction and no storage charge, a return temperature of up to 3 K higher than the circulation temperature is allowed.

- Storage tanks: By using a storage tank, the return temperature of the domestic hot water branch system should not be raised. Basically, a buffer should dampen the daily, house-side load peaks. In addition, the charge must not be made at the time of the daily peak performance. Concerning Legionella issues, it is important to know that from a certain outdoor temperature (usually around $16°\mathrm{C}$) the temperature should never fall below $60°\mathrm{C}$. Legionella bacteria are able to grow in water systems in contact with air at medium to high temperatures, specially if the water is stored, remaining in a tank or any similar configuration , obeying Austrian regulation [101] and [102]

With reference to pressure regulation, the case study follows a clear tree structure, with the substation as starting point followed by a main stream (Figure 3.15, FH), which divides off in such a way that each consumption point has its own branch, one stream for feed and the other for return. This hydraulic system and its components are easily explained by the following diagram:
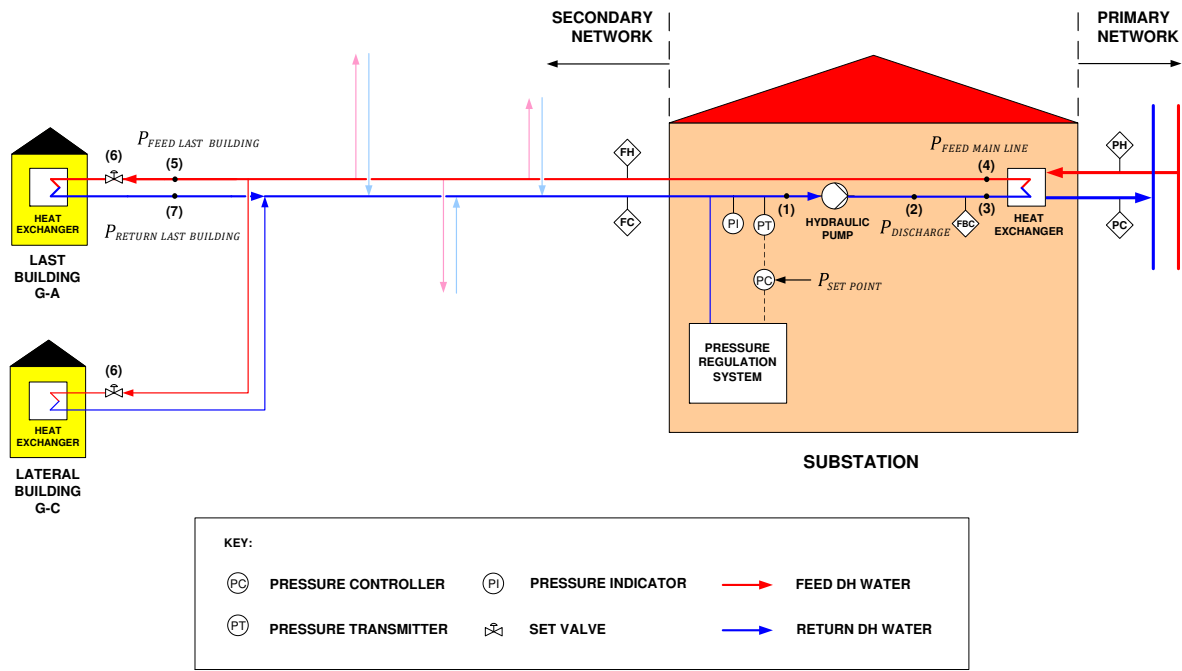
Figure 3.15: Hydraulic system of the secondary network. [32].

Following previous explanations concerning pressure control in hydraulic networks (see figure 2.54), the hydraulic balance is defined:
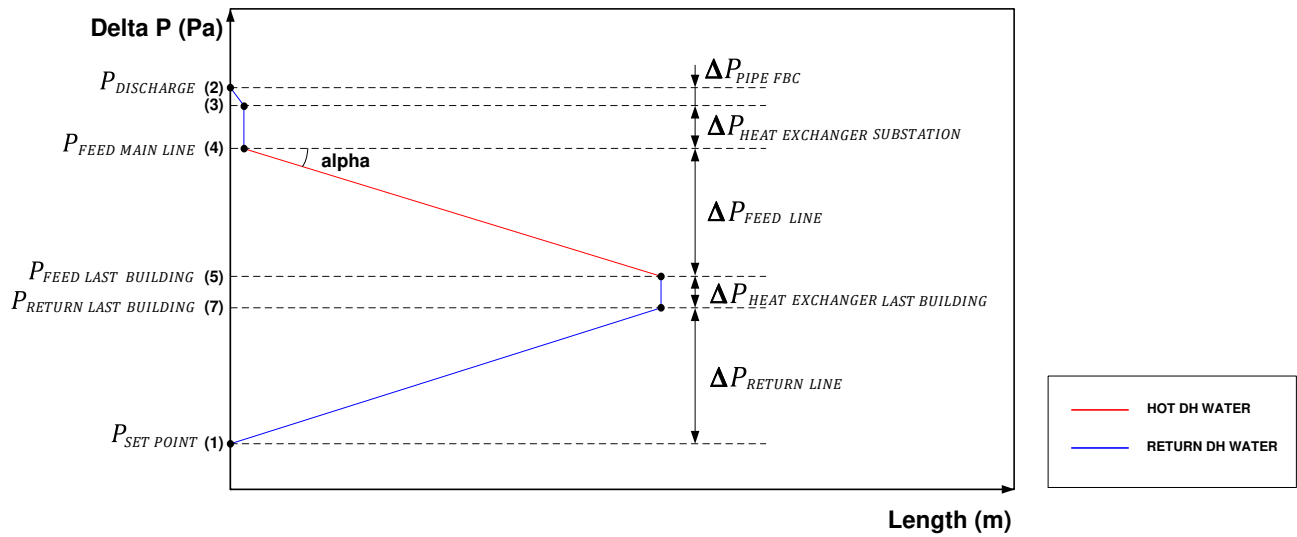
Figure 3.16: Hydraulic balance calculation. [32].

The minimum pressure of the system (Figures 3.15 and 3.16, point 1; $P_{SET\ POINT}$ = 3 bar), is fixed using an unpressurised tank with pump and overflow rate.

In the next step, the main hydraulic line is established: it links the impulsion point of the pump (Figures 3.15 and 3.16, point 2, $P_{DISCHARGE}$) with the last building of the network (Figures 3.15

and 3.16, point 5; $P_{FEED\,LAST\,BUILDING}$). In this way, the length of the pipe to be taken into account when calculating pressure losses ($\Delta P_{FEED\,LINE}$) is defined.

In between, there is a short pipe called FBC connecting the hydraulic pump with the heat exchanger (Figures 3.15 and 3.16, points 2 and 3), giving rise to certain pressure losses ($\Delta P_{PIPE\,FBC}$). The abovementioned heat exchanger also generates pressure losses (Figures 3.15 and 3.16, points 3 and 4; $\Delta P_{HEAT\,EXCHANGER\,SUBSTATION}$).

The water flows through the entire length of the line, reaching the last consumption point (Figures 3.15 and 3.16, point 5, $P_{FEED\,LAST\,BUILDING}$), going into the building substation and losing pressure as it crosses through the heat exchanger (Figures 3.15 and 3.16, point 7, $P_{RETURN\,LAST\,BUILDING}$, generating $\Delta P_{HEAT\,EXCHANGER\,LAST\,BUILDING}$.

On the way back, the fluid crosses the pipes in the opposite direction, returning to point 1.

$$P_{DISCHARGE} = P_{SP} + \Delta P_{RL} + \Delta P_{HE-LB} + \Delta P_{FL} + \Delta P_{PIPE\,FBC} + \Delta P_{HE-S} \qquad (3.2)$$

Since $P_{DISCHARGE}$ is the discharge pressure after the hydraulic pump, P_{SP} is the set point pressure (minimum pressure of the system), ΔP_{RL} is the pressure loss of the return line, ΔP_{HE-LB} is the pressure loss of the heat exchanger of the last building, ΔP_{FL} is the pressure loss of the feed line, $\Delta P_{PIPE\,FBC}$ is the pressure loss of the FBC pipe, ΔP_{HE-S} is the pressure loss of the heat exchanger inside the general substation.

$$\alpha = \frac{\Delta P}{L} \qquad (3.3)$$

The angle α represents the relation between the pressure losses and the length for each element.

3.3 Studied Scenarios

After describing how the Viennese DHN works and the case study, we proceed to define and explain all the new hypotheses studied. Each of them constitutes a new configuration of the network for the aforementioned case study, which implies changes such as replacing some technologies with others, adding new devices connected to the network, or directly removing certain installations.

3.3.1 Scenario 1
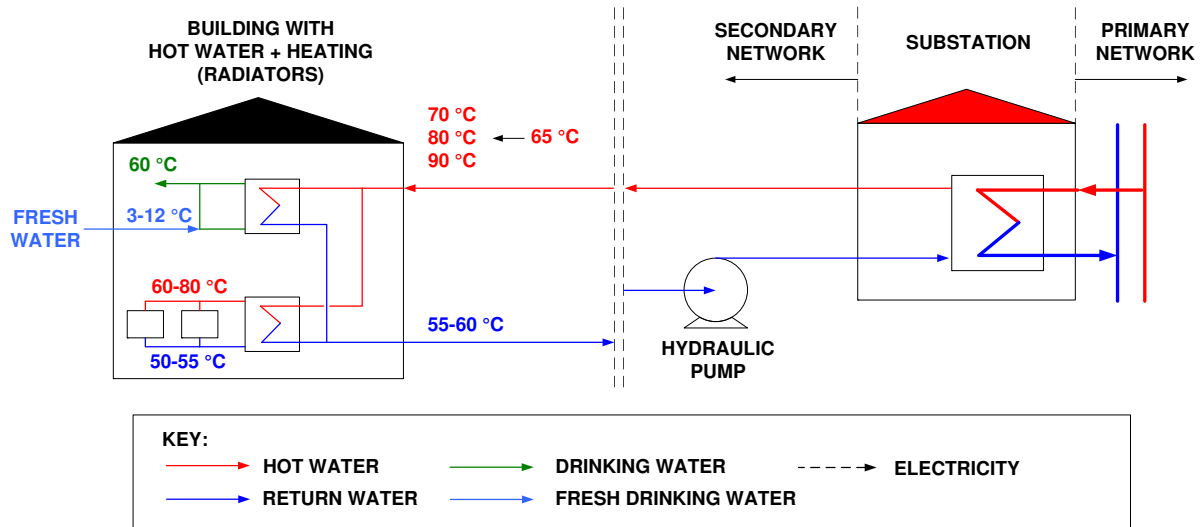
Figure 3.17: SCENARIO 1. Current situation.

- No modification in any building or installation

- Existing heating facilities: radiators

- Temperature regulation by the heating curve (see figure 3.14)

- Hot water production follows Austrian technical regulation ÖNORM B 5019 [102], establishing hot water for human consumption at 60 °C

3.3.2 Scenario 2
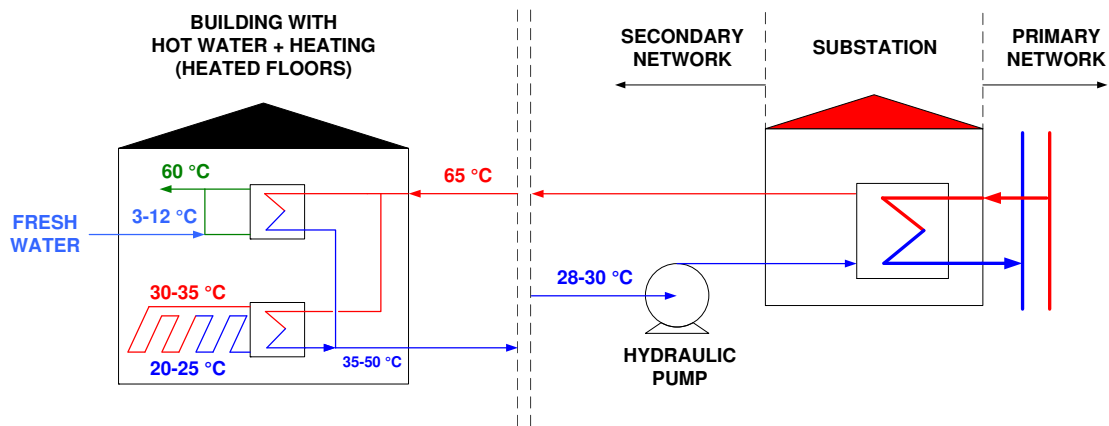
Figure 3.18: SCENARIO 2. Basic refurbishment.

- The radiators are substituted by heated floors for all the buildings

- DHN water temperature changes to 65 °C, constant for all the year

- Domestic hot water at 60 °C

3.3.3 Scenario 3
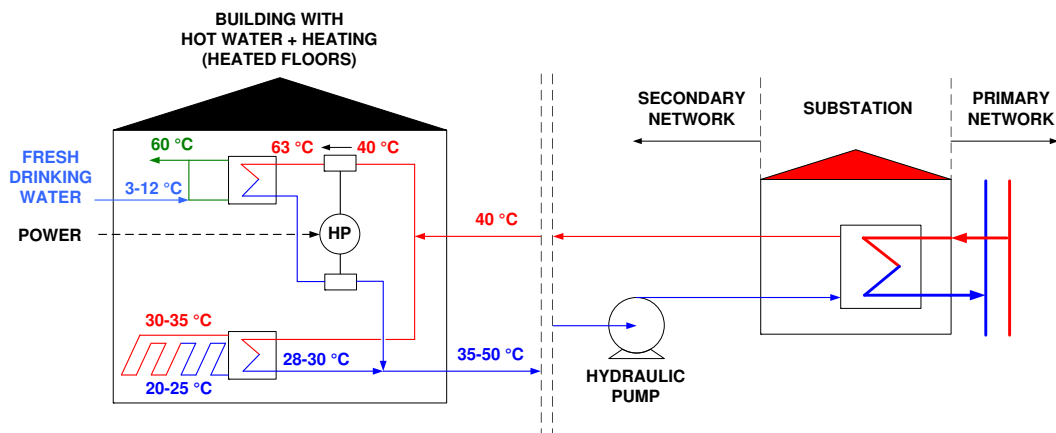
Figure 3.19: SCENARIO 3. Basic refurbishment for LTDHN.

- The radiators are substituted by heated floors for all the buildings

- DHN water temperature changes to 40 °C, constant for all the year (LTDHN)

- Domestic hot water at 60 °C

- In order to satisfy hot drinking water service, the temperature of network water needs to be increased from 40 to 63 °C, Therefore, a heat pump must be simulated, which will be connected next to the hot water heat exchanger

3.3.4 Scenario 4
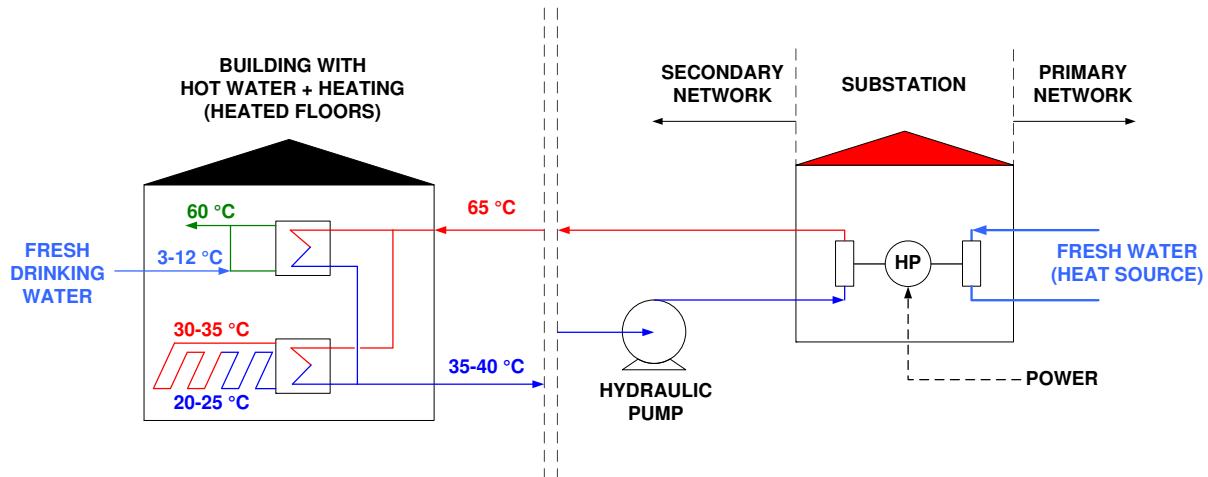
Figure 3.20: SCENARIO 4. Basic refurbishment and central heat pump in the substation.

- The radiators are substituted by heated floors for all the buildings

- DHN water temperature changes to 65 °C, constant for all the year

- Domestic hot water at 60 °C

- The heat exchanger of the general substation is replaced by a central heat pump

- The primary network is replaced by an anergy grid (e. g. river water, ground) to feed the heat pump

3.3.5 Scenario 5
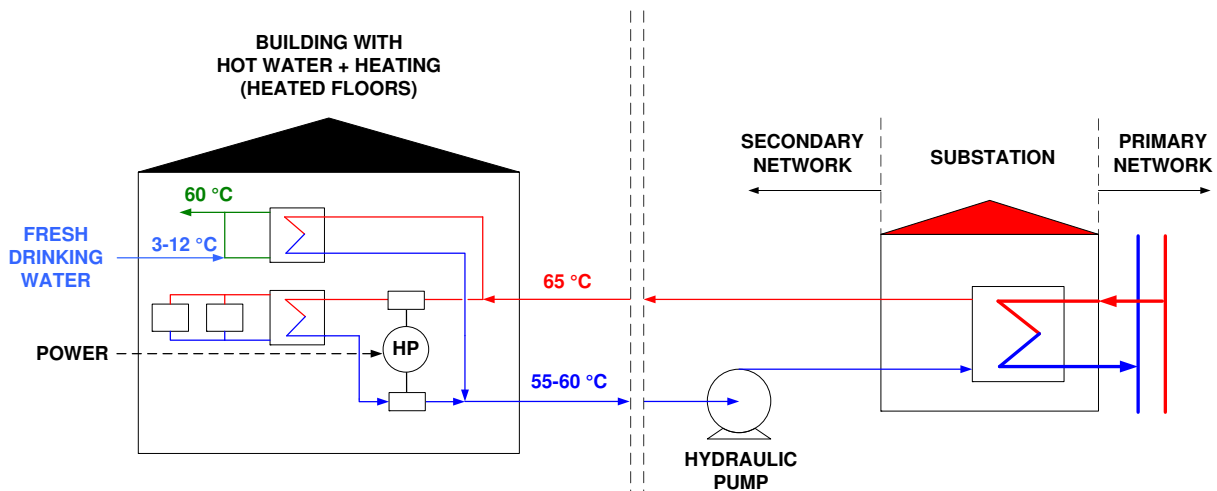
Figure 3.21: SCENARIO 5. Individual heat pumps for heating without refurbishment.

- DHN water temperature changes to 65 °C, constant for all the year

- Domestic hot water at 60 °C

- To satisfy high radiator temperatures for non-refurbished Viennese buildings, an increasing DHN water temperature from 65 to 90 °C is required. Therefore, a heat pump must be simulated, which will be connected next to the heating heat exchanger

3.3.6 Scenario 6
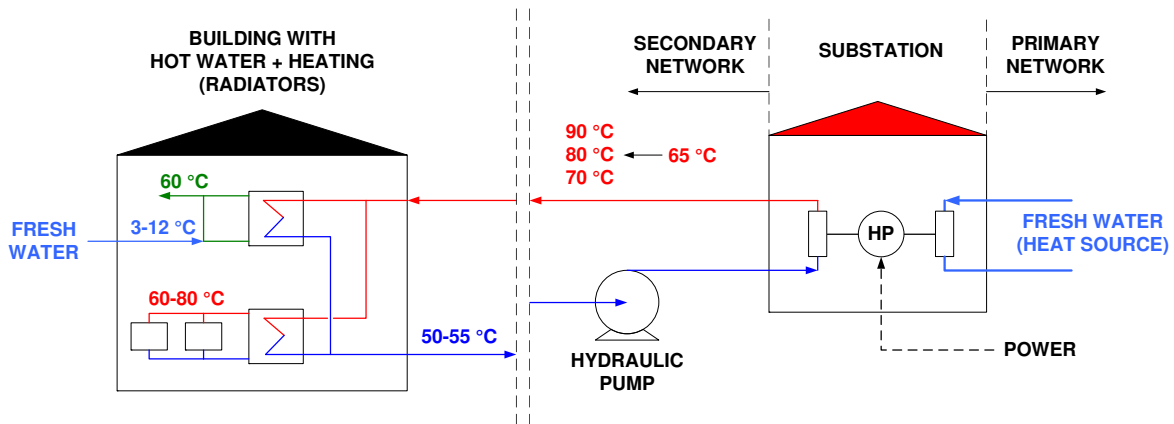
Figure 3.22: SCENARIO 6. Central heat pump without refurbishment.

- Temperature regulation by the heating curve (see figure 3.14, same as scenario 1)

- Domestic hot water at 60 °C

- The heat exchanger of the general substation is replaced by a central heat pump

- The primary network is replaced by an anergy grid (e.g. river water, ground) to feed the heat pump

3.3.7 Scenario 7
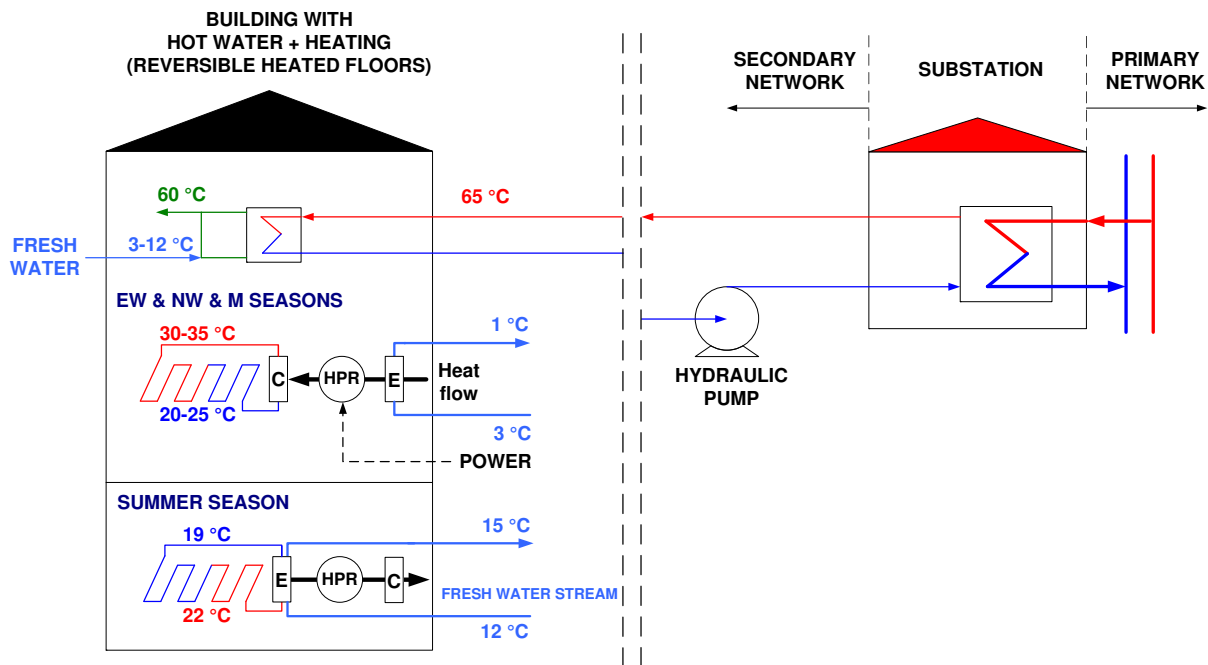
Figure 3.23: SCENARIO 7. Refurbishment installing reversible heat pumps for heating/cooling.

- The radiators are substituted by heated/cooled floors for all the buildings

- DHN water temperature changes to 65 °C, constant for all the year

- Domestic hot water at 60 °C

- To satisfy heated floors requirements for both warm and cold seasons, a reversible heat pump is installed. For cold seasons, the heat pump's evaporator extracts anergy from an external air or water source. For warm seasons, the heat pump's condenser turns into a simple heat exchanger, reducing radiant floor's temperature by exchanging heat with an external fresh water stream (12 °C or lower)

3.3.8 Scenario 8
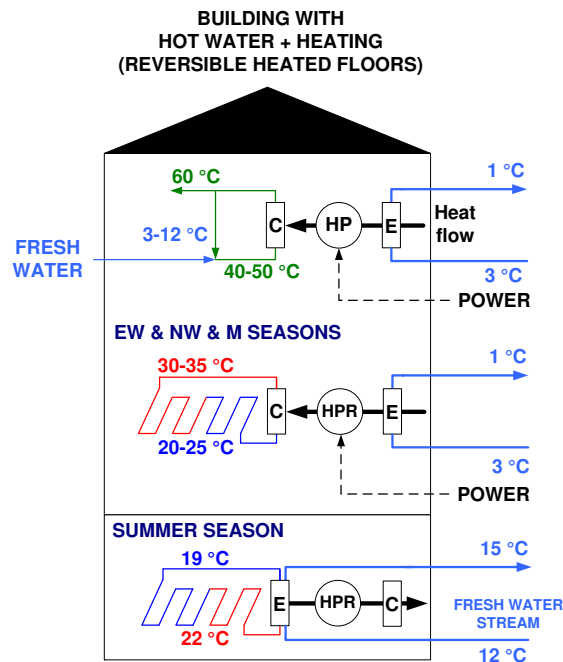
Figure 3.24: SCENARIO 8. Refurbishment with no DH.

- The radiators are substituted by heated/cooled floors for all the buildings

- In this case, there is no DHN

- Domestic hot water at 60 °C

- To satisfy hot water requirements, a heat pump; which uses a low temperature heat source, is installed.

- To satisfy heated floors requirements for both warm and cold seasons, a reversible heat pump is installed. For cold seasons, the heat pump's evaporator extracts anergy from an external air or water source. For warm seasons, the heat pump's condenser turns into a simple heat exchanger, reducing radiant floor's temperature by exchanging heat with an external fresh water stream (12 °C or lower)

The text, pictures and tables described in this chapter (specially sections 3.1 and 3.2) are also included in the book "Urban Energy Systems for Low-Carbon Cities" [32], being Mario Potente Prieto the author of these texts, pictures and other materials.

Chapter 4

Background

4.1   Defining Thermodynamic Systems and Variables

Due to the great complexity of the thermal networks and their large number of variables and parameters, it is necessary to delimit the boundaries of the thermodynamic systems and their corresponding mass, energy and exergy balances. In this way, the system will be subdivided into three fundamental areas with all the variables grouped. The end goal is to understand the behaviour of the DHN from the beginning (substation) to the final consumers (in the buildings).

Based on the information explained in sections 3.2.2 and 3.2.3, the operation of the system is defined, generating the following diagram:
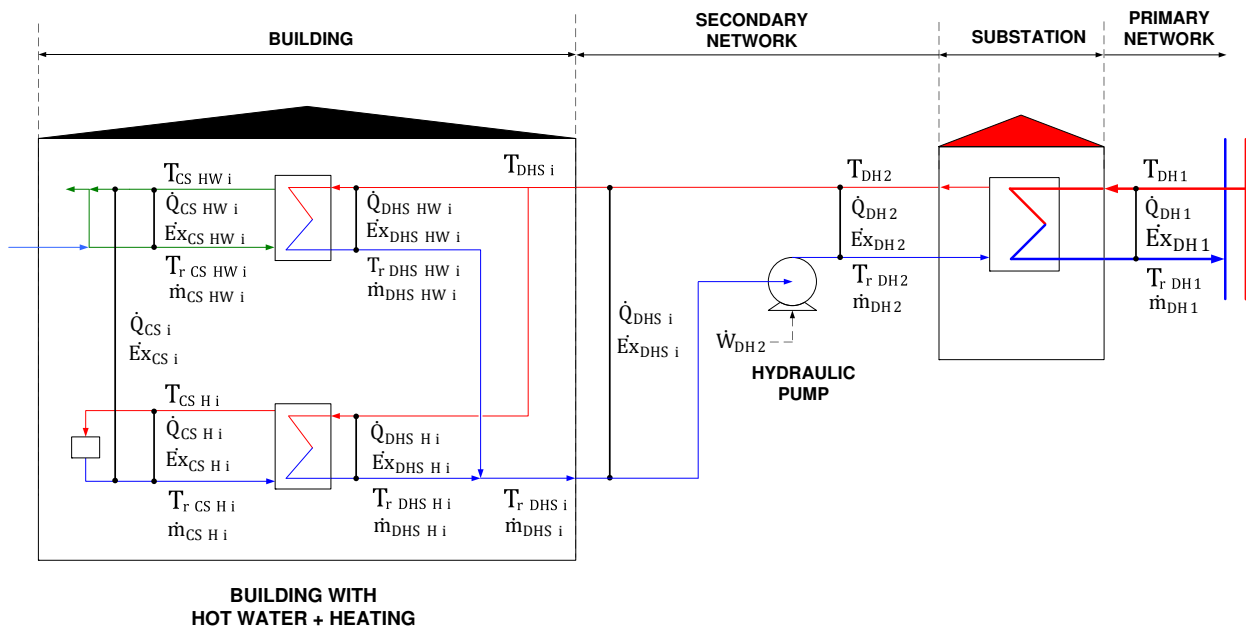
Figure 4.1: Detailed diagram showing the main variables for a local DHN

Which is translated into three independent subsystems and variables, including the corresponding links and connections:

112
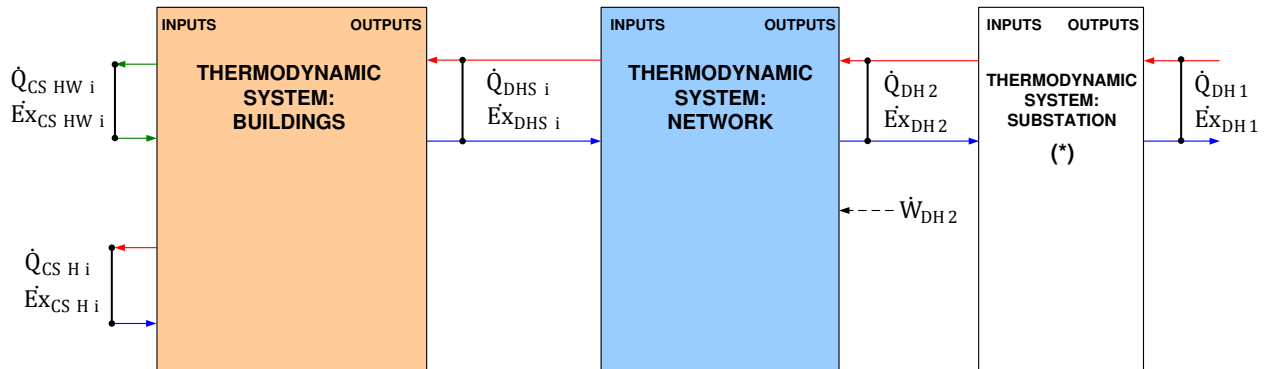
Figure 4.2: Division of the DHN into three thermodynamic systems, with their corresponding variables. (⋆) Although the substation subsystem is defined and appears in the figure, it has been considered in the calculations only in a partial way.

The terms of both figures 4.1 and 4.2 are hereunder explained:

Variables:

- T as the Temperature

- $\dot{m}$ as the Mass flow

- $\dot{Q}$ as the Heat flow

- $\dot{Ex}$ as the Exergy flow

- $\dot{W}$ as the Work flow

Subindexes:

- DH1 as the Primary District Heating

- DH2 as the Secondary District Heating

- DHS as the District Heating Side, before the heat exchanger

- CS as the Client Side, after the heat exchanger

- r as the Return line

- HW as the Hot Water Branch

- H as the Heating Branch

- i as the identifier number for each building

Due to the new scenarios raised in which heat pumps are included in the system (see section 3.3), new variables have to be considered:
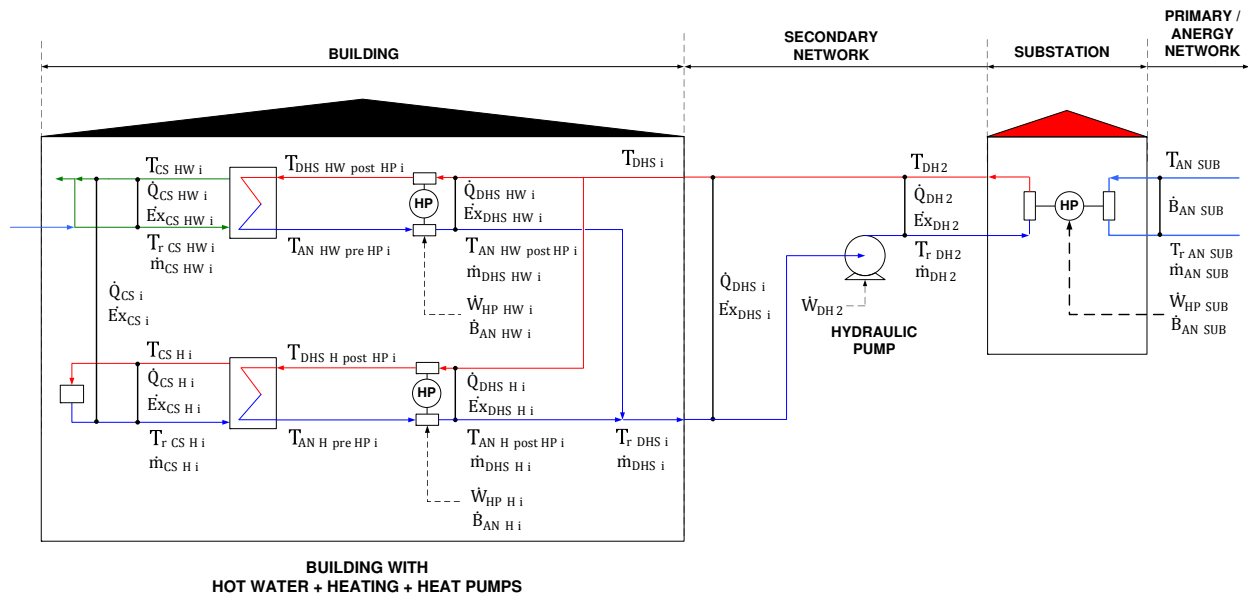
Figure 4.3: Detailed diagram extended, showing the main operation and thermodynamic variables for a local DHN

In this case, the terms of the figure 4.3 are hereunder explained:

Variables:

- $\dot{B}$ as the anergy flow

Subindexes:

- HP as the heat pump

- AN as the anergy Network

- sub as the substation

Again, the three independent subsystems and variables are defined, including the corresponding links and connections:
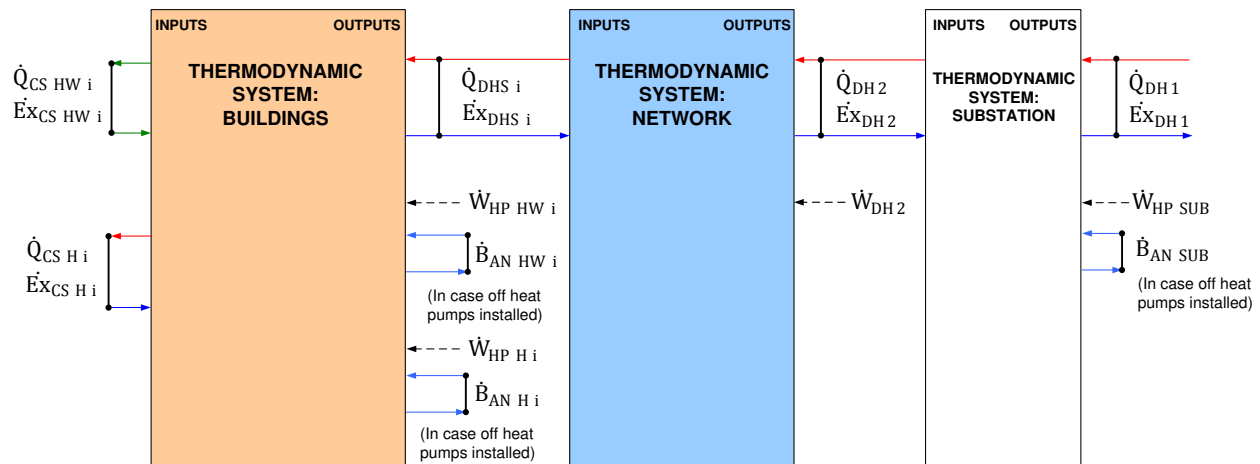
Figure 4.4: Division of the DHN into three thermodynamic systems, with their corresponding variables, heat pumps included

4.2 Main Equations

The behaviour of a thermal network can be described by a set of calculated variables resulting from applying hydraulic, energy and exergy balances. For example, to meet certain heat demand objectives, the system will adapt itself modifying variables such as DH water mass flow, feed temperature or return temperatures, and influencing in turn other variables such as heat losses or destroyed exergy. Each modification influences the hydraulics of the system and, at the end, the final efficiency of the overall installation.

The efficiency is another important indicator related to the behaviour of the system. It is defined as the ratio between supplied and incoming energy/exergy flows. This incoming energy may come either from a production stage or from an intermediate point in the network (heat exchanger, substation etc). Energy and exergy losses are considered to be a valid way to measure the performance of thermodynamic systems.

4.2.1 Global Mass Balance

Once the boundaries of the different thermodynamic systems have been delimited; and before raising any type of energy or exergy balance, it is necessary to quantify the mass flows at all points of the network. These values are not constant throughout the year, they can vary depending on the heat demand consumed in each building through the fundamental equation:

$$\dot{Q} = \dot{m}\,Cp\,(T_{feed} - T_{return}) \tag{4.1}$$

From which the two equations for each branch of service inside the building are obtained (see Figure 4.1):

$$\dot{Q}_{DHS\ HW\ i} = \dot{m}_{DHS\ HW\ i}\, Cp\, (T_{DHS\ i} - T_{r\ DHS\ i}) \tag{4.2}$$

$$\dot{Q}_{DHS\ H\ i} = \dot{m}_{DHS\ H\ i}\, Cp\, (T_{DHS\ i} - T_{r\ DHS\ i}) \tag{4.3}$$

Therefore, the mass flow ($\dot{m}$) will be considered as dependent variable of the energy demand, which will determine the operation of the simulation as we will see in chapter 5.2. In this way, the following equations are obtained:

- Mass balance for each building i:

$$\dot{m}_{DHS\ i} = \dot{m}_{DHS\ HW\ i} + \dot{m}_{DHS\ H\ i} \tag{4.4}$$

- Global mass balance:

$$\dot{m}_{DH2} = \sum_{i}^{n} \dot{m}_{DHS\ i} = \sum_{i}^{n} (\dot{m}_{DHS\ HW\ i} + \dot{m}_{DHS\ H\ i}) \tag{4.5}$$

4.2.2 Global Hydraulic Balance

The overall hydraulic or pressure balance has already been described in the equation (3.2):

$$P_{DISCHARGE} = P_{SP} + \Delta P_{RL} + \Delta P_{HE-LB} + \Delta P_{FL} + \Delta P_{PIPE\ FBC} + \Delta P_{HE-S} \tag{4.6}$$

With the respective equations to calculate the pressure drop for both branches:

$$\Delta P_{RL} = \sum_{i}^{n} \Delta P_{RL\ PIPE\ i} \tag{4.7}$$

$$\Delta P_{FL} = \sum_{i}^{n} \Delta P_{FL\ PIPE\ i} \tag{4.8}$$

This balance will define the hydraulic pump model (hydraulic pump block). The estimation of the different pressure drops is explained in the pipe model (DH pipe block). Both models will appear later in section 4.3.4.

4.2.3 Global Energy Balance

From here, each balance is applied to its corresponding thermodynamic system, obtaining the following equations:

- Substation:

$$\dot{Q}_{losses\ SUBSTATION} = \dot{Q}_{DH1} - \dot{Q}_{DH2} \tag{4.9}$$

$$\eta_{ENERGY\ SUBSTATION} = \frac{\dot{Q}_{DH2}}{\dot{Q}_{DH1}} \tag{4.10}$$

- Network

$$\dot{Q}_{losses\ NETWORK} = \dot{Q}_{DH2} + \dot{W}_{DH2} - \sum_{i}^{n} \dot{Q}_{DHS\ i} \tag{4.11}$$

$$\eta_{ENERGY\ NETWORK} = \frac{\sum_{i}^{n} \dot{Q}_{DHS\ i}}{\dot{Q}_{DH2} + \dot{W}_{DH2}} \tag{4.12}$$

- Buildings

$$\dot{Q}_{losses\ BUILDINGS} = \sum_{i}^{n} \dot{Q}_{DHS\ i} - \sum_{i}^{n} \dot{Q}_{CS\ HW\ i} - \sum_{i}^{n} \dot{Q}_{CS\ H\ i} \tag{4.13}$$

$$\eta_{ENERGY\ BUILDINGS} = \frac{\sum_{i}^{n} \dot{Q}_{CS\ HW\ i} - \sum_{i}^{n} \dot{Q}_{CS\ H\ i}}{\sum_{i}^{n} \dot{Q}_{DHS\ i}} \tag{4.14}$$

It has been assumed that the heat exchangers in the buildings and in the substation are totally isolated; thus, heat losses are negligible in those cases. However, although the pipes are isolated and buried, there are certain pipeline heat losses that must be taken into consideration. Therefore, only equations 4.11 and 4.12 are considered.

4.2.4 Exergy Method

It seems logical to affirm that energy balance and energy efficiency must be considered when evaluating the efficiency of a given thermodynamic system, but why is the exergy balance included in these studies as well? Why is the destroyed exergy so important to evaluate the efficiency of a thermal system?

Essentially, exergy refers to the potential utility of a particular energy source. It is also defined as the maximum theoretical work that could be obtained from the interaction between a certain thermodynamic system and the reference environment. If the state of a quantity of matter is different from that of the environment, there will be the possibility of producing work. As the system evolves towards equilibrium with the environment, this possibility will be reduced [127]. In other words,

exergy is the work available to be used. After the system and surroundings reach the equilibrium, the exergy value is zero [128].

The "reference" is related to a portion of the environment whose intensive properties do not change significantly as a result of any thermodynamic process. In this study, "reference environment" to the DHN is the existing air inside the trench where the pipes are installed. It is considered as a constant value, $T_0 = 281.15$ K.

To calculate the exergy flow attached to the different constituent elements of a DHN, it is necessary to first define the different forms of exergy and their expressions, obtained in turn from the bibliographic sources [127], [129] and [130].

- Exergy of a closed system:

  A closed thermodynamic system does not exchange mass, but rather, energy flow with the environment. The following expression is obtained:

$$Ex = m_{cv} \left[(U - U_0) + P_0(V - V_0) - T_0(s - s_0) + \frac{c^2 - c_0^2}{2} + g\,(z - z_0) \right] \qquad (4.15)$$

  With Ex as the exergy of the system, m_{cv} as the mass in the system, U representing the specific internal energy of the mass in the system, V the specific volume of the mass in the system and s as the specific entropy of the mass in the system. Sub-index 0 represents the correspondent variable (U_0, V_0, h_0, s_0) at reference pressure and temperature conditions (P_0, T_0), whose will be explained later.

  Neglecting the variations of kinetic and potential energy, the expression remains:

$$Ex = m_{cv} \left[(U - U_0) + P_0(V - V_0) - T_0(s - s_0) \right] \qquad (4.16)$$

- Exergy associated to a mass flow:

  In this case, the system is a fixed volume through which a certain flow of matter flows in the form of a current, generating an exergy flow $\dot{Ex}$ and giving rise to the following expression:

$$\dot{Ex} = \dot{m}_{cv} \left[(h - h_0) - T_0(s - s_0) \right] \qquad (4.17)$$

  Since $\dot{m}_{cv}$ is the mass flow crossing the control volume by time unit, and h is the specific enthalpy of the mass flow. Again, the variations of kinetic and potential energy are neglected.

- Exergy transfer associated with a heat flow:

  This is the maximum usable theoretical work $\dot{Ex}_Q$ that could be obtained from the stated heat when it is exchanged with the environment. It is strongly related to Carnot's performance.

$$\dot{Ex}_Q = \int_1^2 \left(1 - \frac{T_0}{T_F} \right) d\dot{Q} \qquad (4.18)$$

  With T_F as the temperature at the external boundary of the thermodynamic system.

- Exergy transfer associated with work:

  This is the maximum usable theoretical work $\dot{Ex}_W = \dot{W}_{useful,max}$ in a thermodynamic process associated to the work flow $\dot{W}$.

- Exergy yield:

  It is defined as the quotient between the exergy which leaves the thermodynamic system and is used for the user and the total exergy provided to the system:

$$\eta_{EX} = \frac{Useful\ exergy\ finally\ supplied\ to\ the\ consumers}{Total\ supplied\ exergy} \tag{4.19}$$

The principal exergy balances applied to the different thermodynamic systems are constituted below.

- Exergy balance for a closed thermodynamic system:
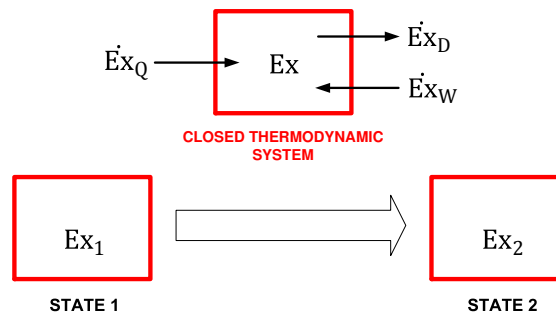
Figure 4.5: Exergy balance for a closed thermodynamic system

As appears in figure 4.5, the closed thermodynamic systems moves from the initial state (STATE 1) to the final state (STATE 2). There is no exchange of mass, but the system exchanges energy with the environment, giving rise to the expression below:

$$Ex_2 - Ex_1 = \int_1^2 \left(1 - \frac{T_0}{T_F}\right) dQ + W - T_0\, m_{cv}\, \sigma \tag{4.20}$$

with σ as the internal entropy generation term and Ex_1 and Ex_2 as the exergy of the system in the initial and final state, respectively.

This is the exergy balance expression for a control volume, which shows how the exergy varies when the system evolves from STATE 1 to STATE 2. Exergy increases in the following cases:

1. By receiving usable work, which is complete exergy

2. By receiving heat flow, which has only one part which contributes to the exergy

And decreases by the internal entropy generation [127].

Therefore, equation 4.20 is simplified:

$$Ex_2 - Ex_1 = Ex_Q + Ex_W - Ex_D \tag{4.21}$$

With $Ex_D = T_0\, m_{cv}\, \sigma$ as the term relative to destroyed exergy. Solving Ex_D:

$$Ex_D = Ex_1 - Ex_2 + Ex_W + Ex_Q \tag{4.22}$$

Calculating the exergy efficiency:

$$\eta_{EX} = \frac{Ex_2}{Ex_1 + supplied\,Exergy\,(Ex_Q, Ex_W)} \tag{4.23}$$

- Exergy balance associated to a non-steady state open thermodynamic system:
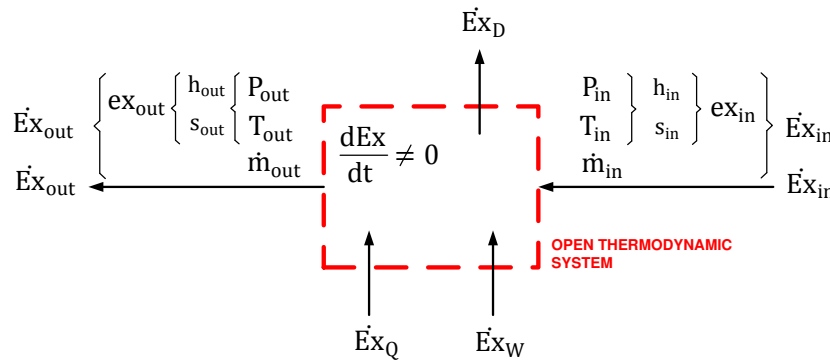
Figure 4.6: Exergy balance associated to a non-steady state open thermodynamic system

There is accumulation of mass inside the system. It could be possible that the system accumulates mass, energy or exergy but those variables are not necessarily coupled. From equation 4.20 the balance is obtained:

$$\sum_{j=1}^{n} \int_{1}^{2} \left(1 - \frac{T_0}{T_F}\right) dQ_j + W_{rev} + W_{irr} + \sum_{n\,inputs} (\dot{m}_{in}\, ex_{in}) - \sum_{n\,outputs} (\dot{m}_{out}\, ex_{out}) - \dot{Ex}_D = \frac{d\,Ex}{dt} \tag{4.24}$$

With j as the subscript related to each heat exchange point between the system and the environment, W_{rev} as the reversible work transported into the system, W_{irr} as the irreversible work transported into the system, and ex_{in} and ex_{out} are the specific exergy values relative to the pressure and temperature for each stream with respect to the reference values, defined by the following equations:

$$ex_{in} = h_{in} - h_0 - T_0(s_{in} - s_0) \tag{4.25}$$

$$ex_{out} = h_{out} - h_0 - T_0(s_{out} - s_0) \tag{4.26}$$

To simplify calculations, for steady state system the exergy flow associated with each stream is directly raised, subtracting the input minus the output, resulting in the expression:

$$\dot{Ex}_{stream} = \dot{m}_{stream\,in}\,ex_{in} - \dot{m}_{stream\,out}\,ex_{out} \tag{4.27}$$

In case of steady-state system, which will be explained later, the equality is written as it follows:

$$\dot{m}_{stream\,in} = \dot{m}_{stream\,out} \tag{4.28}$$

Hence, the following expression is defined for steady-state system:

$$\dot{Ex}_{stream} = \dot{m}_{stream}\,(ex_{in} - ex_{out}) \tag{4.29}$$

Expressing equation 4.24 in simplified form and clearing Ex_D:

$$\dot{Ex}_D = \sum_{n\,inputs} \dot{Ex}_{in} - \sum_{n\,outputs} \dot{Ex}_{out} + \dot{Ex}_W + \sum_{j=1}^{n} \dot{Ex}_Q - \frac{d\,Ex}{dt} \tag{4.30}$$

Simplifying even more:

$$\dot{Ex}_D = \dot{Ex}_{in} - \dot{Ex}_{out} + \dot{Ex}_W + \dot{Ex}_Q - \frac{d\,Ex}{dt} \tag{4.31}$$

And calculating Exergy efficiency:

$$\eta_{EX} = \frac{\dot{Ex}_{out} + \frac{d\,Ex}{dt}}{\dot{Ex}_{in} + supplied\,Exergy(\dot{Ex}_Q, \dot{Ex}_W)} \tag{4.32}$$

Where $\dot{m}_{stream\,in}$ and $\dot{m}_{stream\,out}$ are the input and output mass flows entering or leaving the control volume, and $\frac{d\,Ex}{dt}$ is the accumulation of exergy inside the control volume.

- Exergy balance associated to a steady state open thermodynamic system:
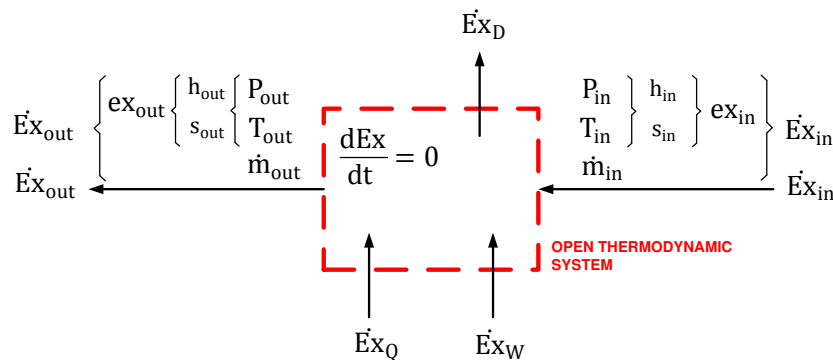
Figure 4.7: Exergy balance associated to a steady state open thermodynamic system

There is no mass variation inside the control volume, from the 4.20 the following expression is obtained:

$$\sum_{j=1}^{n} \int_{1}^{2} \left(1 - \frac{T_0}{T_F}\right) dQ_j + W_{rev} + W_{irr} + \sum_{n\,inputs} (\dot{m}_{in}\,ex_{in}) - \sum_{n\,outputs} (\dot{m}_{out}\,ex_{out}) - \dot{E}x_D = 0 \qquad (4.33)$$

In the same way as before, the expression 4.33 can be simplified:

$$\dot{E}x_D = \sum_{n\,inputs} \dot{E}x_{in} - \sum_{n\,outputs} \dot{E}x_{out} + \dot{E}x_W + \sum_{j=1}^{n} \dot{E}x_Q \qquad (4.34)$$

Simplifying even further:

$$\dot{E}x_D = \dot{E}x_{in} - \dot{E}x_{out} + \dot{E}x_W + \dot{E}x_Q \qquad (4.35)$$

And calculating the Exergy efficiency:

$$\eta_{EX} = \frac{\dot{E}x_{out}}{\dot{E}x_{in} + supplied\,Exergy(\dot{E}x_Q, \dot{E}x_W)} \qquad (4.36)$$

Once all equations are theoretically described, this theory must be applied to all those main systems related to DH networks, defining a set of expressions which constitute the exergetic method.

Applying the previous theoretical balance to our real systems, the following expressions are obtained:

- Exergy balance for a heat exchanger:

  The heat exchanger is considered as an open steady state thermodynamic system that exchanges matter and thermal energy. It is applied to all types of substations, and, in general, to all kinds of heat exchange points.
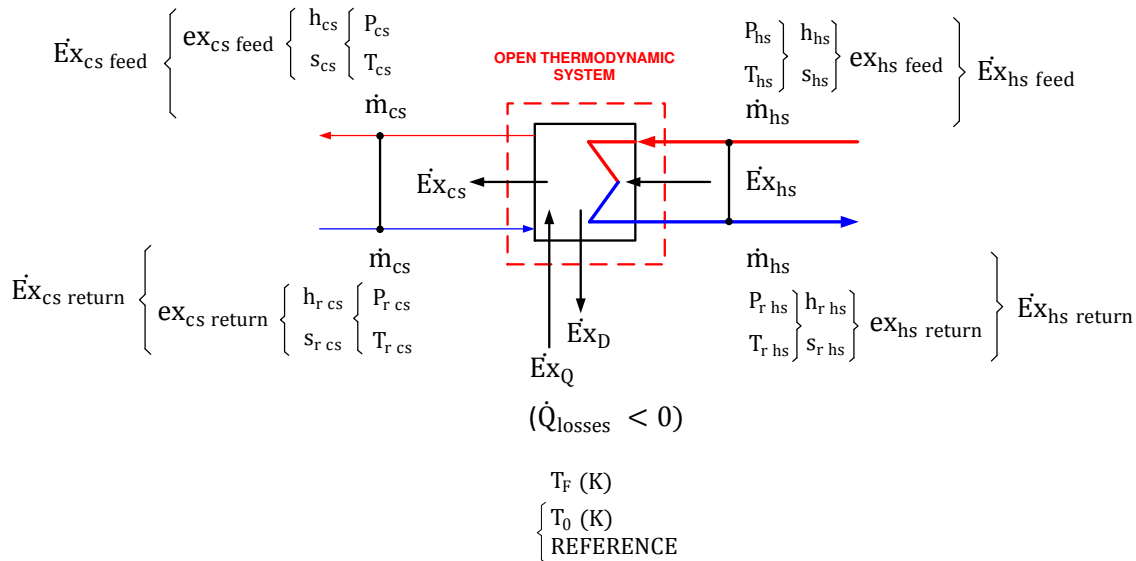
Figure 4.8: Exergy method applied to a heat exchanger.

Subscripts *hs* and *cs* are the hot and the cold side of the heat exchanger, $T_0 = 8°C$ as the reference temperature, corresponding to the average temperature of the trench where the DH pipes are installed, and $T_F = 13°C$ is the external temperature of the boundary that delimits the thermodynamic system, corresponding to the DH substations where the heat exchangers are located. During the calculations, both temperatures have to be expressed in K. The exergy balance applied to this system will be the one corresponding to the equation 4.35, following the sign criterion corresponding to Figure 4.8.

$$\dot{E}x_D = \dot{E}x_{hs} - \dot{E}x_{cs} + \dot{E}x_W + \dot{E}x_Q \tag{4.37}$$

$\dot{E}x_{hs} > 0$, inlet to the control volume

$\dot{E}x_{cs} > 0$, outlet from the control volume and is useful to the user.

$\dot{E}x_W = 0$, no work transferred to the system.

$\dot{E}x_Q = 0$, heat losses are leaving the control volume and are useless.

Where:

$$\dot{E}x_{cs} = \dot{m}_{cs} \cdot \left(ex_{cs\ feed} - ex_{cs\ return}\right) \tag{4.38}$$

$$\dot{E}x_{hs} = \dot{m}_{hs} \cdot \left(ex_{hs\ feed} - ex_{hs\ return}\right) \tag{4.39}$$

From equation 4.18 and assuming that the heat exchanger is totally isolated ($\dot{Q}_{losses} = 0$), $\dot{E}x_Q$ is calculated:

$$\dot{E}x_Q = \int_1^2 \left(1 - \frac{T_0}{T_F}\right) d\dot{Q} = \left(1 - \frac{8 + 273.15}{13 + 273.15}\right) \cdot 0 = 0 \tag{4.40}$$

In this case, $d\dot{Q} = \dot{Q}_{losses} = 0$

Finally, the exergy balance for the heat exchanger will be:

$$\dot{E}x_D = \dot{E}x_{hs} - \dot{E}x_{cs} \tag{4.41}$$

Calculating the exergy efficiency:

$$\eta_{EX} = \frac{\dot{E}x_{cs}}{\dot{E}x_{hs}} \tag{4.42}$$

- Exergy balance for a pipeline network:
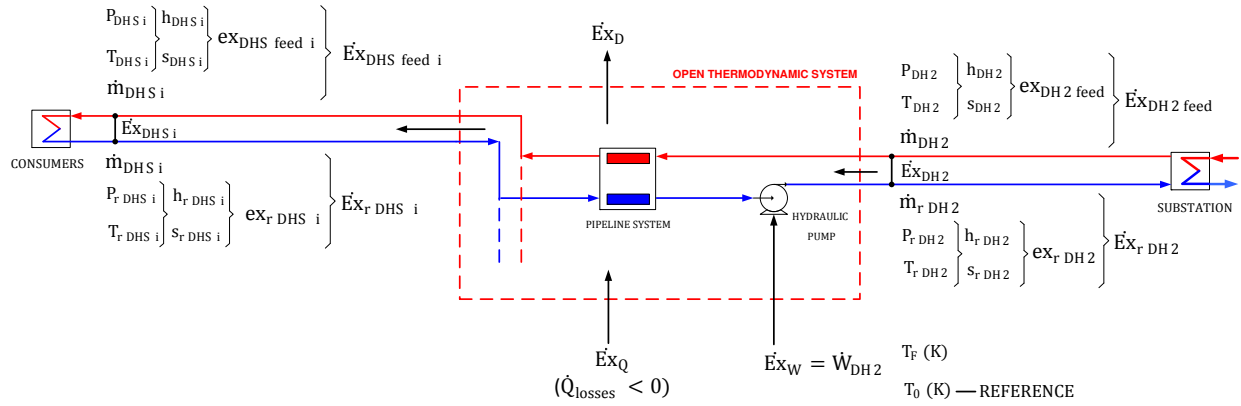
Figure 4.9: Exergy method applied for a DHN pipeline system.

The pipeline network is considered as an open steady-state thermodynamic system that exchanges mass and heat with the environment. It is applied to the entire pipe and branches segment located between substations (see 4.9).

Taking $T_0 = 8°C$ as the reference temperature, corresponding to the average temperature of the trench where the DH pipes are installed, which means that, in this case, T_0 and T_F have the same value.

The exergy balance applied to this system will be modified for a single mass input and several outputs, following the sign criterion corresponding to Figure 4.9:

$$\dot{Ex}_D = \dot{Ex}_{DH2} - \sum_{i=1}^{n\,outputs} \dot{Ex}_{DHS\,i} + \dot{Ex}_W + \dot{Ex}_Q \tag{4.43}$$

$\dot{Ex}_{DH2} > 0$, as inlet to the control volume

$\sum_{i=1}^{n\,outputs} \dot{Ex}_{DHS\,i} > 0$, outlet from the control volume and is useful to the user.

$\dot{Ex}_W > 0$, an input to the control volume, as power for the hydraulic pump.

Where:

$$\dot{Ex}_{DHS\,i} = \dot{Ex}_{DHS\,feed\,i} - \dot{Ex}_{r\,DHS\,i} \tag{4.44}$$

$$\dot{Ex}_{DH2} = \dot{Ex}_{DH2\,feed} - \dot{Ex}_{r\,DH2} \tag{4.45}$$

Again, based on equation 4.18 and considering the values T_0 and T_F, $\dot{Ex}_Q$ is estimated:

$$\dot{Ex}_Q = \int_1^2 \left(1 - \frac{T_0}{T_F}\right) d\dot{Q} = \left(1 - \frac{8 + 273.15}{8 + 273.15}\right) \cdot \dot{Q}_{losses\,DHN} = 0 \tag{4.46}$$

So, the expression for the entire pipeline system will be:

$$\dot{E}x_D = \dot{E}x_{DH2} - \sum_{i=1}^{n\,outputs} \dot{E}x_{DHSi} + \dot{E}x_W \tag{4.47}$$

So, the expression for the exergy efficiency will be:

$$\eta_{EX} = \frac{\sum_{i=1}^{n\,outputs} \dot{E}x_{DHSi}}{\dot{E}x_{DH2} + \dot{E}x_W} \tag{4.48}$$

4.2.5 Global Exergy Balance

As previously explained using the exergy method 4.2.4, equations 4.47, 4.48, 4.41, 4.42 and following figure 4.2, the exergy balances are obtained. All of them are attached to their corresponding thermodynamic systems:

- Substation:

$$\dot{E}x_{losses\ SUBSTATION} = \dot{E}x_{DH1} - \dot{E}x_{DH2} \tag{4.49}$$

$$\eta_{EXERGY\ SUBSTATION} = \frac{\dot{E}x_{DH2}}{\dot{E}x_{DH1}} \tag{4.50}$$

- Network

$$\dot{E}x_{losses\ NETWORK} = \dot{E}x_{DH2} + \dot{W}_{DH2} - \sum_{i}^{n} \dot{E}x_{DHS\ i} \tag{4.51}$$

$$\eta_{EXERGY\ NETWORK} = \frac{\sum_{i}^{n} \dot{E}x_{DHS\ i}}{\dot{E}x_{DH2} + \dot{W}_{DH2}} \tag{4.52}$$

- Buildings

$$\dot{E}x_{losses\ BUILDINGS} = \sum_{i}^{n} \dot{E}x_{DHS\ i} - \sum_{i}^{n} \dot{E}x_{CS\ HW\ i} - \sum_{i}^{n} \dot{E}x_{CS\ H\ i} \tag{4.53}$$

$$\eta_{EXERGY\ BUILDINGS} = \frac{\sum_{i}^{n} \dot{E}x_{CS\ HW\ i} + \sum_{i}^{n} \dot{E}x_{CS\ H\ i}}{\sum_{i}^{n} \dot{E}x_{DHS\ i}} \tag{4.54}$$

$$\dot{E}x_{losses\ BUILDINGS\ HW} = \sum_{i}^{n} \dot{E}x_{DHS\ HW\ i} - \sum_{i}^{n} \dot{E}x_{CS\ HW\ i} \tag{4.55}$$

$$\eta_{EXERGY\ BUILDINGS\ HW} = \frac{\sum_{i}^{n} \dot{E}x_{CS\ HW\ i}}{\sum_{i}^{n} \dot{E}x_{DHS\ HW\ i}} \tag{4.56}$$

$$\dot{Ex}_{losses\ BUILDINGS\ H} = \sum_{i}^{n} \dot{Ex}_{DHS\ HW\ i} - \sum_{i}^{n} \dot{Ex}_{CS\ HW\ i} \tag{4.57}$$

$$\eta_{EXERGY\ BUILDINGS\ H} = \frac{\sum_{i}^{n} \dot{Ex}_{CS\ H\ i}}{\sum_{i}^{n} \dot{Ex}_{DHS\ H\ i}} \tag{4.58}$$

Again, as previously explained using the exergy method, and following figure 4.4 in which all new devices and possibilities are included, the new equations are obtained:

- Substation:

$$\dot{Ex}_{losses\ SUBSTATION} = \dot{W}_{HP\ SUB} + \dot{Ex}_{AN\ SUB} - \dot{Ex}_{DH2} \tag{4.59}$$

$$\eta_{EXERGY\ SUBSTATION} = \frac{\dot{Ex}_{DH2}}{\dot{W}_{HP\ SUB} + \dot{Ex}_{AN\ SUB}} \tag{4.60}$$

- Network

  Same expressions as (4.51) and (4.52).

- Buildings

$$\dot{Ex}_{losses\ BUILDINGS} = \sum_{i}^{n} \dot{Ex}_{DHS\ i} - \sum_{i}^{n} \dot{Ex}_{CS\ HW\ i} - \sum_{i}^{n} \dot{Ex}_{CS\ H\ i}$$
$$+ \sum_{i}^{n} \dot{W}_{HP\ HW\ i} + \sum_{i}^{n} \dot{Ex}_{AN\ HW\ i} + \sum_{i}^{n} \dot{W}_{HP\ H\ i} + \sum_{i}^{n} \dot{Ex}_{AN\ H\ i} \tag{4.61}$$

$$\eta_{EXERGY\ BUILDINGS} = \frac{\sum_{i}^{n} \dot{Ex}_{CS\ HW\ i} - \sum_{i}^{n} \dot{Ex}_{CS\ H\ i}}{\sum_{i}^{n} \dot{Ex}_{DHS\ i} + \sum_{i}^{n} \dot{W}_{HP\ HW\ i} + \sum_{i}^{n} \dot{Ex}_{AN\ HW\ i} + \sum_{i}^{n} \dot{W}_{HP\ H\ i} + \sum_{i}^{n} \dot{Ex}_{AN\ H\ i}} \tag{4.62}$$

$$\dot{Ex}_{losses\ BUILDINGS\ HW} = \sum_{i}^{n} \dot{Ex}_{DHS\ HW\ i} - \sum_{i}^{n} \dot{Ex}_{CS\ HW\ i} + \sum_{i}^{n} \dot{W}_{HP\ HW\ i} + \sum_{i}^{n} \dot{Ex}_{AN\ HW\ i} \tag{4.63}$$

$$\eta_{EXERGY\ BUILDINGS\ HW} = \frac{\sum_{i}^{n} \dot{Ex}_{CS\ HW\ i}}{\sum_{i}^{n} \dot{Ex}_{DHS\ HW\ i} + \sum_{i}^{n} \dot{W}_{HP\ HW\ i} + \sum_{i}^{n} \dot{Ex}_{AN\ HW\ i}} \tag{4.64}$$

$$\dot{Ex}_{losses\ BUILDINGS\ H} = \sum_{i}^{n} \dot{Ex}_{DHS\ H\ i} - \sum_{i}^{n} \dot{Ex}_{CS\ H\ i} + \sum_{i}^{n} \dot{W}_{HP\ H\ i} + \sum_{i}^{n} \dot{Ex}_{AN\ H\ i} \tag{4.65}$$

$$\eta_{EXERGY\ BUILDINGS\ H} = \frac{\sum_{i}^{n} \dot{Ex}_{CS\ H\ i}}{\sum_{i}^{n} \dot{Ex}_{DHS\ H\ i} + \sum_{i}^{n} \dot{W}_{HP\ H\ i} + \sum_{i}^{n} \dot{Ex}_{AN\ H\ i}} \tag{4.66}$$

4.3   Defining District Heating Network's Models

In this section a detailed description of all DHN elements is made, as well as their corresponding representative models. The description contains not only the current elements but also those that would be hypothetically installed in the scenarios proposed (see section 3.3).

The models are grouped according to the three thermodynamic subsystems specified above (see figure 4.3 in section 4.1).

4.3.1   Data treatment

Before raising the equations and building models and simulations, a preliminary analysis and a treatment of the available data was carried out. This information will configure the input of the models, and it is divided into two main categories:

- Structural information of the network

  Several parameters are here described, which necessary to define the network and solve the equations. They are grouped into two main blocks: Buildings (see table A.1 and Pipes (see tables A.2, A.3 and A.4)

- Operation variables

  That is, the profiles of the main variables:

  - Mass flow, district heating side ($\dot{m}_{DHSi}$)
  - Feed temperature, district heating side (T_{DHSi})
  - Return temperature, district heating side (T_{rDHSi})

  All of them recorded over time at the rate of one value every 15 minutes, kindly provided by Wien Energie. For practical reasons, MATLAB will read and generate the profiles considering one value per hour. The data used comes from years 2012 and 2013.

As it will be explained in detail in chapter 5, the model is designed to calculate all operation variables, which depend on the heat demand for domestic hot water production and for heating needed by each building. Based on this, the mass flows of DH water required for each building will be obtained. Based on that, the mass, energy and exergy balances for the entire network will be calculated.

Several issues arised as the model design started, concerning the individual heat demand for each building. As explained before, this magnitude is fundamental and is the main input from which the resolution of the equation system that configures the DHN model begins.

This model is designed to calculate each branch of the DH service (hot water production and heating) for each building, however, the heat demand provided by Wien Energie is the total demand, it is not decoupled in the two specified branches. Given this circumstance, there are two possible strategies to solve this issue:

1. The model is prepared to receive the heat demand profile for each branch as input from an external source (maybe excel files or text files, maybe signals from another software). These profiles can be estimated using a variety of techniques and methods, for which a certain amount of information is required (number of inhabitants per building, meteorological history of the area, heat demand data from previous years, history and structural layout of the building, construction materials, characteristics of the installed heating system, exposure to the solar radiation, exposure to wind ... etc. All this work is not part of this doctoral thesis, although it is a research subject of the CI-NERGY project (see the CI-NERGY project book [32], chapters 3 and 4). Therefore, the methodology and the DH model explained here does not calculate the heat demand, but are prepared to receive these values from abroad. This is the main connection of this project with the rest of the CI-NERGY project.

2. The first option was unfortunately not possible. Therefore, and with the aim to solve the equations systems and obtain results, a calibration method was applied to obtain the dissociated heat demand profiles. This method consists of applying several multiplying factors on the pre-estimated hot water heat demand profiles ($\dot{Q}_{HD\,HW\,i}$), in such a way that by modifying these factors and then running the simulation, the calculated outputs are adjusted to the real values recorded and supplied by Wien Energie ($\dot{m}_{DHS\,i}$, $T_{DHS\,i}$ and $T_{r\,DHS\,i}$) . This profile was obtained using the expression:

$$\dot{Q}_{HD\,HW\,i} = \dot{Q}_{HD\,S\,i} \tag{4.67}$$

Based on the hypothesis that the domestic hot water consumption in summer is the same as during the rest of the year, since in summer the heating consumption is zero.

The initial treatment of the input data of the system is intended to correct peaks and imperfections produced by erroneous measurements, generating realistic profiles.

- Arithmetic average value of three values from 3 different days (3 working days or 3 non-working days) belonging to the period of the year under consideration. For example, considering $\dot{Q}_{HD\,i}$ for a working day :

$$\dot{Q}_{HD\,WD\,EW\,i} = \frac{\dot{Q}_{HD\,WD1\,EW\,i} + \dot{Q}_{HD\,WD2\,EW\,i} + \dot{Q}_{HD\,WD3\,EW\,i}}{3} \tag{4.68}$$

The same operation is made for the other seasons. Finally, the complete profile is defined:

$$\dot{Q}_{HD\,i} = \dot{Q}_{HD\,WD\,EW\,i} + \dot{Q}_{HD\,NWD\,EW\,i} + \dot{Q}_{HD\,WD\,NW\,i} + \dot{Q}_{HD\,NWD\,NW\,i}$$
$$+ \dot{Q}_{HD\,WD\,M\,i} + \dot{Q}_{HD\,NWD\,M\,i} + \dot{Q}_{HD\,WD\,S\,i} + \dot{Q}_{HD\,NWD\,S\,i}$$

- Low-pass filter: Data treatment procedure applied to eliminate the noise and oscillations for statistical distributions and profiles of values, characterized by allowing the passage of lower frequencies and attenuate the higher frequencies.

$$\dot{V}_{f\,(i)} = \frac{\dot{V}_{f\,(i-1)}(F-1) + \dot{V}_{(i)}}{F} \tag{4.69}$$

Since $\dot{V}_{f\,(i)}$ is the filtered value, $\dot{V}_{f\,(i-1)}$ is the previous filtered value of the serie, F is the frecuency, and $\dot{V}_{(i)}$ is the original value without filtering.

4.3.2 Auxiliar models

4.3.2.1 Water Properties
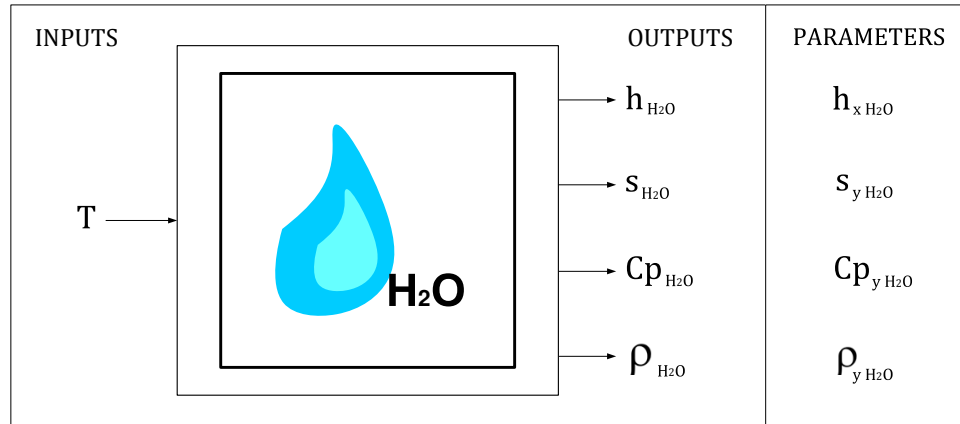
Figure 4.10: Block representing the calculation of the water properties

- Description: This is an auxiliary block used to calculate the physical properties of water extracted from the corresponding tables. For this model, the values were obtained from the XSTEAM Matlab function [131].

  To speed up the calculations, the water properties are only considered dependent on temperature, leaving out the pressure, which influence is not so important for incompressible fluids as in the actual case (liquid water). The output values are calculated by 1-dimensional linear interpolation using the Matlab function interp1, which calculates faster than 2-dimensional interpolation, allowing a shorter simulation time.

- Inputs:

  - $T_{x\,H2O}$ = Input temperature value, in K

- Parameters:

  - $T_{x\,H2O}$ = Temperature values, x axis of the interpolation, in K
  - $h_{y\,H2O}$ = Specific enthalpy of water values, y axis of the interpolation, in J/kg
  - $s_{y\,H2O}$ = Specific entropy of water values , y axis of the interpolation, in J/(kg K)
  - $Cp_{y\,H2O}$ = Specific calorific capacity of water, constant pressure, y axis of the interpolation, in J/(kg K)
  - $\rho_{y\,H2O}$ = Density of water values, y axis of the interpolation, in kg/m^3

- Outputs:

  - h_{H2O} = Specific enthalpy of water, output values, in J/kg
  - s_{H2O} = Specific entropy of water, output values, in J/(kg K)
  - Cp_{H2O} = Specific calorific capacity of water at constant pressure, output values, in J/(kg K)
  - ρ_{H2O} = Density of water, output values, in kg/m^3

4.3.2.2 Temperature Regulation
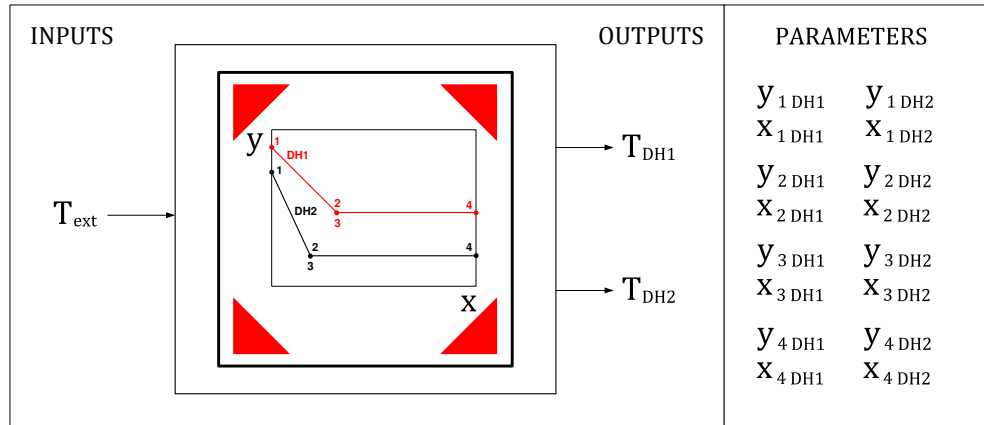
Figure 4.11: Block picture, representing the temperature regulation lines

- Description: Auxiliary block that calculates DH water temperatures for the primary and the secondary network. The block receives the coordinates of the four points which define the two lines that regulate both networks. These parameters are modifiable by the user. Those points and coordinates and lines are represented hereby:
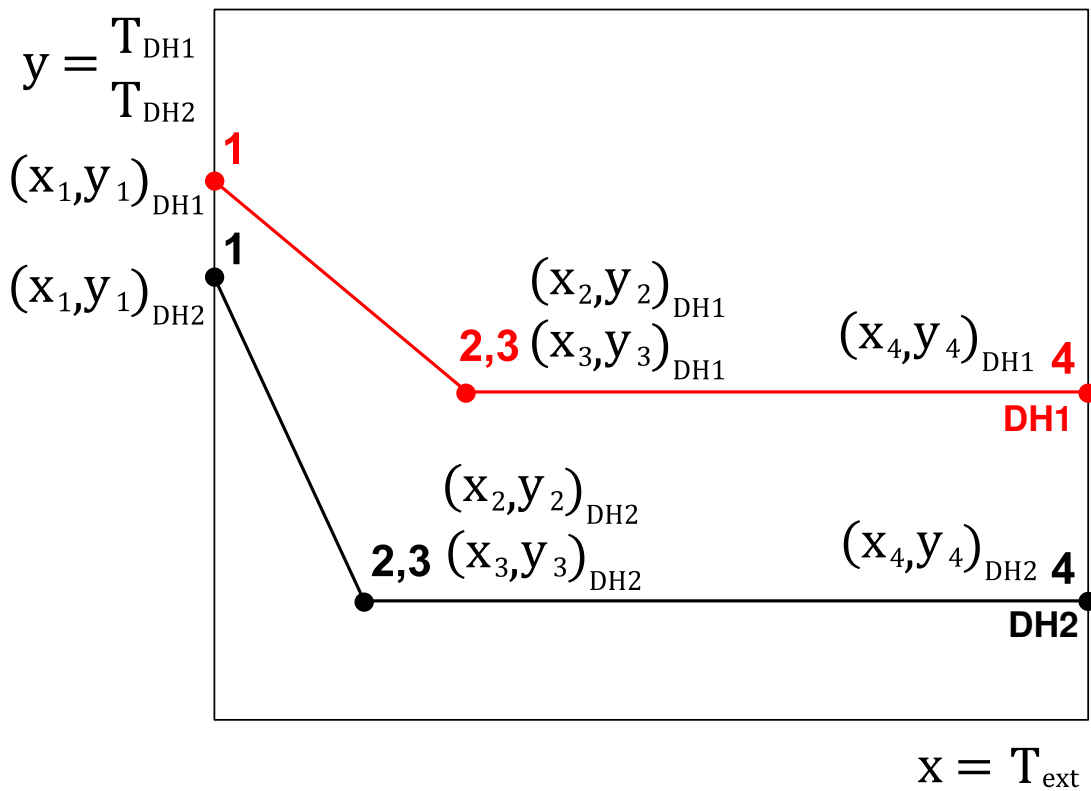
Figure 4.12: Temperature regulation lines for the primary and secondary DH networks

- Inputs:

  - T_{ext} = External temperature profile [=] K

- Parameters:

  - $y_{1,2,3,4\ DH1}$ = Point 1/2/3/4 of the primary network's linear equation, coord. y, in K
  - $x_{1,2,3,4\ DH1}$ = Point 1/2/3/4 of the primary network's linear equation, coord. x, in K
  - $y_{1,2,3,4\ DH2}$ = Point 1/2/3/4 of the secondary network's linear equation, coord. y, in K
  - $x_{1,2,3,4\ DH2}$ = Point 1/2/3/4 of the secondary network's linear equation, coord. x, in K

- Outputs:

  - T_{DH1} = DH water temperature, primary network, in K
  - T_{DH2} = DH water temperature, secondary network, in K

- System of equations:

  1. Calculation of the parameters of the linear equations (Sl = Slope, In = Intercept):

$$Sl_{DH1} = \frac{y_{1\ DH1} - y_{2\ DH1}}{x_{1\ DH1} - x_{2\ DH1}} \tag{4.70}$$

$$In_{DH1} = y_{1\ DH1} - Sl_{DH1} \cdot x_{1\ DH1} \tag{4.71}$$

$$Sl_{DH2} = \frac{y_{1\ DH2} - y_{2\ DH2}}{x_{1\ DH2} - x_{2\ DH2}} \tag{4.72}$$

$$In_{DH2} = y_{1\ DH2} - Sl_{DH2} \cdot x_{1\ DH2} \tag{4.73}$$

  2. Calculation of T_{DH1} and T_{DH2}:
     Constant DH network temperature segment based on the external temperature:

$$T_{DH1} = y_{3\ DH1} \tag{4.74}$$

$$T_{DH2} = y_{3\ DH2} \tag{4.75}$$

     Variable DH network temperature segment based on the external temperature:

$$T_{DH1} = In_{DH1} + Sl_{DH1} \cdot T_{ext} \tag{4.76}$$

$$T_{DH2} = In_{DH2} + Sl_{DH2} \cdot T_{ext} \tag{4.77}$$

4.3.3   Buildings

The elemental blocks of the internal hydraulic network inside the buildings are described below. The constituent blocks of the hot water production branch and the heating branch are distinguished.

4.3.3.1   Heat Demand Distributor
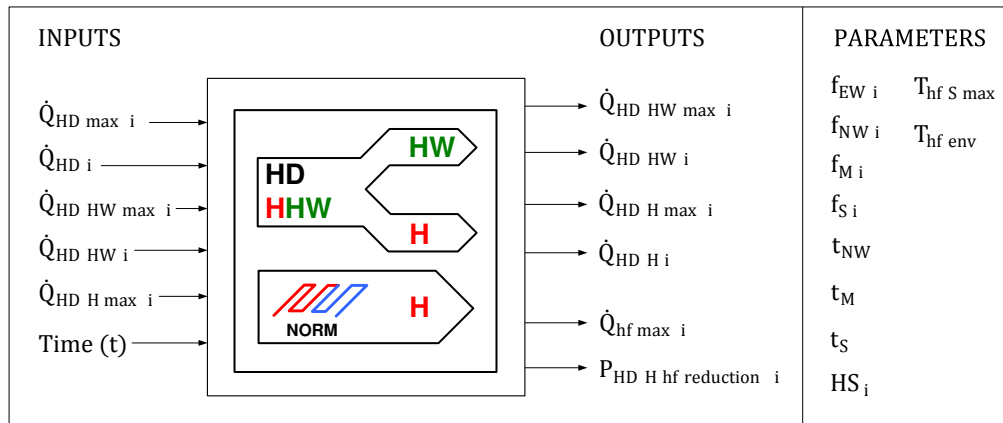
Figure 4.13: Block picture, representing the heat demand calculation model

- Description: This is the initial model and it is integrated inside each building. Based on the known total heat demand, the specific hot water and heating heat demand for each branch is calculated. This block also calculates the heat flow provided by the radiant floor as it is explained in the European regulation and compares it with the heat demand for heating calculated previously, finding in turn the percentage of reduction of heating demand that will be necessary in order to use radiant floor for a building.

- Inputs:

  - $\dot{Q}_{HD\ max\ i}$ = Maximum value of the total heat flow demand profile for building i, in kW

  - $\dot{Q}_{HD\ i}$ = Total heat flow demand profile for building i, in kW

  - $\dot{Q}_{HD\ HW\ max\ i}$ = Estimated maximum value of the heat flow demand profile for hot water production for building i, in kW

  - $\dot{Q}_{HD\ HW\ i}$ = Estimated heat flow demand profile for hot water production for building i, in kW

  - $\dot{Q}_{HD\ H\ max\ i}$ = Estimated maximum value of the heat flow demand for heating for building i, in kW

  - t = time profile, in h

- Parameters:

  - t_{NM} = Time instant that changes from one period to another, in this case from extreme winter to normal winter = 48 h

  - t_M = Time instant that changes from winter to mid season = 96 h

- – t_S = Time instant that changes from mid season to summer = 144 h
- – $T_{hf\ s\ max}$ = Maximum surface temperature with radiant floor heating [132] = 29 °C
- – $T_{hf\ env}$ = Critical ambient air temperature in the room [132] = 20 °C
- – HS_i = Heat Surface for building i, in m^2
- – $f_{EW\ i}$ = multiplication factor over $\dot{Q}_{HD\ HW\ i}$, extreme winter period = 0.2/0.3
- – $f_{NW\ i}$ = multiplication factor over $\dot{Q}_{HD\ HW\ i}$, normal winter period = 0.2/0.3
- – $f_{M\ i}$ = multiplication factor over $\dot{Q}_{HD\ HW\ i}$, mid season period = 0.8/0.9
- – $f_{S\ i}$ = multiplication factor over $\dot{Q}_{HD\ HW\ i}$, summer period = 0.8/0.9

- Outputs:

  - – $\dot{Q}_{HD\ HW\ max\ i}$ = Calculated maximum value of the heat flow demand profile for hot water production for building i, in kW
  - – $\dot{Q}_{HD\ H\ max\ i}$ = Calculated maximum value of the heat flow demand profile for heating for building i, in kW
  - – $\dot{Q}_{HD\ HW\ i}$ = Calculated heat flow demand profile for hot water production for building i, in kW
  - – $\dot{Q}_{HD\ H\ i}$ = Calculated heat flow demand profile for heating for building i, in kW
  - – $\dot{Q}_{hf\ max\ i}$ = Maximum heat flow emitted by the radiant floor for building i, in kW
  - – $P_{HD\ H\ hf\ reduction\ i}$ = Percentage of reduction of heating demand that will be necessary in order to use the radiant floor for a building.

- System of equations:

  1. Calculation of the heat demand profiles for hot water production and heating:
     For all climatic periods:

$$\dot{Q}_{HD\ HW\ max\ i\ (calculated)} = \dot{Q}_{HD\ HW\ max\ i\ (estimated)} \tag{4.78}$$

$$\dot{Q}_{HD\ H\ max\ i\ (calculated)} = \dot{Q}_{HD\ H\ max\ i\ (estimated)} \tag{4.79}$$

Those maximum values will be used later to design the heat exchangers (see sections 4.3.3.3 and 4.3.3.9).
For the extreme winter period, the following equations are fulfilled:

$$\dot{Q}_{HD\ HW\ i\ (calculated)} = f_{EW\ i} \cdot \dot{Q}_{HD\ HW\ i\ (estimated)} \tag{4.80}$$

$$\dot{Q}_{HD\ H\ i\ (calculated)} = \dot{Q}_{HD\ i} - \dot{Q}_{HD\ HW\ i\ (calculated)} \tag{4.81}$$

Similarly, for normal winter period:

$$\dot{Q}_{HD\ HW\ i\ (calculated)} = f_{NW\ i} \cdot \dot{Q}_{HD\ HW\ i\ (estimated)} \tag{4.82}$$

$$\dot{Q}_{HD\ H\ i\ (calculated)} = \dot{Q}_{HD\ i} - \dot{Q}_{HD\ HW\ i\ (calculated)} \tag{4.83}$$

For mid season:

$$\dot{Q}_{HD\ HW\ i\ (calculated)} = f_{M\ i} \cdot \dot{Q}_{HD\ HW\ i\ (estimated)} \tag{4.84}$$

$$\dot{Q}_{HD\ H\ i\ (calculated)} = \dot{Q}_{HD\ i} - \dot{Q}_{HD\ HW\ i\ (calculated)} \tag{4.85}$$

For summer (no heating used):

$$\dot{Q}_{HD\ HW\ i\ (calculated)} = f_{S\ i} \cdot \dot{Q}_{HD\ HW\ i\ (estimated)} \tag{4.86}$$

$$\dot{Q}_{HD\ H\ i\ (calculated)} = 0 \tag{4.87}$$

2. Radiant floor's specifications:

On the other hand, regardless of the climate period studied, the simulation helps to find out if the radiant floor is able meet the energy demands of each building. For this purpose, the norm UNE-EN 1264-2: 2009 + A1: 2013 [132] is applied, defining the following equations which are included in this block:

Maximum heat flow emitted by the radiant floor for building i, in W/m^2:

$$\dot{Q}_{hf\ max\ i} = 8.92 \cdot \left[\left(T_{hf\ s\ max} - T_{hf\ env} \right)^{1.1} \right] \cdot HS_i \tag{4.88}$$

This equation comes from the characteristic curve defined in the aforementioned norm, which fixes the relationship between the thermal flow density $\dot{Q}_{hf\ i}/HS_i$ with $T_{hf\ s\ max}$ and $T_{hf\ env}$

Finally, the block calculates the percentage of reduction of heating demand that will be necessary in order to use the heated floor for a building, only in those cases in which $\dot{Q}_{hf\ i} < \dot{Q}_{HD\ H\ i}$

$$P_{HD\ H\ hf\ reduction\ i} = \frac{\dot{Q}_{HD\ H\ i} - \dot{Q}_{hf\ max\ i}}{\dot{Q}_{HD\ H\ i}} \cdot 100 \tag{4.89}$$

4.3.3.2 Domestic Hot Water Recirculation System
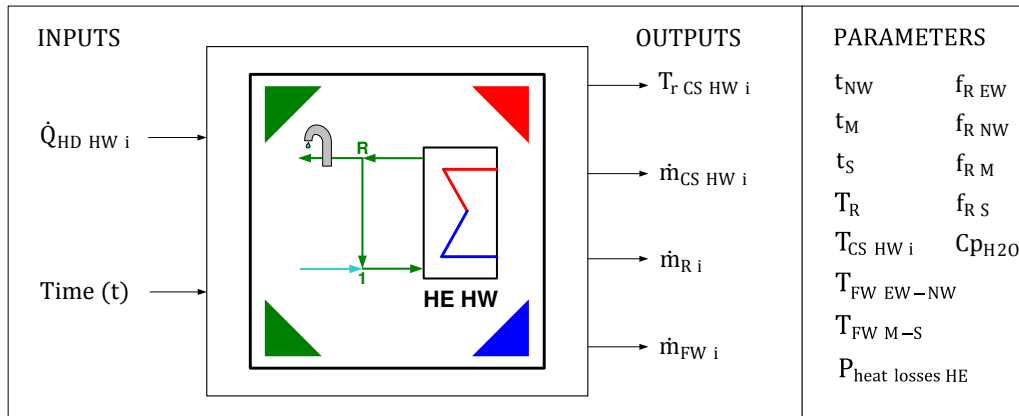
Figure 4.14: Block representing the DHW Recirculation model

- Description: Block mainly intended to estimate DHW return temperature from the internal hydraulic network of the building. This network has been simplified giving rise to the following figure, based in turn on the explanations detailed in the section 3.2.2, figures 3.10 and 3.11:
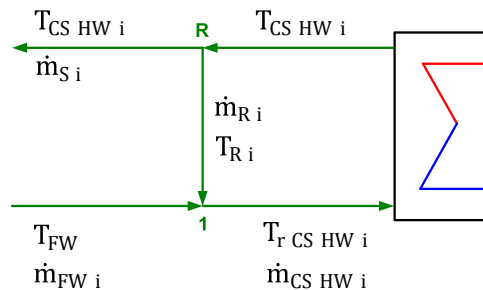
Figure 4.15: Domestic Hot Water Recirculation, simplified grid

- Inputs:

  - $\dot{Q}_{HD\ HW\ i}$ = Heat flow demand profile for hot water production for building i, in kW
  - t = time profile, in h

- Parameters:

  - t_{NM} = Time instant that changes from one period to another, in this case from extreme winter to normal winter = 48 h
  - t_M = Time instant that changes from winter to midseason = 96 h
  - t_S = Time instant that changes from midseason to summer = 144 h
  - $f_{R\ EW\ i}$ = Recirculation factor, extreme winter period = 0.2/0.3 (high DHW consumption)
  - $f_{R\ NW\ i}$ = Recirculation factor, normal winter period = 0.2/0.3 (high DHW consumption)

- $f_{R\,M\,i}$ = Recirculation factor, midseason period = 0.8/0.9 (low DHW consumption)
- $f_{R\,S\,i}$ = Recirculation factor, summer period = 0.8/0.9 (low DHW consumption)
- $T_{cs\,HW\,i}$ = DHW temperature for human consumption and storage, specified in the norms [101] [102] = 60 °C
- T_R = DHW temperature, recirculation line = 55 °C. it is assumed constant, since it comes from a water storage tank (see section 3.11)
- $T_{FW\,EW\,NW}$ = Average value for fresh potable water temperature, cold periods = 3 °C
- $T_{FW\,M\,S}$ = Average value for fresh potable water temperature, warm periods = 13 °C
- $P_{HD\,H\,hf\,reduction\,i}$ = Percentage of heat losses for the heat exchanger, hot water branch = 0 (supposed isolated)
- Cp_{H2O} = Calorific capacity of water at constant pressure, in J/(kg K)

- Outputs:

  - $T_{r\,cs\,HW\,i}$ = return DHW temperature coming from the hydraulic grid, in K
  - $\dot{m}_{cs\,HW\,i}$ = DHW mass flow, in kg/s
  - $\dot{m}_{FW}$ = DHW mass flow, fresh water stream, in kg/s
  - $\dot{m}_R$ = DHW mass flow, recirculation stream, in kg/s

- System of equations:

  The outputs defined are determined by an equations system of four equations with four unknowns explained below:

  1. A part of the heat flow provided by the heat exchanger is carried by the recirculation stream:

  $$\dot{m}_R \cdot Cp \cdot (T_{cs\,HW\,i} - T_R) = \dot{Q}_{HD\,HW\,i} \cdot f_{R\,i} \tag{4.90}$$

  2. While the rest of this heat flow is used to heat the flow of fresh drinking water:

  $$\dot{m}_{FW} \cdot Cp_{H2O} \cdot (T_{cs\,HW\,i} - T_{FW}) = \dot{Q}_{HD\,HW\,i} \cdot (1 - f_{R\,i}) \tag{4.91}$$

  3. Mass balance for point 1:

  $$\dot{m}_{cs\,HW\,i} = \dot{m}_{FW} + \dot{m}_R \tag{4.92}$$

  4. Energy balance for point 1:

  $$\dot{m}_{cs\,HW\,i} \cdot T_{r\,cs\,HW\,i} = \dot{m}_{FW} \cdot T_{FW} + \dot{m}_R \cdot T_R \tag{4.93}$$

  This system is calculated for the four climatic periods specified: EW, NW, M and S

4.3.3.3 Heat Exchanger for DHW production
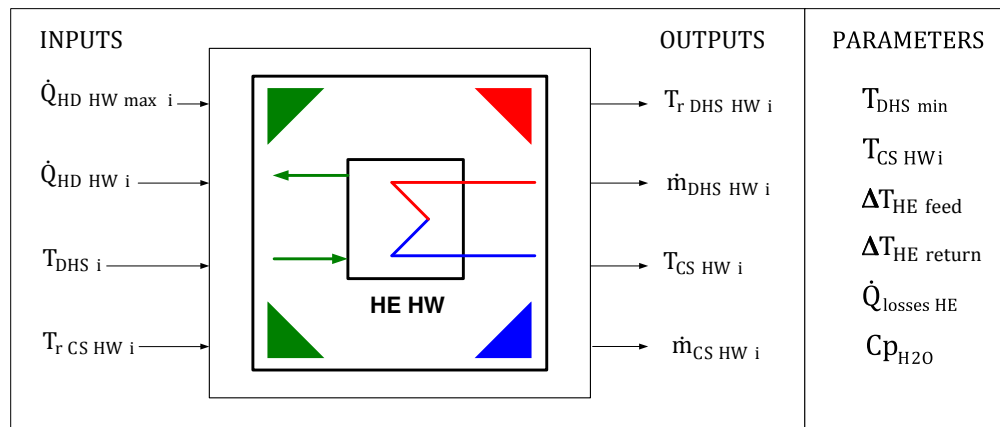
Figure 4.16: Block picture, representing the heat exchanger model for DHW production

- Description: Representative model of the heat exchanger located between the DHN and the DHW water supply grid inside the building. The model consists of two stages. In the first stage, based on the maximum heat demand for hot water production and other parameters, the model calculates the design parameter $(k_i \cdot HTS_i)$, which defines the dimensioning of the heat exchanger. In the second stage, the model calculates both the return temperature and the mass flow of the DH water stream leaving the heat exchanger.

- Inputs:

  - $\dot{Q}_{HD\ HW\ max\ i}$ = Maximum calculated value of the heat flow demand profile for DHW production for building i, in kW
  - $\dot{Q}_{HD\ HW\ i}$ = Heat flow demand profile for hot water production for building i, in kW
  - $T_{DHS\ i}$ = Feed temperature of the DH water for building i, in K
  - $T_{r\ CS\ HW\ i}$ = Return DHW temperature coming from the hydraulic grid, in K

- Parameters:

  - $T_{DHS\ min}$ = Minimum Feed temperature of the DH water, defined by the regulation curve 3.14 = 336.15 K = 63 °C
  - $T_{CS\ HW\ i}$ = Feed DHW temperature required for the inhibition of Legionella and human consumption [101] [102] = 333.15 K = 60 °C
  - $\Delta T_{HE\ feed}$ = Temperature difference supposed between $T_{DHS\ i}$ and $T_{CS\ HW\ i}$ = 3 K
  - $\Delta T_{HE\ return}$ = Temperature difference supposed between $T_{r\ CS\ HW\ i}$ and $T_{r\ DHS\ HW\ i}$ = 2 K
  - $\dot{Q}_{losses\ HE}$ = Heat losses supposed for an isolated plate heat exchanger = 0 kW (negligible)
  - Cp_{H2O} = Calorific capacity of water at constant pressure = 4.18 kJ/(kg K)

- Outputs:

  - $T_{r\ DHS\ HW\ i}$ = Return temperature of the DH water for building i, in K
  - $\dot{m}_{DHS\ HW\ i}$ = Mass flow of the DH water for building i, in kg/s
  - $T_{CS\ HW\ i}$ = previously defined
  - $\dot{m}_{CS\ HW\ i}$ = Mass flow of DHW water for human consumption, building i, in kg/s

- System of equations:

  1. Dimensioning the heat exchanger:

     Following the heat transmission equation for a heat exchanger in the most exigent conditions:

     $$\dot{Q}_{HD\ HW\ max\ i} = k_i \cdot HTS_i \cdot \frac{(T_{DHS\ min} - T_{CS\ HW\ design\ i}) - (T_{r\ DHS\ HW\ design\ i} - T_{r\ CS\ HW\ i})}{Ln\frac{T_{DHS\ min} - T_{CS\ HW\ design\ i}}{T_{r\ DHS\ HW\ design\ i} - T_{r\ CS\ HW\ i}}}$$

     (4.94)

     Since:

     $$T_{CS\ HW\ design\ i} = T_{DHS\ min} - \Delta T_{HE\ feed} \tag{4.95}$$

     $$T_{r\ DHS\ HW\ design\ i} = T_{r\ CS\ HW\ i} + \Delta T_{HE\ return} \tag{4.96}$$

     $(k_i \cdot HTS_i)$ is solved

  2. Calculating DH variables:

     A three-equation system with three unknown variables has to be solved using Matlab command fsolve:

     $$\dot{Q}_{HD\ HW\ i} = (k_i \cdot HTS_i) \cdot \frac{(T_{DHS\ i} - T_{CS\ HW\ i}) - (T_{r\ DHS\ HW\ i} - T_{r\ CS\ HW\ i})}{Ln\frac{T_{DHS\ i} - T_{CS\ HW\ i}}{T_{r\ DHS\ HW\ i} - T_{r\ CS\ HW\ i}}} \tag{4.97}$$

     $$\dot{Q}_{HD\ HW\ i} = \dot{m}_{DHS\ HW\ i} \cdot Cp_{H2O} \cdot (T_{DHS\ i} - T_{r\ DHS\ HW\ i}) \tag{4.98}$$

     $$\dot{Q}_{HD\ HW\ i} = \dot{m}_{CS\ HW\ i} \cdot Cp_{H2O} \cdot (T_{CS\ HW\ i} - T_{r\ CS\ HW\ i}) \tag{4.99}$$

     $T_{r\ CS\ HW\ i}$, $\dot{m}_{DHS\ HW\ i}$ and $\dot{m}_{CS\ HW\ i}$ are calculated

4.3.3.4 Heat Pump for DHW production
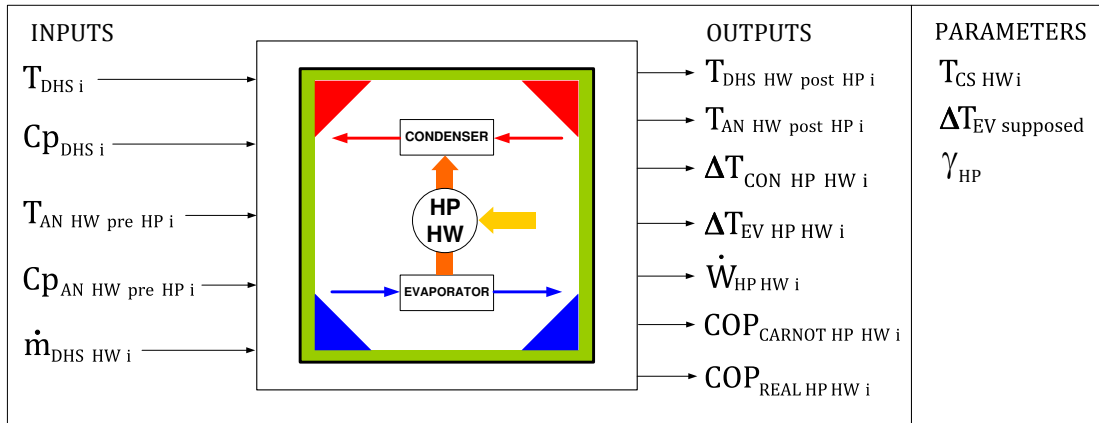
Figure 4.17: Block representing the Heat Pump for DHW production model

- Description: Representative model of a heat pump supporting the heat exchanger for DHW production. The heat pump raises the temperature of the feed DH water stream, whose temperature is insufficient to keep the DHW at the 60 °C required by the regulations. As anergy network, the device extracts heat from the same DH water stream that leaves the heat exchanger, therefore reducing its return temperature (see scenario 3, figure 3.19). For more information about this type of system, see section 2.1.2.2.

- Inputs:

    - $T_{DHS\,i}$ = Feed temperature of the DH water for building i, in K
    - $Cp_{DHS\,i}$ = Calorific capacity of DH water at constant pressure, building i, in $kJ/(kg\,K)$
    - $T_{AN\,HW\,pre\,HP\,i}$ = Return temperature of the DH water between the heat exchanger and the heat pump for building i, in K
    - $Cp_{AN\,HW\,pre\,HP\,i}$ = Calorific capacity of the DH water at constant pressure between the heat exchanger and the heat pump for building i, in $kJ/(kg\,K)$
    - $\dot{m}_{DHS\,HW\,i}$ = Mass flow of the DH water for building i, in kg/s

- Parameters:

    - $T_{CS\,HW\,i}$ = Feed DHW temperature required for the inhibition of Legionella and human consumption [101] [102] = 333.15 K = 60 °C
    - γ_{HP} = Heat pump's efficiency factor, brings together all possible irreversibilities inside the heat pump. The real efficiency of commercial heat pump systems is usually 50 % to 70 % of the theoretical efficiency [133]. For this work, an average value of 55 % (0.55) is used
    - $\Delta T_{EV\,supposed}$ = Supposed temperature difference for the evaporator between $T_{AN\,HW\,pre\,HP\,i}$ and $T_{AN\,HW\,post\,HP\,i}$ = 21 K

- Outputs:

    - $T_{DHS\ HW\ post\ HP\ i}$ = Feed temperature of the DH water to the heat exchanger, in K
    - $T_{AN\ HW\ post\ HP\ i}$ = Return temperature of the DH water after the heat pump for building i, in K
    - $\Delta T_{CON\ HP\ HW\ i}$ = Temperature difference between the input and the output of the condenser for building i, in K
    - $\Delta T_{EV\ HP\ HW\ i}$ = Temperature difference between the input and the output of the evaporator for building i, in K
    - $\dot{W}_{HP\ HW\ i}$ = Electric work flow required by the heat pump for building i, in kW
    - $COP_{CARNOT\ HP\ HW\ i}$ = Theoretical heat pump's operation coefficient for building i (ad.)
    - $COP_{REAL\ HP\ HW\ i}$ = Real heat pump's operation coefficient for building i (ad.)

- System of equations:

The present system of equations can be solved lineally, which allows a higher calculation speed in the simulation. Cp values ($Cp_{H2O\ DHS\ i}$ and $Cp_{H2O\ AN\ HW\ pre\ HP\ i}$) are obtained through the auxiliary block " Water Properties " (see section 4.3.2.1)

A temperature margin of 5 K is established, in order to define the temperature of the district heating side $T_{DHS\ HW\ post\ HP\ i}$ before the heat exchanger:

$$T_{DHS\ HW\ post\ HP\ i} = T_{CS\ HW\ i} + 5K \tag{4.100}$$

Temperature increase of the DH supply line, required to keep the DHW at 60 °C:

$$\Delta T_{CON\ HP\ HW\ i} = T_{DHS\ HW\ post\ HP\ i} - T_{DHS\ i} \tag{4.101}$$

Heat flow supplied to the feed DH line (heat sink):

$$\dot{Q}_{H\ i} = \dot{m}_{DHS\ HW\ i} \cdot Cp_{H2O\ DHS\ i} \cdot \Delta T_{CON\ HP\ HW\ i} \tag{4.102}$$

Hereinafter, it is necessary to assume a certain temperature difference in the evaporator ($\Delta T_{EV\ supposed}$), from which the calculations continue:

$$T_{AN\ HW\ post\ HP\ supposed\ i} = T_{AN\ HW\ pre\ HP\ i} - \Delta T_{EV\ supposed} \tag{4.103}$$

In the next step, both heat pump efficiencies are calculated:

$$COP_{CARNOT\ HP\ HW\ i} = \frac{T_{DHS\ HW\ post\ HP\ i}}{T_{DHS\ HW\ post\ HP\ i} - T_{AN\ HW\ post\ HP\ supposed\ i}} \tag{4.104}$$

$$COP_{REAL\ HP\ HW\ i} = COP_{CARNOT\ HP\ HW\ i} \cdot \gamma_{HP} \tag{4.105}$$

After all these operations and considerations, it is possible to obtain the electric work flow required from the heat pump to operate:

$$\dot{W}_{HP\ HW\ i} = \frac{\dot{Q}_{H\ i}}{COP_{REAL\ HP\ HW\ i}} \tag{4.106}$$

The energy balance allows to calculate the heat flow extracted from the anergy network (cold heat source)

$$\dot{Q}_{H\ i} = \dot{Q}_{C\ i} + \dot{W}_{HP\ HW\ i} \tag{4.107}$$

From where $\dot{Q}_{C\ i}$ is calculated

Subsequently, $T_{AN\ HW\ post\ HP\ i}$ is obtained from the energy balance of the evaporator:

$$\dot{Q}_{C\ i} = \dot{m}_{DHS\ HW\ i} \cdot Cp_{H2O\ AN\ HW\ pre\ HP\ i} \cdot (T_{AN\ HW\ pre\ HP\ i} - T_{AN\ HW\ post\ HP\ i}) \tag{4.108}$$

Finally, it is important to check if the supposed temperature difference $\Delta T_{EV\ supposed}$, which was introduced as a parameter in the equation system, is equal or similar to the calculated $\Delta T_{EV\ calculated}$ (see equation (4.103))

Regarding this, the simulation of scenario 3 yields the following results:

– $\Delta T_{EV\ supposed}$ = 21 K

– $\Delta T_{EV\ calculated}$ = 19.5 K - 21.7 K

The difference between both values is very small, therefore the model is assumed to be valid.

4.3.3.5   Heat Pump for DHW production at continuous operation
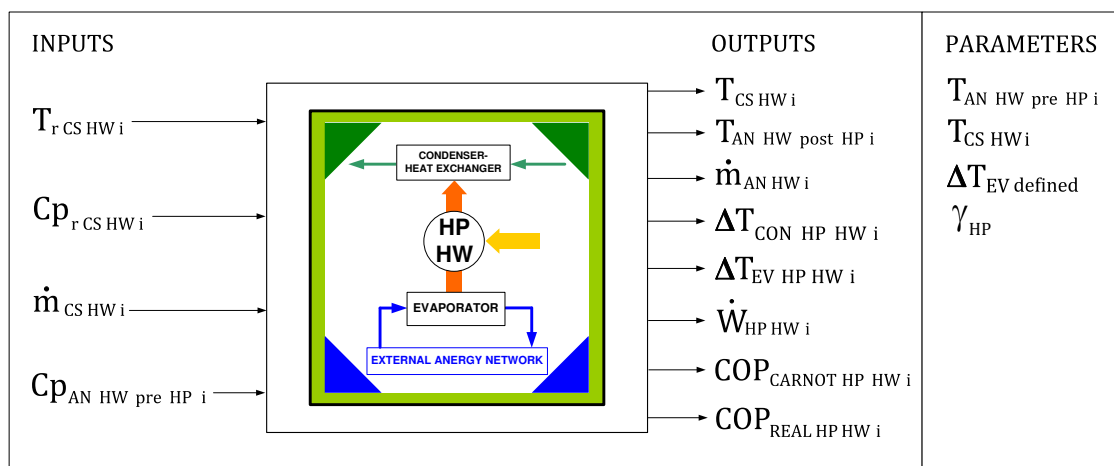
Figure 4.18: Block picture, representing the Heat Pump for DHW production (No DHN)

- Description: Representative model of a heat pump working at continuous operation. In this case, the condenser makes the role of the heat exchanger for DHW production branch without any support of the DHN. Therefore, this device is the only heat source available for this branch.

This block is very similar to the Heat Pump for DHW branch model (see section 4.3.3.4) with some differences. Firstly, the heat pump raises directly the potable water temperature until the required consumption temperature $T_{CS\ HW\ i}$ = 60 ° C, so, the DHW stream will be the hot sink in this case. Secondly, the anergy network is no longer DH water, but water coming from an external network that has nothing to do with the district heating. The block receives the water coming from the source (river, lake ... etc) at the temperature $T_{AN\ HW\ pre\ HP\ i}$ and extracts the necessary heat for the hot stream, calculating the mass flow of the anergy network $\dot{m}_{AN\ HW\ post\ HP\ i}$ required in those conditions. The rest of the functions are the same as in the Heat Pump for DHW branch model.

- Inputs:

    - $T_{r\ CS\ HW\ i}$ = Return DHW temperature coming from the hydraulic grid for building i, in K

    - $Cp_{r\ CS\ HW\ i}$ = Calorific capacity of DHW water at constant pressure, in kJ/(kg K)

    - $\dot{m}_{CS\ HW\ i}$ = Mass flow of DHW water for human consumption, building i, in kg/s

    - $Cp_{AN\ HW\ pre\ HP\ i}$ = Calorific capacity of the DH water at constant pressure between the heat exchanger and the heat pump for building i, in kJ/(kg K)

- Parameters:

    - $T_{AN\ HW\ pre\ HP\ i}$ = Feed temperature of the anergy network (AN), in K

    - $T_{CS\ HW}$ = Feed DHW temperature required for the inhibition of Legionella and human consumption [101] [102] = 333.15 K = 60 °C

    - γ_{HP} = Heat pump's efficiency factor, brings together all possible irreversibilities inside the heat pump. The real efficiency of commercial heat pump systems is usually 50 % to 70 % of the theoretical efficiency [133]. For this work, an average value of 55 % (0.55) is used

    - $\Delta T_{EV\ defined}$ = Defined Temperature difference for the evaporator between $T_{AN\ HW\ pre\ HP\ i}$ and $T_{AN\ HW\ post\ HP\ i}$ = 21 K

- Outputs:

    - $T_{CS\ HW}$ = Same as the same previous parameter

    - $T_{AN\ HW\ post\ HP\ i}$ = Return temperature of the AN after crossing the heat pump for building i, in K

    - $\dot{m}_{AN\ HW\ i}$ = Mass flow of AN water for building i, in kg/s

    - $\Delta T_{CON\ HP\ HW\ i}$ = Temperature difference between the input and the output of the condenser for building i, in K

    - $\Delta T_{EV\ HP\ HW\ i}$ = Temperature difference between the input and the output of the evaporator for building i, in K

    - $\dot{W}_{HP\ HW\ i}$ = Electric work flow required by the heat pump for building i, in kW

    - $COP_{CARNOT\ HP\ HW\ i}$ = Theoretical heat pump's operation coefficient for building i (ad.)

    - $COP_{REAL\ HP\ HW\ i}$ = Real heat pump's operation coefficient for building i (ad.)

- System of equations:

Again, in the present system, Cp values ($Cp_{H2O\ DHS\ i}$ and $Cp_{H2O\ AN\ HW\ pre\ HP\ i}$) are obtained through the auxiliary block " Water Properties " (see section 4.3.2.1)

$$T_{CS\ HW\ (output)} = T_{CS\ HW\ (parameter)} \tag{4.109}$$

Temperature increase of the DHW supply line, required to keep it at 60 °C:

$$\Delta T_{CON\ HP\ HW\ i} = T_{r\ CS\ HW\ i} - T_{CS\ HW} \tag{4.110}$$

Heat flow supplied to the feed DH line (heat sink):

$$\dot{Q}_{HW\ i} = \dot{m}_{CS\ HW\ i} \cdot Cp_{r\ CS\ HW\ i} \cdot \Delta T_{CON\ HP\ HW\ i} \tag{4.111}$$

Hereinafter, it is necessary to define a certain temperature difference in the evaporator (ΔT_{EV}):

$$T_{AN\ HW\ post\ HP\ i} = T_{AN\ HW\ pre\ HP\ i} - \Delta T_{EV\ defined} \tag{4.112}$$

From there, both heat pump efficiencies are calculated:

$$COP_{CARNOT\ HP\ HW\ i} = \frac{T_{CS\ HW}}{T_{CS\ HW} - T_{AN\ HW\ post\ HP\ i}} \tag{4.113}$$

$$COP_{REAL\ HP\ HW\ i} = COP_{CARNOT\ HP\ HW\ i} \cdot \gamma_{HP} \tag{4.114}$$

After all these operations and considerations, it is possible to obtain the electric work flow required from the heat pump to operate:

$$\dot{W}_{HP\ HW\ i} = \frac{\dot{Q}_{H\ i}}{COP_{REAL\ HP\ HW\ i}} \tag{4.115}$$

The energy balance allows to calculate the heat flow extracted from the anergy network (cold heat source)

$$\dot{Q}_{H\ i} = \dot{Q}_{C\ i} + \dot{W}_{HP\ HW\ i} \tag{4.116}$$

From where $\dot{Q}_{C\ i}$ is calculated

Subsequently, $\dot{m}_{AN\ HW\ i}$ is obtained from the energy balance of the evaporator:

$$\dot{Q}_{C\ i} = \dot{m}_{AN\ HW\ i} \cdot Cp_{AN\ HW\ pre\ HP\ i} \cdot (T_{AN\ HW\ pre\ HP\ i} - T_{AN\ HW\ post\ HP\ i}) \tag{4.117}$$

4.3.3.6 Radiators
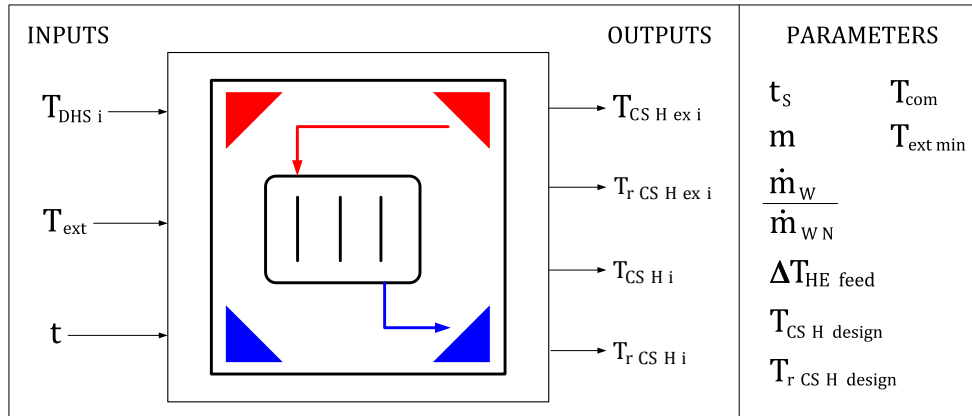
Figure 4.19: Block picture, representing the radiators system inside the building

- Description: The present model represents the heating system serving the building's habitants, consisting on radiators. The model calculates the return temperature of the water coming from the radiators ($T_{r\ CS\ H\ i}$), based on the comfort temperature parameters (T_{com}) and the external temperature (T_{ext}). This value is essential for the resolution of the model inside the next block (Heat Exchanger for Heating 4.3.3.9). The algorithm applied here is a simplification of the Recknagel-Schramek-Sprenger method [47], carried out in the department of Energy systems and Thermodynamics of the TU Wien.

- Inputs:

  - $T_{DHS\ i}$ = Feed temperature of the DH water for building i, in K
  - T_{ext} = External temperature profile, in K
  - t = time profile, in h

- Parameters:

  - t_S = Time instant that changes from midseason to summer = 144 h
  - $T_{ext\ min}$ = Minimum external temperature value = 260.89 K = -12,26 °C
  - T_{com} = Comfort temperature value = 297.15 K = 24 °C
  - $T_{CS\ H\ design}$ = Feed temperature of the heating water in design (extreme) conditions = 351.15 K = 78 °C
  - $T_{r\ CS\ H\ design}$ = Return temperature of the heating water in design (extreme) conditions = 331.15 K = 58 °C
  - $\Delta T_{HE\ feed}$ = Temperature difference supposed between $T_{DHS\ i}$ and $T_{CS\ H\ i}$ = 3 K
  - m = Correction factor = 1.33 for radiators [47]
  - $\frac{\dot{m}_W}{\dot{m}_{W\ N}}$ = Relationship between the circulating mass flow for design conditions and normal conditions = 1 (constant mass flow considered)

- Outputs:

    - $T_{CS\,H\,ex\,i}$ = Feed temperature of the heating water in design conditions for building i, in K

    - $T_{r\,CS\,H\,ex\,i}$ = Return temperature of the heating water in design conditions for building i, in K

    - $T_{CS\,H\,i}$ = Feed temperature of the heating water for building i, in K

    - $T_{r\,CS\,H\,i}$ = Return temperature of the heating water for building i, in K

- System of equations:

    The simplified Recknagel method is based on considering that the radiator's heating power P and the difference between T_{com} and T_{ext} follow a linear relationship:

    $$P \alpha T_{com} - T_{ext} \tag{4.118}$$

    Taking the main heat equation (see equation (4.1)) both in operation and design mode, the following expressions are obtained:

    $$P = \dot{m}\,Cp\,\Delta T \tag{4.119}$$

    $$P_N = \dot{m}_N\,Cp\,\Delta T_N \tag{4.120}$$

    Since the subindex N represents design/extreme conditions.

    Relating both equations:

    $$\frac{P}{P_N} = \frac{\dot{m}_W}{\dot{m}_{W\,N}} \cdot \frac{\Delta T_W}{\Delta T_{W\,N}} \tag{4.121}$$

    To solve this equation it is necessary to solve the following expressions:

    1. Power relation considering external and comfort temperatures:

    $$\frac{P}{P_N} = \frac{T_{com} - T_{ext}}{T_{com} - T_{ext\,min}} \tag{4.122}$$

    2. Temperature difference in design conditions:

    $$\Delta T_{W\,N} = T_{CS\,H\,design} - T_{r\,CS\,H\,design} \tag{4.123}$$

    From the equation (4.121), ΔT_W is obtained.

    The model calculates the supply temperature of the circulating water through the radiators ($T_{CS\,H\,i}$) as a dependent variable from the DH water temperature ($T_{DHS\,i}$), by the expression:

    $$T_{CS\,H\,i} = T_{DHS\,i} - \Delta T_{HE\,feed} \tag{4.124}$$

    Finally, $T_{r\,CS\,H\,i}$ is obtained using the ecuation:

$$T_{r\ CS\ H\ i} = T_{CS\ H\ i} - \Delta T_W \tag{4.125}$$

In the summer period, the heatings are switched off, which is also reflected in the model through the following equalities:

$$\Delta T_W = 0 \tag{4.126}$$

$$T_{CS\ H\ i} = T_{r\ CS\ H\ i} = 295.15 K = 22°C \tag{4.127}$$

.

On the other hand, the following expressions are used to calculate the maximum temperature required by the radiators to satisfy the comfort temperature inside the rooms:

$$\Delta T_N = \frac{T_{CS\ H\ design} + T_{r\ CS\ H\ design}}{2} - T_{com} \tag{4.128}$$

$$\left(\frac{P}{P_N}\right)_{max} = \frac{T_{com} - T_{ext\ min}}{T_{com} - T_{ext\ min}} = 1 \tag{4.129}$$

$$T_{CS\ H\ ex\ i} = T_{com} + \frac{\dot{m}_W}{\dot{m}_{W\ N}} \cdot \frac{\Delta T_{W\ N}}{2} \cdot \left(\frac{P}{P_N}\right)_{max} + \left(\frac{P}{P_N}\right)_{max}^{1/m} \cdot \Delta T_N \tag{4.130}$$

In design conditions, $\Delta T_{W\ ex}$ is obtained from the equation:

$$\left(\frac{P}{P_N}\right)_{max} = \frac{\dot{m}_W}{\dot{m}_{W\ N}} \cdot \frac{\Delta T_{W\ ex}}{\Delta T_{W\ N}} \tag{4.131}$$

Which is used to solve the last equation:

$$T_{r\ CS\ H\ ex\ i} = T_{CS\ H\ ex\ i} - \Delta T_{W\ ex} \tag{4.132}$$

4.3.3.7   Heated Floors
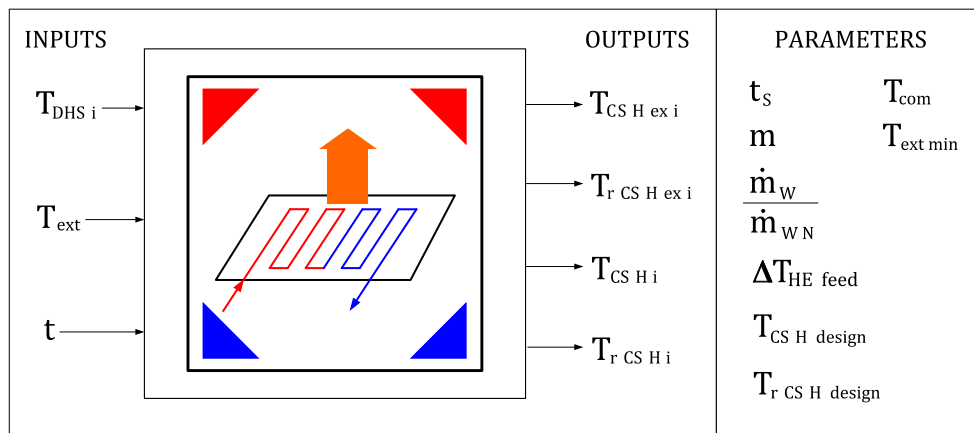
Figure 4.20: Block picture, representing the heated floors system inside the building

- Description: Representative model of the heating system composed by radiant floors instead of radiators. Like in the previous block, the same model is used, but modifying the following parameters:

  - $T_{CS\ H\ design}$ = Feed temperature of the heating water in design conditions = 35 °C
  - $T_{r\ CS\ H\ design}$ = Return temperature of the heating water in design conditions = 25 °C
  - m = Correction factor = 1.1 for heated floors [47]

4.3.3.8 Heated/Cooled Floors
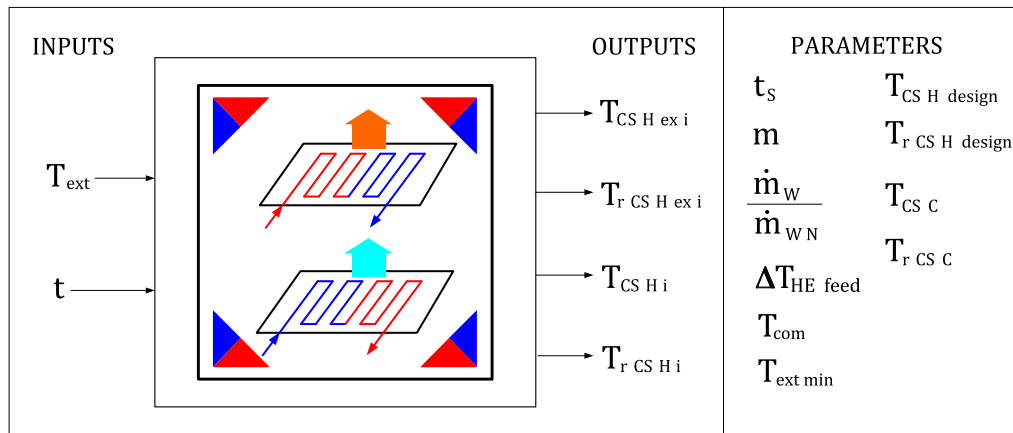
Figure 4.21: Block picture, representing the reversible radiant floors system inside the building

- Description: Representative model of the heating system formed by radiant/cooling floors adapted to work for both, winter and summer periods. This block follows the same equations system as the one for radiators and floor heating models (see sections 4.3.3.6 and 4.3.3.7). There is only one difference: in summer mode, the heating is not switched off and it is still running, with the heating water circulating at the following temperatures:

  - $T_{CS\ C}$ = Feed temperature of the cooling water to the radiant floors = 19 °C.
    Minimum required temperature to avoid condensation drops on the pavement's surface [132]
  - $T_{r\ CS\ C}$ = Return temperature of the cooling water in design conditions = 21 °C [52] [54] [53]

This block is intimately linked to the reversible heat pump for the heating branch model (see section 4.3.3.11), which will be explained later.

4.3.3.9 Heat Exchanger for Heating
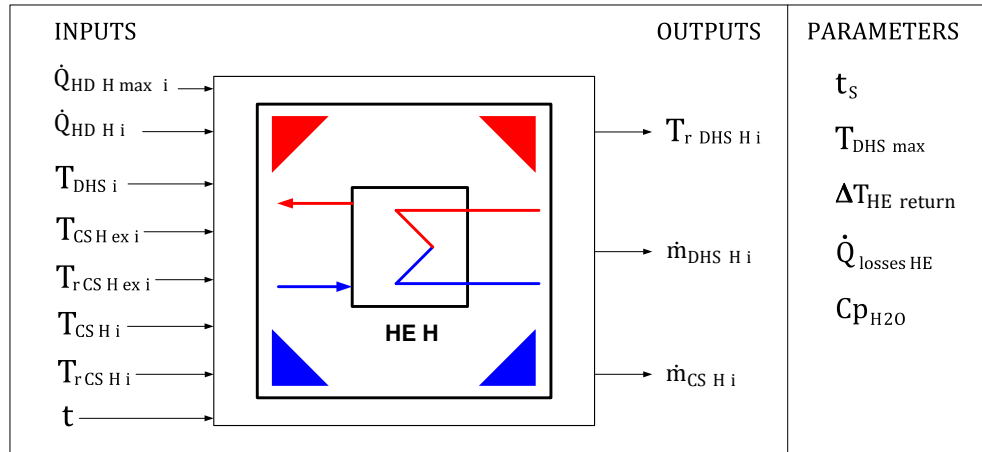
Figure 4.22: Block representing the Heat Exchanger for Heating

- Description: Representative model of the heat exchanger connected to the internal heating network of the building. It is very similar to the heat exchanger model for hot water production (see 4.3.3.3). In this case, the block receives the feed ($T_{CS\,H\,i}$) and return temperatures ($T_{r\,CS\,H\,i}$) from the heating network as already known values. In addition, this model also takes into account the shutdown during the summer months.

- Inputs:

  - $\dot{Q}_{HD\,H\,max\,i}$ = Maximum calculated value of the heat flow demand profile for heating for building i, in kW
  - $\dot{Q}_{HD\,H\,i}$ = Heat flow demand profile for heating for building i, in kW
  - $T_{DHS\,i}$ = Feed temperature of the DH water for building i, in K
  - $T_{CS\,H\,ex\,i}$ = Feed temperature of the heating water in design conditions for building i, in K
  - $T_{r\,CS\,H\,ex\,i}$ = Return temperature of the heating water in design conditions for building i, in K
  - $T_{CS\,H\,i}$ = Feed temperature of the heating water for building i, in K
  - $T_{r\,CS\,H\,i}$ = Return temperature of the heating water for building i, in K
  - t = time profile, in h

- Parameters:

  - t_S = Time instant that changes from mid-season to summer = 144 h
  - $T_{DHS\,max}$ = Maximum Feed temperature of the DH water, defined by the regulation curve 3.14 = 363.15 K = 63 °C
  - $\Delta T_{HE\,return}$ = Temperature difference supposed between $T_{r\,CS\,HW\,i}$ and $T_{r\,DHS\,HW\,i}$ = 2 K
  - $\dot{Q}_{losses\,HE}$ = Heat losses supposed for an isolated plate heat exchanger = 0 kW

- Cp_{H2O} = Calorific capacity of water at constant pressure = 4.18 kJ/(kg K)

- Outputs:

  - $T_{r\,DHS\,H\,i}$ = Return temperature of the DH water of the heating branch for building i, in K

  - $\dot{m}_{DHS\,H\,i}$ = Mass flow of the DH water of the heating branch for building i, in kg/s

  - $\dot{m}_{CS\,H\,i}$ = Mass flow of heating water, building i, in kg/s

- System of equations:

  1. Dimensioning the heat exchanger:

     Following the heat transmission equation for a heat exchanger with the most exigent conditions:

     $$\dot{Q}_{HD\,H\,max\,i} = k_i \cdot HTS_i \cdot \frac{(T_{DHS\,max} - T_{CS\,H\,ex\,i}) - (T_{r\,DHS\,H\,design\,i} - T_{r\,CS\,H\,ex\,i})}{ln\frac{T_{DHS\,max} - T_{CS\,H\,ex\,i}}{T_{r\,DHS\,H\,design\,i} - T_{r\,CS\,H\,ex\,i}}} \qquad (4.133)$$

     Since:

     $$T_{r\,DHS\,H\,design\,i} = T_{r\,CS\,H\,ex\,i} + \Delta T_{HE\,return} \qquad (4.134)$$

     $(k_i \cdot HTS_i)$ is solved

  2. Calculating DH variables:

     In the same procedure as before, a three-equation system with three unknown variables has to be solved using Matlab command fsolve:

     $$\dot{Q}_{HD\,H\,i} = (k_i \cdot HTS_i) \cdot \frac{(T_{DHS\,i} - T_{CS\,H\,i}) - (T_{r\,DHS\,H\,i} - T_{r\,CS\,H\,i})}{Ln\frac{T_{DHS\,i} - T_{CS\,H\,i}}{T_{r\,DHS\,H\,i} - T_{r\,CS\,H\,i}}} \qquad (4.135)$$

     $$\dot{Q}_{HD\,H\,i} = \dot{m}_{DHS\,H\,i} \cdot Cp_{H2O} \cdot (T_{DHS\,i} - T_{r\,DHS\,H\,i}) \qquad (4.136)$$

     $$\dot{Q}_{HD\,H\,i} = \dot{m}_{CS\,H\,i} \cdot Cp_{H2O} \cdot (T_{CS\,H\,i} - T_{r\,CS\,H\,i}) \qquad (4.137)$$

     $T_{r\,CS\,H\,i}$, $\dot{m}_{DHS\,H\,i}$ and $\dot{m}_{CS\,H\,i}$ are calculated

  3. Specifications for the summer period:

     In this periods, the heatings are switched off, which is also reflected in the model through the following equalities:

     $$\dot{m}_{CS\,H\,i} = \dot{m}_{DHS\,H\,i} = 0 \qquad (4.138)$$

     $$T_{r\,DHS\,H\,i} = 295.15K = 22°C \qquad (4.139)$$

4.3.3.10   Heat Pump for Heating
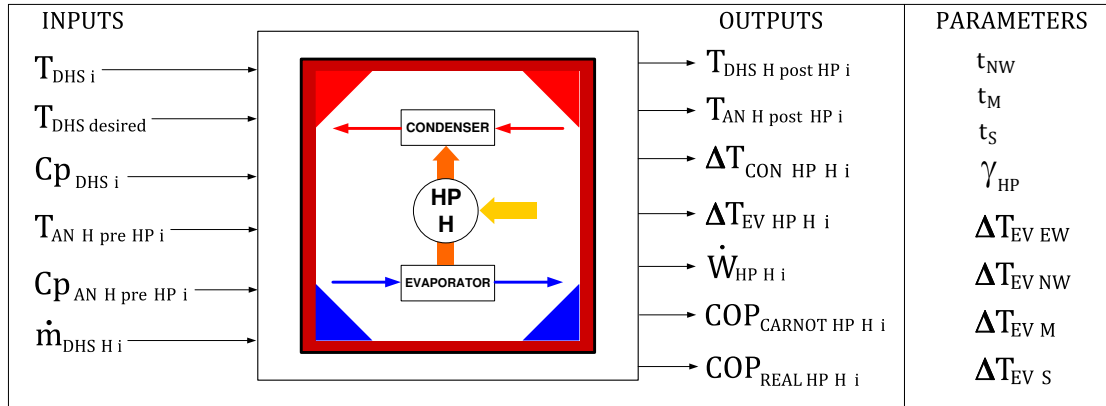
Figure 4.23: Block picture, representing the Heat Pump for Heating model

- Description: Representative model of a heat pump supporting the heat exchanger of the heating branch. As in the heat pump for DHW production (see 4.3.3.4, this device raises the DH water temperature ($T_{DHS\ i}$) whose temperature can be, in certain periods, insufficient to keep the radiators at the necessary temperature to maintain the comfort of the room. The new input is the variable $T_{DHS\ desired}$ defined by the temperature regulation curve (see section 4.3.2.2). This model also uses the return DH stream from the heat exchanger as anergy network (see 3.21)

- Inputs:

    - $T_{DHS\ i}$ = Feed temperature of the DH water for building i, in K

    - $T_{DHS\ required}$ = Required DH water temperature obeying the regulation curve, in K (see section 3.14)

    - $Cp_{DHS\ i}$ = Calorific capacity of DH water at constant pressure, building i, in kJ/(kg K)

    - $T_{AN\ H\ pre\ HP\ i}$ = Return temperature of the DH water between the heat exchanger and the heat pump for building i, in K

    - $Cp_{AN\ H\ pre\ HP\ i}$ = Calorific capacity of the DH water at constant pressure between the heat exchanger and the heat pump for building i, in kJ/(kg K)

    - $\dot{m}_{DHS\ H\ i}$ = Mass flow of the DH water for building i (heating branch), in kg/s

- Parameters:

    - t_{NM} = Time instant that changes from one period to another, in this case from extreme winter to normal winter = 48 h

    - t_{M} = Time instant that changes from winter to mid-season = 96 h

    - t_{S} = Time instant that changes from mid-season to summer = 144 h

    - γ_{HP} = Heat pump's efficiency factor, brings together all possible irreversibilities inside the heat pump. For this work, an average value of 55 % (0.55) is used

    - $\Delta T_{EV\ EW}$ = Supposed Temperature difference for the evaporator between $T_{AN\ HW\ pre\ HP\ i}$ and $T_{AN\ HW\ post\ HP\ i}$ for extreme winter = 18.5 K

– $\Delta T_{EV\ NW}$ = Supposed temperature difference for the evaporator for normal winter = 9 K

– $\Delta T_{EV\ M}$ = Supposed temperature difference for the evaporator for mid-season = 1 K

– $\Delta T_{EV\ S}$ = Supposed temperature difference for the evaporator for summer period = 0 K

- Outputs:

    – $T_{DHS\ H\ post\ HP\ i}$ = Feed temperature of the DH water after crossing the heat pump for building i, in K

    – $T_{AN\ H\ post\ HP\ i}$ = Return temperature of the DH water after crossing the heat pump for building i, in K

    – $\Delta T_{CON\ HP\ H\ i}$ = Temperature difference between the input and the output of the condenser for building i, in K

    – $\Delta T_{EV\ HP\ H\ i}$ = Temperature difference between the input and the output of the evaporator for building i, in K

    – $\dot{W}_{HP\ H\ i}$ = Electric work flow required by the heat pump for building i, in kW

    – $COP_{CARNOT\ HP\ H\ i}$ = Theoretical heat pump's operation coefficient for building i, ad.

    – $COP_{REAL\ HP\ H\ i}$ = Real heat pump's operation coefficient for building i, ad.

- System of equations:

    In this case, the model has been adapted for a type of heat pump that works only during those periods when it is necessary, that is, when the DH water temperature is lower than the DH temperature indicated by the temperature regulation line. In addition, the assumed temperature difference ΔT_{EV} is not constant, but varies according to the season of the year. All these considerations give rise to the following algorithm:

    – Extreme Winter period (time <= t_{NM}):
    If $T_{DHS\ i} < T_{DHS\ required} \rightarrow$ Heat pump H switched on:

$$T_{DHS\ H\ post\ HP\ i} = T_{DHS\ required} \tag{4.140}$$

$$\Delta T_{CON\ HP\ H\ i} = T_{DHS\ H\ post\ HP\ i} - T_{DHS\ i} \tag{4.141}$$

Heat flow supplied to the feed DH line (heat sink):

$$\dot{Q}_{H\ i} = \dot{m}_{DHS\ H\ i} \cdot Cp_{DHS\ i} \cdot \Delta T_{CON\ HP\ H\ i} \tag{4.142}$$

Hereinafter, it is necessary to assume a certain temperature difference in the evaporator $\Delta T_{EV\ EW}$, from which the calculations continue:

$$T_{AN\ H\ post\ HP\ supposed\ i} = T_{AN\ H\ pre\ HP\ i} - \Delta T_{EV\ EW} \tag{4.143}$$

In the next step, both heat pump efficiencies are calculated:

$$COP_{CARNOT\ HP\ H\ i} = \frac{T_{DHS\ H\ post\ HP\ i}}{T_{DHS\ H\ post\ HP\ i} - T_{AN\ H\ post\ HP\ supposed\ i}} \tag{4.144}$$

$$COP_{REAL\ HP\ H\ i} = COP_{CARNOT\ HP\ H\ i} \cdot \gamma_{HP} \tag{4.145}$$

Afterwards, the electric work flow is obtained:

$$\dot{W}_{HP\ H\ i} = \frac{\dot{Q}_{H\ i}}{COP_{REAL\ HP\ H\ i}} \tag{4.146}$$

The energy balance allows to calculate the heat flow extracted from the anergy network (cold heat source)

$$\dot{Q}_{H\ i} = \dot{Q}_{C\ i} + \dot{W}_{HP\ H\ i} \tag{4.147}$$

From where $\dot{Q}_{C\ i}$ is calculated

Subsequently, $T_{AN\ H\ post\ HP\ i}$ is obtained from the energy balance of the evaporator:

$$\dot{Q}_{C\ i} = \dot{m}_{DHS\ H\ i} \cdot Cp_{AN\ H\ pre\ HP\ i} \cdot (T_{AN\ H\ pre\ HP\ i} - T_{AN\ H\ post\ HP\ i}) \tag{4.148}$$

Finally, it is important to check if the supposed temperature difference $\Delta T_{EV\ EW}$, which was introduced as a parameter in the equation system, is equal or similar to the calculated $\Delta T_{EV\ HP\ H\ i}$.

Regarding this, the simulation of SCENARIO 5 generates the following results:

* $\Delta T_{EV\ supposed} = \Delta T_{EV\ EW} = 18.5$ K
* $\Delta T_{EV\ calculated} = \Delta T_{EV\ HP\ H\ i} = 15.9$ K, up to 19.8 K

The difference between both values is very small, therefore the model is assumed to be valid.

Even during the winter period, the DH water temperature could be greater or equal than the required (unexpected DH network operation or other eventualities). Then, the algorithm responds switching the heat pump off:

If $T_{DHS\ i} >= T_{DHS\ required} \rightarrow$ Heat pump H switched off:

$$T_{DHS\ H\ post\ HP\ i} = T_{DHS\ i} \tag{4.149}$$

From here in advance, the equation system is the same, just substituting $\Delta T_{EV\ EW}$ by $\Delta T_{EV\ S}$, which is the parameter used for summer periods, when the heat pump is not operating.

For Normal Winter and Mid-season, the procedure is the same:

– Normal Winter period ($t_{NW} < $ time $<= t_M$):

If $T_{DHS\ i} < T_{DHS\ required} \rightarrow$ Heat pump H is switched on:

After solving the equations system, the supposed temperature difference $\Delta T_{EV\ NW}$, which was introduced as a parameter in the equation system, has to be equal or similar to the calculated $\Delta T_{EV\ HP\ H\ i}$.

Regarding this, for normal winter period, the simulation of SCENARIO 5 generates the following results:

* $\Delta T_{EV\ supposed} = \Delta T_{EV\ NW} = 9$ K
* $\Delta T_{EV\ calculated} = \Delta T_{EV\ HP\ H\ i} = 6.5$ K, up to 11.2 K

Again, the difference between both values is small, therefore the model is assumed to be valid.

– Mid-season period (t_M < time <= t_S):

If $T_{DHS\ i}$ < $T_{DHS\ required}$ → Heat pump H is switched on:

Again, for mid-season period, the simulation of SCENARIO 5 generates the following results:

  * $\Delta T_{EV\ supposed} = \Delta T_{EV\ M} = 0.5$ K
  * $\Delta T_{EV\ calculated} = \Delta T_{EV\ HP\ H\ i} = 0.2$ K, up to 1 K

Here, the temperature difference is much smaller than previous periods, due to the low deployment of the heat pump during spring and autumn seasons. Therefore, for mid-season periods maybe it could be a better option to increase slightly the DHN temperature and switch off the heat pump.

– Summer period → Heat pump H switched off:

$$T_{DHS\ H\ post\ HP\ i} = T_{DHS\ i} \qquad (4.150)$$

Same equation system, just using $\Delta T_{EV\ S}$, which is the parameter used when the heat pump is not operating.

4.3.3.11 Reversible Heat Pump for Heating-Cooling
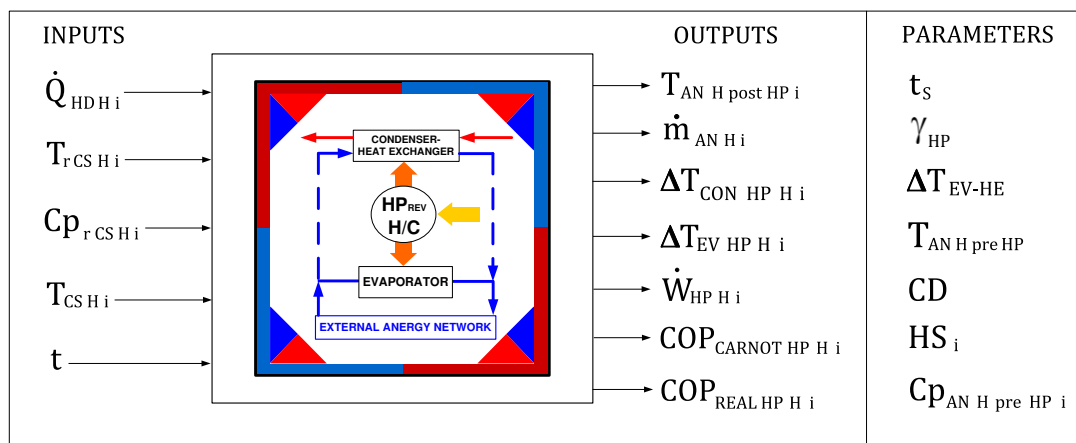
Figure 4.24: Block picture, representing the reversible heat pump model

• Description: Representative model of a reversible heat pump capable of heating the rooms during the winter season and cooling them in summer. This model is associated with the heated-cooled floors, previously explained (see section 4.3.3.8).

In heating mode, the device uses the anergy network and the electric current to heat the circulating water through the radiant floors to the corresponding temperature. The anergy network used is water from an external network (usually a river or lake) at temperature $T_{AN\ H\ pre\ HP}$.

In cooling mode, the condenser is transformed into a simple heat exchanger that reduces the radiant floor's circulating water temperature, keeping it at 18-19 °C established in the regulations [132]. The water flow used as an anergy network is redirected, so that now it

serves as a cooling fluid for the heat exchanger. Therefore, this heat pump is switched off during the summer season and will not consume any electrical work.

This model will be used in the last two scenarios that progressively eliminate the relevance of the DH network (see chapter 3.3, figures 3.23 and 3.24)

- Inputs:

    - $\dot{Q}_{HD\,H\,i}$ = Heat flow demand profile for heating, building i, in kW
    - $T_{CS\,H\,i}$ = Feed temperature of the heating water to the radiant floors, in K
    - $T_{r\,CS\,H\,i}$ = Return temperature of the heating water from the radiant floors, in K
    - $Cp_{r\,CS\,H\,i}$ = Calorific capacity of the circulating water at constant pressure, in kJ/(kg K)
    - $\dot{m}_{CS\,H\,i}$ = Mass flow of the circulating water, in kg/s
    - t = time profile, in h

- Parameters:

    - t_S = Time instant that changes from mid-season to summer = 144 h
    - γ_{HP} = Heat pump's efficiency factor, brings together all possible irreversibilities inside the heat pump. For this work, an average value of 55 % (0.55) is used
    - $T_{AN\,H\,pre\,HP}$ = temperature of the anergy network feeding the heat pump = 7 °C
    - $Cp_{AN\,H\,pre\,HP}$ = Calorific capacity of the anergy network water, in kJ/(kg K)
    - $\Delta T_{EV\,HE}$ = Supposed Temperature difference for the evaporator - heat exchanger during heating - cooling mode. This value is fixed by the user = 5 K.
    - HS_i = Heat Surface for building i, in m^2
    - SC = Estimated cooling demand ratio. The rule of thumb establishes values between 10 and 42 kW/m^2

- Outputs:

    - $T_{AN\,H\,post\,HP\,i}$ = Return temperature of the anergy network water after crossing the heat pump, building i, in K
    - $\dot{m}_{AN\,H\,i}$ = Mass flow of the circulating water through the anergy network, in kg/s
    - $\Delta T_{CON\,HP\,H\,i}$ = Temperature difference between the input and the output of the condenser (heating-cooling branch) for building i, in K
    - $\Delta T_{EV\,HP\,H\,i}$ = Temperature difference between the input and the output of the evaporator (heating-cooling branch), in K
    - $\dot{W}_{HP\,H\,i}$ = Electric work flow required by the heat pump (heating branch), in kW
    - $COP_{CARNOT\,HP\,H\,i}$ = Theoretical heat pump's operation coefficient (heating-cooling branch) (ad.)
    - $COP_{REAL\,HP\,H\,i}$ = Real heat pump's operation coefficient (heating-cooling branch) (ad.)

- System of equations:

In accordance with the characteristics of the device, the algorithm also works differently, depending on the seasonal period considered. In this way, 2 operating modes are distinguished:

– Cold Season (time <= t_S) = Heating mode:
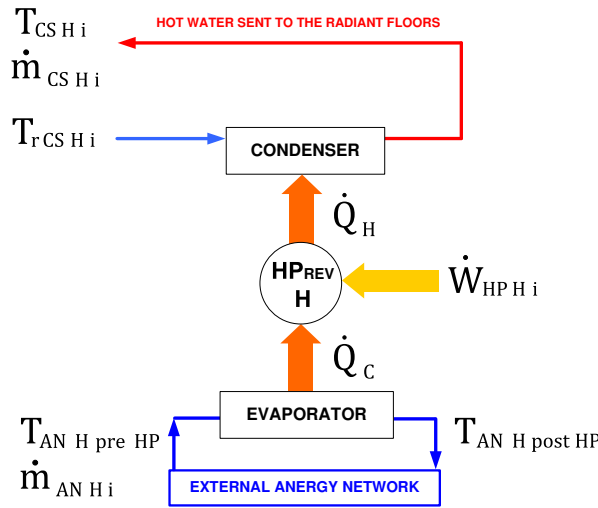
Figure 4.25: Reversible heat pump working on heating mode

1. Calculation of the mass flow circulating inside the radiant floors: From the main heat equation (see equation (4.1)) the following expression is obtained:

$$\dot{Q}_{HD\,H\,i} = \dot{m}_{CS\,H\,i} \cdot Cp_{r\,CS\,H\,i} \cdot (T_{CS\,H\,i} - T_{r\,CS\,H\,i}) \qquad (4.151)$$

$\dot{m}_{CS\,H\,i}$ is obtained.

2. Normal heat pump operation:

$T_{CS\,H\,i} > T_{r\,CS\,H\,i}$

A fixed temperature difference is used ($\Delta T_{EV\,HE}$), from which the mass flow of water will be supplied from the anergy network. the mass flow $\dot{m}_{AN\,H\,i}$ will be the dependent variable.

$$\Delta T_{CON\,HP\,H\,i} = T_{CS\,H\,i} - T_{r\,CS\,H\,i} \qquad (4.152)$$

Heat balance applied to the condenser:

$$\dot{Q}_{H\,i} = \dot{m}_{CS\,H\,i} \cdot Cp_{r\,CS\,H\,i} \cdot \Delta T_{CON\,HP\,H\,i} \qquad (4.153)$$

Looking at the evaporator branch, this relation is fulfilled:

$$T_{AN\,H\,post\,HP\,i} = T_{AN\,H\,pre\,HP\,i} - \Delta T_{EV\,HE} \qquad (4.154)$$

In the next step, both heat pump efficiencies are calculated:

$$COP_{CARNOT\,HP\,H\,i} = \frac{T_{CS\,H\,post\,HP\,i}}{T_{CS\,H\,post\,HP\,i} - T_{AN\,H\,post\,HP\,i}} \qquad (4.155)$$

$$COP_{REAL\,HP\,H\,i} = COP_{CARNOT\,HP\,H\,i} \cdot \gamma_{HP} \qquad (4.156)$$

Afterwards, the electric work flow is obtained:

$$\dot{W}_{HP\,H\,i} = \frac{\dot{Q}_{H\,i}}{COP_{REAL\,HP\,H\,i}} \qquad (4.157)$$

The energy balance allows to calculate the heat flow extracted from the anergy network (cold heat source):

$$\dot{Q}_{H\ i} = \dot{Q}_{C\ i} + \dot{W}_{HP\ H\ i} \tag{4.158}$$

From where $\dot{Q}_{C\ i}$ is calculated. Subsequently, $\dot{m}_{AN\ H\ i}$ is obtained from the energy balance of the evaporator:

$$\dot{Q}_{C\ i} = \dot{m}_{AN\ H\ i} \cdot Cp_{AN\ H\ pre\ HP\ i} \cdot \Delta T_{EV\ HE} \tag{4.159}$$

$\dot{m}_{AN\ H\ i}$ is finally solved.

3. Heat pump switched off:
   $T_{CS\ H\ i} = T_{r\ CS\ H\ i}$
   Same equations system as in the previous situation. In this case, the heat pump is switched off and there is no power consumption. Therefore:

   * $T_{AN\ H\ post\ HP\ i} = T_{AN\ H\ pre\ HP\ i}$
   * $\dot{m}_{AN\ H\ i} = 0$
   * $\dot{W}_{HP\ H\ i} = 0$

– Summer Season (time >= t_S) = Cooling mode:
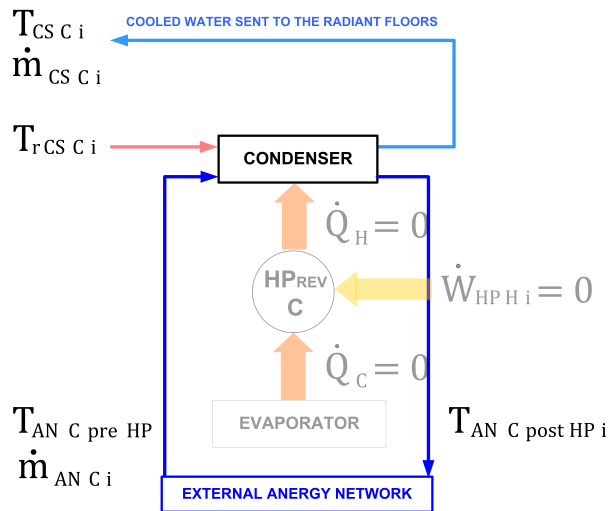
Figure 4.26: Reversible heat pump working in cooling mode

1. Calculation of the mass flow circulating inside the radiant floors:
   The heat flow extracted from the building can be obtained using the following expression:

$$\dot{Q}_{CD\ i} = SC \cdot HS_i \tag{4.160}$$

Again, from the main heat equation (see equation (4.1)) the mass flow of refreshing water circulating through the radiant floors is calculated using the following expression:

$$\dot{Q}_{CD\ i} = \dot{m}_{CS\ C\ i} \cdot Cp_{r\ CS\ H\ i} \cdot (T_{r\ CS\ H\ i} - T_{CS\ H\ i}) \tag{4.161}$$

$\dot{m}_{CS\ C\ i}$ is obtained.

2. Heat pump switched off. Condenser working in simple heat exchanger mode:

$$\Delta T_{CON\ HP\ H\ i} = T_{r\ CS\ H\ i} - T_{CS\ H\ i} \tag{4.162}$$

The notation changes because the system no longer works in heating mode (H), but cooling mode (C), and the condenser is turned into a heat exchanger (HE), thus:

$$\Delta T_{HE\ HP\ H\ i} = T_{r\ CS\ C\ i} - T_{CS\ C\ i} \tag{4.163}$$

From here in advance, all the equations are the same, but taking into account all modifications and notation changes.

Heat balance applied to the condenser (now behaving as a heat exchanger):

$$\dot{Q}_{refreshing\ i} = \dot{m}_{CS\ H\ i} \cdot Cp_{r\ CS\ H\ i} \cdot \Delta T_{HE\ HP\ H\ i} \tag{4.164}$$

$$T_{AN\ H\ post\ HP\ i} = T_{AN\ H\ pre\ HP\ i} - \Delta T_{EV\ HE} \tag{4.165}$$

Calculating heat pump efficiencies:

$$COP_{CARNOT\ HP\ H\ i} = 0 \tag{4.166}$$

$$COP_{REAL\ HP\ H\ i} = 0 \tag{4.167}$$

Afterwards, the electric work flow is obtained:

$$\dot{W}_{HP\ H\ i} = 0 \tag{4.168}$$

Heat flow extracted from the anergy network in the heat exchanger:

$$\dot{Q}_{refreshing\ i} = \dot{m}_{AN\ C\ i} \cdot Cp_{AN\ H\ pre\ HP} \cdot \Delta T_{EV\ HE} \tag{4.169}$$

From where $\dot{m}_{AN\ C\ i}$ is calculated.

4.3.3.12 Building's Linker Pipe
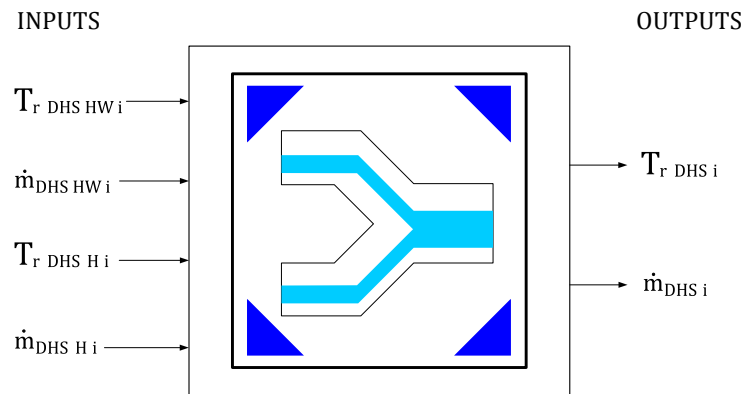
Figure 4.27: Block picture, representing the linker "T" pipe for return DH water flow inside the building

- Description: This is a very simple model that represents the union of the two DH water flows coming from the 2 branches in service (hot water and heating) inside the building.

- Inputs:

  - $T_{r\,DHS\,HW\,i}$ = Return temperature of the DH water for building i, hot water branch, in K
  - $\dot{m}_{DHS\,HW\,i}$ = Mass flow of the DH water for building i, hot water branch, in kg/s
  - $T_{r\,DHS\,H\,i}$ = Return temperature of the DH water for building i, heating branch, in K
  - $\dot{m}_{DHS\,H\,i}$ = Mass flow of the DH water for building i, heating branch, in kg/s

- Parameters: No parameters needed

- Outputs:

  - $T_{r\,DHS\,i}$ = Return temperature of the DH water for building i, in K
  - $\dot{m}_{DHS\,i}$ = Mass flow of the DH water for building i, in kg/s
  - System of equations:
    * Mass flow calculation:

$$\dot{m}_{DHS\,i} = \dot{m}_{DHS\,HW\,i} + \dot{m}_{DHS\,H\,i} \tag{4.170}$$

    * Temperature calculation:

$$T_{r\,DHS\,i} = \frac{\dot{m}_{DHS\,HW\,i}}{\dot{m}_{DHS\,HW\,i} + \dot{m}_{DHS\,H\,i}} \cdot T_{r\,DHS\,HW\,i} + \frac{\dot{m}_{DHS\,H\,i}}{\dot{m}_{DHS\,HW\,i} + \dot{m}_{DHS\,H\,i}} \cdot T_{r\,DHS\,H\,i} \tag{4.171}$$

4.3.4   Network

The representative elementary blocks of each member of the DHN are described below. No complex blocks appear in this case.

4.3.4.1   District Heating Pipe
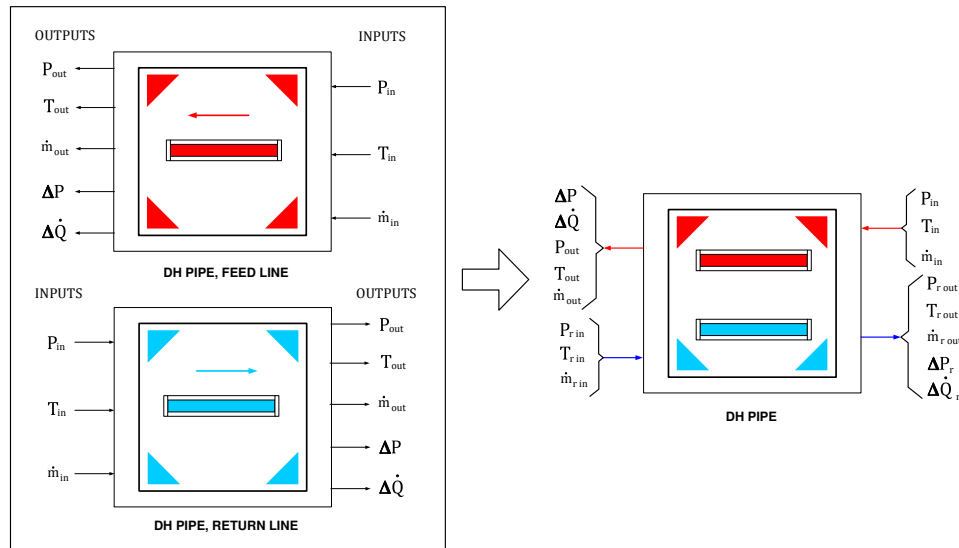
Figure 4.28: Block picture, representing the DH pipe, feed and return flow

- Description: The present block represents the pipeline through the DH water flows. Each block represents a segment of individual pipe with its length, nominal diameter and insulation layer. The model is a simplification of a real DH pipe in which both tubes (supply and return) are wrapped by the same insulating body and contained inside the same tube (see figure 2.60).

  The final goal is the calculation of the pressure drop (ΔP) and the heat losses ($\Delta \dot{Q}$), as well as the associated temperature drop.

- Inputs:

    - P_{in} = Pressure of the incoming DH water in the pipeline, in Pa
    - T_{in} = Temperature of the incoming DH water in the pipeline, in K
    - $\dot{m}_{in}$ = Mass flow of the incoming DH water in the pipeline, in kg/s

- Parameters:

    - $D_{N\,j}$ = Nominal diameter of the pipe, in m
    - L_j = Pipe length, in m
    - ρ_{H2O} = Water density at mean feed/return temperature, in kg/m^3 [131]
    - μ_{H2O} = Water viscosity at mean feed/return temperature, in kg/(m s) [131]

- Cp_{H2O} = Calorific capacity of water at constant pressure. Feed/return line, in kJ/(kg K) [131]

- π = Pi number = 3.1416

- g = Gravitational acceleration value = 9.81 m/s^2

- Re_x = Reynolds values, x axis of Moody's diagram (ad.) [134]

- ϕ_y = Friction factor values, y axis of Moody's diagram (ad.) K [134]

- Z_{in} = Height of the first pipe endpoint (+ or -), in m

- Z_{out} = Height of the second pipe endpoint (+ or -), in m

- T_0 = Reference temperature, corresponding to the average temperature of the trench where the DH pipes are installed = 281.15 K = 8 °C

- ρ_{AIR} = Air density at T_0, in kg/m^3 [135]

- μ_{AIR} = Air viscosity at T_0, in kg/(m s) [135]

- Cp_{AIR} = Calorific capacity of the air at constant pressure at T_0, in kJ/(kg K) [135]

- k_{AIR} = Thermal conductivity of the air at T_0, in W/(m K) [135]

- β_{AIR} = Thermal expansion coefficient of the air at T_0, in K^{-1}) [135]

- T_s = Supposed temperature of the external pipe surface = 318.15 K = 45 °C

- e_{PVC} = Pipe's wall thickness = 0.005 m

- e_{INS} = Pipe's insulation thickness = 0.01 m

- k_{PVC} = Thermal conductivity of PVC material = 0.16 W/(m K) [136], [137]

- k_{INS} = Thermal conductivity of insulation material = 0.032 W/(m K) [138], [139], [140]

- Outputs:

  - P_{out} = Pressure of the outgoing DH water in the pipeline, in Pa

  - T_{out} = Temperature of the outgoing DH water in the pipeline, in K

  - $\dot{m}_{out}$ = Mass flow of the outgoing DH water in the pipeline, in kg/s

  - ΔP = Pressure drop, in Pa

  - $\Delta\dot{Q}$ = = Heat losses, in kW

- System of equations:

  1. Mass balance: Straight pipe segment without branches or mass inputs or outputs

$$\dot{m}_{out} = \dot{m}_{in} \qquad (4.172)$$

  2. Calculation of pressure losses:

     - Preliminary estimations

$$\dot{q} = \frac{\dot{m}_{in}}{\rho_{H2O}} \qquad (4.173)$$

$$A_{pipe\ j} = \pi \cdot \left(\frac{D_{N\ j}}{2}\right)^2 \qquad (4.174)$$

$$u_j = \frac{\dot{q}}{A_{pipe\ j}} \quad (4.175)$$

Since u is the fluid velocity [=] m/s

– Hydraulic balances

The Reynolds number then is calculated, which will characterize the fluid movement and determine whether the flow regime is laminar or turbulent [141].

$$Re = \frac{u_j \cdot D_{N\ j} \cdot \rho_{H2O}}{\mu_{H2O}} \quad (4.176)$$

The Reynolds values are their correspondent regimes are the following:

Re $\leq$ 2000 $\rightarrow$ Laminar flow 2000 < Re < 4000 $\rightarrow$ Transition phase Re $\geq$ 4000 $\rightarrow$ Turbulent flow

In the next step, the Darcy-Weisbach friction factor is calculated (ϕ). In fluid dynamics, this factor is used to estimate the pressure drop inside horizontal cylindrical pipes due to the friction of fluids.

In case of laminar flow, ϕ depends only on Reynolds number. For turbulent flow, ϕ factor depends on the Reynolds number and the relative pipe roughness (ϵ/D). In this project, all DH pipes are smooth and made of PVC, which offers a very low resistance to the flow circulation. For this material, $\epsilon/D = 0.000001$.

From this value, and its correspondent curve in Moody's diagram (see ANNEX: Figure B.1), the table ϕ - Re is obtained. This table is introduced as a block parameter.

By means of interpolation, and depending on the Reynolds number calculated for each instant, a ϕ value is obtained.

Finally, ΔP is calculated from the Darcy-Weisbach equation [134]:

$$h_f = \frac{8 \cdot phi \cdot L_j \cdot u_j^2}{D_{N\ j} \cdot 2 \cdot g} \quad (4.177)$$

Finally, using the hydraulic balance:

$$\Delta P = \left[Z_{out} + Z_{in} + \frac{8 \cdot \phi \cdot L_j \cdot u_j^2}{D_{N\ j} \cdot 2 \cdot g} \right] \cdot \rho_{H2O} \cdot g \quad (4.178)$$

$$P_{out} = P_{in} - \Delta P \quad (4.179)$$

Due to the relatively small pipe lengths present in this case study, the variations of the physical properties of the circulating fluid are considered negligible.

3. Calculation of heat and temperature losses:

Considering the heat transmission mechanisms (conduction and convection), the following schema is obtained:
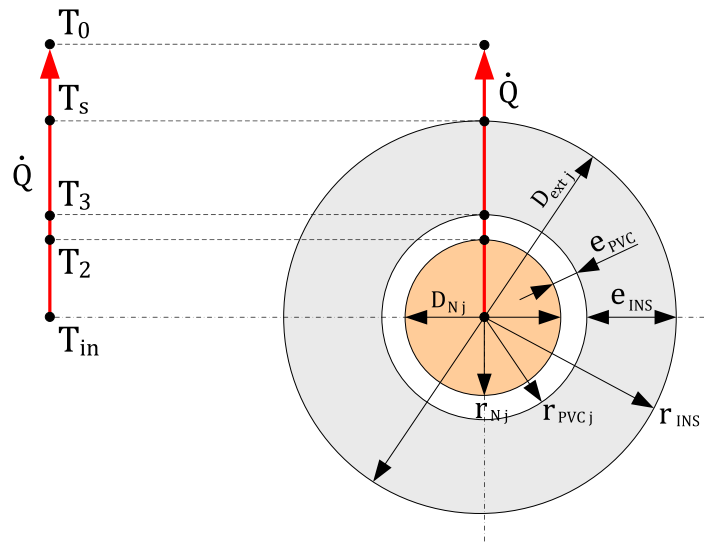
Figure 4.29: Pipe section scheme and heat transmission mechanisms detailed

Since $r_{N\,j}$ is the nominal radius, r_{PVC} is the distance between the pipe center and the external pipe layer, r_{INS} is the external radius, considering the insulation layer, and $D_{ext\,j}$ as the external diameter, all of them in m.

– Preliminary calculations:

$$r_{N\,j} = \frac{D_{N\,j}}{2} \tag{4.180}$$

$$r_{PVC\,j} = r_{N\,j} + e_{PVC} \tag{4.181}$$

$$r_{INS\,j} = r_{N\,j} + e_{PVC} + e_{INS} \tag{4.182}$$

$$D_{ext\,j} = 2 \cdot (r_{N\,j} + e_{PVC} + e_{INS}) \tag{4.183}$$

$$A_{LMHT\,j} = \frac{2\,\pi\,(r_{INS\,j} - r_{N\,j})}{Ln\left(\frac{r_{INS\,j}}{r_{N\,j}}\right)} \tag{4.184}$$

$$A_{LMHT\,PVC\,j} = \frac{2\,\pi\,(r_{PVC\,j} - r_{N\,j})}{Ln\left(\frac{r_{PVC\,j}}{r_{N\,j}}\right)} \tag{4.185}$$

$$A_{LMHT\,INS\,j} = \frac{2\,\pi\,(r_{INS\,j} - r_{PVC\,j})}{Ln\left(\frac{r_{INS\,j}}{r_{PVC\,j}}\right)} \tag{4.186}$$

Since $A_{LMHT\,j}$, $A_{LMHT\,PVC\,j}$ and $A_{LMHT\,INS\,j}$ are logarithmic mean heat transmission areas for the entire pipe, the PVC layer and the insulation layer, respectively.

For 1 m length:

$$A_{ext\ j} = 2 \cdot \pi \cdot r_{INS\ j} \cdot 1 \tag{4.187}$$

– Grashof (Gr), Prandtl (Pr) and Rayleigh (Ra) numbers:

$$Gr = g \cdot \beta_{AIR} \cdot (T_s - T_0) \cdot \left(D_{ext\ j}^3\right) \cdot \left(\frac{\rho_{AIR}}{\mu_{AIR}}\right)^2 \tag{4.188}$$

$$Pr = \frac{\mu_{AIR} \cdot Cp_{AIR} \cdot 1000}{k_{AIR}} \tag{4.189}$$

$$Ra = Gr \cdot Pr \tag{4.190}$$

– Calculation of the heat transmission coefficient by natural convection ($h_{CN\ AIR}$ [=] W/(m^2 K)):
In order to calculate the Nusselt number, the Churchill & Chu correlation for turbulent regime will be used [142]:

$$Nu = \left[0.6 + 0.387 \cdot \left[\frac{Ra}{\left[1 + \left(\frac{0.559}{Pr}\right)^{\frac{9}{16}}\right]^{\frac{16}{9}}}\right]^{\frac{1}{6}}\right]^2 \tag{4.191}$$

This formula is valid for the following conditions:

  * Rayleigh number range has to be between 10^{-5} and 10^{12}
  * Applied for natural convection for horizontal cylinders
  * The diameter is the characteristic dimension assumed
  * The external surface temperature (T_s) is assumed constant

Consequently, $h_{CN\ AIR}$ is calculated:

$$h_{CN\ AIR} = \frac{Nu \cdot k_{AIR}}{D_{ext\ j}} \tag{4.192}$$

– Calculation of the global heat transmission coefficient (U [=] W/(m^2 K)) (see figure 4.29:

$$U = \frac{1}{\frac{e_{PVC}}{K_{PVC} \cdot A_{LMHT\ PVC\ j}} + \frac{e_{INS}}{K_{INS} \cdot A_{LMHT\ INS\ j}} + \frac{1}{h_{CN\ AIR} \cdot A_{ext\ j}}} \tag{4.193}$$

Finally, $\Delta \dot{Q}$ is calculated using the heat transmission equation:

$$\Delta \dot{Q} = U \cdot A_{LMHT\ j} \cdot L_j \cdot (T_{in} - T_0) \tag{4.194}$$

And therefore, T_{out} is calculated from the energy balance:

$$\Delta \dot{Q} = \dot{m}_{in} \cdot Cp_{H2O} \cdot (T_{in} - T_{out}) \tag{4.195}$$

4.3.4.2 District Heating Linker Pipe (2,3,4 branches)
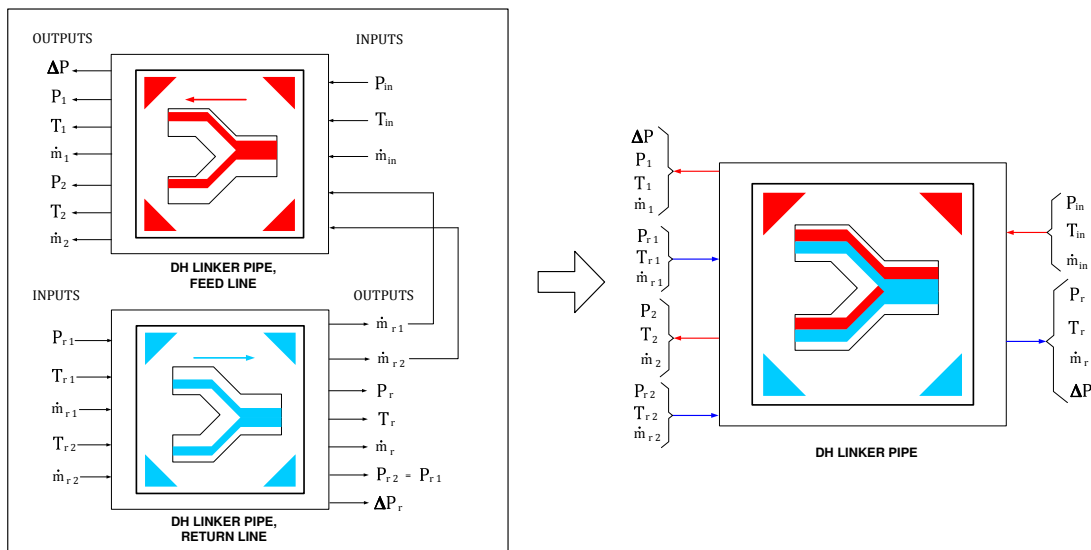
Figure 4.30: Block picture, representing the DH Linker pipe for feed and return flows

- Description: Representative block of a union-branching node of 2, 3 and up to 4 DH pipes. In this case, only the two branches model is described.

  The model calculates pressures, temperatures and mass flows of all outputs, including the pressure losses both for the feed return line. For this kind of pipeline accessories, the heat losses are considered negligible.

  Regarding to the pressure calculation in the return line, the block determines the return pressure of the lateral branches (P_r) based on the return pressures of the main line (see explanation in section 3.2.3)

  In addition, the block calculates the mass flows circulating through the feed line based on the return line, obeying to the circulation of data in the simulation.

- Inputs:

  - P_{in} = Pressure of the incoming DH water, in Pa
  - T_{in} = Temperature of the incoming DH water, in K
  - $\dot{m}_{in}$ = Mass flow of the incoming DH water, in kg/s
  - $P_{r\,1}$ = Pressure of the return DH water, first branch, in Pa
  - $T_{r\,1}$ = Temperature of the return DH water, first branch, in K
  - $\dot{m}_{r\,1}$ = Mass flow of the return DH water, first branch, in kg/s
  - $P_{r\,2}$ = Pressure of the return DH water, second branch, in Pa
  - $T_{r\,2}$ = Temperature of the return DH water, second branch, in K
  - $\dot{m}_{r\,2}$ = Mass flow of the return DH water, second branch, in kg/s

- Parameters:

- $D_{N\ AC\ j}$ = Nominal diameter of this pipe accessory, in m

- $L_{EQ\ AC\ j}$ = Equivalent Pipe length, in m [143], [144]

- ρ_{DH2} = Water density at mean feed temperature, in kg/m^3 [131]

- $\rho_{r\ DH2}$ = Water density at mean return temperature, in kg/m^3 [131]

- μ_{H2O} = Water viscosity at mean feed/return temperature, in kg/(m s) [131]

- π = pi number = 3.1416

- g = gravitational acceleration value = 9.81 m/s^2

- Re_x = Reynolds values, x axis of Moody's diagram (ad.) [134]

- ϕ_y = Friction factor values, y axis of Moody's diagram (ad.) K [134]

- Z_{in} = Height of the first pipe endpoint, in m

- Z_{out} = Height of the second pipe endpoint, in m

- Outputs:

  - ΔP = Pressure drop, feed line, in Pa

  - ΔP_r = Pressure drop, return line, in Pa

  - P_1 = Pressure of the outgoing DH water, feed line, first branch, in Pa

  - T_1 = Temperature of the outgoing DH water, feed line, first branch, in K

  - $\dot{m}_1$ = Mass flow of the outgoing DH water, feed line, first branch, in kg/s

  - P_2 = Pressure of the outgoing DH water, feed line, second branch, in Pa

  - T_2 = Temperature of the outgoing DH water, feed line, second branch, in K

  - $\dot{m}_2$ = Mass flow of the outgoing DH water, feed line, second branch, in kg/s

  - P_r = Pressure of the return DH water, in Pa

  - T_r = Temperature of the return DH water, in K

  - $\dot{m}_{r\ 1}$ = Mass flow of the return DH water, in kg/s

- System of equations:

  1. Pressure drop calculation:

     ΔP is calculated following the same process as in the previous block (see section 4.3.4.1)

     For the feed line, using the hydraulic balance:

     $$\Delta P = \left[Z_{out} - Z_{in} + \frac{8 \cdot \phi_{feed\ line} \cdot L_{EQ\ AC\ j} \cdot u^2_{feed\ line\ j}}{D_{N\ AC\ j} \cdot 2 \cdot g} \right] \cdot \rho_{DH2} \cdot g \qquad (4.196)$$

     $$P_1 = P_2 = P_{in} - \Delta P \qquad (4.197)$$

     For the return line:

     $$\Delta P = \left[Z_{out} - Z_{in} + \frac{8 \cdot \phi_{r\ line} \cdot L_{EQ\ AC\ j} \cdot u^2_{r\ line\ j}}{D_{N\ AC\ j} \cdot 2 \cdot g} \right] \cdot \rho_{r\ DH2} \cdot g \qquad (4.198)$$

$$P_r = P_{r\,1} - \Delta P_r \tag{4.199}$$

$$P_{r\,2} = P_{r\,1} \tag{4.200}$$

2. Mass flow:
   For the return line:

$$\dot{m}_r = \dot{m}_{r\,1} - \dot{m}_{r\,2} \tag{4.201}$$

For the feed line:

$$\dot{m}_1 = \dot{m}_{r\,1} \tag{4.202}$$

$$\dot{m}_2 = \dot{m}_{r\,2} \tag{4.203}$$

3. Temperatures:
   For the feed line:

$$T_1 = T_2 = T_{in} \tag{4.204}$$

For the return line:

$$T_r = \frac{T_{r\,1} \cdot \dot{m}_{r\,1} + T_{r\,2} \cdot \dot{m}_{r\,2}}{\dot{m}_r} \tag{4.205}$$

4.3.4.3 Hydraulic Pump
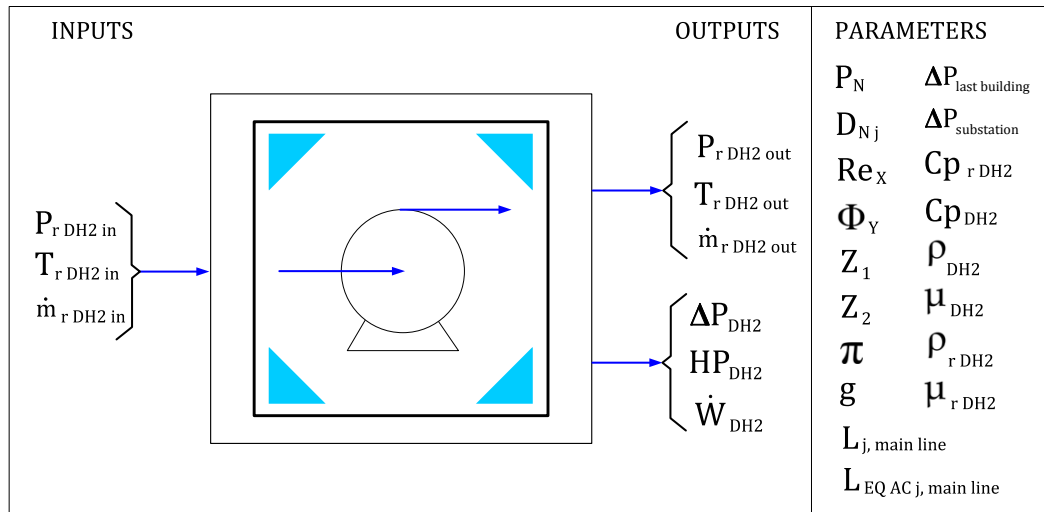
Figure 4.31: Block picture, representing the Hydraulic Pump

- Description: This model represents the hydraulic pump that drives the DH water from the substation to the last building. The model calculates the total pressure drop associated with the main hydraulic line and, based on this value, calculates the impulsion pressure required to overcome those pressure losses. Likewise, it calculates the electrical energy flow consumed by the pump. The increase of water temperature due to the impulsion is considered negligible.

- Inputs:

    - $P_{r\,DH2\,in}$ = Pressure of the incoming DH water, in Pa
    - $T_{r\,DH2\,in}$ = Temperature of the incoming DH water, in K
    - $\dot{m}_{DH2\,in}$ = Mass flow of the incoming DH water, in kg/s

- Parameters:

    - $D_{N\,j}$ = Nominal diameter of the pipe, in m
    - $L_{j\,main\,line}$ = Pipe length of those pipes belonging to the main hydraulic line, in m
    - $L_{EQ\,j\,main\,line}$ = Pipe length of those pipe accessories belonging to the main hydraulic line, in m
    - P_N = Nominal pressure, in Pa
    - ρ_{DH2} = Water density of water, feed DH line, in kg/m^3 [131]
    - μ_{DH2} = Water viscosity of water, feed DH line, in kg/(m s) [131]
    - Cp_{DH2} = Calorific capacity of water at constant pressure, feed DH line, in kJ/(kg K) [131]
    - $\rho_{r\,DH2}$ = Water density of water, return DH line, in kg/m^3 [131]
    - $\mu_{r\,DH2}$ = Water viscosity of water, return DH line, in kg/(m s) [131]

- – $Cp_{r\,DH2}$ = Calorific capacity of water at constant pressure, return DH line, in kJ/(kg K) [131]
- – π = pi number = 3.1416
- – g = Gravitational acceleration value = 9.81 m/s^2
- – Re_x = Reynolds values, x axis of Moody's diagram, in K [134]
- – ϕ_y = Friction factor values, y axis of Moody's diagram, in K [134]
- – Z_1 = Height where the hydraulic pump is located (+ or -), in m
- – Z_2 = Height of the last building of the DH network (+ or -), in m
- – $\Delta P_{last\,building}$ = Pressure drop assumed for heat exchangers in the buildings, in Pa
- – $\Delta P_{substation}$ = Pressure drop assumed for the heat exchanger in the substation, in Pa

- Outputs:

  - – $P_{r\,DH2\,out}$ = Pressure of the incoming DH water[=] Pa
  - – $T_{r\,DH2\,out}$ = Temperature of the incoming DH water [=] K
  - – $\dot{m}_{DH2\,out}$ = Mass flow of the incoming DH water [=] kg/s
  - – ΔP_{DH2} = Pressure difference supplied by the hydraulic pump [=] Pa
  - – $\dot{q}_{DH2}$ = = Volumetric flow [=] m^3/s
  - – HP_{DH2} = Impulse charge [=] m
  - – $\dot{W}_{DH2}$ = Electric work flow [=] W

- System of equations:

  Pressure losses are calculated for both branches: feed and return.

  1. Mass balance: The device is considered as a watertight compartment without liquid leakages.

$$\dot{m}_{DH2\,out} = \dot{m}_{DH2\,in} \tag{4.206}$$

  2. Calculation of pressure losses: return line

$$\dot{q}_{DH2\,return\,line} = \frac{\dot{m}_{DH2}}{\rho_{r\,DH2}} \tag{4.207}$$

$$A_{pipe\,j} = \pi \cdot \left(\frac{D_{N\,j\,main\,pipe}}{2}\right)^2 \tag{4.208}$$

$$u_{DH2\,j} = \frac{\dot{q}_{DH2\,return\,line}}{A_{pipe\,j}} \tag{4.209}$$

$$Re = \frac{u_{DH2\,j} \cdot D_{N\,j\,main\,pipe} \cdot \rho_{r\,DH2}}{\mu_{r\,DH2}} \tag{4.210}$$

  By means of interpolation, and depending on the Reynolds number calculated for each instant, a ϕ value is obtained. Again, $\varepsilon/D = 0.000001$ (same procedure as in previous block models).

Total length is calculated following the expression:

$$L_{total\ main\ line} = \sum_{j}^{npipes} L_{j\ main\ line} + \sum_{j}^{naccessories} L_{eq\ j\ main\ line} \qquad (4.211)$$

Therefore, pressure drop for the return line is calculated:

$$\Delta P_{DH2\ return\ line} = \left[Z_{out} + Z_{in} + \frac{8 \cdot \phi \cdot L_{total\ main\ line} \cdot u_j^2}{D_{N\ j} \cdot 2 \cdot g} \right] \cdot \rho_{r\ DH2} \cdot g \qquad (4.212)$$

$\Delta P_{DH2\ feed\ line}$ is obtained using the same procedure, but using ρ_{DH2} and μ_{DH2}.

3. Hydraulic balance (see section 3.2.3

$$\Delta P_{DH2} = \Delta P_{DH2\ return\ line} + \Delta P_{DH2\ feed\ line} + \Delta P_{last\ building} + \Delta P_{SUB} \qquad (4.213)$$

Finally, discharge pressure is obtained:

$$P_{r\ DH2\ out} = P_N + \Delta P_{DH2} \qquad (4.214)$$

Thus, impulse charge is calculated:

$$HP_{DH2} = \frac{\Delta P_{DH2}}{\rho_{r\ DH2} \cdot g} \qquad (4.215)$$

4. Electric work flow

The impulse energy consumed by the hydraulic pump is calculated by the following expression:

$$\dot{W}_{DH2} = HP_{DH2} \cdot \dot{m}_{DH2\ in} \cdot g \qquad (4.216)$$

4.3.5 Substation

Hereunder, the representative elementary blocks of each element inside the substation are described:

4.3.5.1 Mass-Energy balances in the Substation
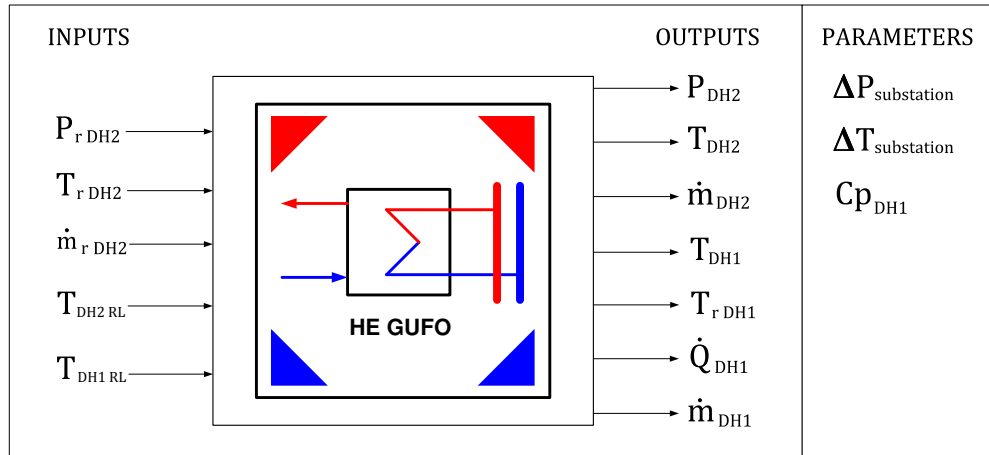
Figure 4.32: Block picture, representing the Mass-Energy balances calculated in the substation

- Description: This model is used to calculate pressure, temperature and mass flow variables for the substation for both the primary and secondary networks. The results associated with the primary network will not be considered because this project focuses on the local network. In addition, there is a lack of information about the primary network's operation. For more information, see section 4.1

- Inputs:

  - $P_{r\ DH2}$ = Pressure of the incoming DH water, in Pa
  - $T_{r\ DH2}$ = Temperature of the incoming DH water, in K
  - $\dot{m}_{r\ DH2}$ = Mass flow of the incoming DH water, in kg/s
  - $T_{DH1\ RL}$ = Temperature of the DH water defined by the regulation lines, primary network (see section 4.3.2.2), in K
  - $T_{DH2\ RL}$ = Temperature of the DH water defined by the regulation lines, secondary network (see section 4.3.2.2), in K

- Parameters:

  - $\Delta P_{substation}$ = Pressure drop supposed in the substation, in Pa
  - $\Delta T_{substation}$ = Temperature difference supposed in the heat exchanger of the substation, hot side, in K
  - Cp_{DH1} = Calorific capacity of water at constant pressure, in $J/(kg\,K)$

- Outputs:

  - P_{DH2} = Pressure of the outgoing DH water, feed line of the secondary network, in Pa

  - T_{DH2} = Temperature of the outgoing DH water, feed line of the secondary network, in K

  - $\dot{m}_{DH2}$ = Mass flow of the outgoing DH water, feed line of the secondary network, in kg/s

  - T_{DH1} = Temperature of the DH water defined by the regulation line, primary network, in K

  - $T_{r\,DH1}$ = Return temperature of the DH water, primary network, in K

  - $\dot{Q}_{DH1}$ = Heat flow extracted from the primary network to the secondary network, in kW. (Again as before, the heat losses in the heat exchanger are considered negligible)

  - $\dot{m}_{DH1}$ = Mass flow of DH water used from the primary network, in kg/s

- System of equations:

  1. Secondary network:

$$P_{DH2} = P_{r\,DH2} + \Delta P_{substation} \tag{4.217}$$

$$T_{DH2} = T_{DH2\,RL} \tag{4.218}$$

$$\dot{m}_{DH2} = \dot{m}_{r\,DH2} \tag{4.219}$$

  2. Primary network:

$$T_{DH1} = T_{DH1\,RL} \tag{4.220}$$

$$T_{r\,DH1} = T_{DH1} - \Delta P_{substation} \tag{4.221}$$

$$\dot{Q}_{DH1} = \dot{Q}_{DH2} = \dot{m}_{DH1} \cdot C_{P DH1} \cdot (T_{DH2} - T_{r\,DH2}) \tag{4.222}$$

$\dot{m}_{DH1}$ is calculated.

Another strategy is possible, defining a fixed mass flow $\dot{m}_{DH1}$ and leaving $T_{r\,DH2}$ as the dependent variable.

For this model, it has been decided to define a constant $\Delta T_{substation}$ on the hot side and leave $\dot{m}_{DH1}$ as the independent variable. However, another control strategy would be possible, defining a fixed mass flow $\dot{m}_{DH1}$ and leaving $T_{r\,DH2}$ as the dependent variable.

The lack of information regarding the operation of the substation prevents us to know which control strategy is used.

4.3.5.2   Substation's Heat Pump
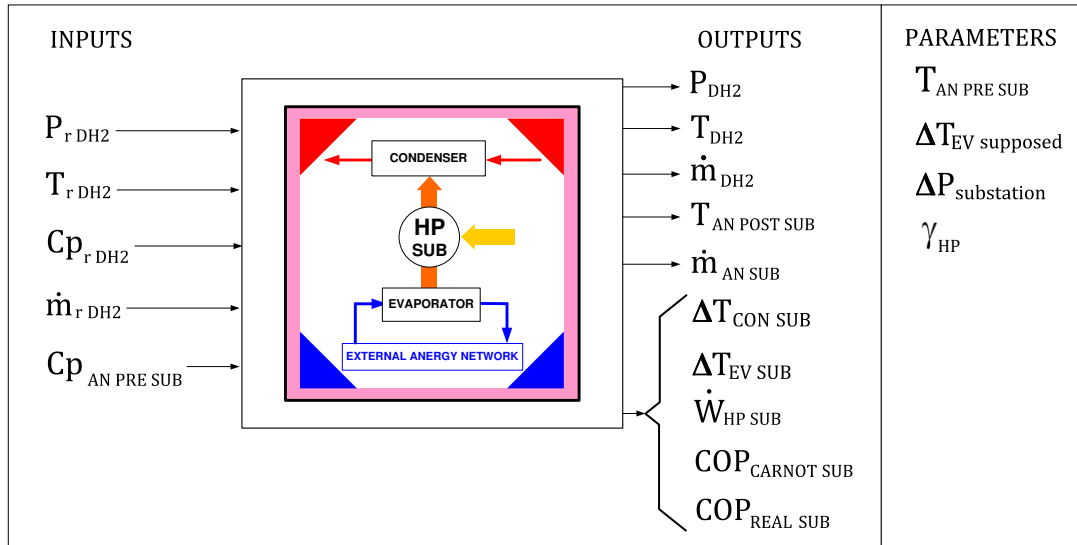
Figure 4.33: Block picture, representing the General Heat Pump installed in the substation

- Description: Representative model of a heat pump working at continuous operation. Her capacity is greater than previous devices. This heat pump is located inside the substation, and its function consists of raise DH water temperature in the same way as the heat exchanger would do in her place. The temperature is indicated by the regulation line, in the same way as in previous model.

  This kind of device appears in those hypotheses in which no connection with the primary network is needed. Instead, a water stream from an external anergy network is modelled. This water comes from industrial effluents and it is considered thermally usable, due to the relative high temperature it has (around 25 - 30 °C).

- Inputs:

  - $P_{r\,DH2}$ = Pressure of the incoming DH water, in Pa
  - $T_{r\,DH2}$ = Temperature of the incoming DH water, in K
  - $Cp_{r\,DH2}$ = Calorific capacity of water at constant pressure, at $T_{r\,DH2}$, in $J/(kg\,K)$
  - $\dot{m}_{r\,DH2}$ = Mass flow of the incoming DH water, in kg/s
  - $Cp_{AN\,PRE\,SUB}$ = Calorific capacity of water at constant pressure, at $T_{AN\,PRE\,SUB}$, in $J/(kg\,K)$
  - $T_{DH2\,RL}$ = Temperature of the DH water defined by the regulation lines, secondary network (see section 4.3.2.2), in K

- Parameters:

  - $\Delta P_{substation}$ = Pressure drop supposed in the substation, in Pa
  - $T_{AN\,pre\,SUB}$ = Feed temperature of the substation's anergy network (AN) = 30 °C

- – γ_{HP} = Heat pump's efficiency factor, brings together all possible irreversibilities inside the heat pump. The real efficiency of commercial heat pump systems is usually 50% to 70% of the theoretical efficiency [133]. For this work, an average value of 55% (0.55) is used

    - – $\Delta T_{EV\ defined}$ = Defined Temperature difference for the evaporator between $T_{AN\ HW\ pre\ HP\ i}$ and $T_{AN\ HW\ post\ HP\ i} = 21$ K

- • Outputs:

    - – P_{DH2} = Pressure of the DH water, feed line of the secondary network, in Pa
    - – T_{DH2} = Temperature of the DH water, feed line of the secondary network, in K
    - – $\dot{m}_{DH2}$ = Mass flow of the DH water, feed line of the secondary network, in kg/s
    - – $T_{AN\ post\ SUB}$ = Return temperature of the AN after crossing the heat pump, in K
    - – $\dot{m}_{AN\ HW\ i}$ = Substation's AN water mass flow, in kg/s
    - – $\Delta T_{CON\ SUB}$ = Heat pump's Temperature difference (condenser), in K
    - – $\Delta T_{EV\ SUB}$ = Heat pump's Temperature difference (evaporator), in K
    - – $\dot{W}_{HP\ SUB}$ = Electric work flow required by the substation's heat pump, in kW
    - – $COP_{CARNOT\ SUB}$ = Theoretical heat pump's operation coefficient, ad.
    - – $COP_{REAL\ SUB}$ = Real heat pump's operation coefficient, ad.

- • System of equations:

    This model has the same operation as the previous block Direct Heat Pump for DHW branch, used in scenarios 7 and 8 (see section 4.3.3.5).

Chapter 5

Methodology

5.1 About the Software

MATLAB® (MATrix LABoratory) is a fourth-generation high-level programming language and interactive environment for numerical computation, visualization and programming.

Among the great variety of applications it has, the following ones are highlighted:

- Creation of functions and databases

- Data analysis

- Plotting and Mapping

- Development and implementation of algorithms

- Creation of models, user interfaces and other applications

- interfacing with programs written in other languages, including C, C++, Java, and FORTRAN

In addition, MATLAB has numerous built-in commands and math functions that help in mathematical calculations, generating plots, and performing numerical methods. In addition, it provides an interactive environment able to link with other softwares and applications, like Simulink or Excel.

Simulink (also developed by MathWorks) is a data flow graphical programming language tool for modelling, simulating and analyzing multi-domain dynamic systems. It is basically a graphical block diagramming tool with customizable set of block libraries. It allows the incorporation of MATLAB algorithms into models as well as export the simulation results into MATLAB for further analysis [145].

174

5.2   Workflow
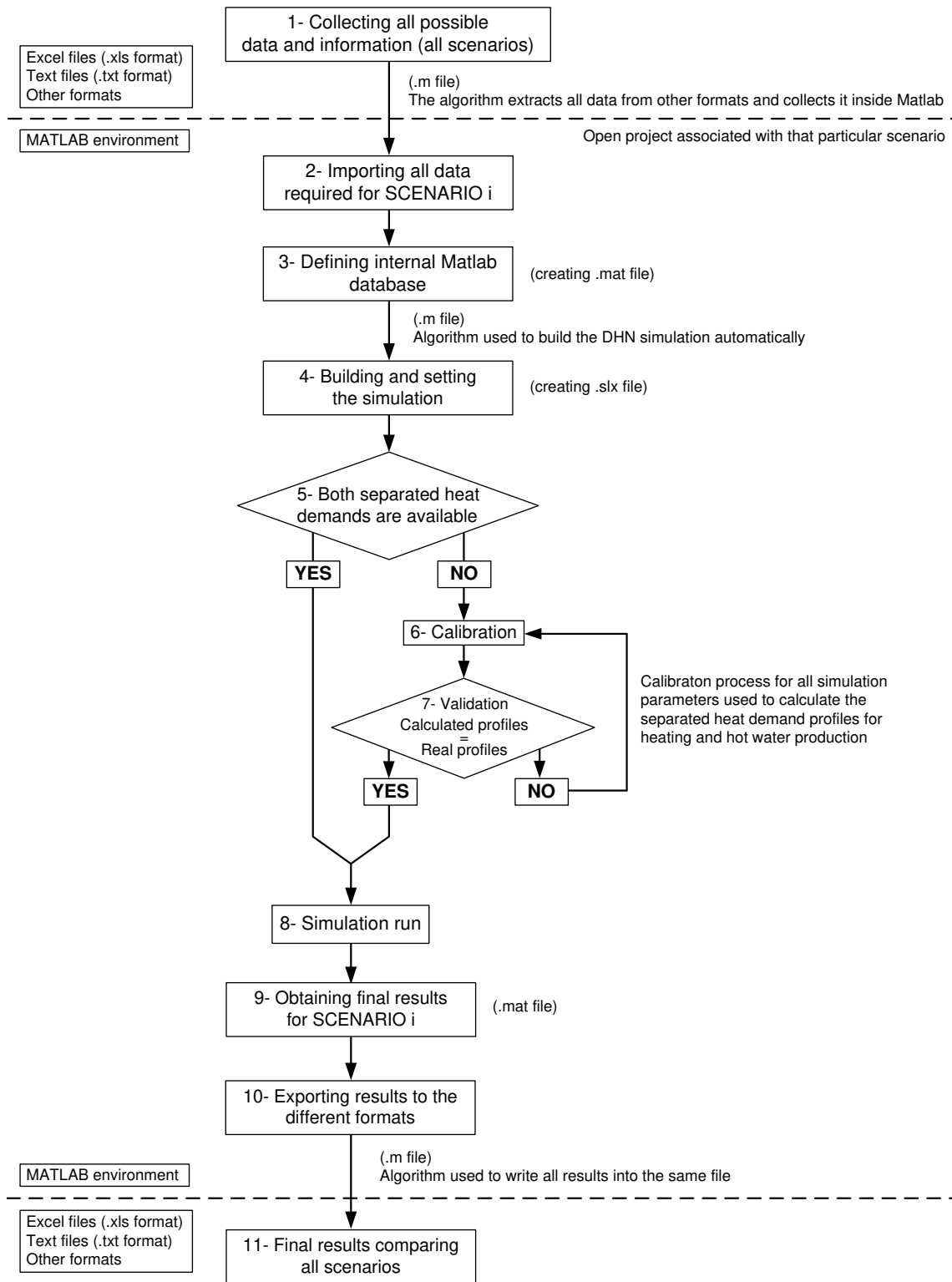
Figure 5.1: Sequential process of the model.

Once all particular mathematical models integrating a thermal network are known, then it is possible to set up the general model. The number of equations to be considered and calculations to be solved becomes large as the complexity of the network increases, so simulators are the necessary tools in order to make all these calculations automatically.

Due to the idea of refurbishing and transforming the heating systems inside the buildings, the desired methodology should be able to modellize and simulate their internal networks and facilities, in order to understand how these systems work and how to modify them with the aim of generate new simulations representing new scenarios.

Finally, a detailed simulation representing each of the elements of the network (pipes, substations, hydraulic pumps) is needed. Other elements inside the buildings must be considered, such as radiators or recirculation systems. For example, in order to simulate a hot water stream flowing from a pipe to a building, a pipe block and a building block connected to each other will be required, so that the outputs of the pipe block are the inputs of the building block. In this way the user easily visualises how the models are linked and how the different variables interact each other.

If the purpose is to show the effects of refurbishing all buildings changing from radiators to heated floors, it will first be necessary to simulate a network with radiators installed in the buildings and compare it with a second simulation in which these radiators are replaced by radiant floors. The software used here must be flexible and capable to construct each representative simulation.

On this basis, different simulations will be constructed. Throughout figure 5.1, the different stages constituting this workflow and the district network model are explained, including the corresponding algorithms that must be executed in order to advance from one stage to the next. The different events are happening in sequential order through MATLAB®, which is the engine program that links with other software applications and orchestrates the entire process.

The first step consists on reading and collecting the different input data to build and simulate the network (Figure 5.1, steps 1 and 2) and store all processed information inside the internal database of Matlab, called workspace (step 3). This data comes from different formats, such as Excel sheets, text, xml files etc. The main input data required for the simulation is described here:

- Hourly resolved annual heat demand profiles

- Separated annual heat demand profiles for heating and hot water production (if possible)

- External temperature profiles

- Feed and return temperatures for each building and the general substation

- Other parameters, (temperature regulation curves, equipment characteristics, etc)

During step 4, the simulation i (i = 1 to 8, representing 8 scenarios) is built using the required structural data, including network topology, number of consumption points, number of pipes and connection layout between pipes and substations, and parameters such as nominal diameters, width and thermal properties of insulation material, etc. Before that, the library of representative blocks has to be created.

As explained before (see section 4.3), each DHN component can be modelled as a system of equations, synthesised as visual blocks with inputs, outputs and all the necessary parameters required.
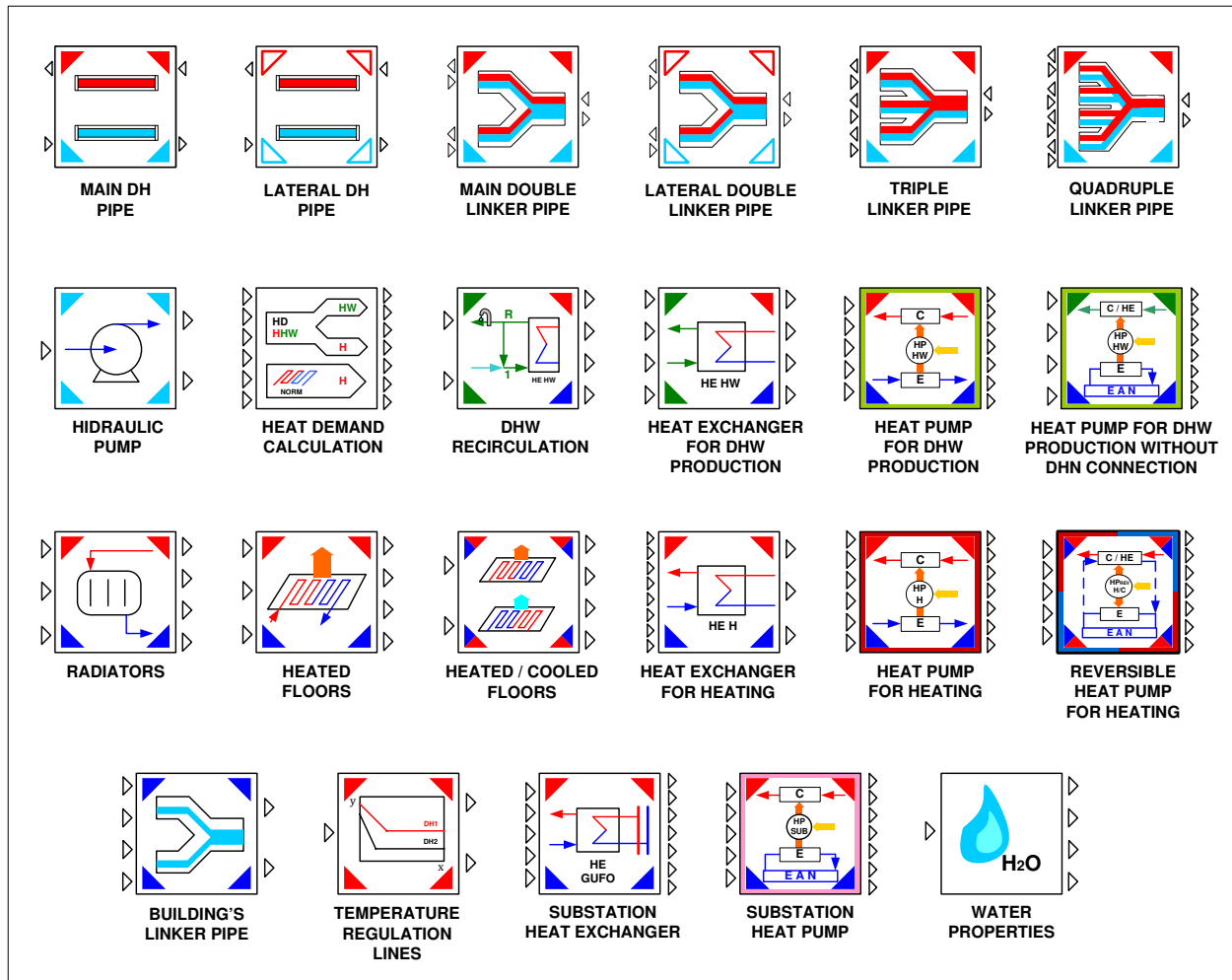
Figure 5.2: Library of basic blocks

After combining and connecting the different simple blocks in a proper way, more complex elements can be modelled, such as the different types of buildings (Figures 5.3 and 5.4), or the substation itself (Figures 5.5 and 5.6).
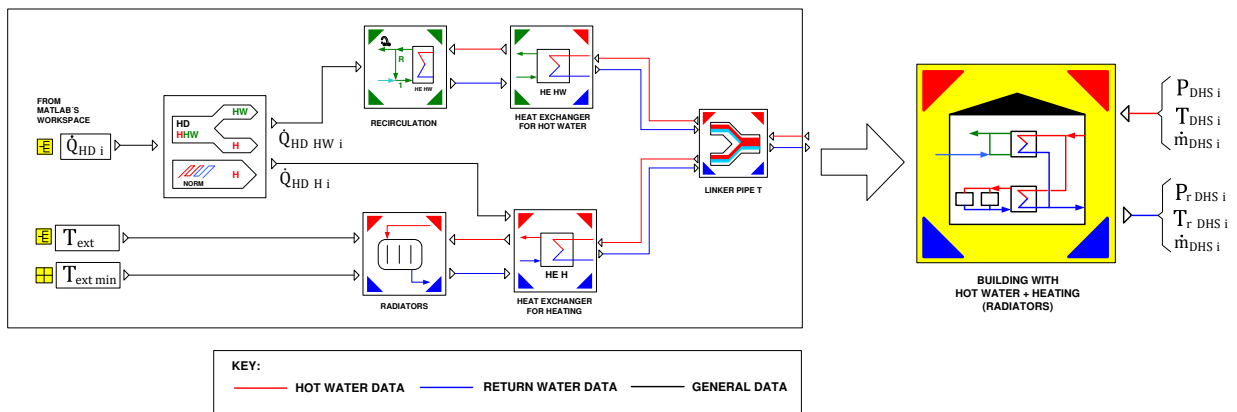
Figure 5.3: Representative diagram showing the internal configuration of the building block (DHW + Heating) (scenario 1, see figure 3.17)
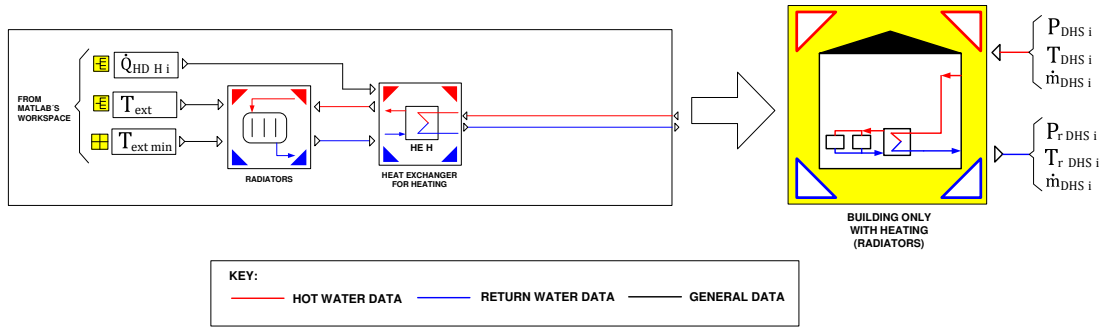
Figure 5.4: Representative diagram showing the internal configuration of the building block (Only Heating) (scenario 1, see figure 3.17)

Likewise, the rest of the complex blocks representing the new modified buildings of scenarios 2, 3, 5, 7 and 8 are obtained (see section 3.3, figures 3.18, 3.19, 3.21, 3.23, 3.24)
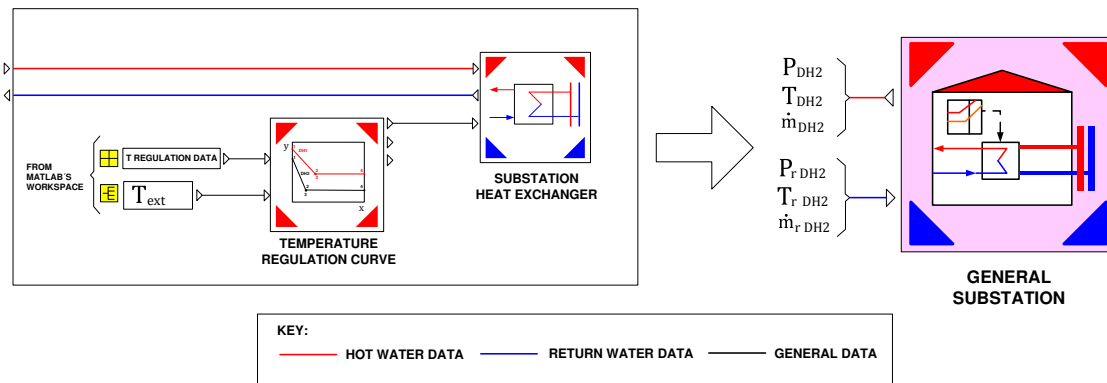
Figure 5.5: Representative diagram showing the actual internal configuration of the substation block (see figures 3.17, 3.18, 3.19, 3.21 and 3.23)
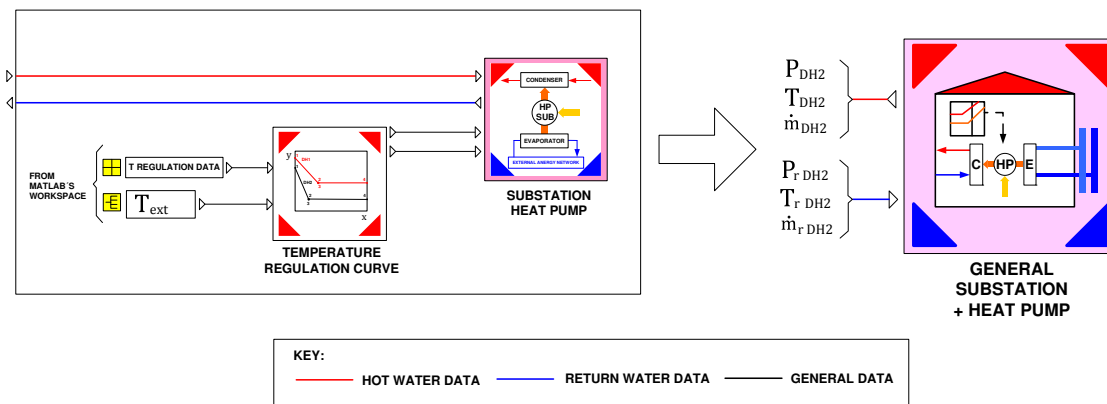
Figure 5.6: Representative diagram showing the internal configuration of the substation block, scenarios 4 and 6 (see figures 3.20 and 3.22)

In this way, the user can open each block and observe what is inside. Several kinds of information

are available:

- Existing devices inside the facilities

- Internal configuration and connections between these devices

- Input values and output results inside the buildings, as well as their calculation parameters

Finally, all the blocks are stored and organized into the same place, creating the library of blocks. All the complex models used to build the simulations will be gathered there.
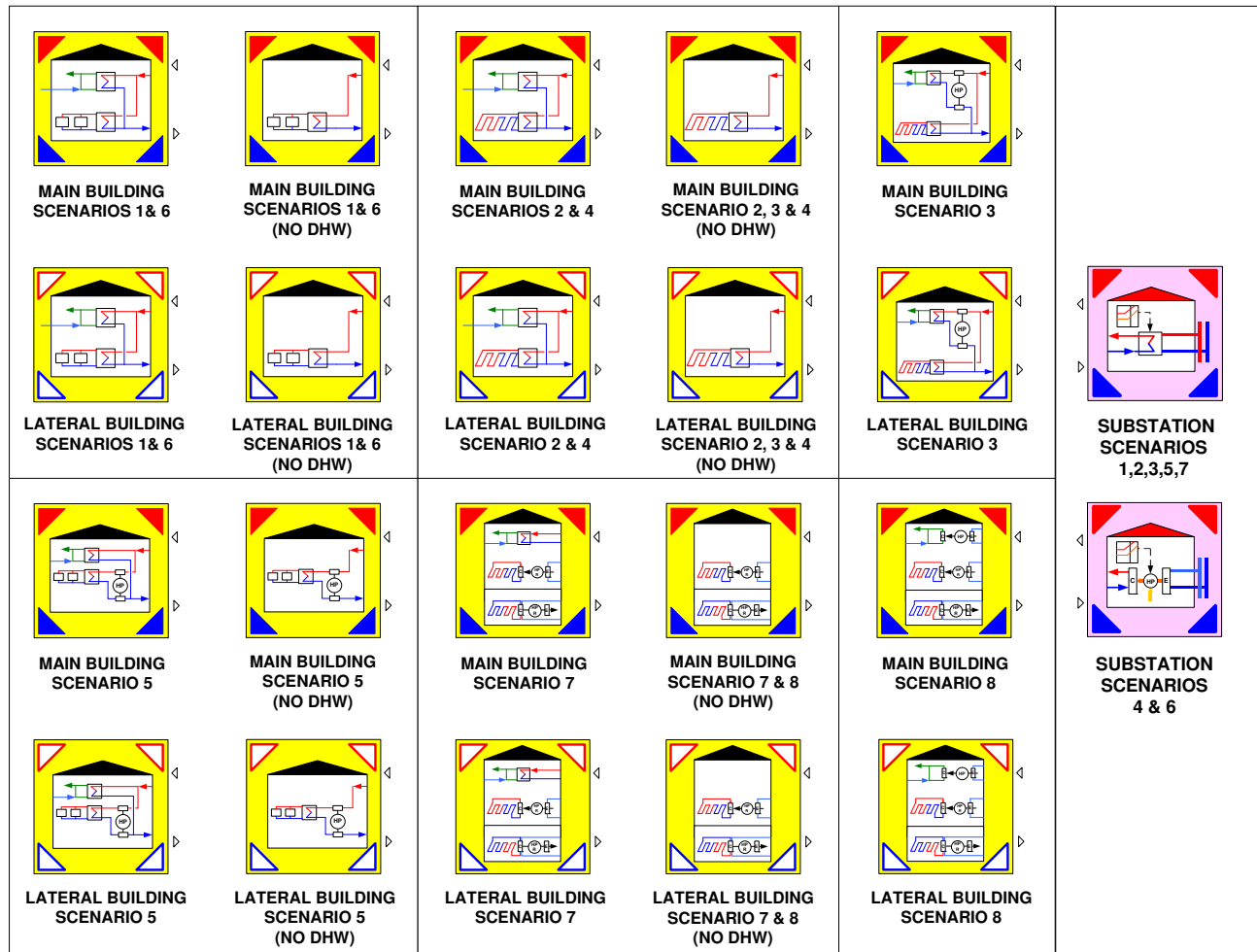
Figure 5.7: Collection of complex blocks, added to the previous library

Furthermore, it is possible to build the simulation an carry on the fourth step (Figure 5.1, step 4). The blocks are extracted from the library and the position where they have to be placed is generated according to what is specified in the structural layout data. Furthermore, all required parameters are assigned to their corresponding blocks (Figure 5.8).
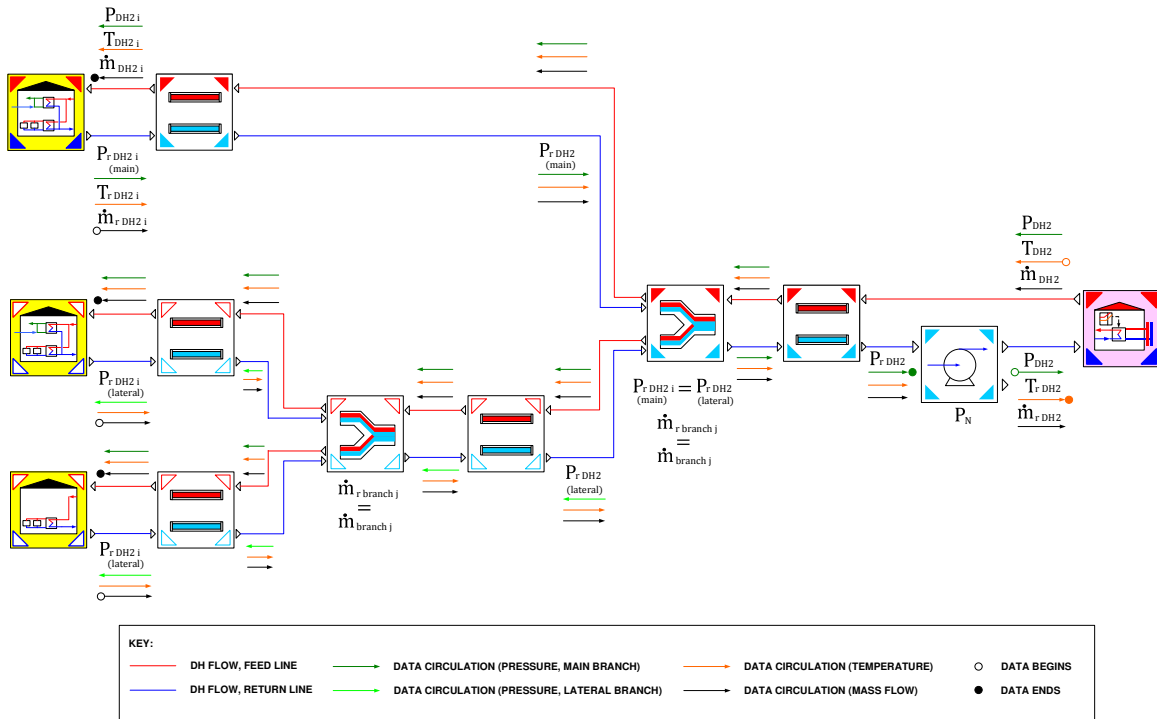
Figure 5.8: Conceptual diagram representing the layout of the blocks for a small DHN with three buildings

The pressure variable is defined from the hydraulic pump onwards. The temperature value starts from the substation towards the buildings, later defining all temperatures for all network points. Regarding the mass flow, the information circulates from the buildings to the substation through the return line and returns to the buildings through the feed line. Thus, buildings energy demand is the key data that defines the circulation of mass flow throughout the network. The system is designed and programmed in order to avoid loops, interruptions or failures during the simulation running.

After indicating whether there are separated heat demand profiles available for DHW and heating or not (Figure 5.1, step 5), the model will move to one or another direction depending on the answer. If this is negative, the procedure continues to the calibration phase (Figure 5.1, step 6), where all simulation parameters are adjusted to obtain the separated profiles.

Afterwards, the simulation is executed, obtaining all calculated temperatures, mass flows and enthalpy profiles of the inlet and outlet streams for each building. Furthermore, real and calculated profiles are compared (5.1, step 7, validation). If the parameters are acceptably well adjusted, then the system moves to the next step: if not, returns to step 6.

Hereafter, the simulation continues (5.1, step 8), solving all mass, energy and exergy balances and generating all pressure, temperature, enthalpy and exergy profiles for the whole network and for the entire time-profiles.

During step 9, all results for each scenario are obtained and stored inside MATLAB's internal Workspace. After running the data exportation algorithm, the system creates an Excel file containing all results for each scenario i (figure 5.1, step 10) and another one where all results for all scenarios are compared (figure 5.1, step 11).

Chapter 6

Results and Discussion

As it was previously mentioned (Section 4.3.1), each graph appearing in this section distinguishes four periods, described from left to right: extreme winter (EW), moderate winter (NW), midseason (M) and summer (S). All are 48-hour segments, with the first 24 hours corresponding to a working day and the other 24 hours to a weekend. In total, eight days are displayed in hourly resolution. In this way, a representative profile for each period of the year is obtained.
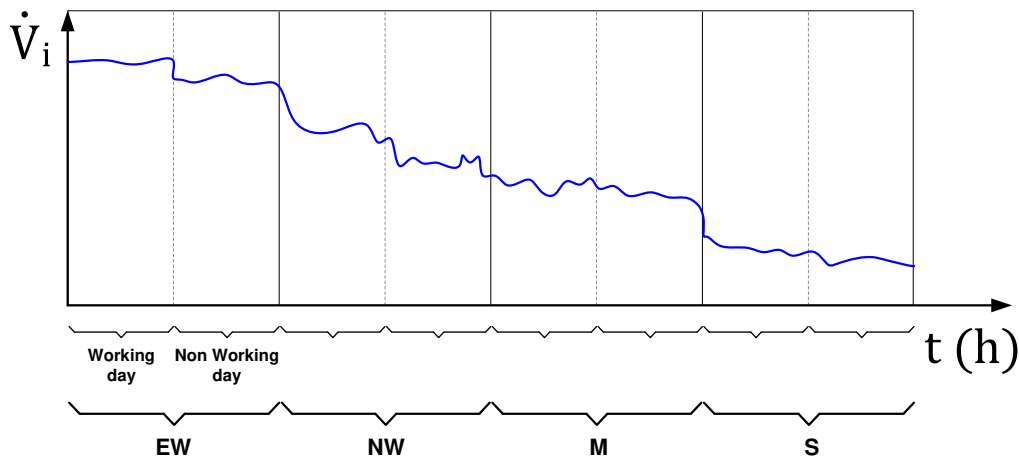
Figure 6.1: Temporal profiles format. Since $\dot{V}_i$ is the variable to be considered for each building (i), and t the time elapsed

6.1 Calibration

Previously to the validation phase, several calibration actions were carried on:

6.1.1 Modifying the temperature regulation line

Initially, the temperature regulation line for the secondary network (see section 4.3.2.2) was the same as Figure 3.14. Later, after running the simulation, a great discrepancy between real measured data and calculated data was discovered. Therefore, the regulation curve had to be modified, resulting in the following figure:
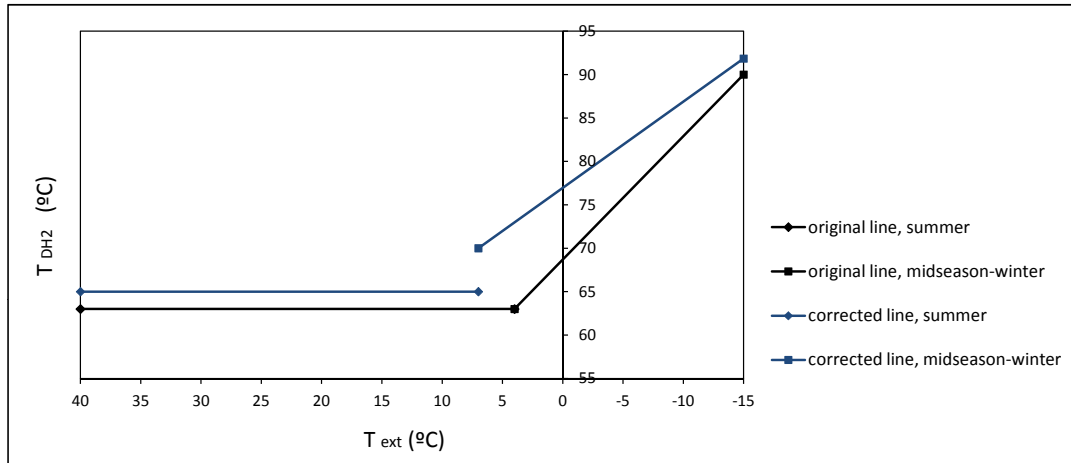
Figure 6.2: Comparison between the previous and the new heating curve, both for the secondary network (See figure 3.14)

- Highest value: If $T_{ext} = -15°C. \Rightarrow T_{DH2} = 91.85°C$

- Transition value: If $T_{ext} = 7° \Rightarrow T_{DH2} = 70°C$

- Lowest value: If $T_{ext} \leq 7° \Rightarrow T_{DH2} = 65°C.$

In this way, temperature values are calculated with higher accuracy, adjusted to the real measured values.

6.1.2 Calibrating multiplication factors for heat demand calculation

This action was previously explained (see section 4.3.3.1)

6.2 Validation

After performing the calibration actions, feed temperature (T_{DHSi}), return temperature (T_{rDHSi}) and mass flow ($\dot{m}_{DHSi}$) profiles related to the buildings are obtained. The profiles shown below compare calculated values obtained from the simulation with real registered values measured in the current Viennese installations for a sample of three of the 21 buildings studied.
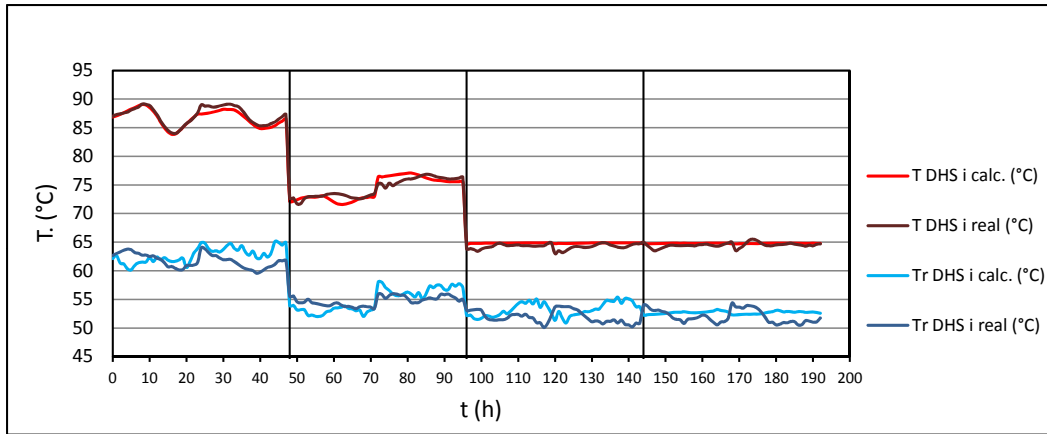
Figure 6.3: Comparison between real and calculated temperatures for building 8
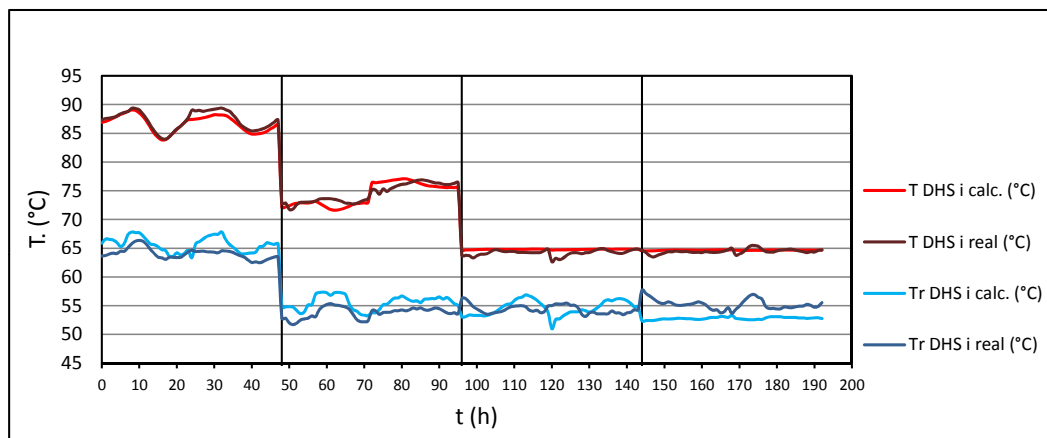
Figure 6.4: Comparison between real and calculated temperatures for building 14
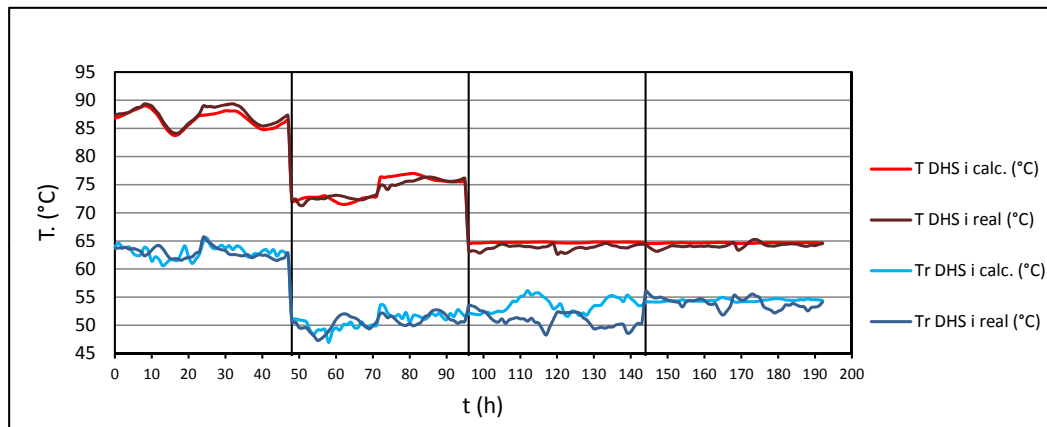
Figure 6.5: Comparison between real and calculated temperatures for building 38

Calculated Feed temperature profile has an average error of 0.87% with respect to the real recorded values. With the return temperature, such a value is somewhat higher (3.03%), probably due to inaccuracies regarding radiator's ΔT calculation using the approximate method of Recknagal-Schramek-Sprenger [47].

Regarding mass flow, the average error is significantly higher (13.02% with respect to the real measurement), especially for consumption peaks. This is due to the inaccuracies generated by estimating separately hot water and heating demands, which also generates an error by calculating heat exchanger parameters for each service.
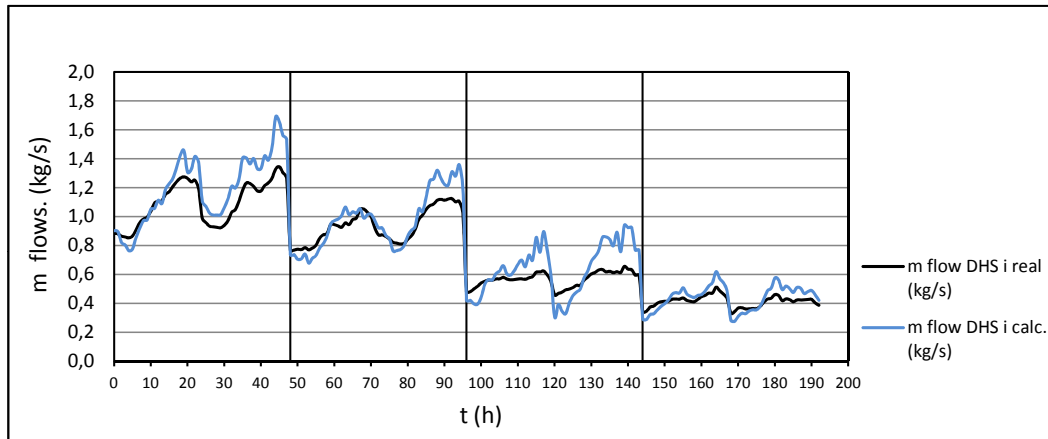
Figure 6.6: Comparison between real and calculated mass flows for building 8
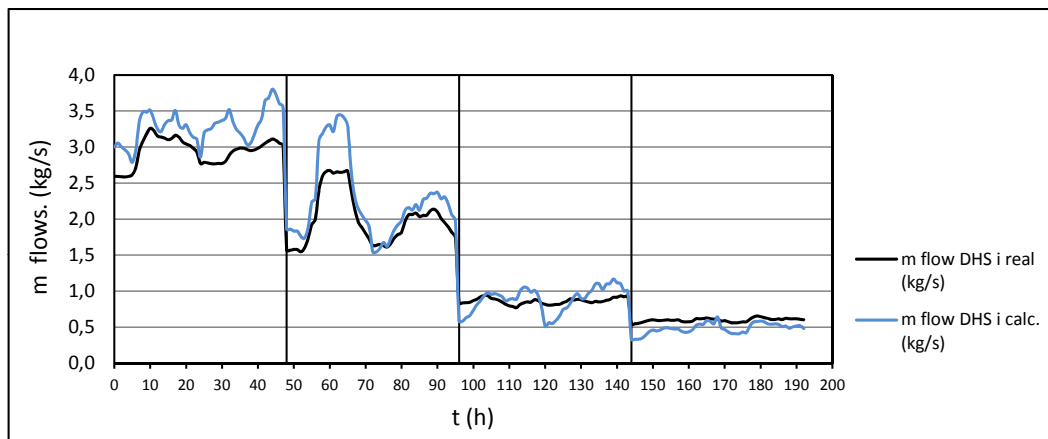
Figure 6.7: Comparison between real and calculated mass flows for building 14
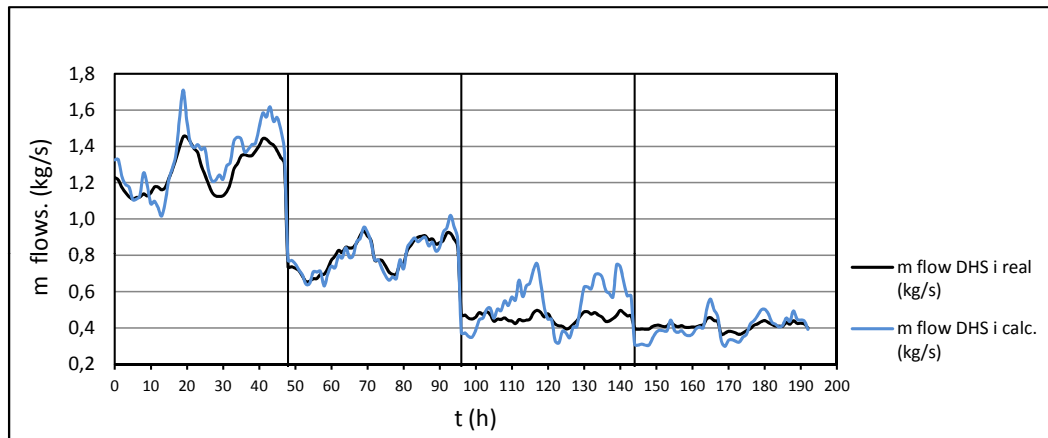
Figure 6.8: Comparison between real and calculated mass flows for building 38

Both variables define the enthalpy flow, which graphs are obtained as well:
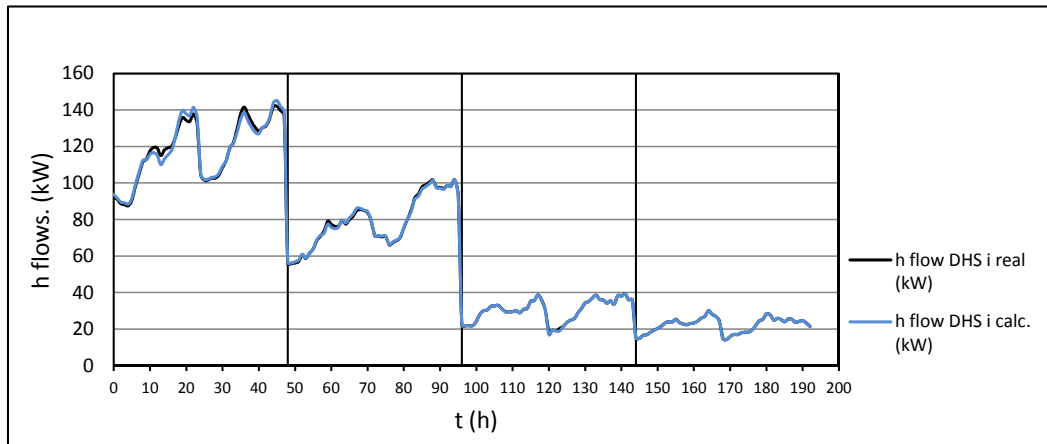
Figure 6.9: Comparison between real and calculated enthalpy flows for building 8
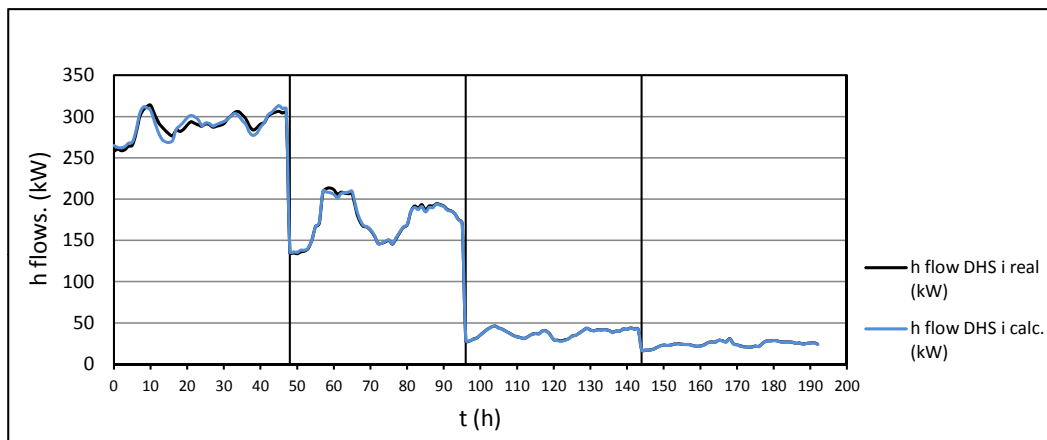
Figure 6.10: Comparison between real and calculated enthalpy flows for building 14
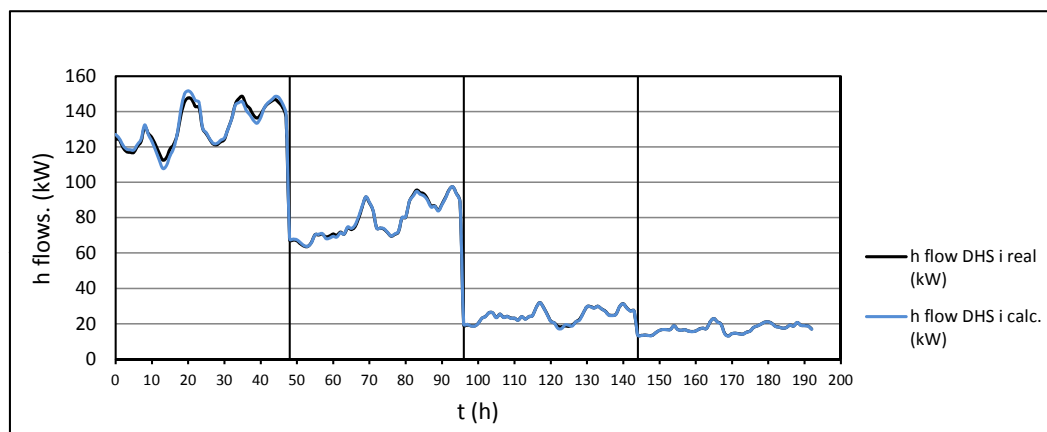
Figure 6.11: Comparison between real and calculated enthalpy flows for building 38

In light of the results shown in the graphs and since the profiles of calculated variables follow the same trend as the real registered variables, it can be assumed that the model is realistic and the

methodology is suitable for other hypotheses and case studies. The accuracy of the model will be greater if the energy demand values are provided separately from the beginning.

6.3 Results for the Current Situation

Results are displayed below, defining the actual network's performance. All variables and profiles are grouped according to the different thermodynamic systems, defined in section 4.1

6.3.1 Operation Variables

6.3.1.1 Pressure
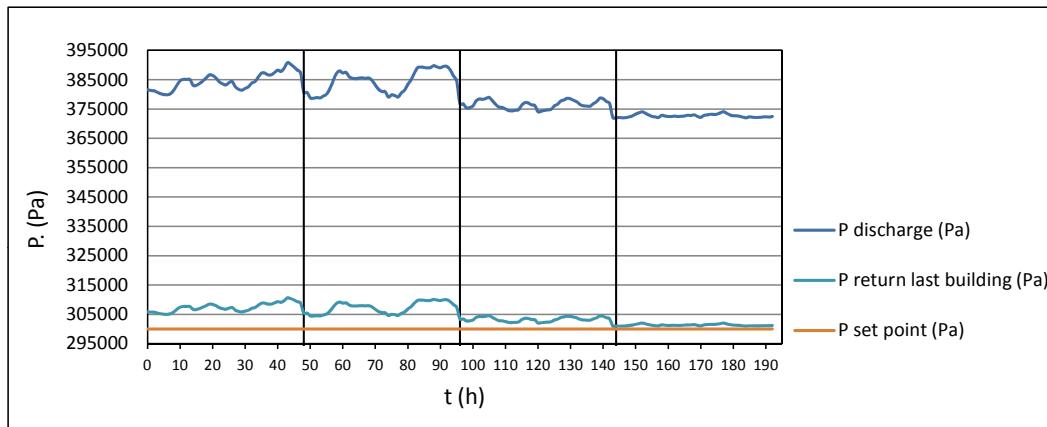
Figure 6.12: Pressure evolution throughout the network.

As shown in figure 6.12, the pressure immediately after the hydraulic pump ($P_{DISCHARGE}$) is much higher than the calculated pressure in the last building ($P_{RETURN\ LAST\ BUILDING}$) and at the suction point of the pump ($P_{SET\ POINT}$). This large difference is due to the hydraulic balance (see Figures 3.15 and 3.16). For mild winter and extreme winter days, heating demand is higher; which leads to a greater flow of water circulating through the network. Therefore, pressures will be higher in comparison with other periods of the year.

6.3.1.2 Temperatures
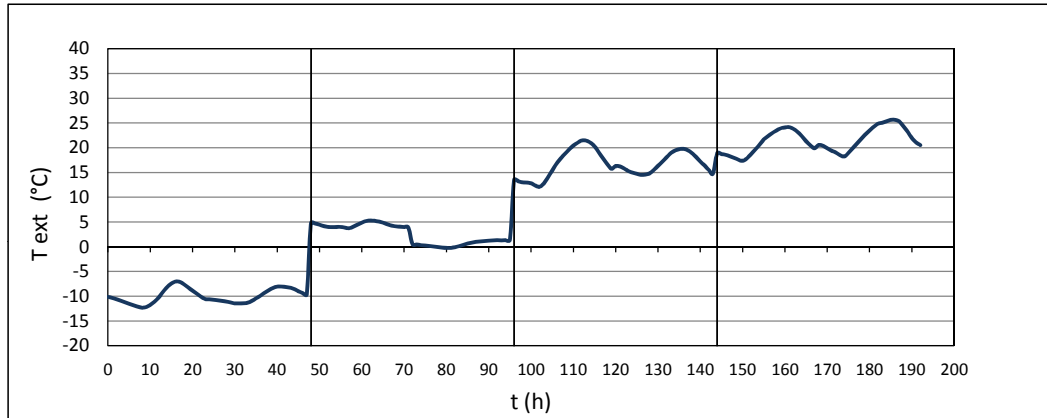
Figure 6.13: External temperature evolution along the year.
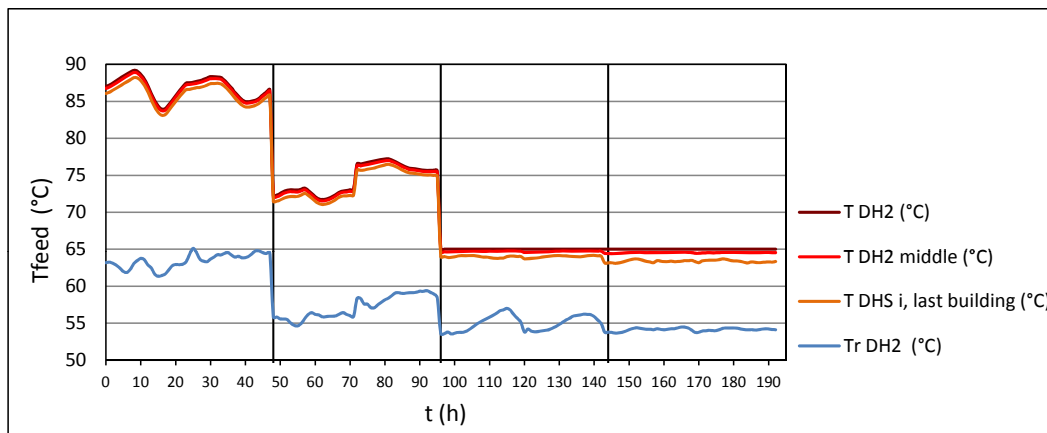
Figure 6.14: Temperatures evolution throughout the network.

Figure 6.14 shows the evolution of the main temperatures for the four temporal periods studied. T_{DH2} is the DH water temperature just after the general district substation, and $T_{DHS\,i,last\,building}$ is the temperature of the water flow reaching the last building. By comparing both variables, the data reflect an average temperature decrease of 0.84 K for extreme winter and 0.736 K for winter, while in the warm months, the decrease is more pronounced (1.02 K in midseason and 1.6 K in summer).

It might be assumed that the greatest temperature decrease occurs in winter and extreme winter, when the temperature gradient between circulating water and the environment surrounding the pipes is higher: however this does not happen for two main reasons:

1. Pipes are installed throughout a buried ditch sealed just below the pavement, conferring them some protection and insulation, keeping a constant ambient temperature throughout the year.

2. During the cold seasons, the mass flow of DHN water is higher (see Figure 6.15), resulting in a greater velocity and, thus, less time for the fluid to lose heat . Exactly the opposite situation happens during warm periods, especially in summer when the flow of DHN water is much lower and used only for hot water production.

Thus, the temperature profiles are more distanced from each other and the heat losses are steeper as we move from colder to warmer periods of the year.

The graph also shows the global return temperature, whose performance is conditioned to the feeding temperatures. Both variables - return temperature ($T_{r\,DH2}$) and the difference between feed and return values ($T_{DH2} - T_{r\,DH2}$) - decrease when moving from colder to warmer seasons through the year. In extreme winter this difference is maximum (23.3 K), and in winter stays around 17 K: in warm periods it decreases to 10-11 K.

The lower the external temperature (Figure 6.13), the greater the heat losses between the rooms and the external air. A high thermal gradient is necessary between the temperature of the radiator's metal plate and the comfort temperature inside the habitable rooms in order to ensure a constant heat flow to keep the comfort temperature constant, overcoming the heat losses. Therefore, the use of low heat exchange area devices (such as radiators) leads to high feed temperatures, guaranteeing high temperature gradients. At the same time, the lower the outside temperature, the greater the heat losses from the rooms to the external air, and therefore, the greater the water temperature decrease in the radiator, justifying the values shown in Figure 6.14.

6.3.1.3   Mass flows
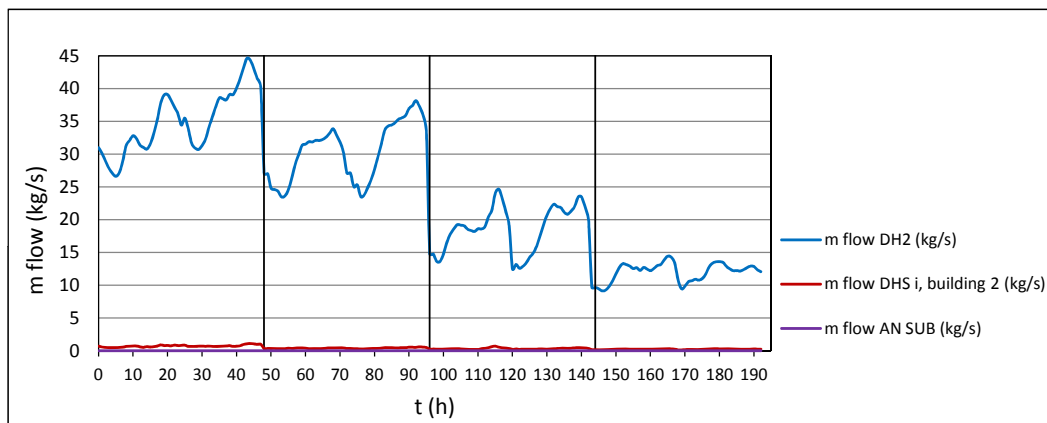
Figure 6.15: Mass flows evolution throughout the network.

Total DHN water mass flow and consumption peaks are higher for cold seasons and lower for the summer season. The frequency of peaks and troughs is similar throughout the seasons. The DHN's water flow for building 2 is shown, to see a comparison between the flow for an individual building and the flow for the entire neighbourhood. In addition, the mass flow of network water from where a hypothetical heat pump would extract energy ($\dot{m}_{AN\,SUB}$), is shown (For Scenario 1, this value equals 0).

6.3.2   Energy Balance

The results below were obtained using the expressions 4.11 and 4.12, gathered in section 4.2.3 and following figure 4.2.

The electric consumption of the hydraulic pump and the mass flow (figure 6.15) both follow a similar shape, undoubtedly due to the direct relationship between the fluid velocity and the electric power. Therefore, figure 6.16 is obtained:
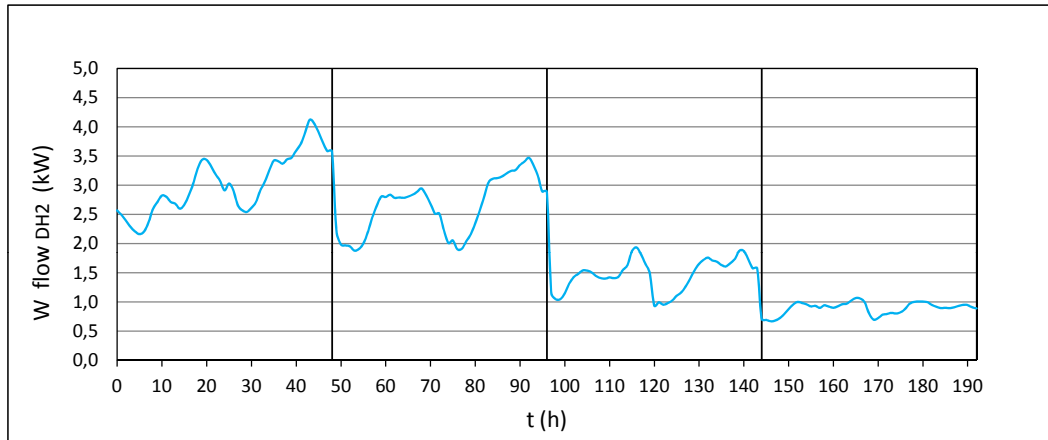
Figure 6.16: Electric flow consumption by the hydraulic pump

Note that this value is very small in comparison with other magnitudes, since the hydraulic pumping is usually not very important in the energy balance, especially in networks with short distances.

Concerning the heat losses, those are greater in extreme winter than other periods of the year, as show in figure 6.17:
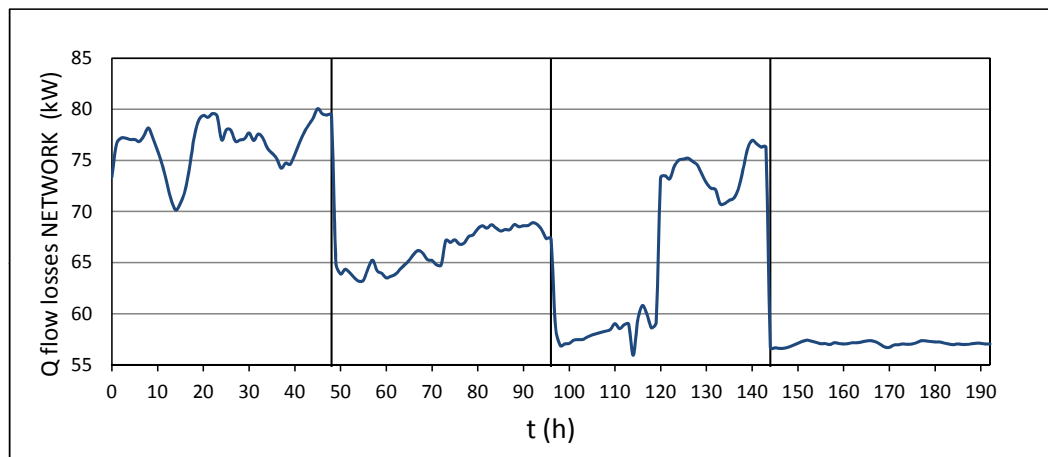
Figure 6.17: Evolution of the heat losses in the DH Network

However, this does not necessarily mean that energy efficiency is going to be lower during this period. In fact, the opposite may be true: heat losses can be quantitatively greater between periods within the same profile, but after taking into account the different energy flows, it can be concluded that energy yields are relatively higher in cold periods than in warm periods.

Furthermore, it is interesting to discover how in a mid-season segment the consumption profile can suddenly change from working day to a weekend day. Heat losses are increased after approx. 120 h. There is a drop in the weekend consumption, leading to a reduction of DHN water and therefore a sudden rise of the heat losses.

Due to high absolute consumption in winter, the efficiency is higher than in a low consumption period such as the summer season, despite the greater heat losses:
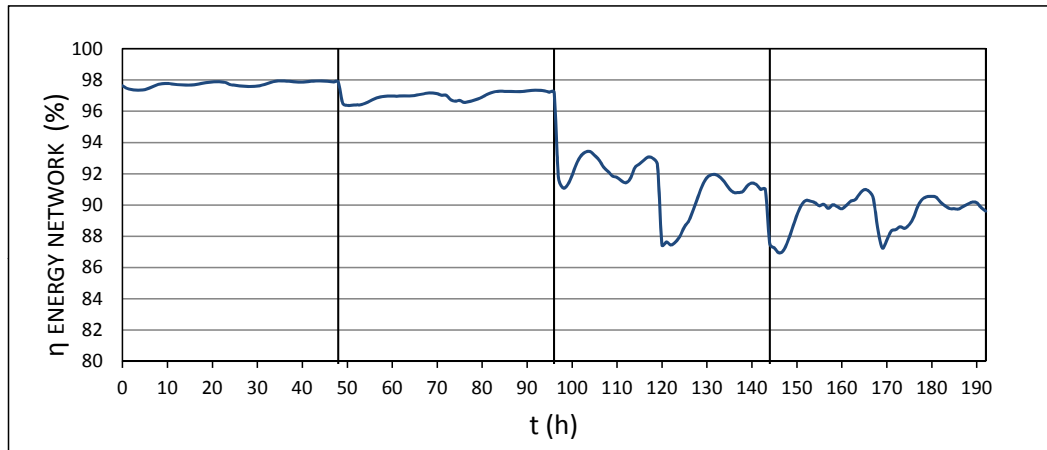
Figure 6.18: Evolution of the energy efficiency in the DH Network

The energy yield decreases clearly during spring - summer months (6.61% and 8.45% decrease with respect to the maximum winter period values) because the heating service is losing relevance and hot water consumption becomes significant, especially at the beginning and the end of the day (7:00 and 21:00 for weekdays, 11:00 and 22:00 for weekends), when the users spend more hot water on showers, bath, toilet, cooking etc..

Following the previous argument, it can be concluded that the higher the mass flow, the lower the relative heat losses and therefore the greater the energy efficiency.

6.3.3 Exergy Balance

For this scenario, the following expressions are used:

- Substation: equations 4.49 and 4.50

- Network: equations 4.51 and 4.52

- Buildings: equations 4.53 and 4.54

- Buildings, DHW branch: equations 4.55 and 4.56

- Buildings, Heating branch: equations 4.57 and 4.58

All of them are gathered along the section 4.2.5, obtained from Figure 4.2, and giving rise to the following results:
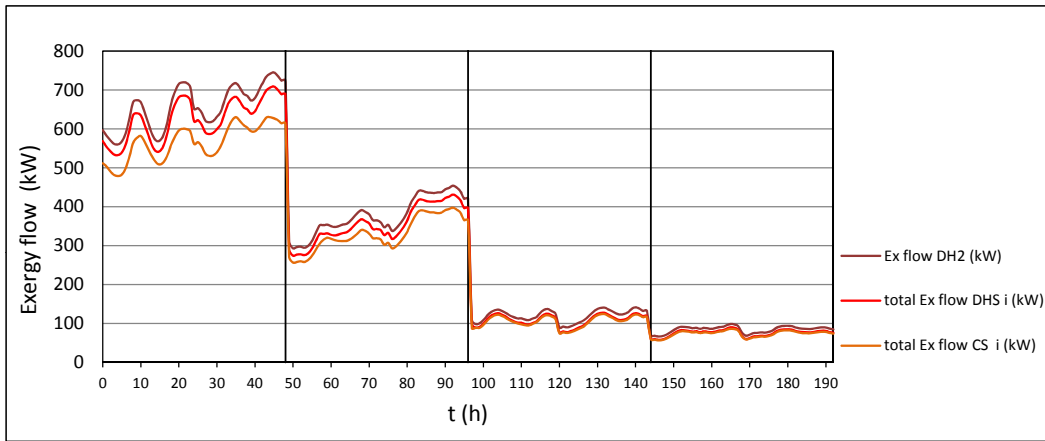
Figure 6.19: Exergy balance
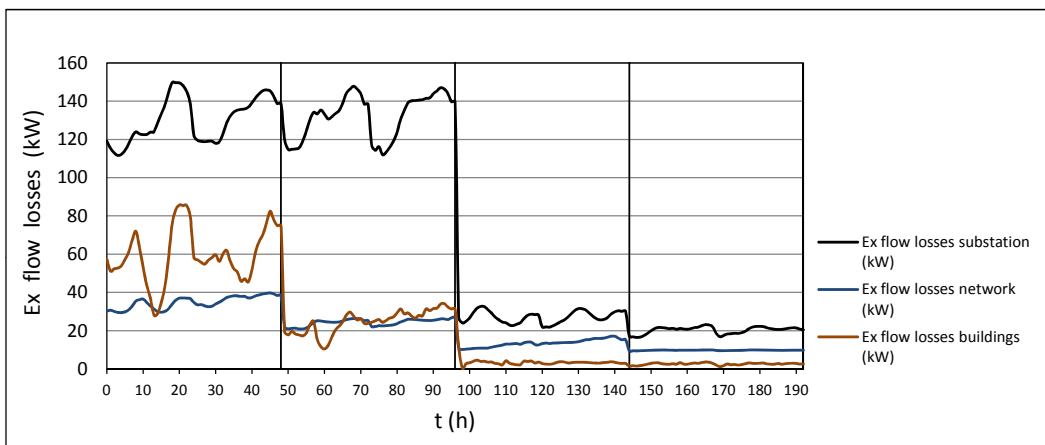
Figure 6.20: Evolution of the exergy losses for the three thermodynamic subsystems
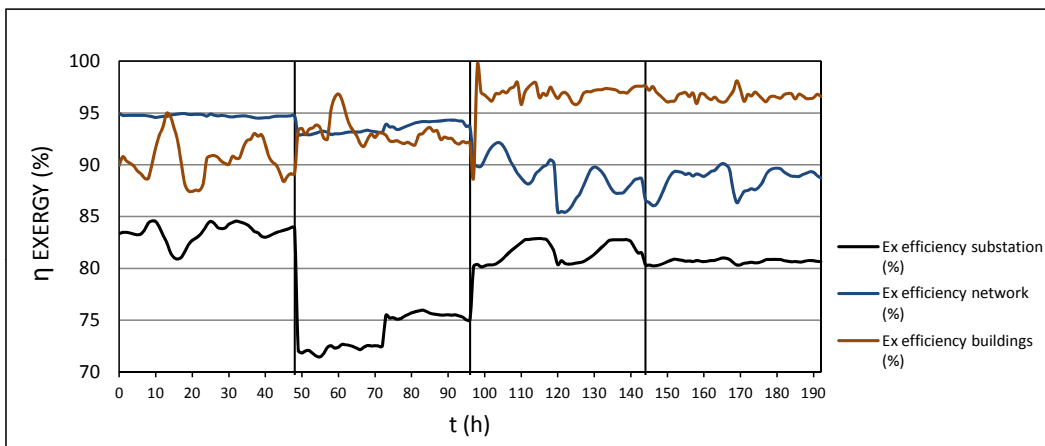
Figure 6.21: Evolution of the exergy efficiency for the three thermodynamic subsystems

Figure 6.20 compares $\dot{Ex}_{losses\ substation}$ and $\dot{Ex}_{losses\ buildings}$, that is to say, those thermodynamic subsystems in which heat exchangers are involved. Greater exergy losses are produced during winter and extreme winter, matching higher temperatures along the system. It is possible to conclude

that in the presence of heat exchangers, exergy losses are mainly produced by the temperature differences.

On the other hand, Figure 6.21 shows how the exergetic efficiency increases 2.87% in winter and approximately 7% in mid-summer with respect to the minimum extreme winter values. Therefore, it is proved that the lower the temperature difference on both sides of the heat exchanger, the lower the exergy destruction, and the better the performance.

However, in the case of the network ($\dot{Ex}_{losses\ network}$) the situation follows exactly the opposite pattern. As we move from extreme winter to summer, exergy losses decrease. This is because in this thermodynamic subsystem, the exergy contained is only associated with the heat flow. Consequently, the destruction of exergy is intimately associated with the heat losses of the circulating water in the pipeline. This is the reason why both variables in Figure 6.18 and Figure 6.21 describe similar patterns. All of this will result in a systematic efficiency loss with respect to extreme winter values when moving from cold to warm seasons (1.25% for normal winter, 6.17% for mid-season and 6.47% for summer), as shown in Figure 6.21.

Going deep inside the thermodynamic system of a building, a detailed exergy analysis is made for both services (heating and domestic hot water):
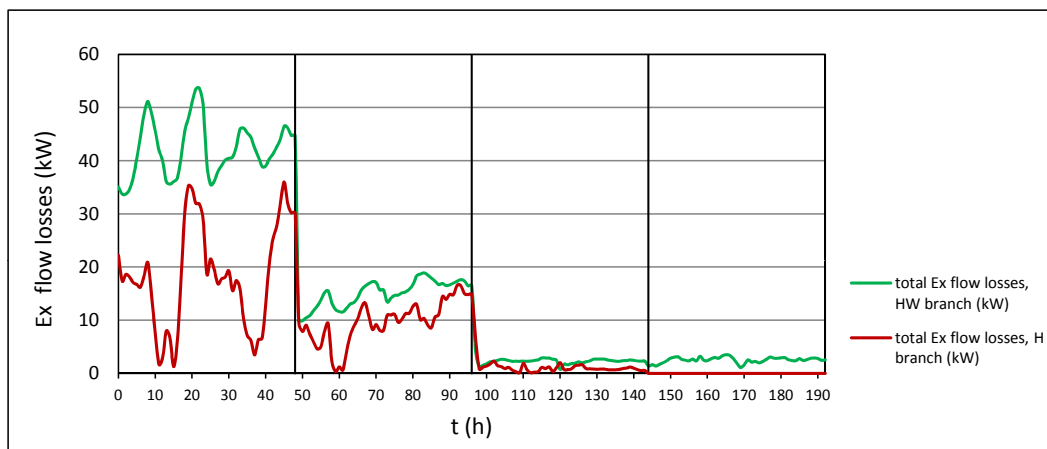
Figure 6.22: Evolution of the exergy losses for both branches
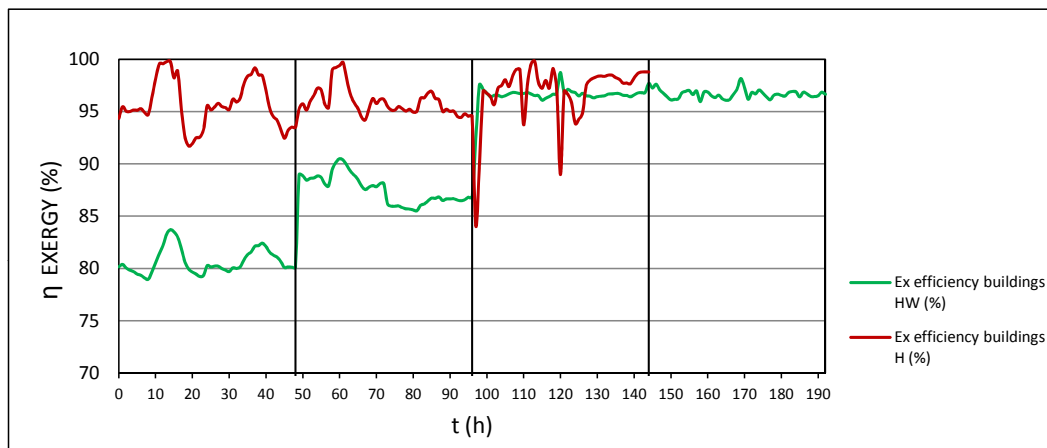
Figure 6.23: Evolution of the exergy efficiency for both branches

Looking at Figure 6.23, within the extreme winter period, building's exergetic efficiency for heating branch is on average a 15.8% greater than the DHW branch performance. Both yields are closer as we move to warm seasons, with a 8.8% difference in winter and almost equal values in mid-season. In summer, the comparison is not possible since there is no heating service.

The main difference between both branches is the ΔT between the heat exchangers. For example, in the domestic hot water branch, the heat exchanger receives water at almost 90°C on the network side during the cold seasons; meanwhile, on the client side the temperature is fixed at 60°C in order to avoid the formation of Legionella, leading to a temperature difference of 30 K. In the heating branch, the heat exchanger also receives water at almost 90°C, but on the client side temperature is much higher, approximately 80-83°C. In this case the temperature difference is only 10 K.

Using the same argument as before, the higher the temperature difference, the greater the exergy destruction, because the high quality of the energy carried by a high temperature stream is wasted by transferring heat inefficiently from high to lower temperatures, even if the heat losses are zero or close to zero. Consequently, from the exergetic point of view, the heating branch is more efficient than the domestic hot water branch, especially during cold seasons.

6.4 Buildings insulation

As a previous consideration to scenarios 2,3,4,7 and 8, and considering section 4.3.3.1, it is necessary to ensure that the maximum heat provided by the radiant floors ($\dot{Q}_{hf\,max\,i}$) is enough to satisfy the heating demand ($\dot{Q}_{HD\,H\,i}$). In this regard, the simulation indicates 2 buildings which do not meet this condition:
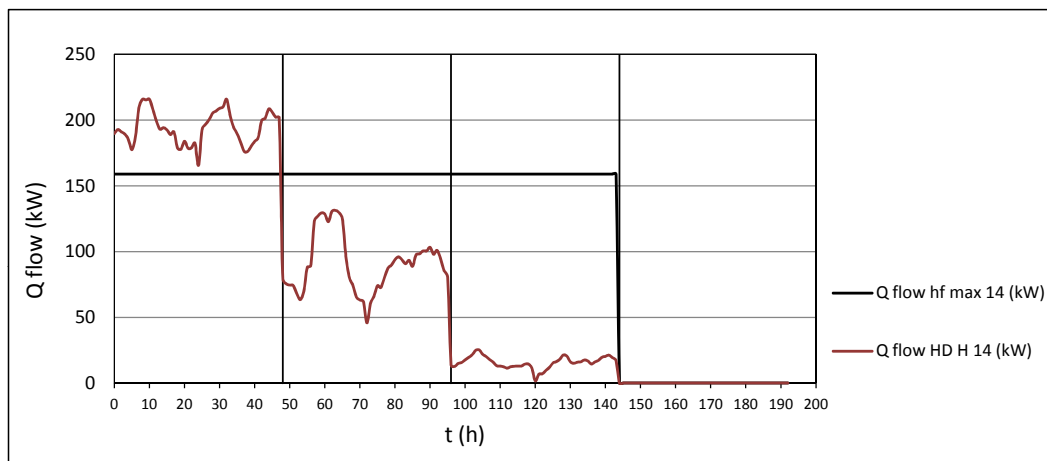
Figure 6.24: Comparison between $\dot{Q}_{hf\,max\,i}$ and $\dot{Q}_{HD\,H\,i}$, building 14
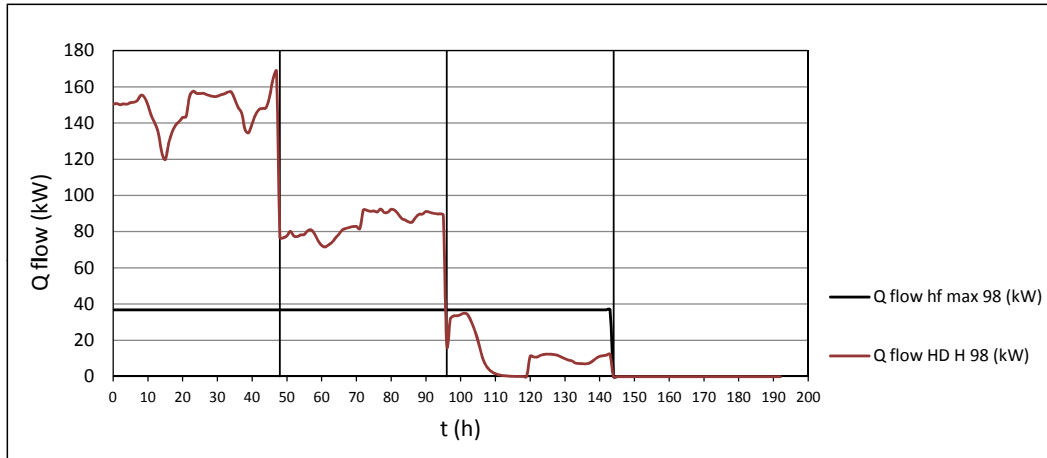
Figure 6.25: Comparison between $\dot{Q}_{hf\ max\ i}$ and $\dot{Q}_{HD\ H\ i}$, building 98

The analysis of these profiles indicates that, in certain periods of the year, the maximum heating power of the radiant floors will not be sufficient to maintain the comfort temperature in the habitable rooms of those buildings. As shown in the graphs, this deficit occurs during extreme winter and mild winter periods. As explained in the equation (4.89), it will be necessary to increase the insulation degree of these buildings, in order to reduce the heating demand by a certain percentage (-26.22 % for building 14 and -78.11 % for building 98)

6.5 Comparative Results for all Scenarios

This section presents a comparative overview describing how each variable evolves for each calculated hypothesis, giving an idea about all pros and cons for the various improvements and changes which can be applied. Again, all results are grouped in three blocks: Operation variables, Energy balance and Exergy Balance.

6.5.1 Scenario 2 vs scenario 1 (see section 3.3.2)

6.5.1.1 Operation variables
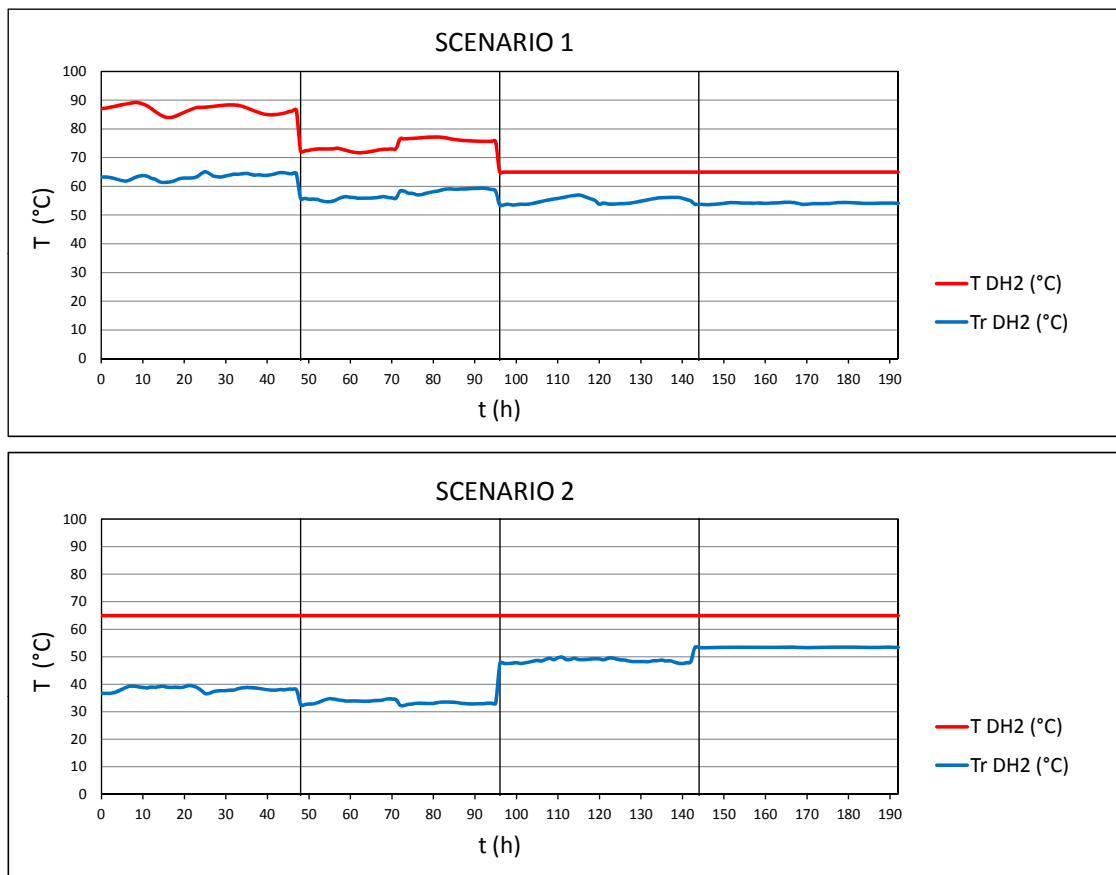
Figure 6.26: Temperatures evolution. Comparison scenarios 1 and 2

Changing from scenario 1 to scenario 2 leads to a reduction of network's feed temperature (T_{DH2}), which is decreased to a fixed value of 65°C. In addition, radiators are replaced by radiant floors for all the buildings.
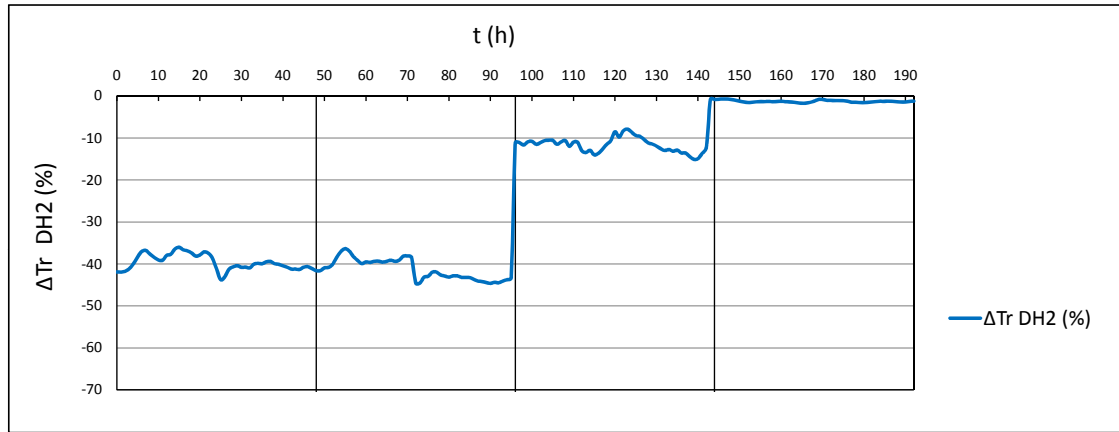
Figure 6.27: Return temperature variation respect to scenario 1

These measures contribute to an important reduction of the return temperature ($T_{r\,DH2}$), which changes from 60°C to 35°C in winter (average values, see figure 6.26), generating a percentage reduction of -40/-45% in comparison with scenario 1 (average values, see figure 6.27).
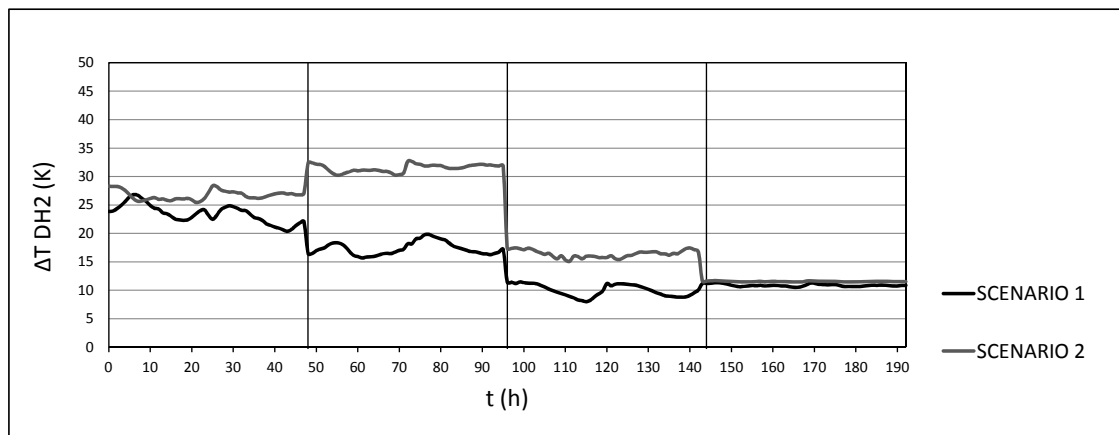
Figure 6.28: ΔT evolution. Comparison scenarios 1 and 2

Therefore, new temperature differences will be defined, as shown in figure 6.28. A ΔT is observed for both winter seasons and mid-season periods. This situation leads to several changes, reasoning in agreement with the general expression (4.1):

$$\dot{Q}_{DH2} = \dot{m}_{DH2} \cdot Cp \cdot \Delta T_{DH2} \tag{6.1}$$
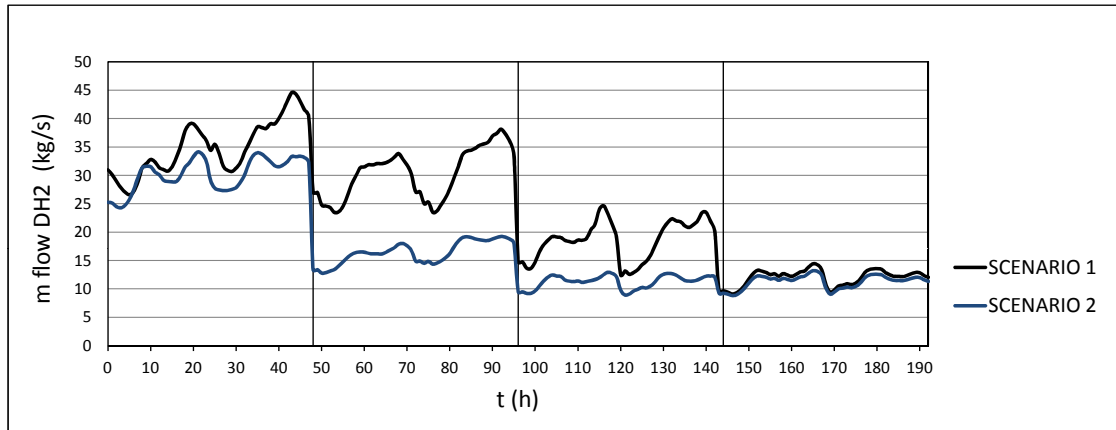
Figure 6.29: Mass flow evolution. Comparison scenarios 1 and 2

An increase of ΔT allows a decrease of the mass flow ($\dot{m}_{DH2}$), as shown in figure 6.29. This decrement is highly accused in winter ($\overline{\Delta \dot{m}_{DH2\ NW}}$ = -45%) and mid-season ($\overline{\Delta \dot{m}_{DH2\ M}}$ = -45%), where the temperature differences are greater in comparison with extreme winter period.
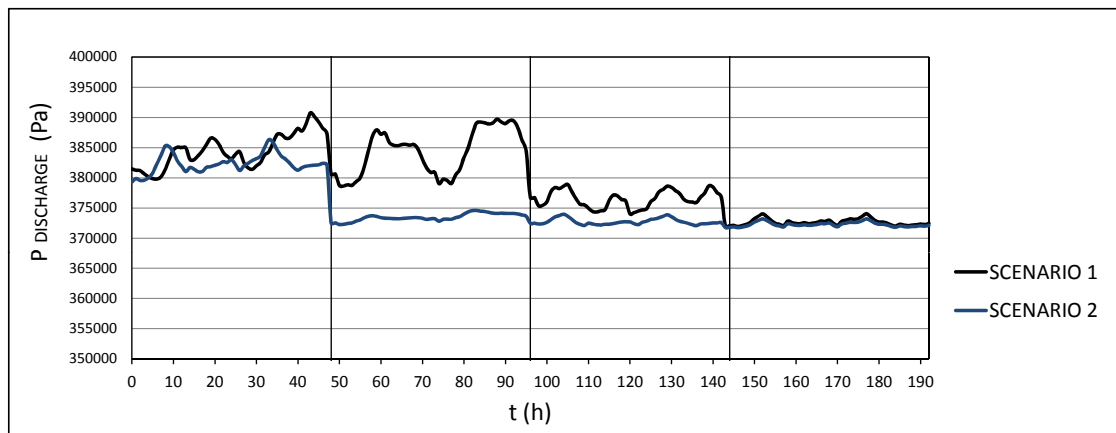
Figure 6.30: Discharge pressure evolution. Comparison scenarios 1 and 2

Decreasing the mass flow leads to a reduction of the pumping pressure (more accused in normal winter and mid-season). In fact, looking at both figures 6.29 and 6.30 it is possible to observe how both magnitudes follow similar behaviours due to the high dependence of the pumping pressure ($P_{DISCHARGE}$) with the mass flow ($\dot{m}_{DH2}$).

All those changes will generate an important decrease of the hydraulic pump's power consumption, as shown in figure 6.31. Approximately a 50% of this power is reduced in normal winter and mid-season periods (see figure 6.32).

The units are W/m^2, showing the density of energy or exergy flow for the total heating surface.
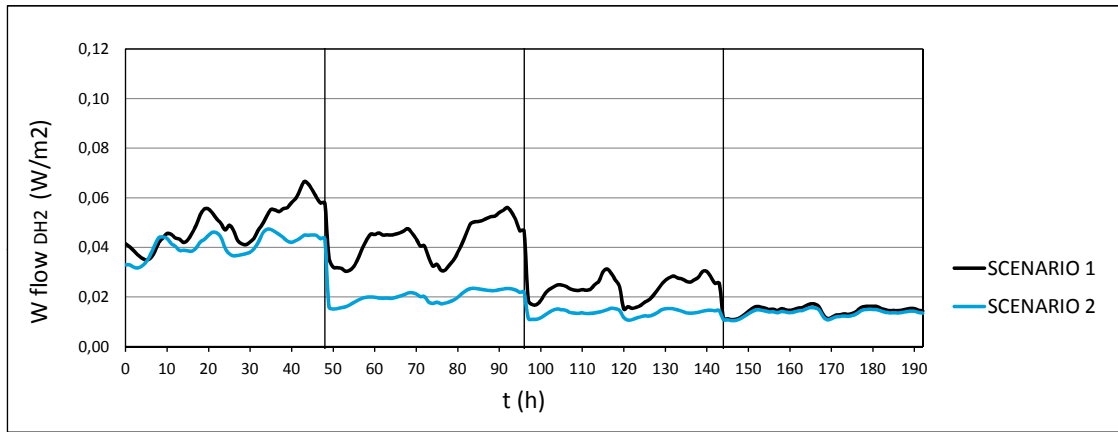
Figure 6.31: Hydraulic pump's electric consumption. Comparison scenarios 1 and 2
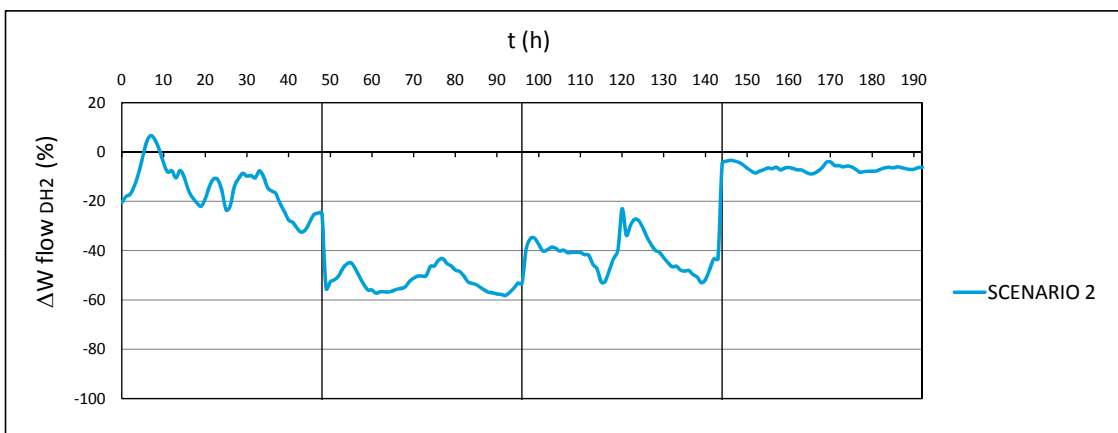
Figure 6.32: Hydraulic pump's electric consumption variation respect to scenario 1

6.5.1.2 Energy Balance

The same expressions of scenario 1 are used here, generating the following results:
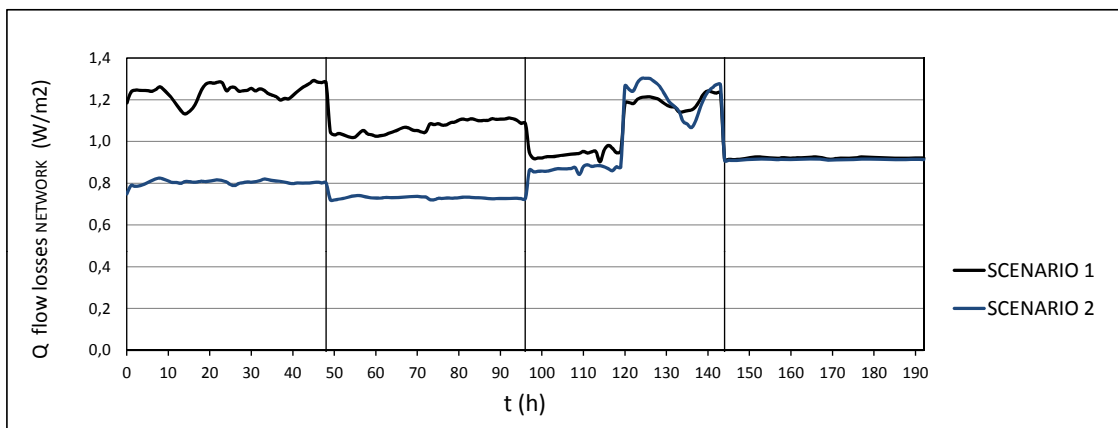
Figure 6.33: Energy flow losses along the network. Comparison scenarios 1 and 2

Decreasing network's temperature decreases, in turn, the energy losses along the pipes due to the reduction of the temperature gradient between the circulating water inside the pipe and the surrounding external air. This effect is remarkable during extreme winter and normal winter periods, as we can see in figure 6.33. During mid-season, temperature levels are closer each other (see figure 6.26), making the heat losses to be similar as well.

Looking at different periods within the same profile shows the same phenomenon described in section 6.3.2; the greater the circulating mass flow, the less energy losses in the pipe network. The same behaviour will be observed for the other hypotheses as well.
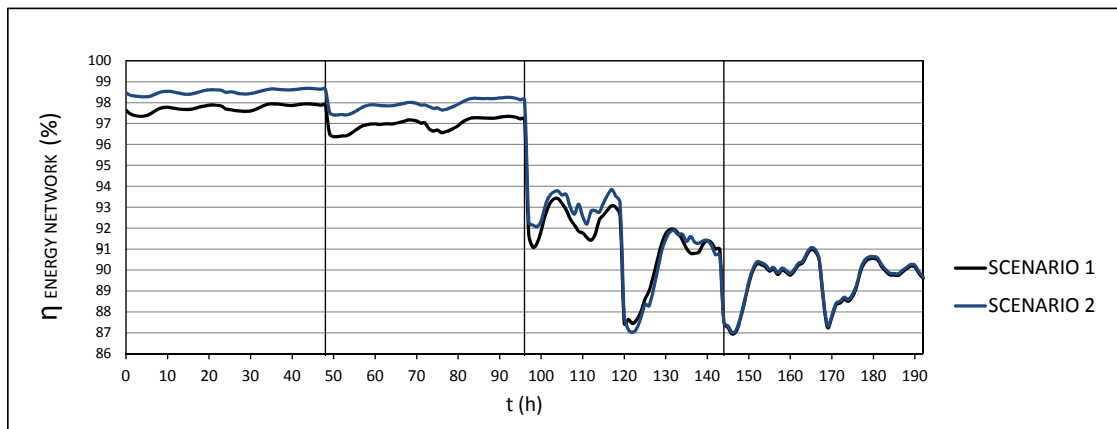
Figure 6.34: Energy efficiency along the network. Comparison scenarios 1 and 2
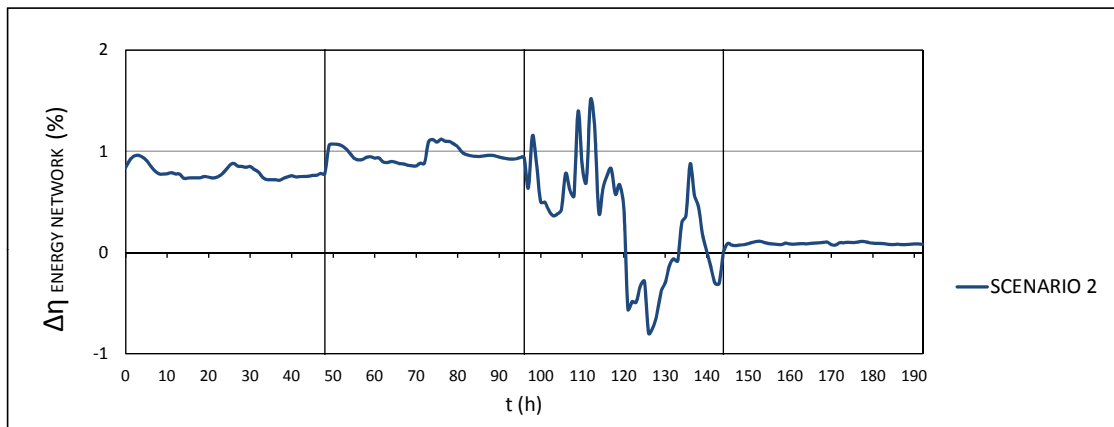
Figure 6.35: Energy efficiency variation respect to scenario 1

Focusing at figure 6.35, when moving from scenario 1 to scenario 2, an improvement of the pipeline's energy efficiency is achieved (around 1% in the winter period and less than 1% in extreme winter. In mid-season this improvement has a minor role, fluctuating between 1% and -1%.

6.5.1.3 Exergy Balance

The same expressions of scenario 1 are used here, generating the following results:
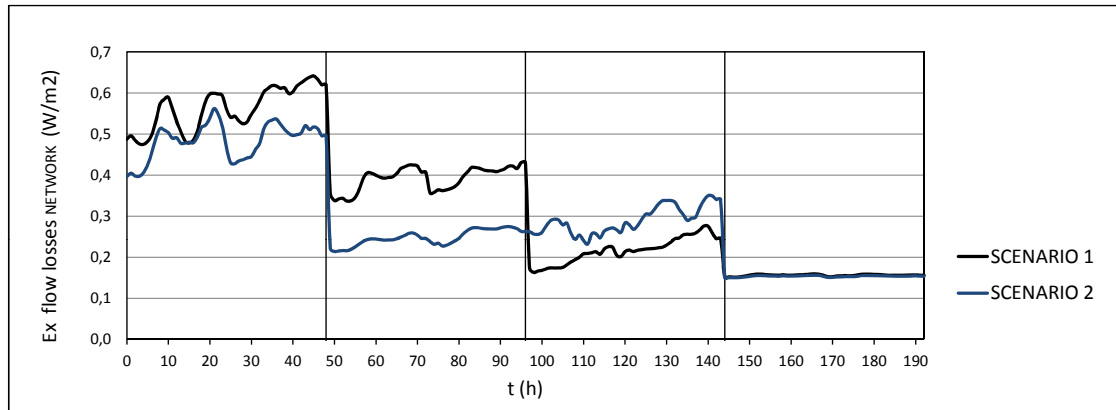
Figure 6.36: Exergy flow losses along the network. Comparison scenarios 1 and 2

As previously explained, exergy is the maximum useful work that can be obtained from a given thermodynamic system which is not in equilibrium with the environment. The further this system is from the environmental pressure and temperature conditions, the more useful work can be extracted from it, and therefore the greater the exergy content will be. Therefore, it is a thermodynamic magnitude which gives an idea of the quality of the thermal energy, and not quantity.

During winter and extreme winter periods, the temperature reduction from the first to the second scenario collaborates with decreasing the energy losses, influencing on the exergy losses in the same direction.

However, in mid-season this trend does not happen in the same way. The temperature levels are similar for both hypotheses ($T_{DH2} = 65\,^{\circ}C$, $\overline{T_{r\ DH2\ sc1}} = 55\,^{\circ}C$, $\overline{T_{r\ DH2\ sc2}} = 49\,^{\circ}C$), but the low mass flow rate (much lower than in scenario 1) results in a lower grade of the energy utilization, that is, a greater exergy destruction.
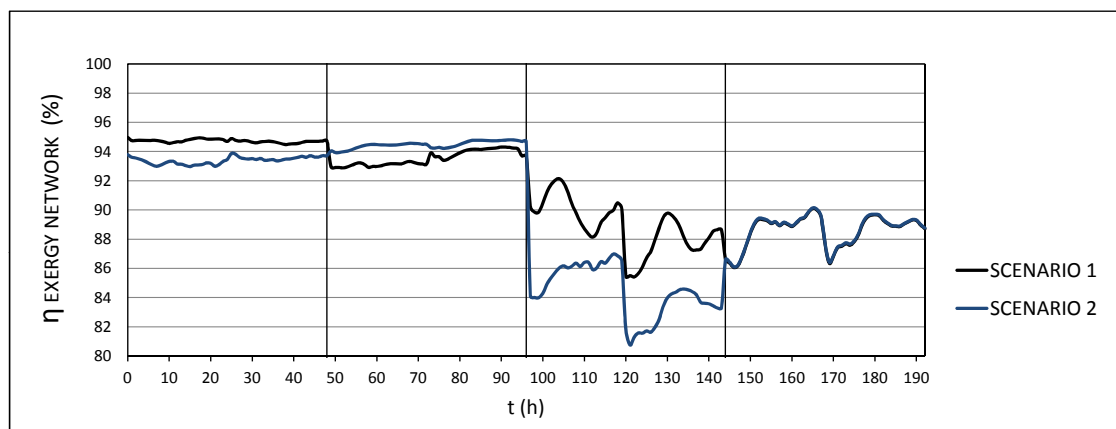
Figure 6.37: Exergy efficiency along the network. Comparison scenarios 1 and 2
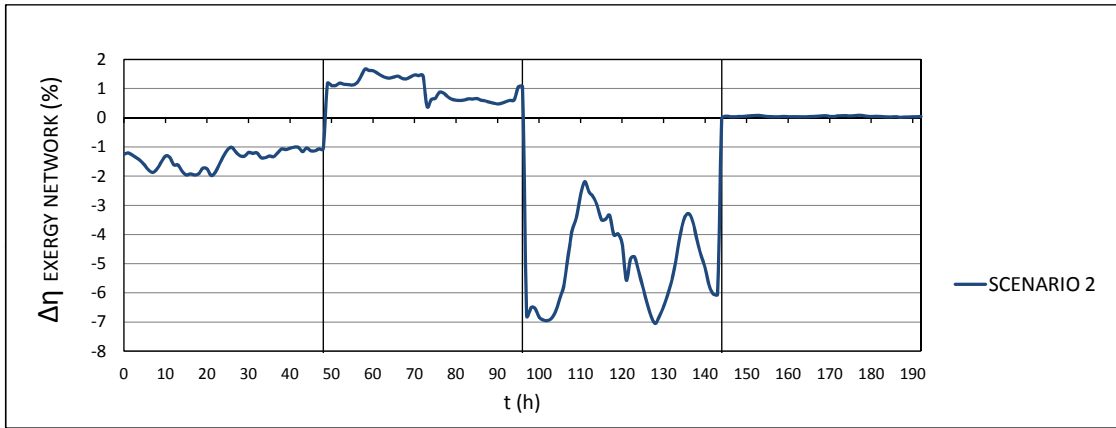
Figure 6.38: Exergy efficiency variation respect to scenario 1

The consequence is a relative improvement in the average exergy efficiency in the pipe network ($\eta_{\text{EXERGY NETWORK}}$) of 1% in the winter period. On the other hand, in mid-season this magnitude falls significantly, and may decrease to values between 86 and 82%.
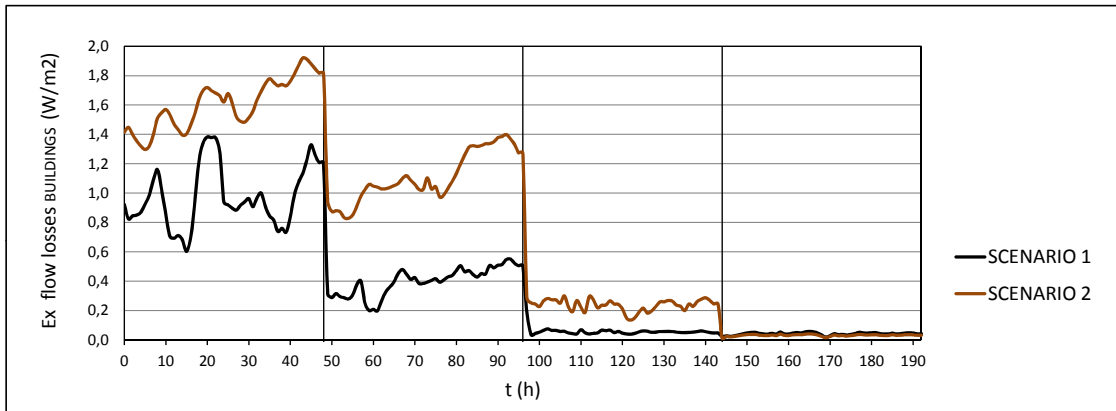
Figure 6.39: Exergy flow losses for all buildings. Comparison scenarios 1 and 2
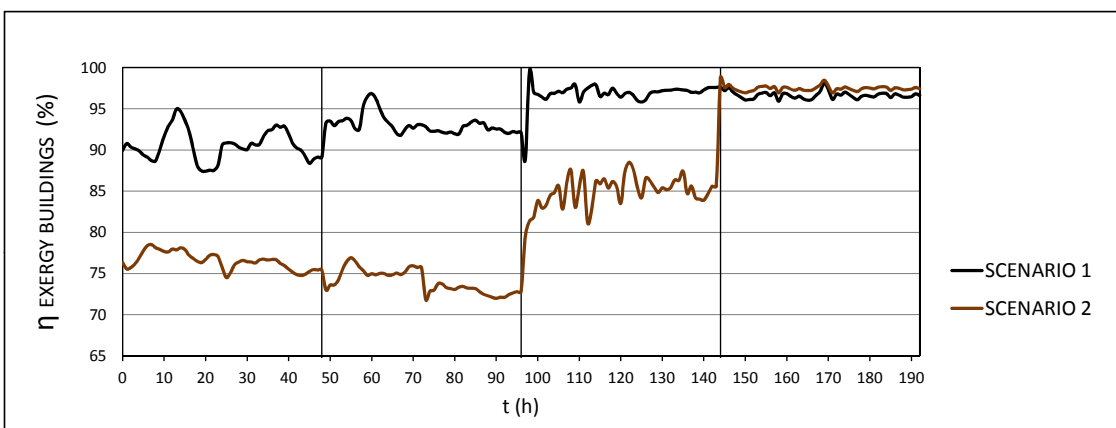
Figure 6.40: Exergy efficiency for all buildings. Comparison scenarios 1 and 2

Going deep into the analysis of the thermodynamic subsystem of the buildings, there is a general

increase of the exergy losses for the first three periods (see figure 6.39). This fact means a significant reduction of the exergy efficiency in the whole set of buildings. From scenario 1 to 2, the average values change from 90-95 % to 77 % in extreme winter and to 75% in normal winter. In mid-season the change is smaller, reaching 85 %.

To understand what happens, it is required to study each of the two branches that operate inside the buildings separately, as shown below.
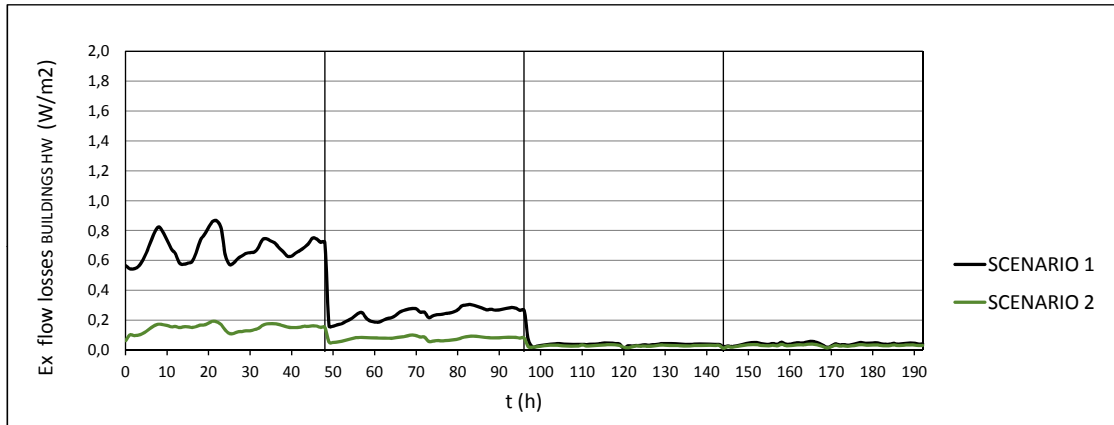
Figure 6.41: Exergy flow losses for all buildings, DHW branch. Comparison scenarios 1 and 2

Focusing on figure 6.41, there is a significant decrease of the exergy losses in the hot water production branch. This improvement is due to the approximation of the temperature profiles at both sides of the heat exchanger, as it was previously explained (see section 6.3.3, figure 6.23.
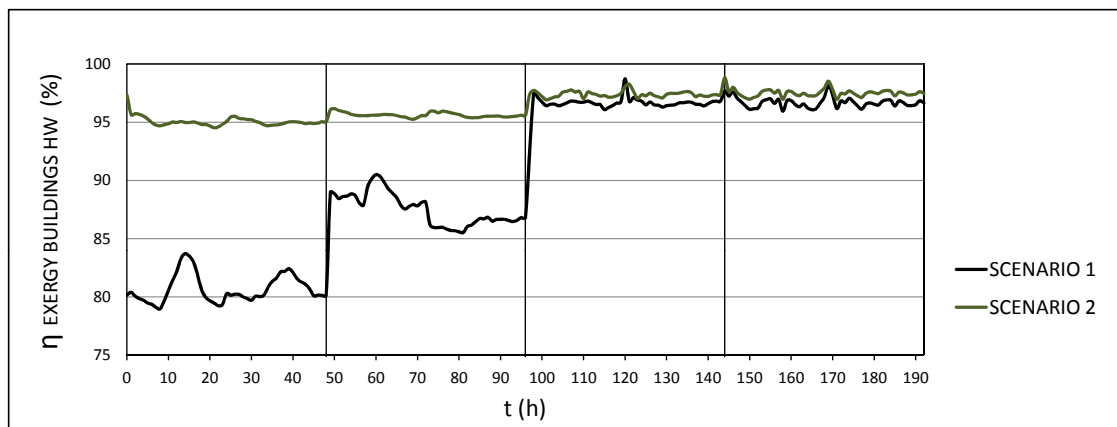
Figure 6.42: Exergy efficiency for all buildings, DHW branch. Comparison scenarios 1 and 2

Therefore, in comparison with scenario 1, in this branch there will be an increase of the exergy efficiency of almost +20% in extreme winter and +10% in normal winter. In mid-season and summer both profiles are similar (figure 6.42).

However, the opposite effect is observed in the DHW branch, as shown in figure 6.43.
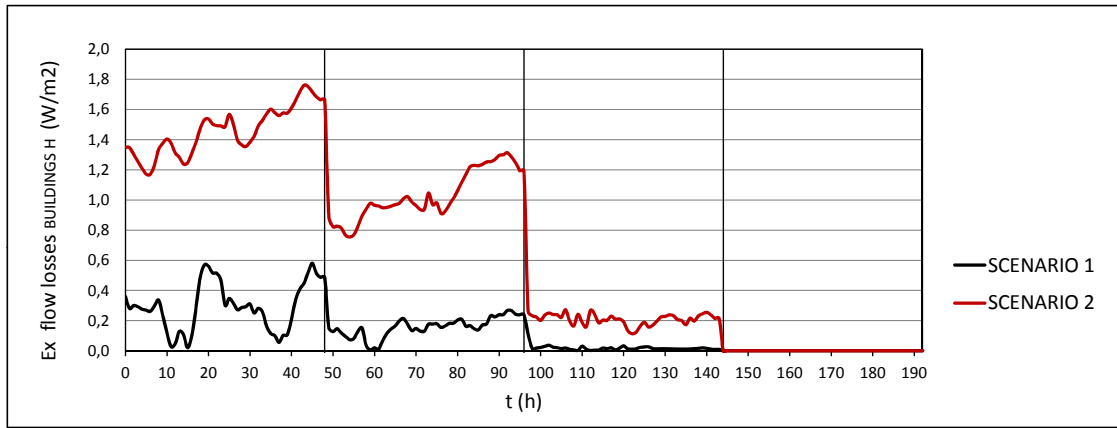
Figure 6.43: Exergy flow losses for all buildings, Heating branch. Comparison scenarios 1 and 2

In this case, after replacing the radiators with underfloor heating, there is a significant decrease in the level of temperature on the consumer side ($T_{CS\,H\,i}$ = 35° C, $T_{r\,CS\,H\,i}$ = 25°C. However, the temperature on the other side of the heat exchanger is still quite high ($T_{DHS\,i}$ = 65°C). Therefore, in scenario 2 a large difference between both sides of the heat exchanger, which gives rise to a high exergy destruction.
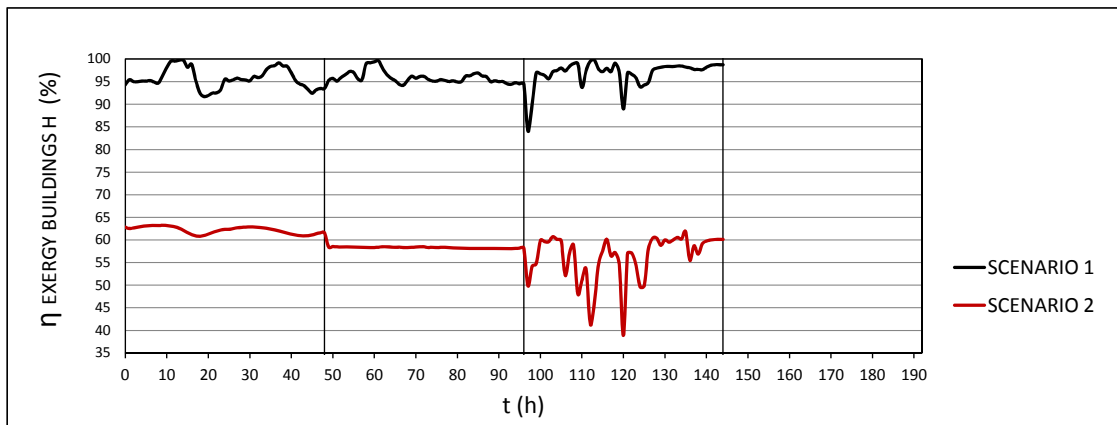
Figure 6.44: Exergy efficiency for all buildings, heating branch. Comparison scenarios 1 and 2

The exergy destruction means a significant reduction of the exergy efficiency in this branch, going from average values of 95% to 63% in extreme winter and even up to 57% in normal winter (see figure 6.44)

Subsequently, the decrease of the exergy efficiency in buildings comes mainly from the heating branch, whose effect is preponderant against the hot water production branch (see figure 6.40).

6.5.2 Scenario 3 vs scenario 1 (see section 3.3.3)

6.5.2.1 Operation variables
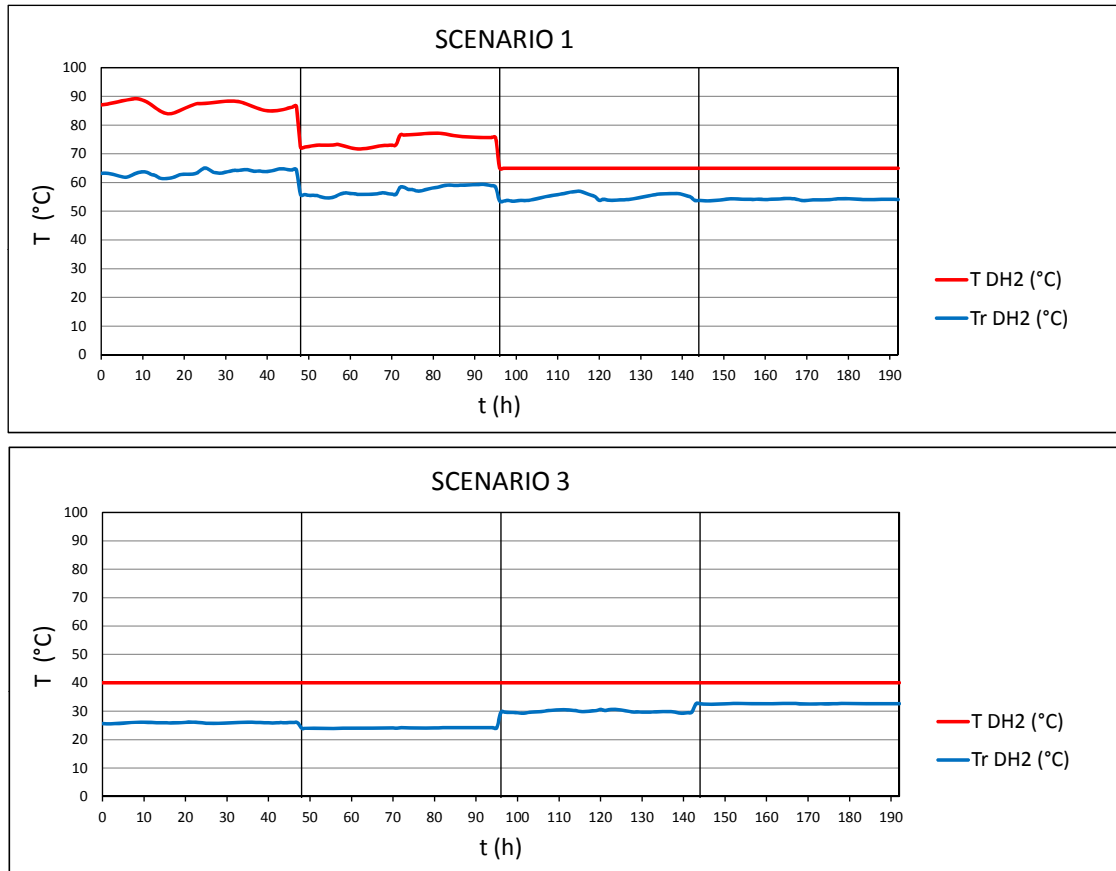
Figure 6.45: Temperatures evolution. Comparison scenarios 1 and 3
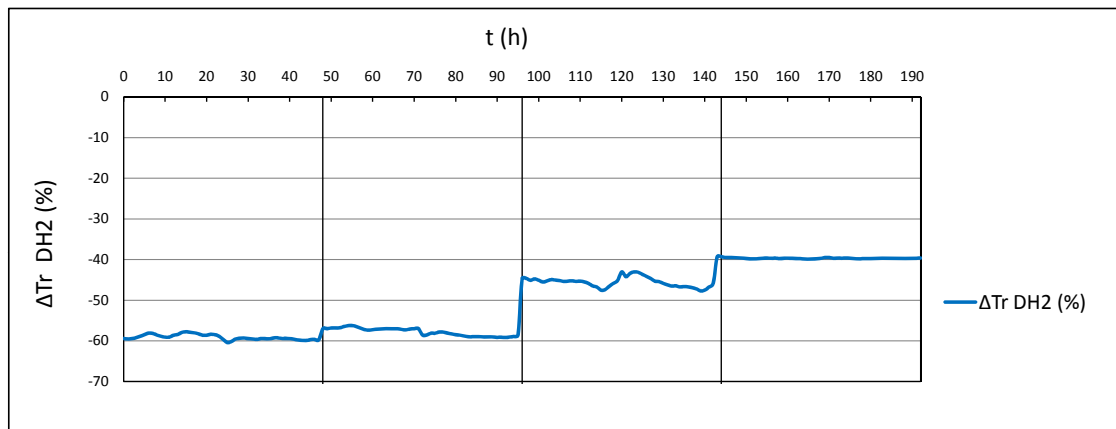
Figure 6.46: Return temperature variation respect to scenario 1

After replacing radiators by radiant floors and decreasing drastically the feed temperature, LTDHN conditions are reached for this scenario. Temperature levels are the lowest possible for all the cases

studied. ΔT values will be generally lower than scenario 1. In extreme winter the difference is more pronounced, implying consequences related to the increase of the mass flow, as it will be seen later.

The first relevant fact is the sharp decrease of the return temperature, which moves from 65/55 °C (scenario 1, winter) to approx. 25 °C (scenario 3, same period). More than 55% of the return temperature is decreased in winter and in extreme winter, and around 45% in mid-season (figure 6.46).
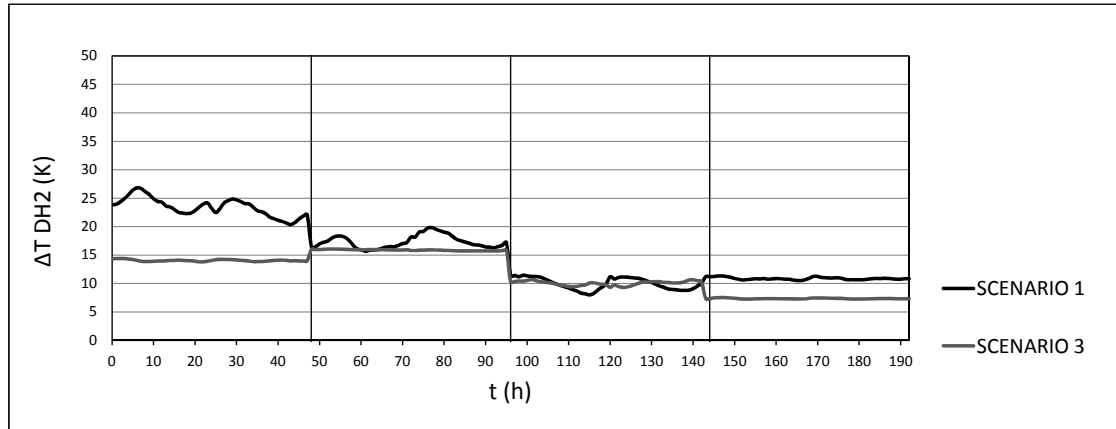
Figure 6.47: ΔT evolution. Comparison scenarios 1 and 3

Although $T_{r\,DH2}$ has been widely reduced for all periods, this does not necessarily mean that ΔT values have to decrease as well. In fact, only a significant change of this magnitude is observed for extreme winter period (from 25 to 14 K, approx.) and summer (from 11 to 7.3 K, approx.). For the rest of the year the values are similar.
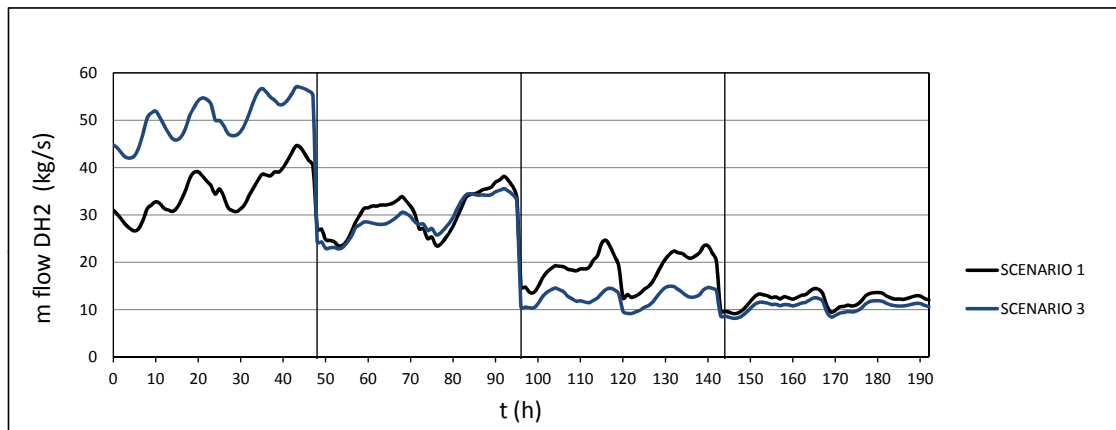
Figure 6.48: Mass flow evolution. Comparison scenarios 1 and 3

For extreme winter, a strong decrease of ΔT allows the correspondent increase of the mass flow, as shown in figure 6.48. For winter period, where ΔT for both scenarios are closer, mass flows are also similar.

In the mid-season there is a slight increase of ΔT on the hot side of the heat exchanger (DHN side) in comparison with scenario 1. This gain is also observed in the heating branch. However, during

this period of the year, the hot water consumption is predominant. The final consequence will be also a mass flow reduction, but slightly smaller than in scenario 2.
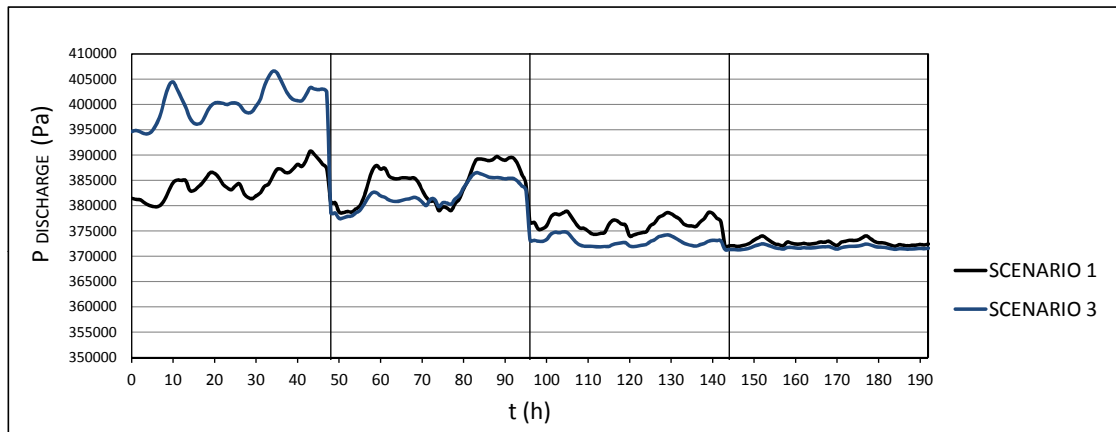
Figure 6.49: Discharge pressure evolution. Comparison scenarios 1 and 3
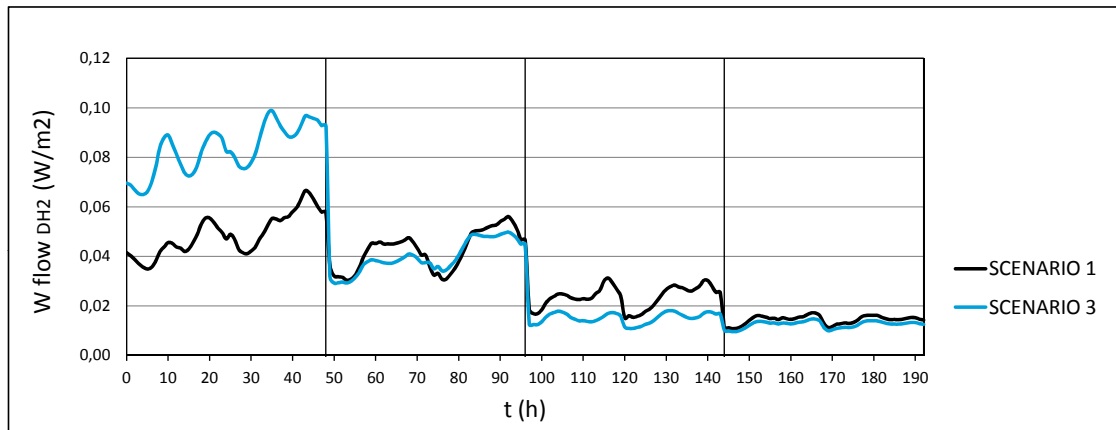
Figure 6.50: Hydraulic pump's electric consumption. Comparison between scenarios 1 and 3
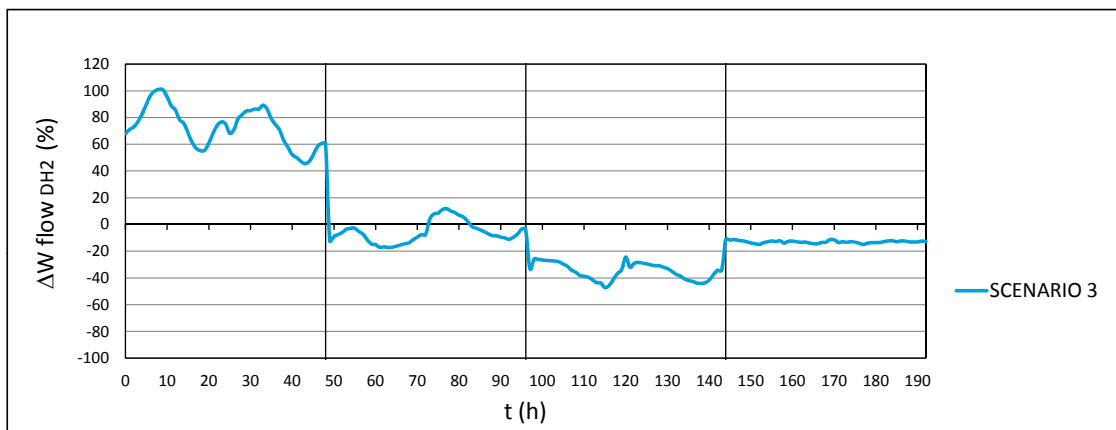
Figure 6.51: Hydraulic pump's electric consumption variation respect to scenario 1

Again, both the pressure and the electrical hydraulic pump's consumption describe parallel profiles, following figure 6.48. For the second variable, the maximum values appear during the extreme winter time ($\overline{\dot{W}}_{DH2}$), reaching consumption peaks of about 0.09 W/m^2 and even of 0.1 W/m^2, which represents increases of 80% or even 100% for several consumption peaks (see figures 6.50 and 6.51).

6.5.2.2 Energy Balance

The same expressions of scenario 1 are used here, generating the following results:
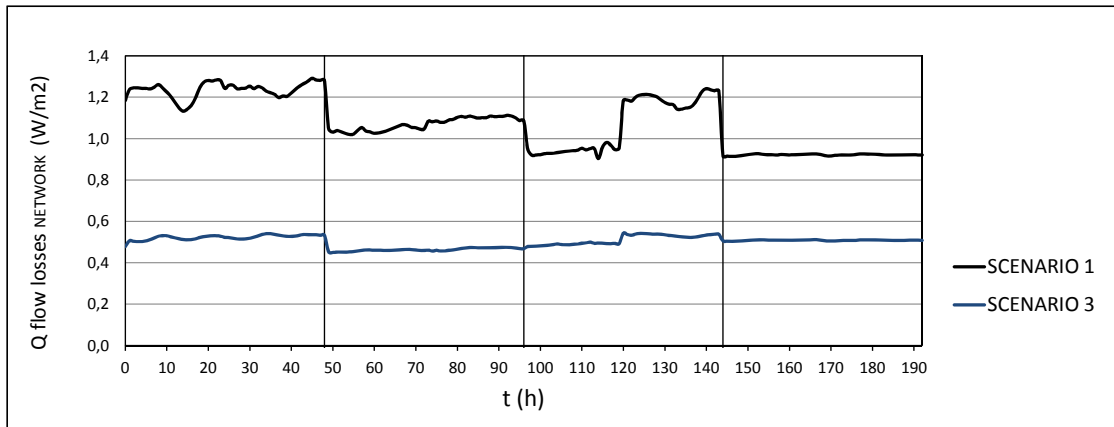
Figure 6.52: Energy flow losses along the network. Comparison scenarios 1 and 3

As shown in figure 6.52, reducing the temperature levels leads to a significant decrease of the energy losses of the pipe network. Unlike scenario 2, this decrease occurs for all periods of the year studied.
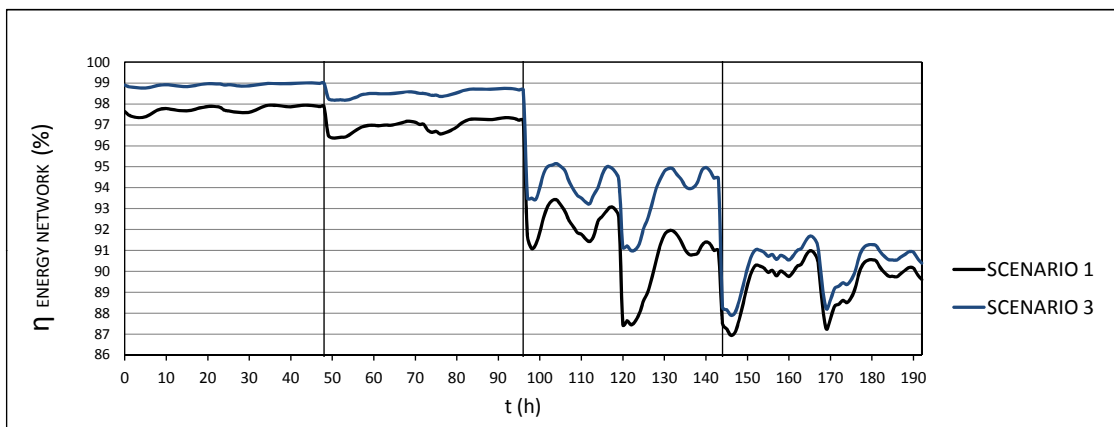
Figure 6.53: Energy efficiency along the network. Comparison scenarios 1 and 3

The generalized fall of the energy losses are good news, leading to the increase of the energy efficiency for all periods studied. For extreme winter, average values moving from 97.6% to 99% are reached, which means a relative improvement of the energy efficiency higher than 1%. In

normal winter the improvement is even greater, going from 97 to 98.5%, leading to a relative improvement greater than 1.5% (figure 6.54).
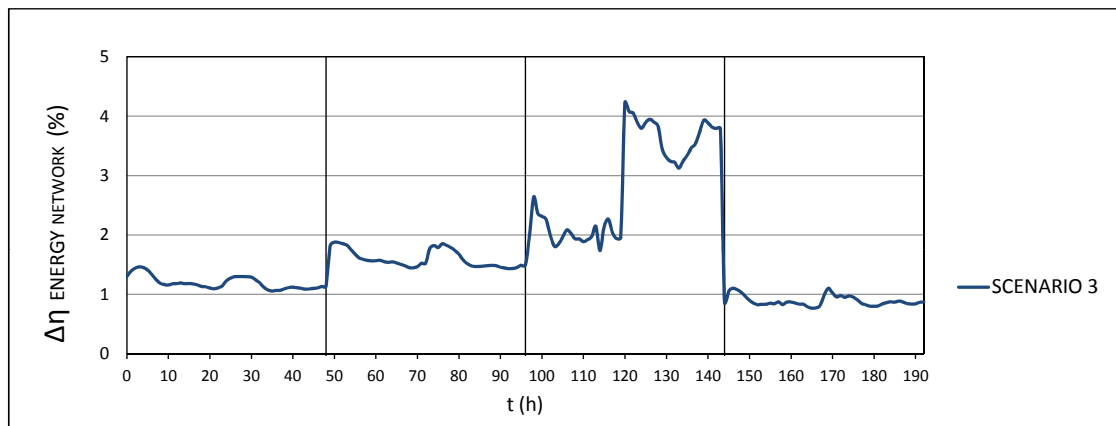
Figure 6.54: Energy efficiency variation respect to scenario 1

In essence, when moving from scenario 1 to 3, an improvement of the pipeline's energy efficiency is achieved (around 1.5% in winter period and 1.4% in extreme winter. In mid-season this improvement could be even higher, reaching up to 2% or even more.

6.5.2.3   Exergy Balance

For this scenario, the following expressions are used:

- Substation: equations 4.49 and 4.50

- Network: equations 4.51 and 4.52

- Buildings: equations 4.61 and 4.62

- Buildings, DHW branch: equations 4.63 and 4.64

- Buildings, Heating branch: equations 4.57 and 4.58

For the equations 4.61, 4.62, 4.63 and 4.64, the term $\sum_i^n \dot{B}_{AN\ HW\ i} = 0$, because this magnitude appears inside the borders of the control volume where the balance is applied, so, it is implicitly considered in the balance.

All those equations can be found in section 4.2.5, obtained from figure 4.4. Results are displayed along the following graphs:
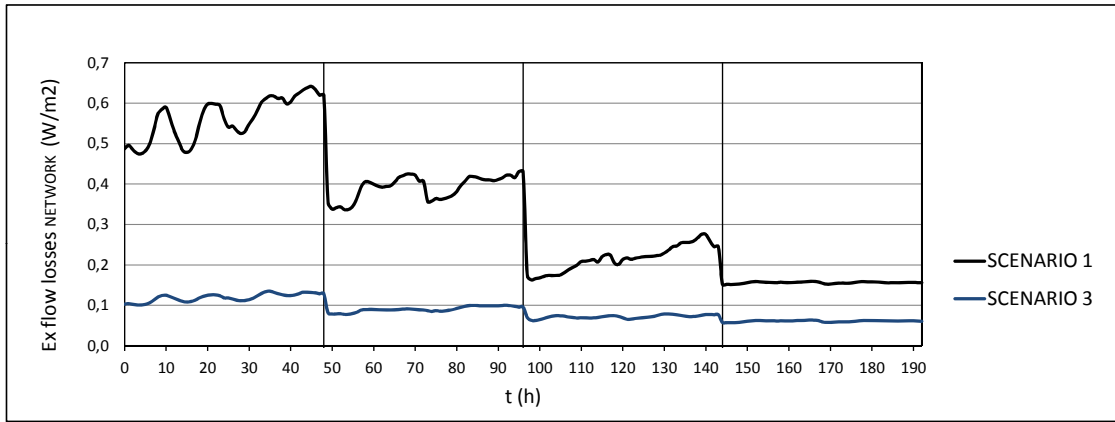
Figure 6.55: Exergy flow losses along the network. Comparison scenarios 1 and 3

The drastic temperature reduction brings these values closer to the reference ones, reducing the gradient. Therefore, the exergy of the system will be significantly reduced, with the consequent drop-off of the exergy losses.
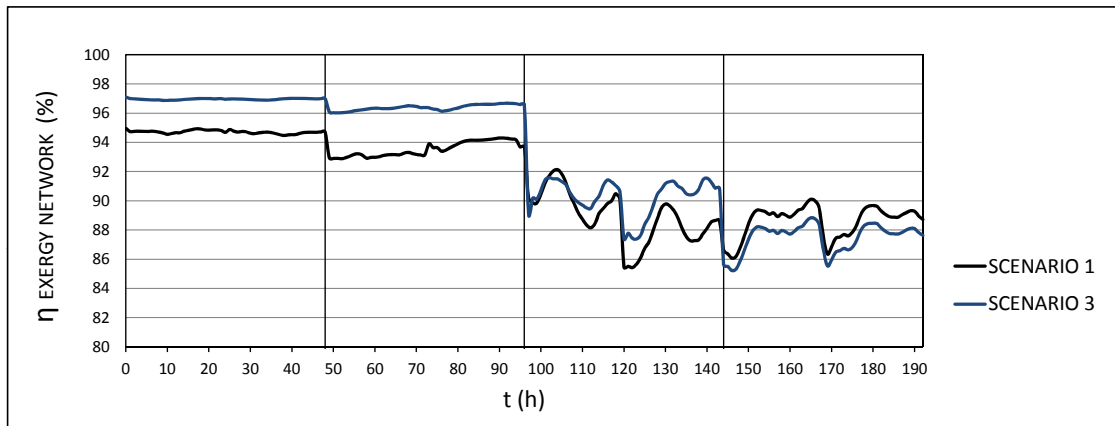
Figure 6.56: Exergy efficiency along the network. Comparison scenarios 1 and 3
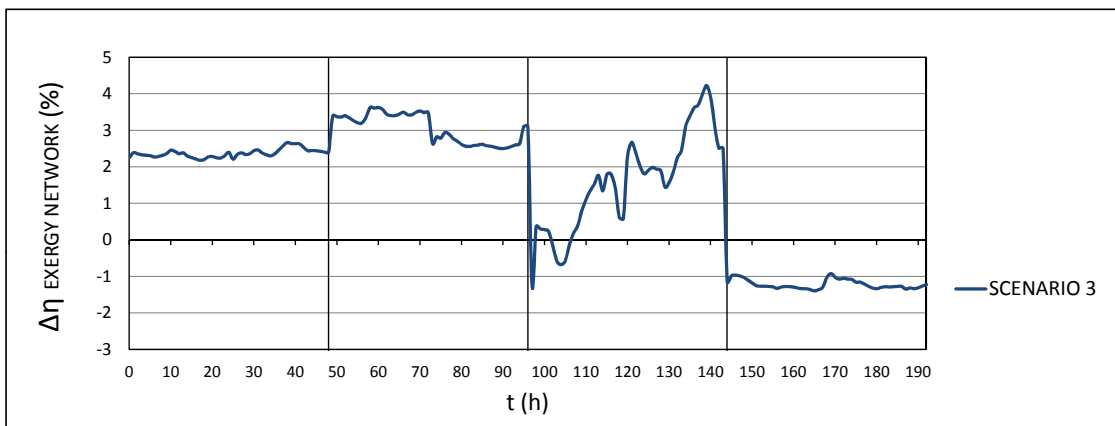
Figure 6.57: Exergy efficiency variation respect to scenario 1

This time, the relative improvement of the average exergy efficiency will be higher for all periods. The greater improvement comes for normal winter time ($\eta_{\text{EXERGY NETWORK}}$ = +3.5%). For extreme winter days, the improvement exceeds 2.3%. In mid-season this magnitude varies significantly, making values between -0.6/+4%.
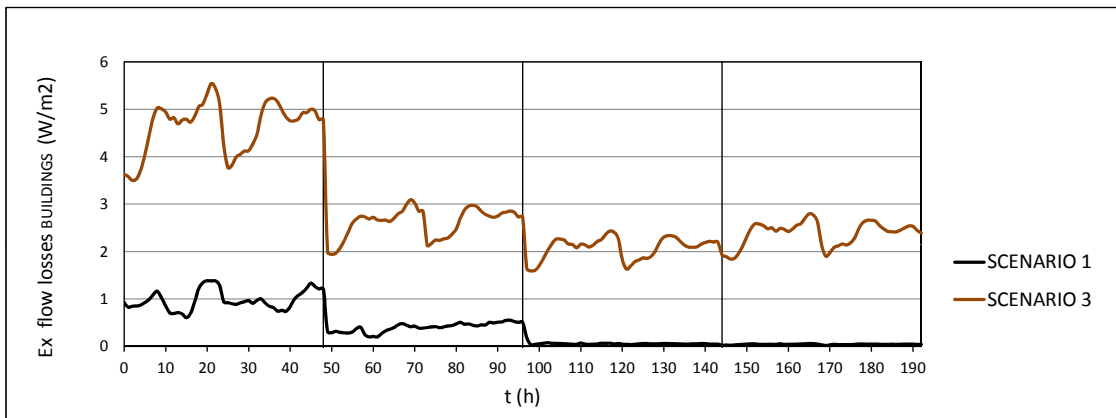
Figure 6.58: Exergy flow losses for all buildings. Comparison scenarios 1 and 3
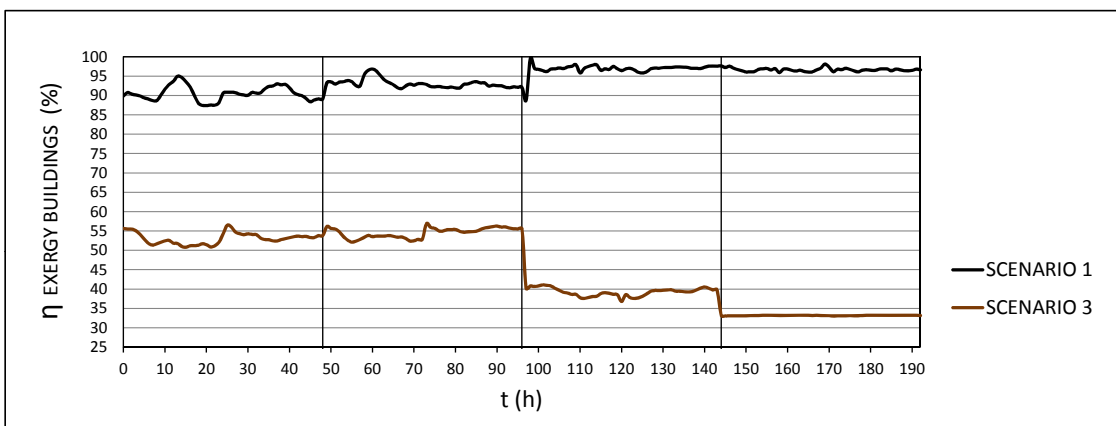
Figure 6.59: Exergy efficiency for all buildings. Comparison scenarios 1 and 3

As the figure 6.58 shows, the exergy losses for the buildings subsystem are much greater here than in the previous scenario. These losses are evenly generated along the year, in coincidence with the hot water consumption.
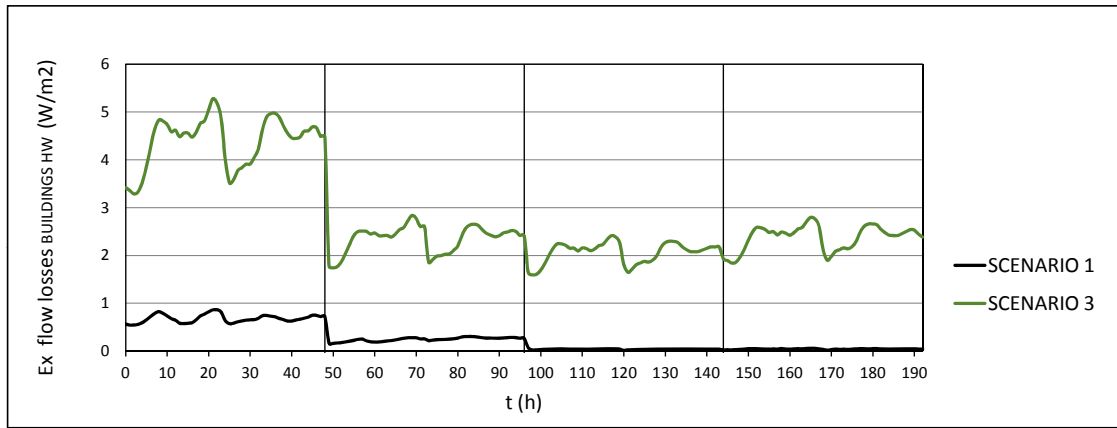
Figure 6.60: Exergy flow losses for all buildings, DHW branch. Comparison scenarios 1 and 3
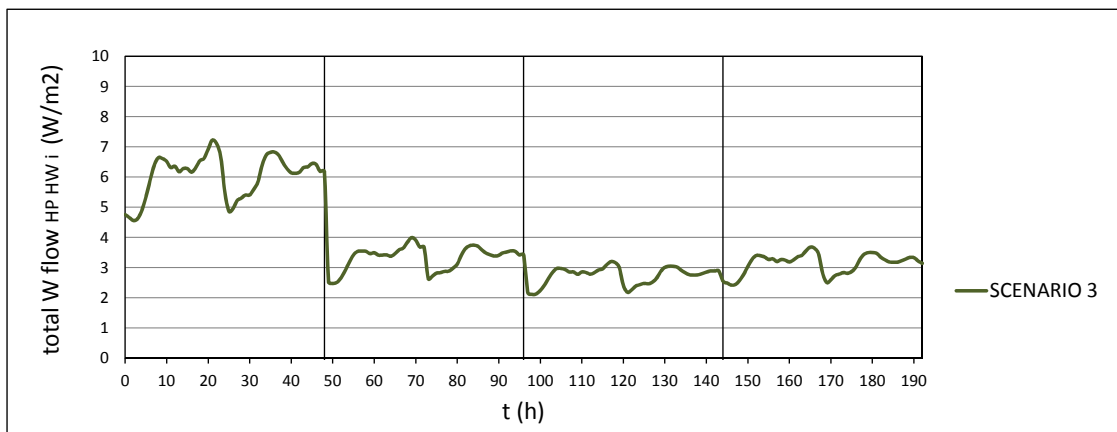
Figure 6.61: Heat pump's electric consumption, DHW branch

Once again, both separated branches have to be analysed, in order to understand the reasons of this performance.

The analysis of figure 6.61 is the key to understand the reason of this behaviour. It shows the total electrical consumption required by all the heat pumps of all buildings to operate ($\sum_{j=1}^{n} \dot{W}_{\text{HP HW i}}$). This device is continuously raising the DH water temperature from 40 to 65°C, using between 2.1 and 7.2 W/m^2. This is a continuous injection of electric flow, which definitely means pure exergy and increases the external exergy flow rate fed to the thermodynamic system in comparison with the exergy flow that is finally supplied to the consumer. The consequence will be a sharp decrease of the exergy performance (figure 6.62).
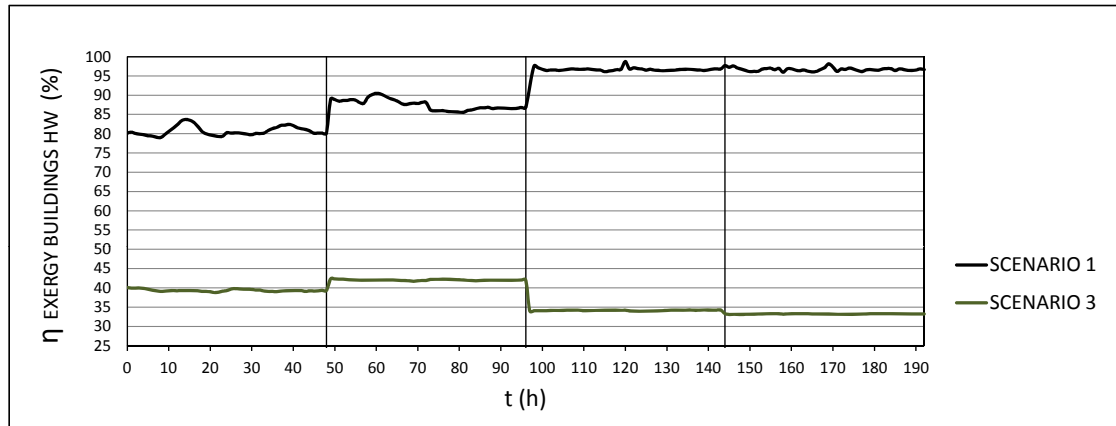
Figure 6.62: Exergy efficiency for all buildings, DHW branch. Comparison scenarios 1 and 3

On the other hand, on the heating side there are several instants during the extreme winter time segment (consumption peaks) where the exergy losses are considerably reduced (figure 6.63).
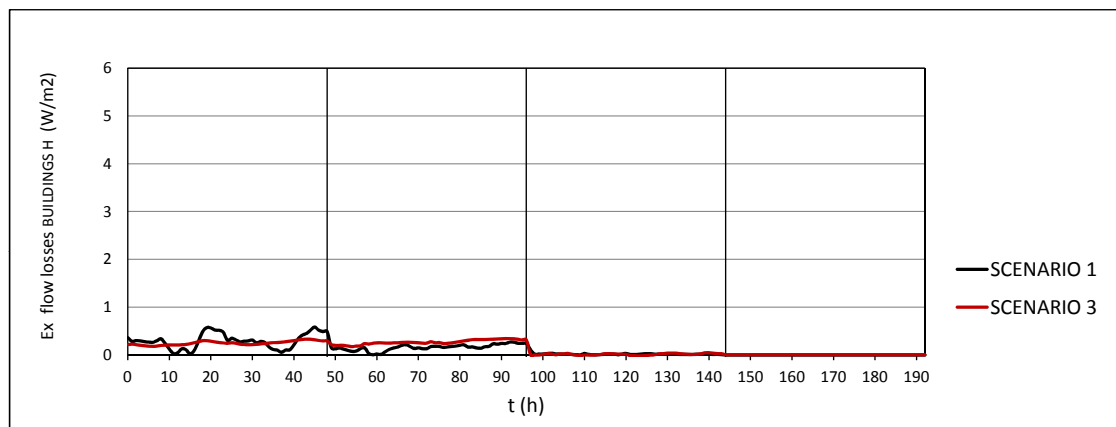
Figure 6.63: Exergy flow losses for all buildings, Heating branch. Comparison scenarios 1 and 3

There is a certain uniformity of these losses in both winter seasons, mainly due to the small variation of the temperature values for these periods. In normal winter period, the exergy losses are slightly higher than in scenario 1, probably due to the greater temperature difference between the hot side of the heat exchanger (DHN side $\rightarrow T_{DHS\,i} \simeq 40°$C) and the cold side (radiant floor side $\rightarrow T_{CS\,H\,i} \simeq$ 35°C). Spring and summer are seasons in which the heating consumption is very low or zero, therefore the losses will follow the same trend.
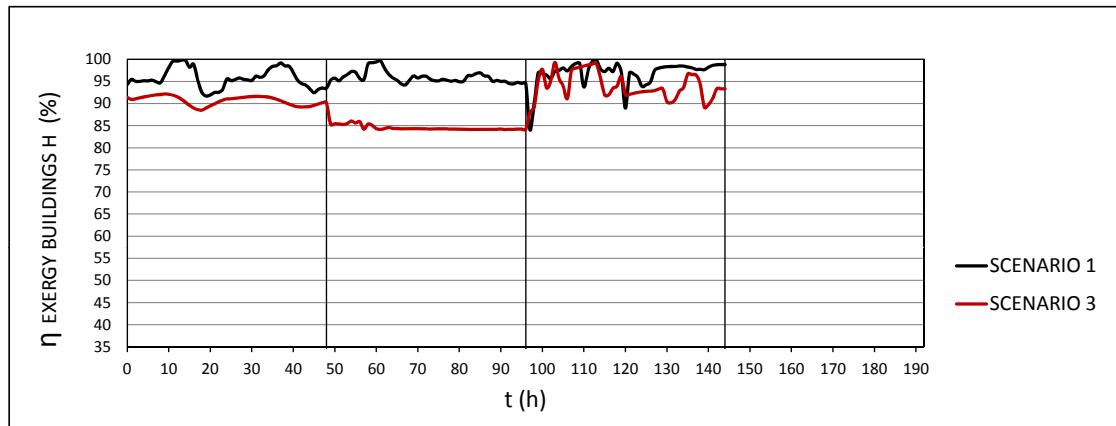
Figure 6.64: Exergy efficiency for all buildings, heating branch. Comparison scenarios 1 and 3

The consequence will be a reduction of the exergy performance for winter periods (around -5% for extreme winter, and -10% for normal winter. In midseason the exergy balance values are very small, generating strong fluctuations for the calculated values. During this period, it is considered that the exergy efficiency remains the same as scenario 1 (see figure 6.64).

6.5.3 Scenario 4 vs scenario 1 (see section 3.3.4)

The general balance expressions used for this scenario are the same as scenario 1, except the substation subsystem (equations 4.59 and 4.60).

This scenario has the same characteristics and results profiles as scenario 2 (see section 6.5.1). The main difference lies in the principal heat flow, which is not provided anymore from the primary network. Instead, there is a general heat pump installed in the substation, which consumes power ($\dot{W}_{HP\ SUB}$) and requires a constant mass flow of anergy water ($\dot{m}_{AN\ SUB}$). For more information, see section 4.3.5.2.
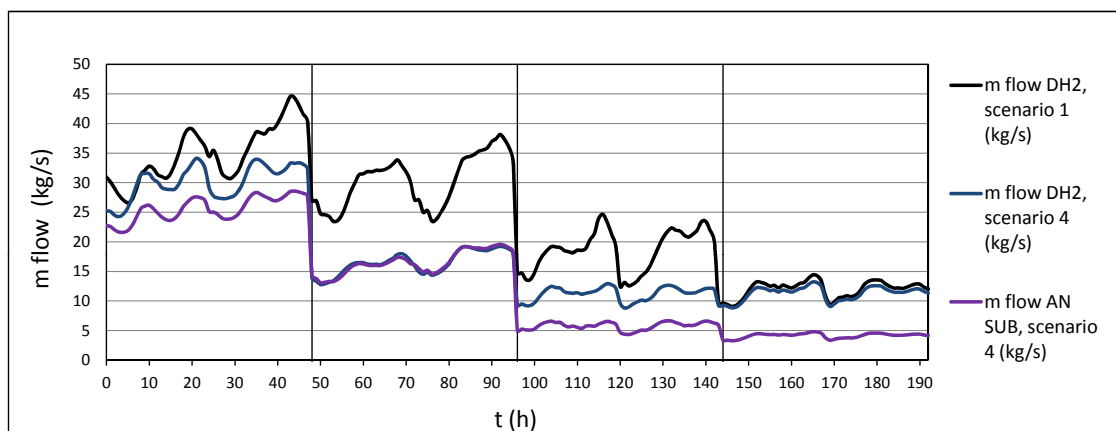
Figure 6.65: Comparison between the different mass flows related to the DHN.

As it is shown in figure 6.65, the mass flow consumed by the substation is lower than the total DH water flow used in both scenarios 1 and 4. nevertheless, it is still a very important flow that has

to be returned to the original place where it comes from, or sent to the corresponding treatment process. Thus, like the district heating network, the urban anergy network is able to work as a cooling medium for water from thermal processes whose temperature is too high to be expelled into the environment (rivers, lakes...etc)

The second variable to be considered in this study is the electrical consumption of the heat pump, reflected in the following figure:
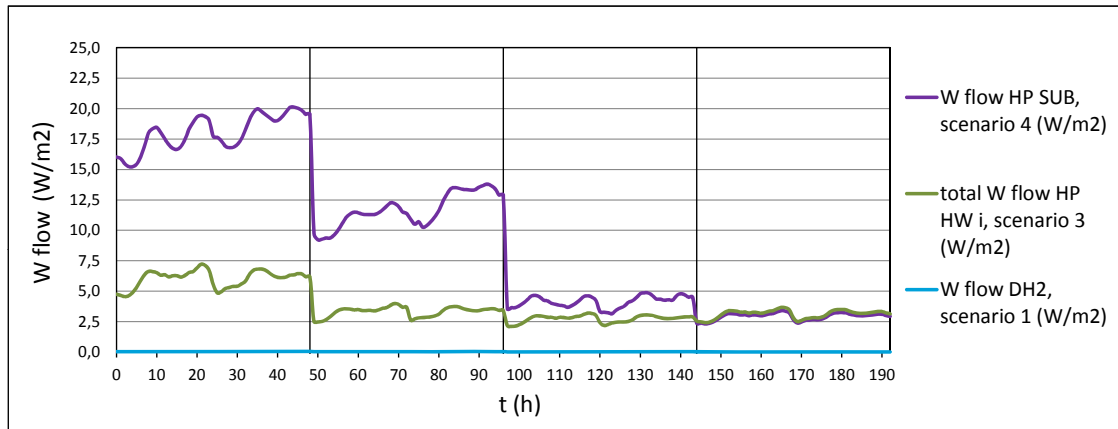
Figure 6.66: Heat pump's electric consumption in the substation. Comparison with other electric flows

This comparison gives an idea about the power that is required by the substation's heat pump in comparison with other systems; and therefore, proceed with the appropriate design of the power supply system in the absence of another available heat source.

Obviously, $\dot{W}_{HP\,SUB}$ reaches maximum values in extreme winter, making a consumption peak of 20 W/m^2. For both winter seasons, this variable is practically doubled $\sum_{j=1}^{n} \dot{W}_{HP\,HW\,i}$ (between 13.65 W/m^2 as maximum value and 9.21 W/m^2 as minimum value). It is reasonable, since this is the only exergy source available for the DHW production and heating generation for the entire group of buildings.

For this hypothesis and also for scenario 6, the used water here comes from several origins (industrial processes, urban waste) which temperature is still usable ($T_{AN\,pre\,SUB} = 30\,°C$). As a comment, it would be possible to increase the efficiency of the heat pump and reduce its electrical consumption if the water temperature was higher, leading to another range of improvement for the whole system.

6.5.4 Scenario 5 vs scenario 1 (see section 3.3.5)

6.5.4.1 Operation variables
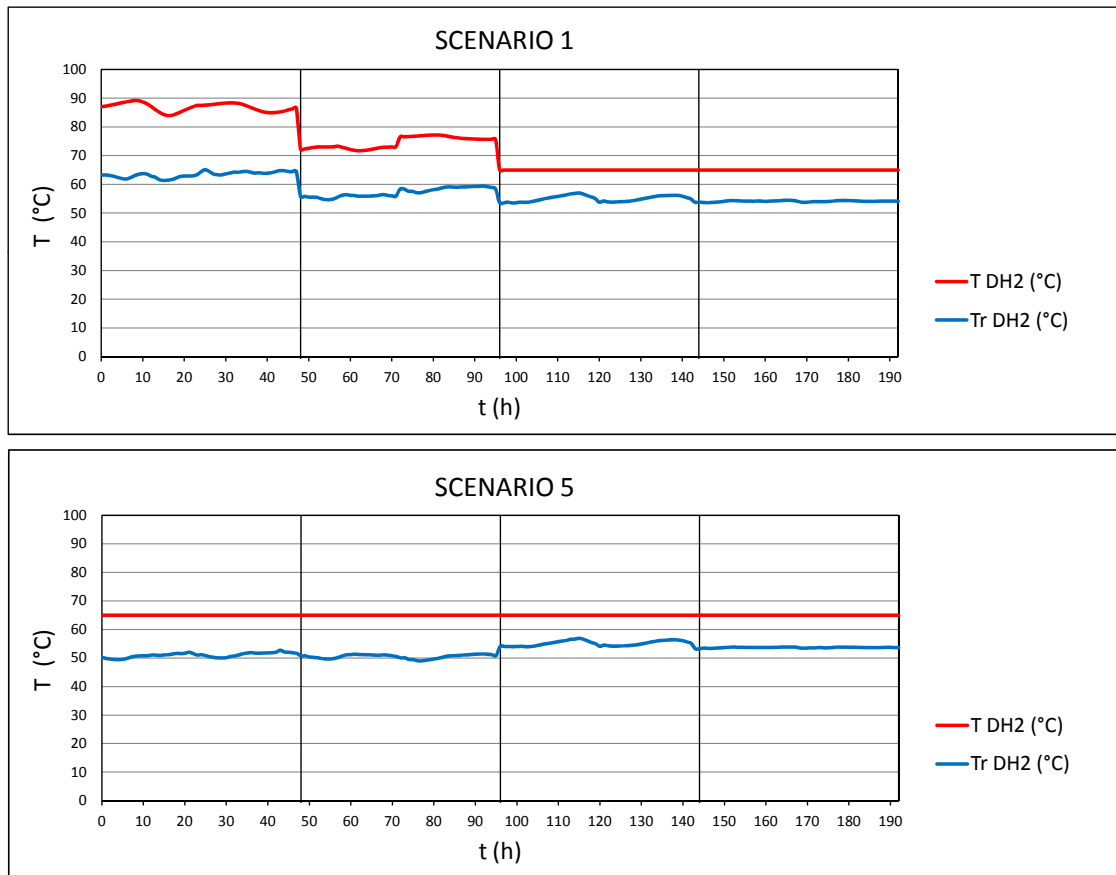
Figure 6.67: Temperatures evolution. Comparison scenarios 1 and 5
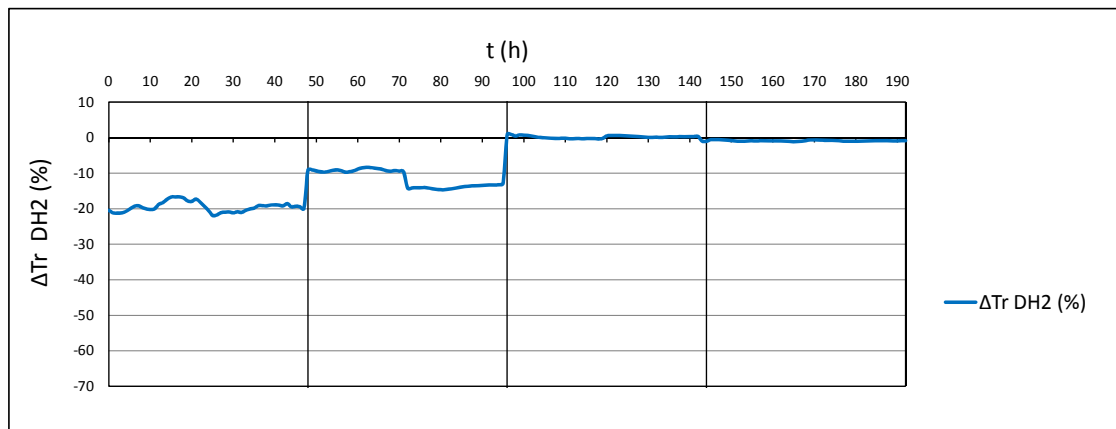
Figure 6.68: Return temperature variation respect to scenario 1

In this new variant the goal consists of satisfying buildings heat demand at constant network temperature, following the same temperature regulation as scenario 2, but without replacing radiators

or performing any kind of refurbishment works. Again, a good solution would be the installation of support heat pumps that are switched on only if the incoming T_{DH} is not sufficient to keep the comfort temperature inside the buildings. Hence, instead of increasing the entire DH water stream temperature above 65°C (which is not necessary in the DHW production branch), the mentioned increase is punctually carried out only for the heating branch and only when it is necessary.

Therefore, the systems will work intermittently instead of continuously, like the case explained in scenario 3 (section 6.5.2). Hence, during mid-season, feed and return temperatures will have the same profile for both scenarios, as it can be observed in figure 6.67.

Keeping the radiator system leads to a higher return temperature than scenario 2 ($T_{r\,DH2}$ = 50°C approx.), but still lower than in scenario 1 (-20% in extreme winter, and -10/-15% in normal winter). There are no differences during the rest of the year respect to scenario 1. This is logical, since all variations will occur only in winter, when the heat pumps are activated.
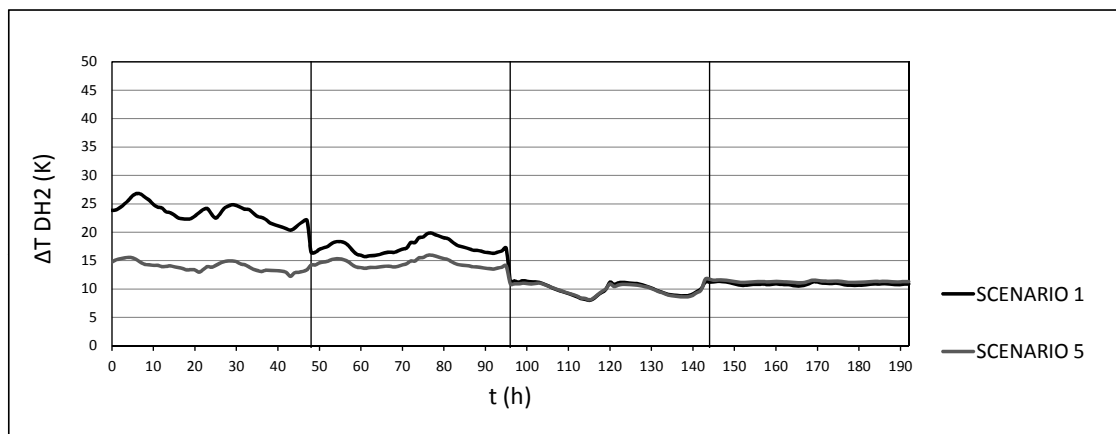
Figure 6.69: ΔT evolution. Comparison scenarios 1 and 5

As a consequence, ΔT will decrease only for winter periods, as shown in figure 6.69.
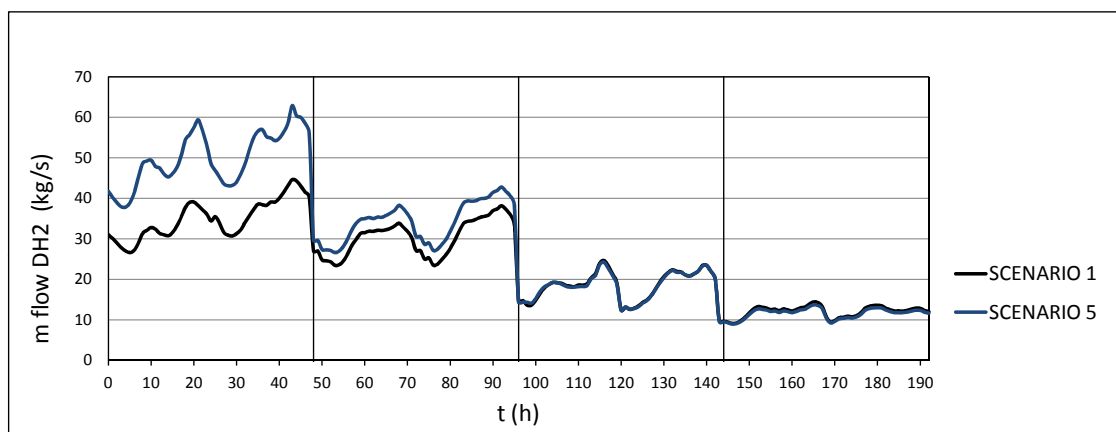
Figure 6.70: Mass flow evolution. Comparison scenarios 1 and 5

As mentioned before, modifying all the heating branches for all the buildings will give raise to a decrease of ΔT, producing a generalized increase of the mass flow during the winter seasons.

The change is more pronounced in extreme winter (+55% in consumption peaks) than in normal winter (approx. +15%). Also in extreme winter, the system reaches a record of 62.85 kg/s, which is the highest flow for all the studied scenarios. In the same way as before, there are practically no variations in mid-season and summer.
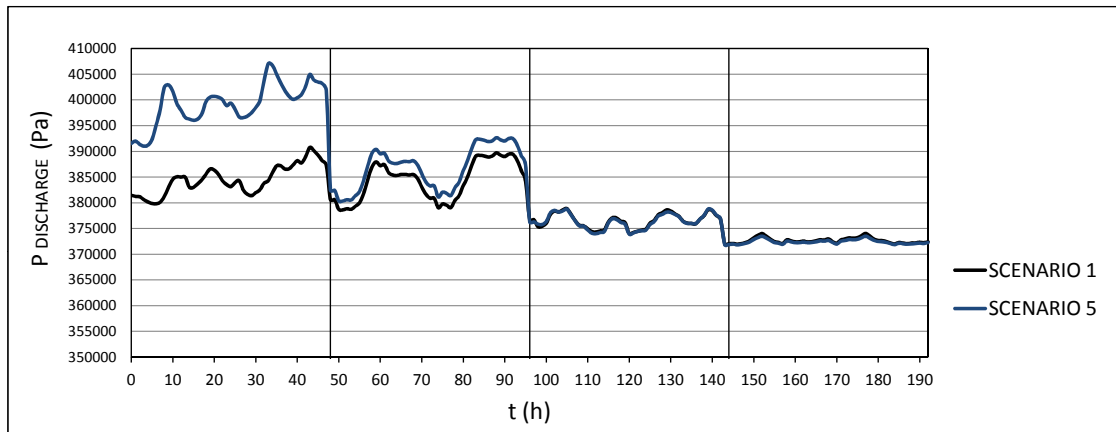
Figure 6.71: Discharge pressure evolution. Comparison scenarios 1 and 5
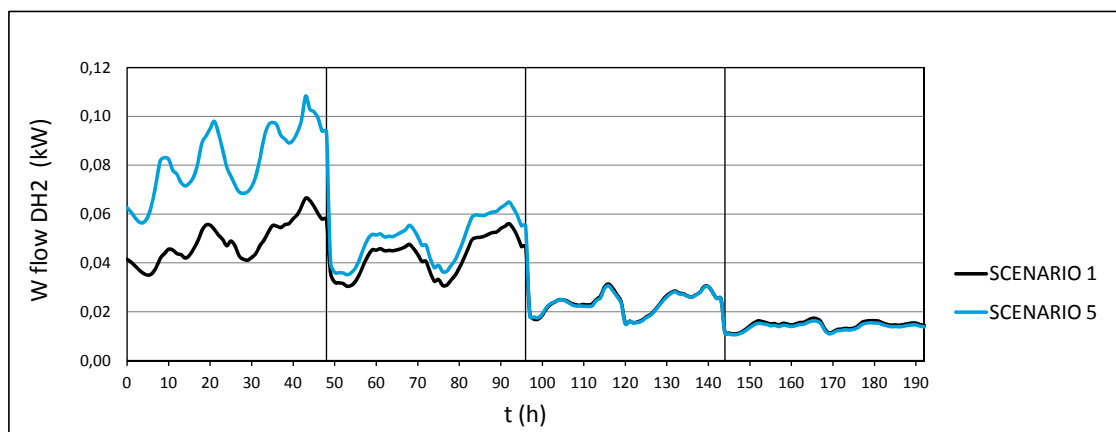
Figure 6.72: Hydraulic pump's electric consumption. Comparison scenarios 1 and 5
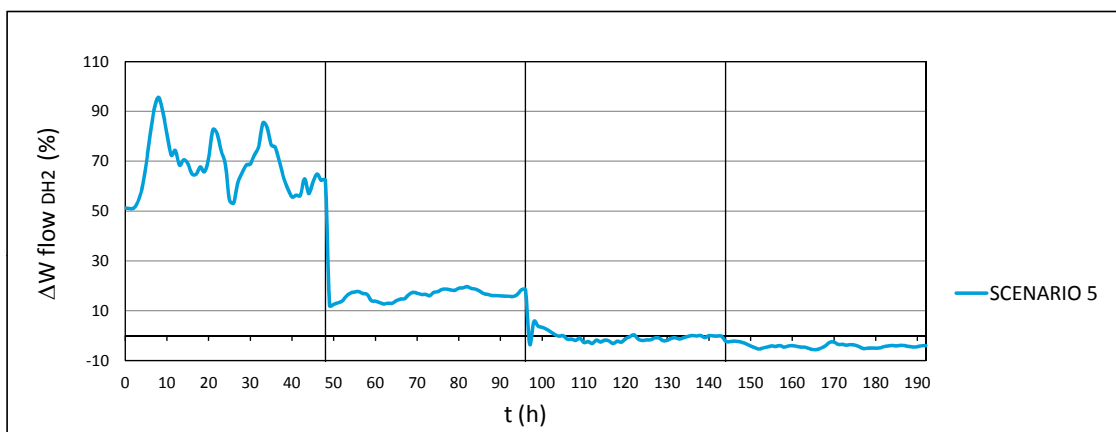
Figure 6.73: Hydraulic pump's electric consumption variation respect to scenario 1

Again, both the pressure and the electrical hydraulic pump's consumption describe parallel profiles, following figure 6.48. For the second variable, the maximum values appear during the extreme winter time, reaching consumption peaks of about 0.09 W/m² and even of 0.1 W/m², which represents increases of 80% or even 100% for several consumption peaks (see figures 6.72 and 6.73).

After analysing scenarios 3 and 5, one conclusion can be obtained from here: installing individual heat pumps in buildings influences on the mass flow, generating the corresponding increase of the hydraulic pump's power consumption.

6.5.4.2   Energy Balance

The same expressions of scenario 1 are used here, generating the following results:
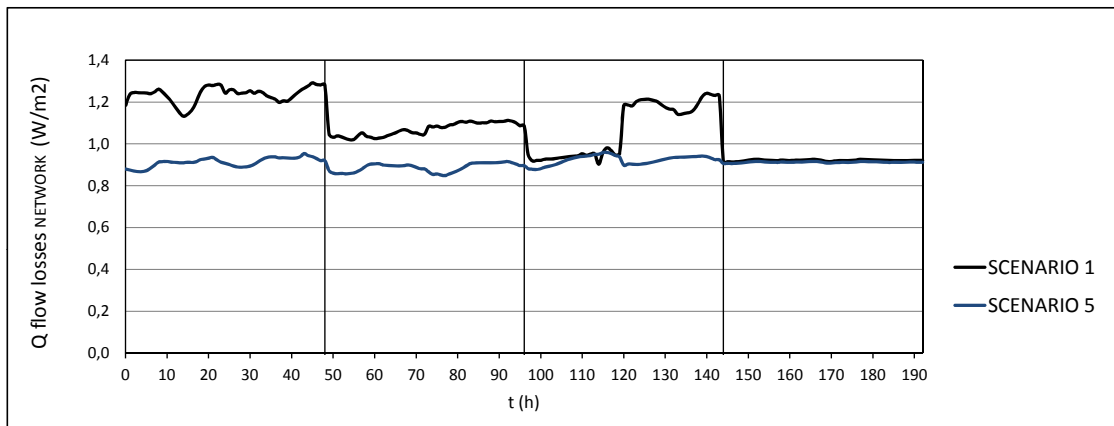
Figure 6.74: Energy flow losses along the network. Comparison scenarios 1 and 5
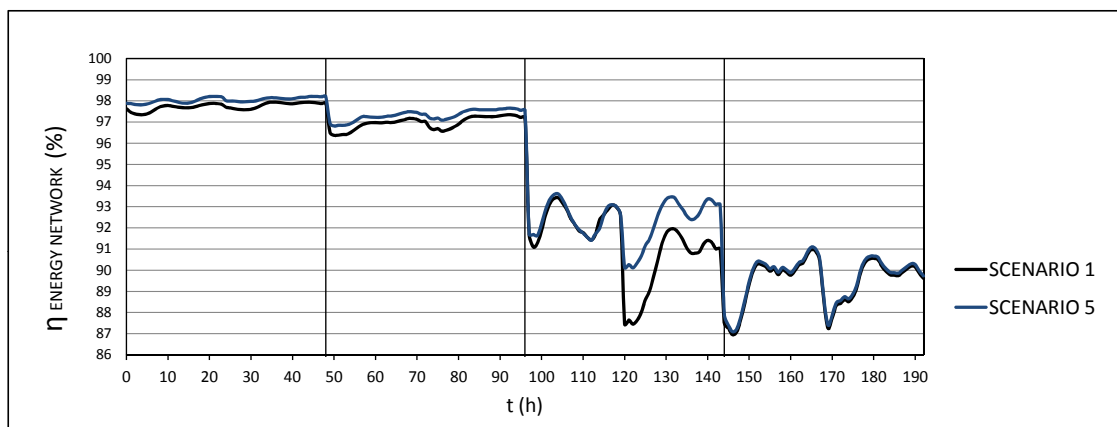
Figure 6.75: Energy efficiency along the network. Comparison scenarios 1 and 5

In this case, the only two variables that influence the energy losses are the return temperature and the mass flow, since the feed temperature is fixed in the same way as it happens in scenario 2. In winter periods, the heat losses are also reduced with respect to scenario 1 but not as much as in scenario 2. The reason here is the return temperature, which decreases more in scenario 2 than in scenario 5 (see and compare figures 6.26, 6.33, 6.67 and 6.74).

Following the same behaviour as the mass flow variable, the heat losses are more strongly reduced in extreme winter than in normal winter, demonstrating the dominant influence of the mass flow over the rest of the variables. The result will be a small improvement of the energy efficiency, less than 0.5% for both winter seasons (figure 6.76).
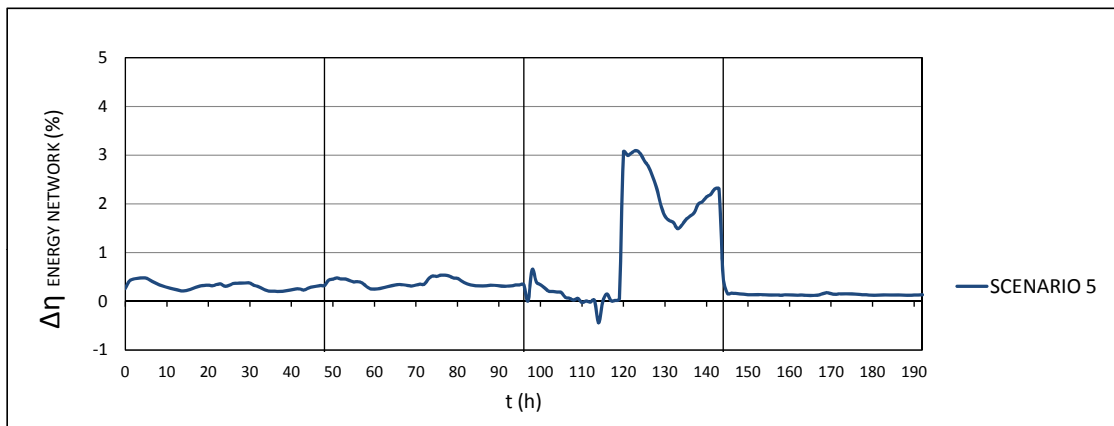
Figure 6.76: Energy efficiency variation respect to scenario 1

6.5.4.3   Exergy Balance

In this case, the following expressions are used:

- Substation: equations 4.49 and 4.50

- Network: equations 4.51 and 4.52

- Buildings: equations 4.61 and 4.62

- Buildings, DHW branch: equations 4.55 and 4.56

- Buildings, Heating branch: equations 4.65 and 4.66

For the equations 4.61, 4.62, 4.65 and 4.66, the term $\sum_{i}^{n} \dot{B}_{AN\ H\ i} = 0$, because this magnitude is contained inside the borders of the control volume where the balance is applied, so, it is already implicitly considered in the balance.

All those equations can be found in section 4.2.5, obtained from figure 4.4. Results are displayed along the following graphs:
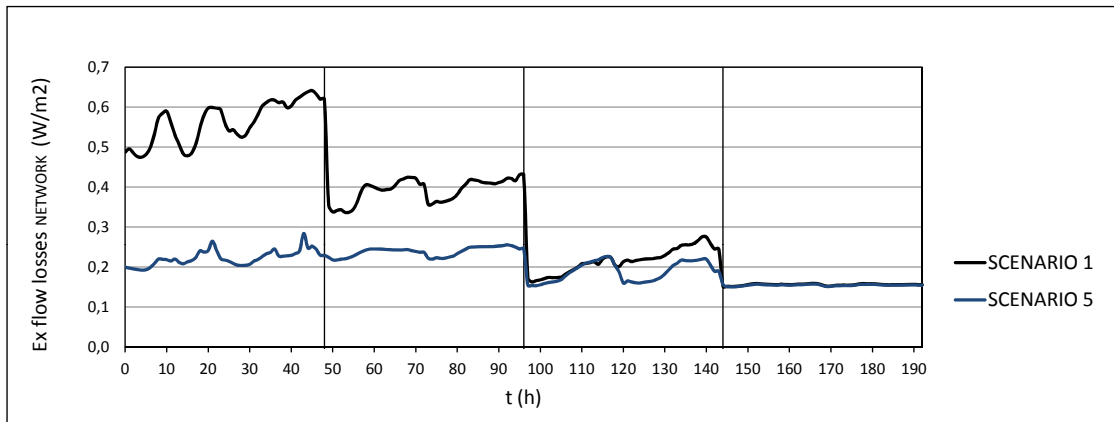
Figure 6.77: Exergy flow losses along the network. Comparison scenarios 1 and 5
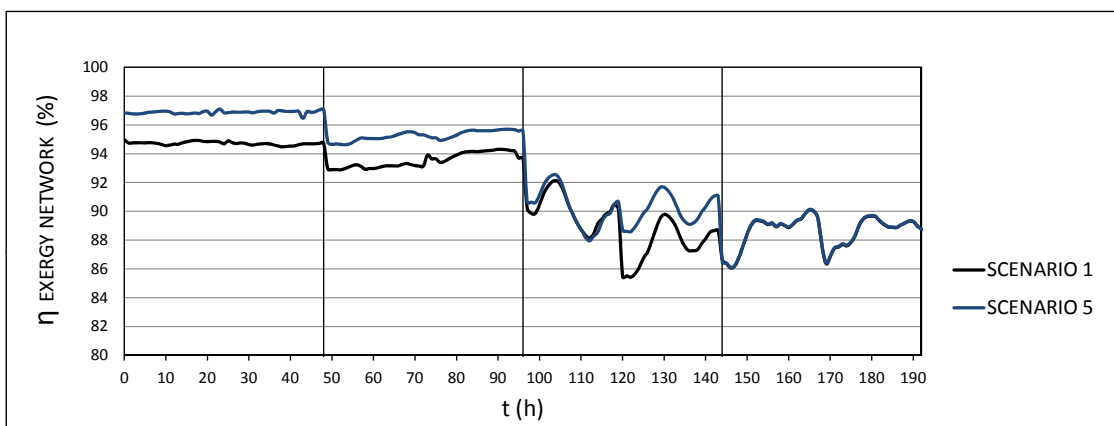
Figure 6.78: Exergy efficiency along the network. Comparison scenarios 1 and 5

During winter and extreme winter periods, the temperature reduction from the first to the fifth scenario and the greater mass flow collaborates in decreasing the energy losses, influencing again on the exergy losses in the same direction. The same performance is observed for all the previous situations.

As shown in figures 6.75 and 6.78, energy and exergy efficiencies both follow very similar profiles. In this case, the exergy efficiency will be increased for all periods except summer. The greater improvement comes for both winter segments, changing from 95% to 97% in extreme winter and from 93% to 95.5% in normal winter, giving a relative increase of +2.5%.
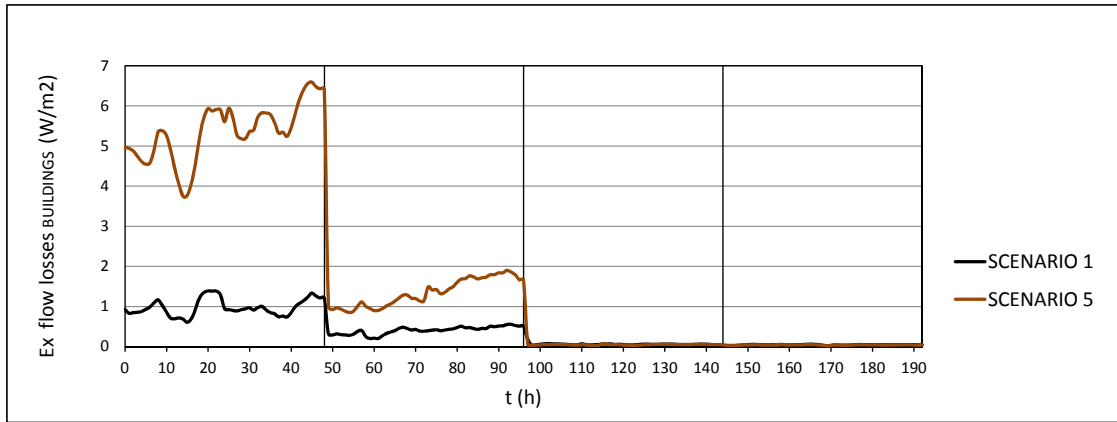
Figure 6.79: Exergy flow losses for all buildings. Comparison scenarios 1 and 5
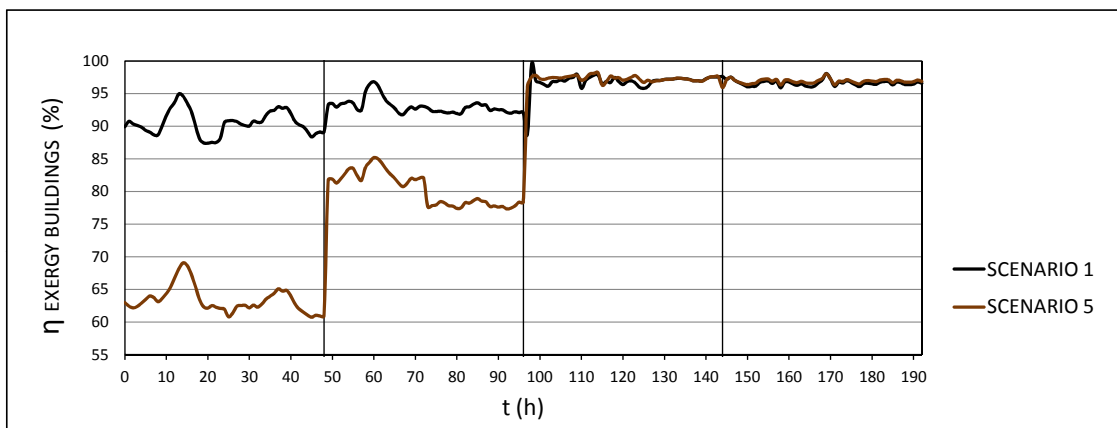
Figure 6.80: Exergy efficiency for all buildings. Comparison scenarios 1 and 5

Looking at the figure 6.79 it is possible to see how the exergy losses are increasing dramatically, exactly when the heat pumps are switched on. These circumstances lead to a very marked decrease of the exergy efficiency 6.80, which moves from 90 to 63% in extreme winter, and from 93 to 80% in normal winter. Both drops involve an efficiency decrease of 30 and 15% for both periods, respectively.
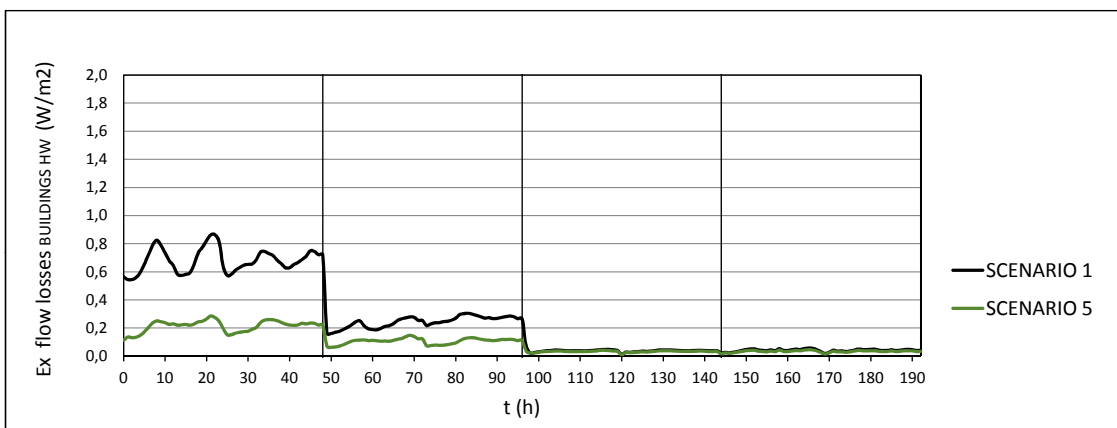
Figure 6.81: Exergy flow losses for all buildings, DHW branch. Comparison scenarios 1 and 5
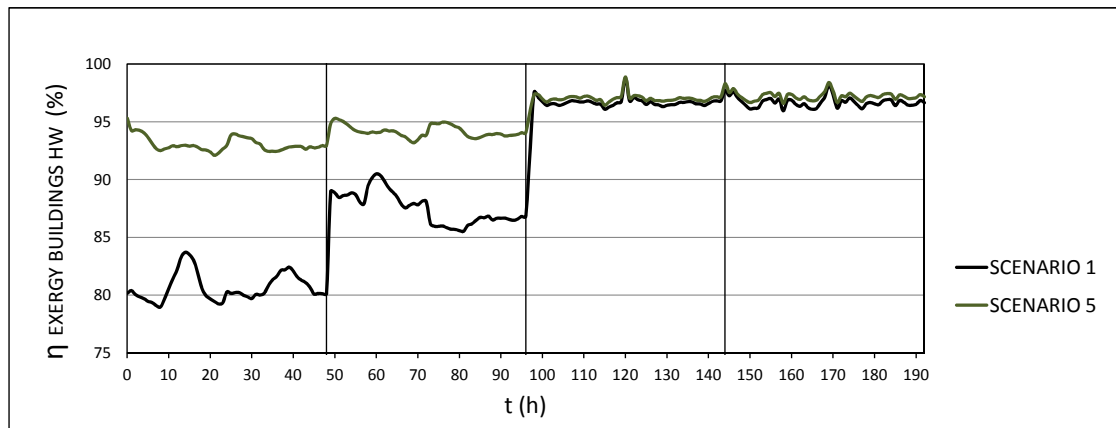
Figure 6.82: Exergy efficiency for all buildings, DHW branch. Comparison scenarios 1 and 5

In the same way as figure 6.41, there is a significant decrease of the exergy losses in the DHW branch. This improvement is observable but it is slightly smaller than in scenario 2. This is because $\dot{m}_{DH2}$ is greater here than scenario 2, leading to smaller temperature losses throughout the network and giving rise to higher temperature values (T_{DH2} and $T_{DHS\,i}$). Then, the variable ($\sum_{j=1}^{n} \dot{Ex}_{DHS\,HW\,i}$) will be mildly increased, producing a very small increment of the exergy losses for that branch.

The analysis of figure 6.83 reveals the total electrical consumption required by all the individual heat pumps ($\sum_{j=1}^{n} \dot{W}_{HP\,H\,i}$). This device is raising the DH water temperature to the required temperature established by the regulation curve from 65 up to 90°C, following the regulation curve (figure 3.14). The power supplied reaches a maximum value up to 9 W/m^2 in extreme winter, and lower values between 1.3 and 2.6 W/m^2 for normal winter periods. Obviously, there is no power consumption in mid-season and summer.

Considering a heat pump and the corresponding power consumption generates this "distorting" effect on the exergy efficiency, as explained in section 6.5.2. The performance is here decreased as well, falling from 95 to a 55% in extreme winter and 75% in mid-season (figure 6.85).
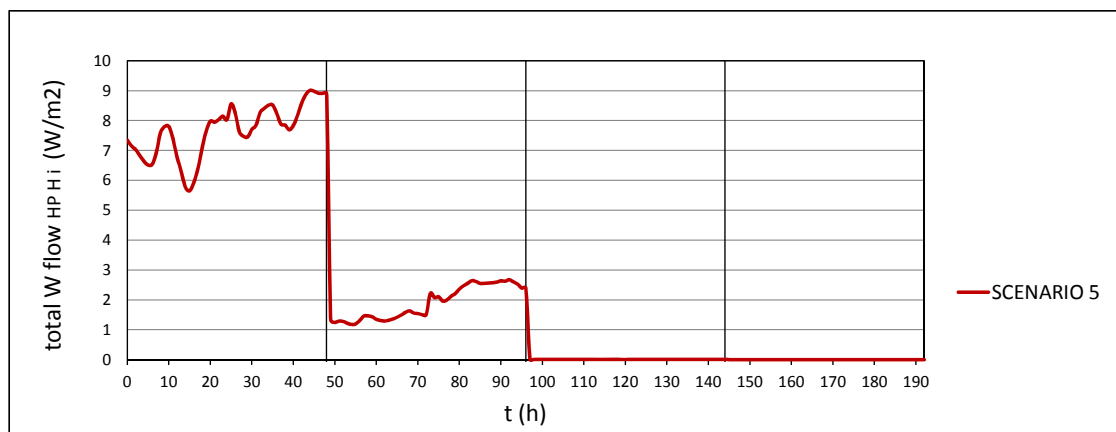
Figure 6.83: Heat pump's electric consumption, heating branch
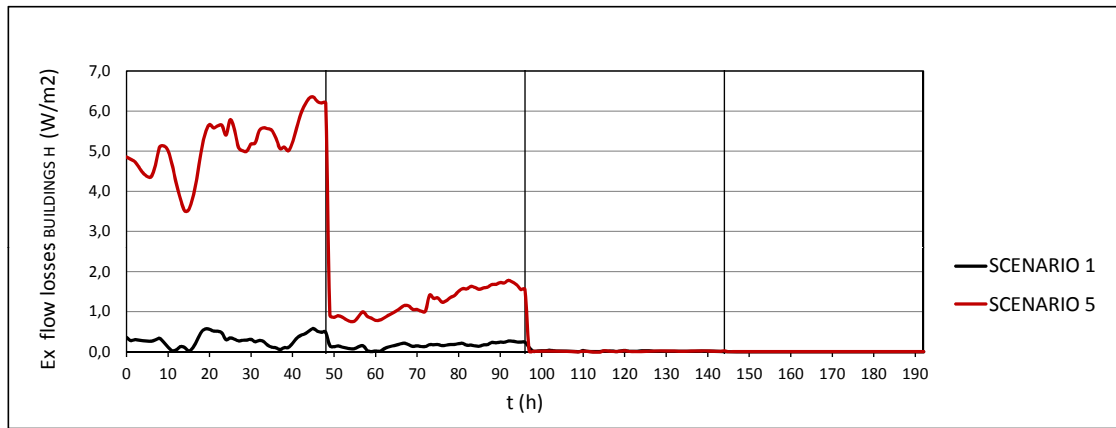
Figure 6.84: Exergy flow losses for all buildings, heating branch. Comparison scenarios 1 and 5
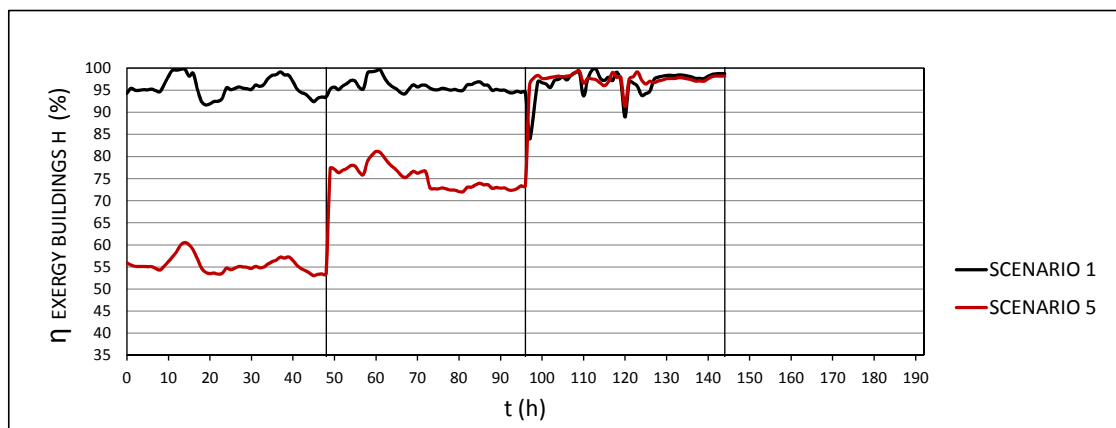
Figure 6.85: Exergy efficiency for all buildings, heating branch. Comparison scenarios 1 and 5

6.5.5 Scenario 6 vs scenario 1 (see section 3.3.6)

In this configuration, all buildings and networks operate in the same way as in scenario 1, generating the same results profiles (see section 6.3). Again, the heat exchangers installed inside the substation are substituted by a general heat pump, proceeding in the same way as scenario 4 (see section 6.5.3).

To analyse the consequences of this new installation, it was preferred to compare this scenario with scenario 4, since both systems have the same configuration in the substation, and therefore, the same equations.

As already stated in the model of sections 4.3.5.2 and 4.18, the general heat pump in the substation follows the same parameters for both scenarios. On the other hand, network's feed temperature (T_{DH2}) is higher in scenario 6 than in scenario 4, which increases the exigency of the device and reduces its efficiency ($COP_{REAL\ SUB}$). If the COP is low, the power consumption increases, as shown in figure 6.86.
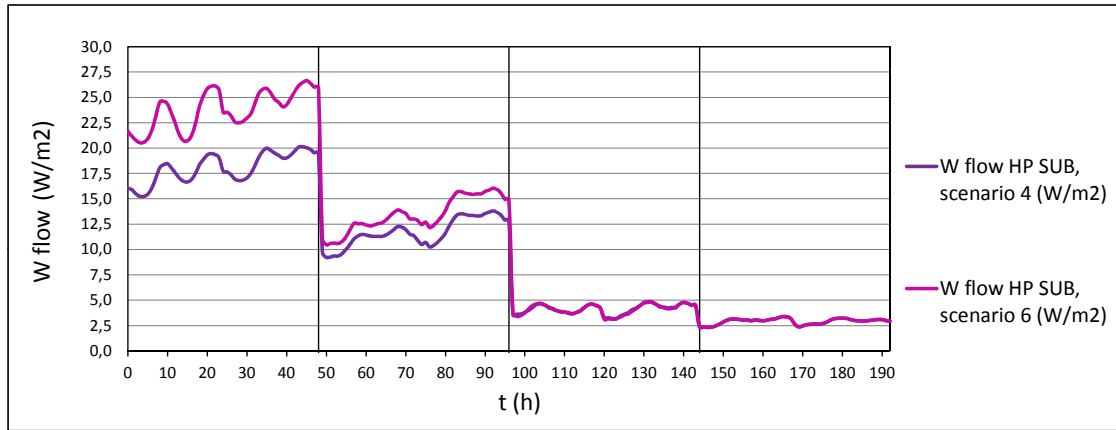
Figure 6.86: Comparison between $\dot{W}_{HP\ SUB}$ for scenarios 4 and 6

The increase of electricity consumption occurs in the two winter periods, in which T_{DH2} moves from 65 to 90°C. This temperature level is much higher than the 65°C value, which is set as a constant temperature in the temperature regulation curve of scenario 4. However, in mid-season and summer, T_{DH2} is the same for both configurations and hence $\dot{W}_{HP\ SUB}$ will be the same as well.

Therefore, comparing scenarios 6 and 4 it can be concluded that a general heat pump needs 28.57% more electricity in extreme winter and 12.7% in normal winter to provide the same heat to the same DHN system.

For the water consumption variable from where the anergy is extracted, from equation (4.116) the following expression is obtained:

$$\dot{Q}_{C\ i} = \dot{Q}_{H\ i} - \dot{W}_{HP\ HW\ i} \tag{6.2}$$

By increasing $\dot{W}_{HP\ SUB}$ with respect to scenario 4, and keeping $\dot{Q}_{H\ i}$ constant, a lower $\dot{Q}_{C\ i}$ is obtained from the balance, leading to a $\dot{m}_{AN\ SUB}$ decrease for both winter seasons (14.7% for extreme winter and 8.1 % for normal winter), as shown in figure 6.87.
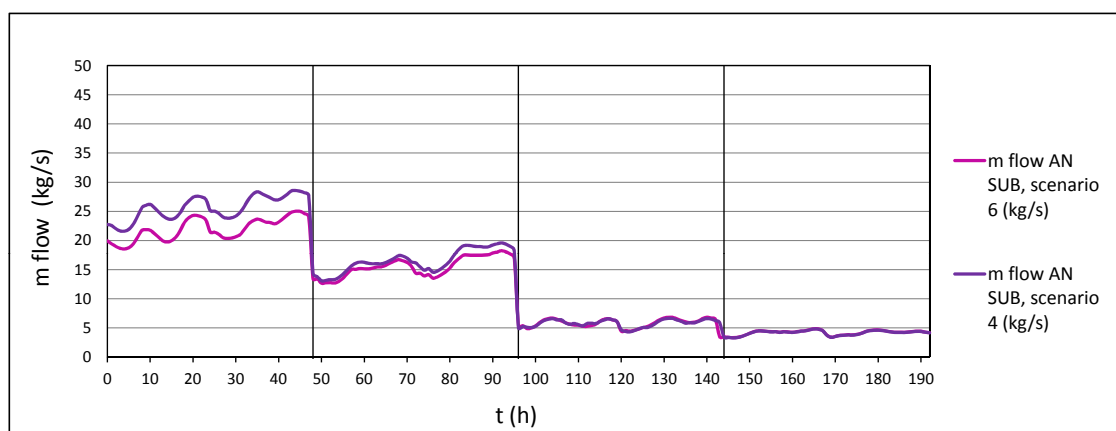
Figure 6.87: Comparison between $\dot{m}_{AN\ SUB}$ for scenarios 4 and 6

6.5.6 Scenario 7 vs scenario 1 (see section 3.3.7)

6.5.6.1 Operation variables
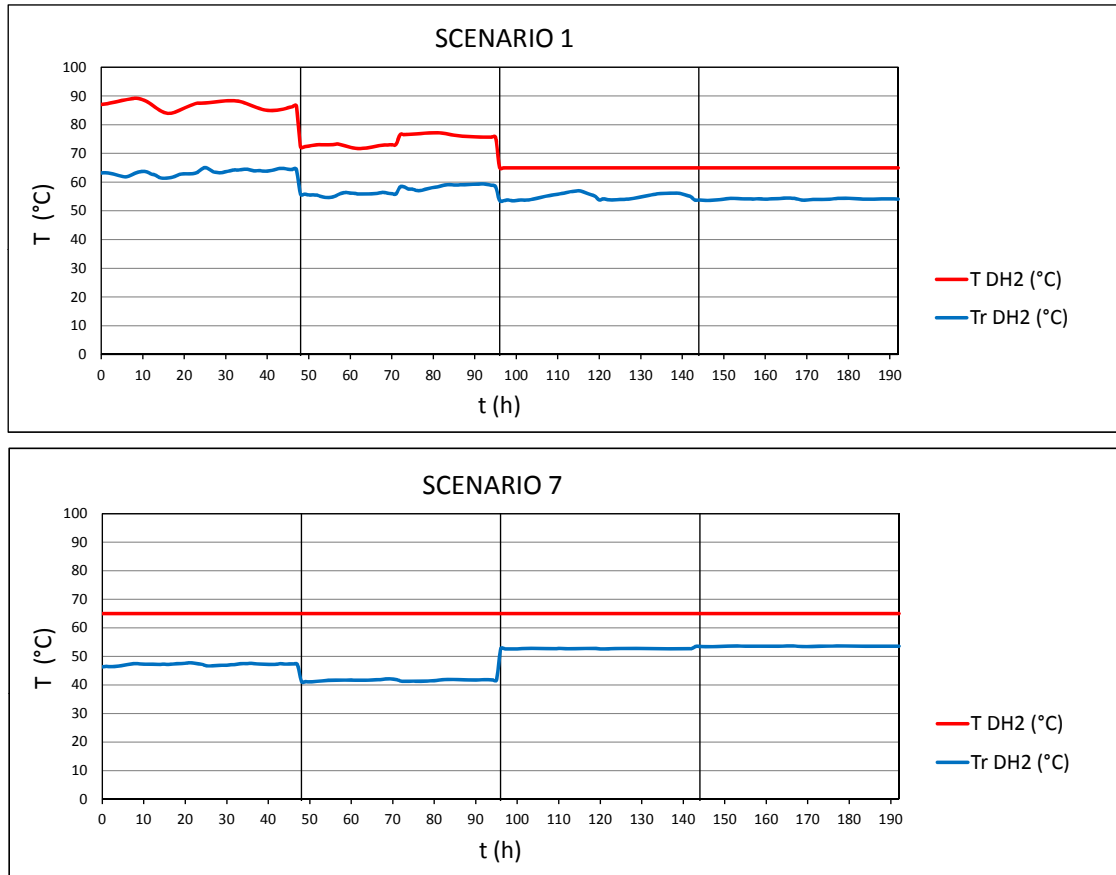
Figure 6.88: Temperatures evolution. Comparison scenarios 1 and 7
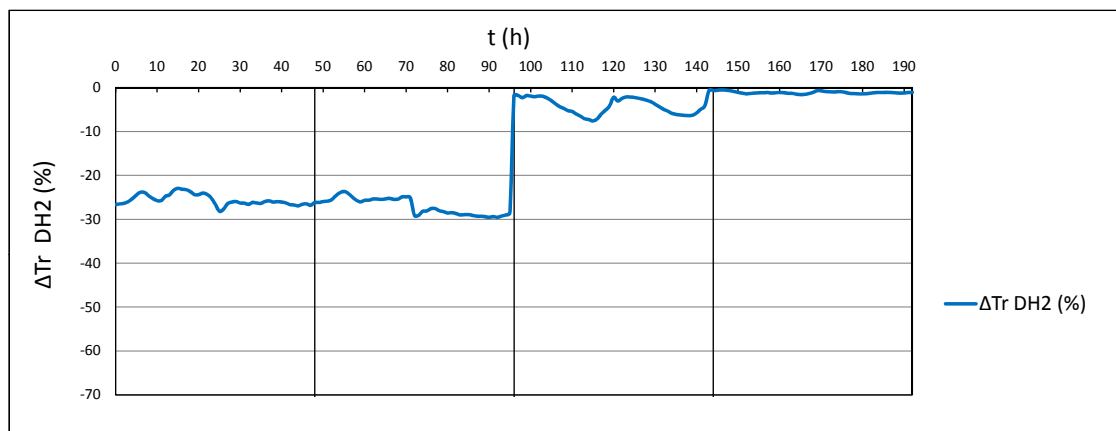
Figure 6.89: Return temperature variation respect to scenario 1

Although scenarios 4 and 6 bring the possibility of resorting to other urban energy systems different from the primary network, scenarios 7 and 8 are deepening in this direction. In scenario 7, both the

primary network and secondary networks continue there, although they are only used to feed the DHW branch inside the buildings. The heating service is provided by a reversible heat pump (see section 4.3.3.11) connected to the adapted radiant floors.

Therefore, $T_{r\ DH2}$ will be fully conditioned by the DHW branch, which will result in the temperature reduction reflected in the figure 6.88. This decrease is approx. quantified by -25% in the winter periods (figure 6.89).
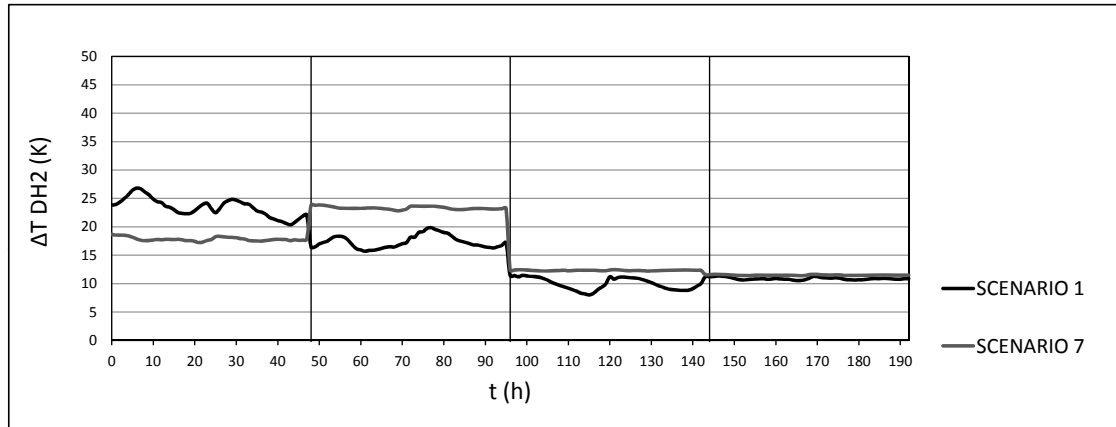
Figure 6.90: ΔT evolution. Comparison scenarios 1 and 7

In conclusion, new temperature differences will be defined, as shown in figure 6.28. The maximum increase of ΔT is observed for both normal winter seasons and mid-season periods, in a similar way to scenarios 2 and 4. However, in this case the ΔT between feed and return DH streams is not the predominant factor that influences on the mass flow, but the fact that DH is not used as a heat source for the heatings anymore. This situation will lead to a dramatic decrease of the DH water, reaching values below 20 kg/s in extreme winter and 10 kg/s in normal winter (figure 6.92).
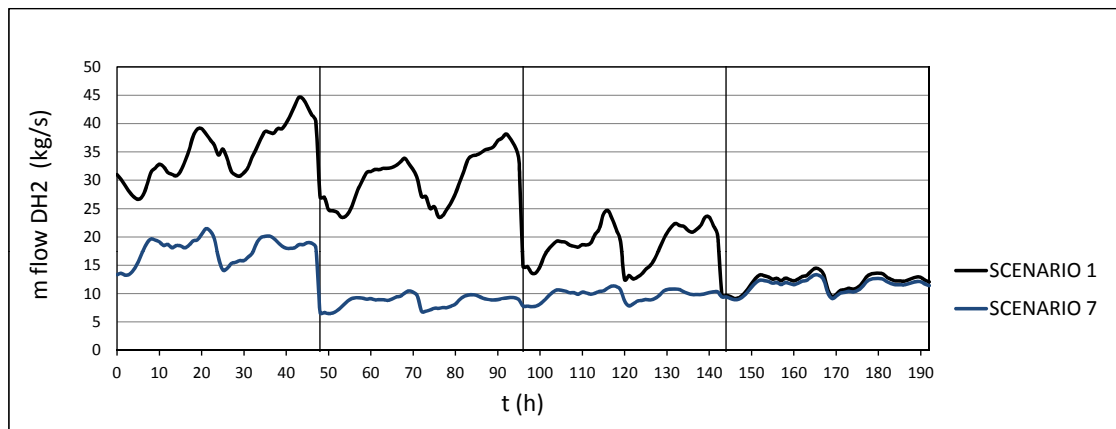
Figure 6.91: Mass flow evolution. Comparison scenarios 1 and 7
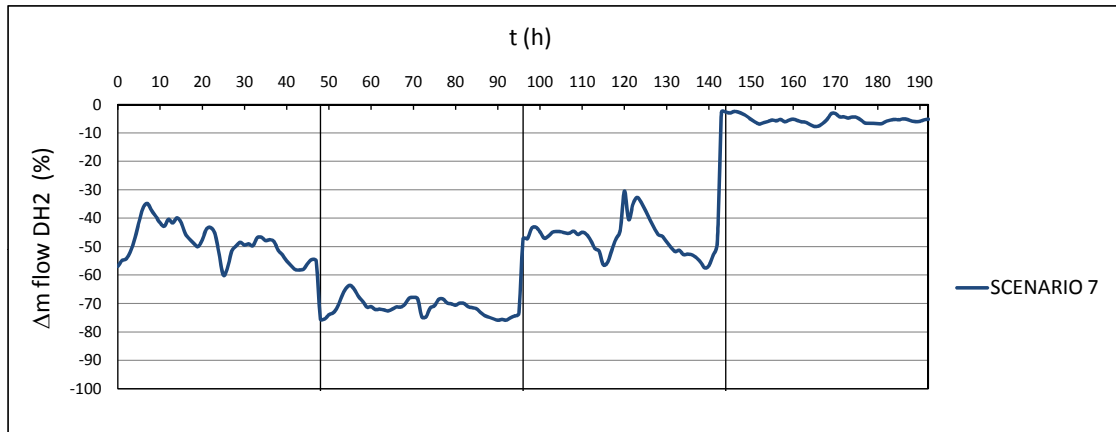
Figure 6.92: Mass flow variation respect to scenario 1

Both are the lowest obtained values from all the hypotheses investigated, resulting in a 50/60% reduction in extreme winter and more than 70% in normal winter. In mid-season this reduction is not so drastic and remains in values between -30 and -55%, due to, this time yes, a greater influence of the ΔT.
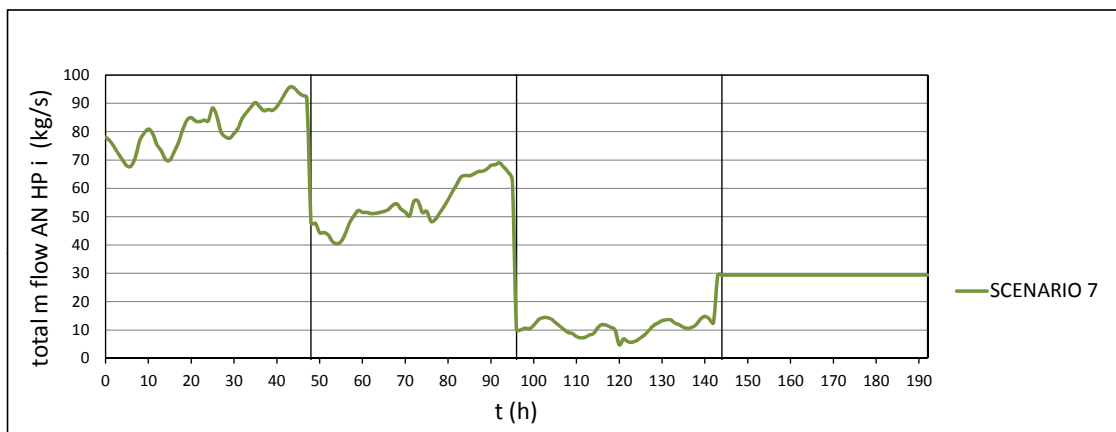
Figure 6.93: Mass flow of water supplied to the anergy network

A new variable comes into play in this scenario, the total mass flow of water used by all reversible heat pumps combined in the building set. This variable is interesting to give an idea about the dimensions that the supply network (anergy network) should have. This situation could influence a reconfiguration or transformation of the current DH networks [104].
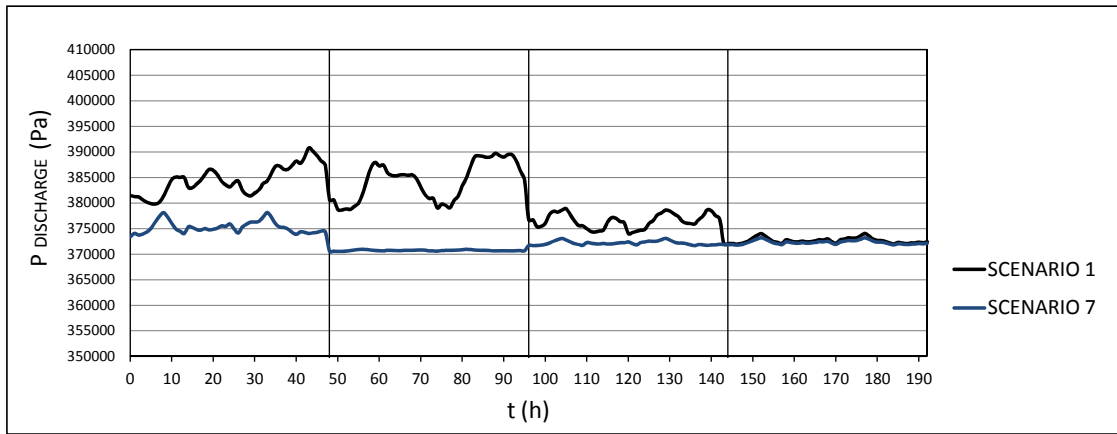
Figure 6.94: Discharge pressure evolution. Comparison scenarios 1 and 7
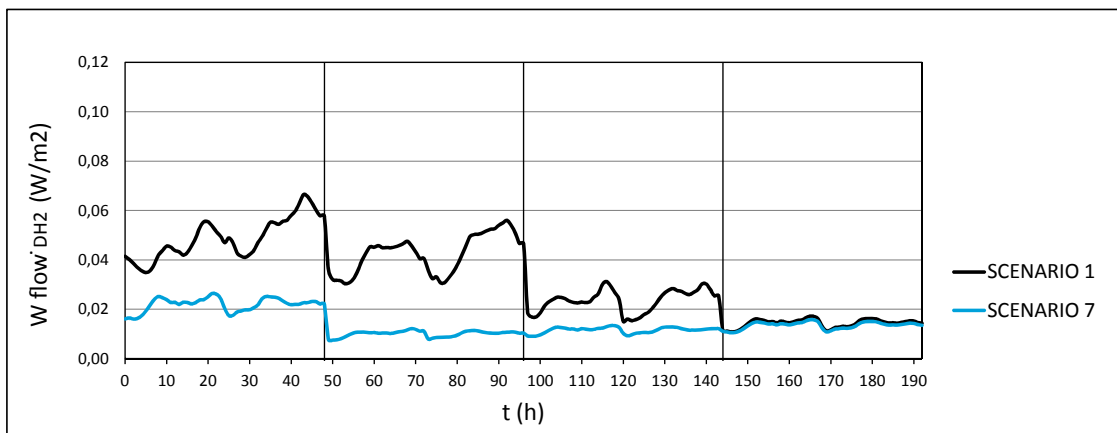
Figure 6.95: Hydraulic pump's electric consumption. Comparison scenarios 1 and 7
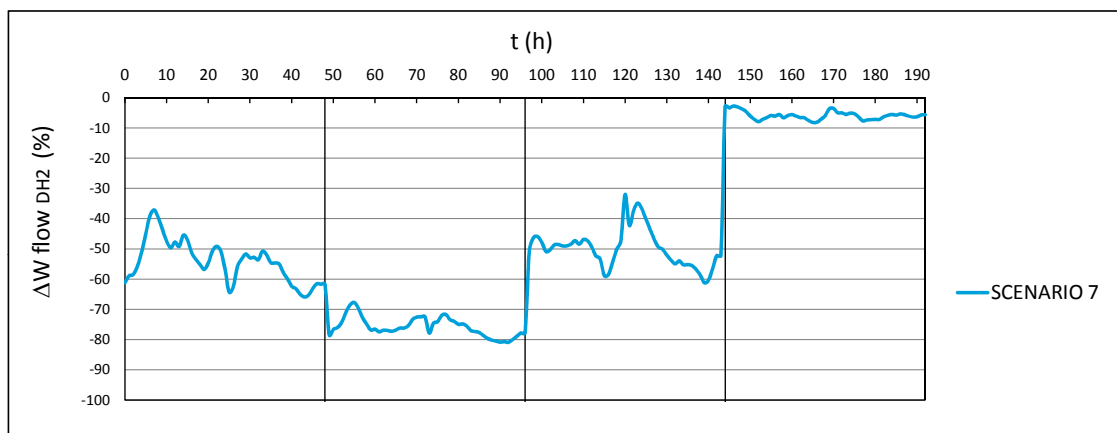
Figure 6.96: Hydraulic pump's electric consumption variation respect to scenario 1

As in the previous scenarios, the mass flow determines both the discharge pressure and the electrical consumption profiles for the hydraulic pump, reaching the minimum values of the overall data series studied. The minimum $\dot{W}_{DH2}$ value is 0.02 W/m^2 for extreme winter and 0.01 W/m^2 for

normal winter (approximate magnitudes, see figure 6.95), which entail a reduction of more than 70% in normal winter (figure 6.96).

6.5.6.2   Energy Balance

Same expressions as scenario 1, resulting in the following figures:
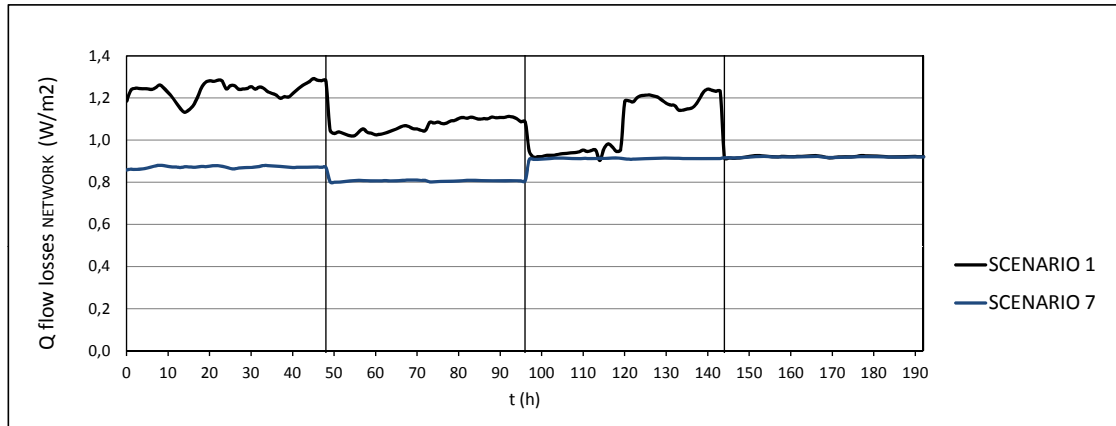
Figure 6.97: Energy flow losses along the network. Comparison scenarios 1 and 7

The sharp decrease of the DH water mass flow, and therefore the speed reduction of the fluid inside the pipes contributes to increase the energy losses of the network. On the other hand, the temperature reduction influences a decrease of these losses. Combining both opposed effects ultimately results in a net decrease to scenario 5 but not as pronounced as in scenarios 2, 3 or 4. Subsequently, reducing the temperature is predominant versus reducing the mass flow (figure 6.97).
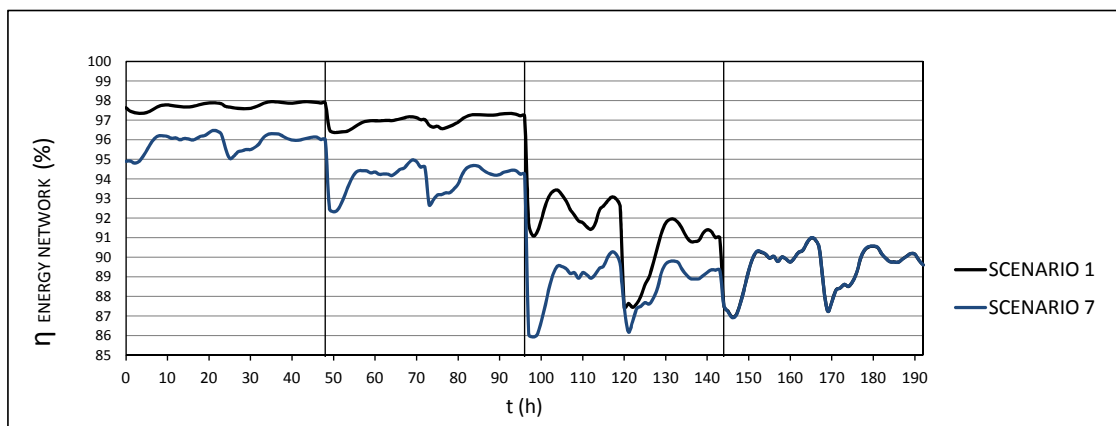
Figure 6.98: Energy efficiency along the network. Comparison scenarios 1 and 7
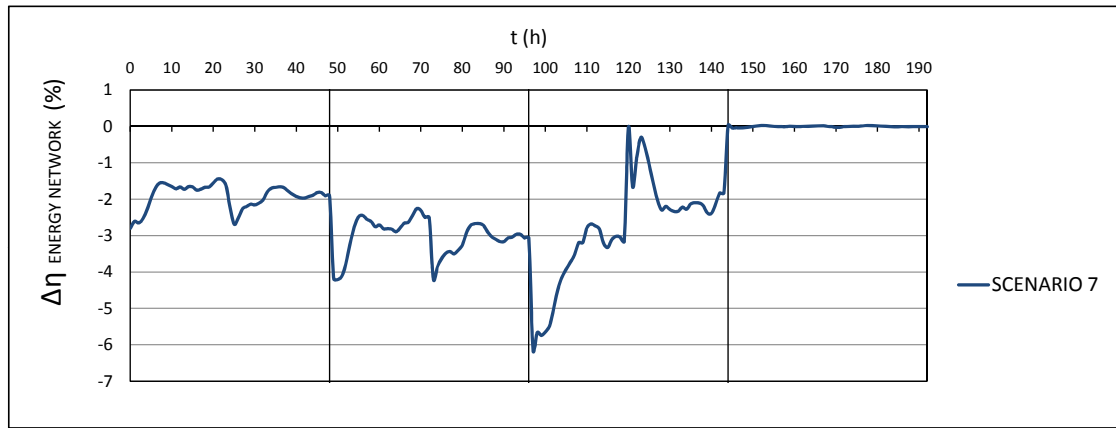
Figure 6.99: Energy efficiency variation respect to scenario 1

While it is true that the energy losses here are smaller than scenario 1, this fact does not necessarily imply an increase of the energy efficiency. The graphs 6.98 and 6.99 show how the energy efficiency drops by approximately 2 points in extreme winter, around 3/4% in normal winter and between -5 and -2% in mid-season. This is the only scenario in which the energy losses are not small enough to increase or at least maintain the energy efficiency as in scenario 1.

6.5.6.3   Exergy Balance

In this case, the following expressions are used:

- Substation: equations 4.49 and 4.50

- Network: equations 4.51 and 4.52

- Buildings: equations 4.61 and 4.62

- Buildings, DHW branch: equations 4.55 and 4.56

- Buildings, Heating branch: equations 4.65 and 4.66

For the equations 4.61, 4.62, 4.65 and 4.66, the term $\sum_i^n \dot{Ex}_{\text{DHS H } i} = 0$, because this magnitude is not supplied from the DHN any more.

All those equations can be found in section 4.2.5, obtained from figure 4.4. Results are displayed along the following graphs:
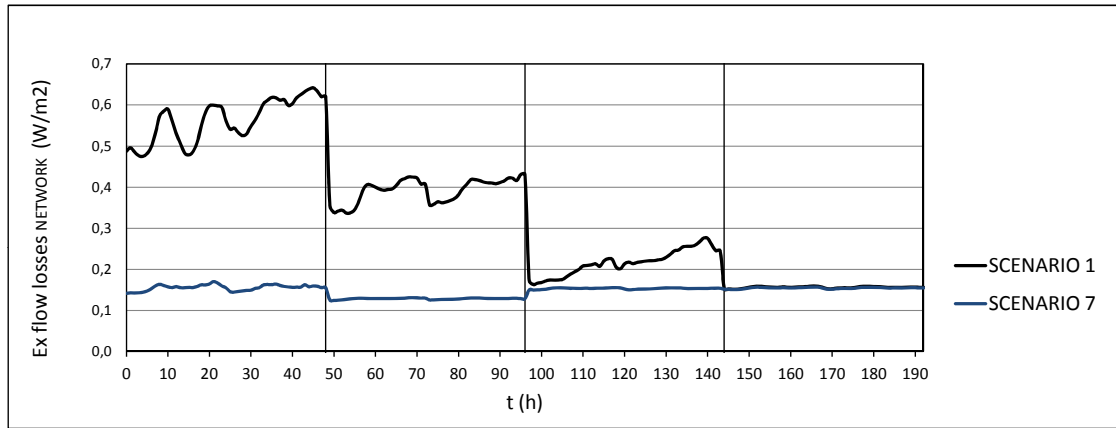
Figure 6.100: Exergy flow losses along the network. Comparison scenarios 1 and 7

The mass flow and temperature drops are reducing all exergy values in both sides of the exergy balance (equation (4.51)), also decreasing the exergy losses. Nevertheless, this situation does not necessarily imply a better performance. Figure 6.101 shows how the exergy efficiencies of scenarios 1 and 7 are very similar. Except for certain moments - normally consumption peaks - it cannot be considered any appreciable improvement.
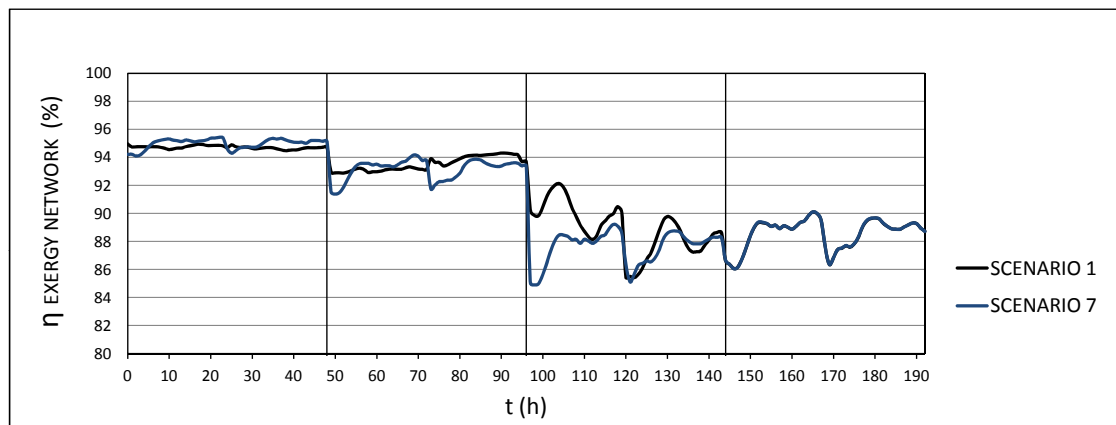
Figure 6.101: Exergy efficiency along the network. Comparison scenarios 1 and 7
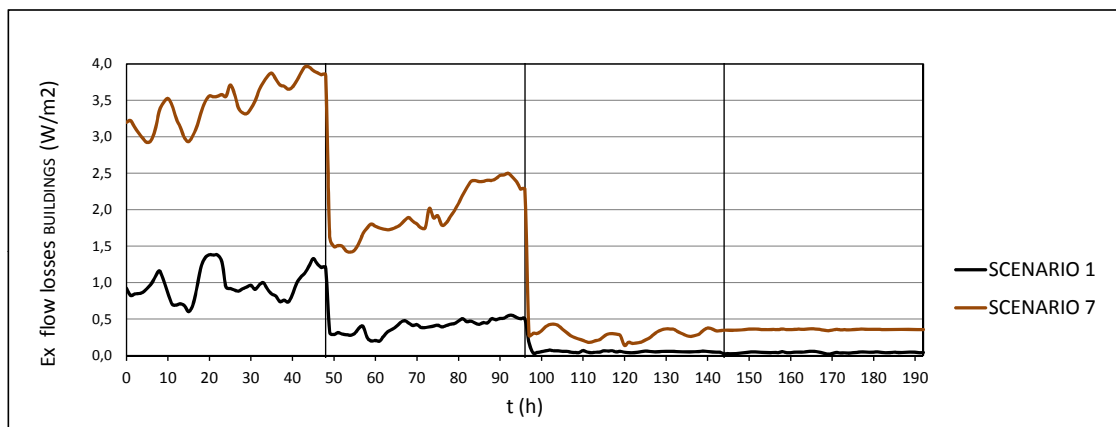
Figure 6.102: Exergy flow losses for all buildings. Comparison scenarios 1 and 7
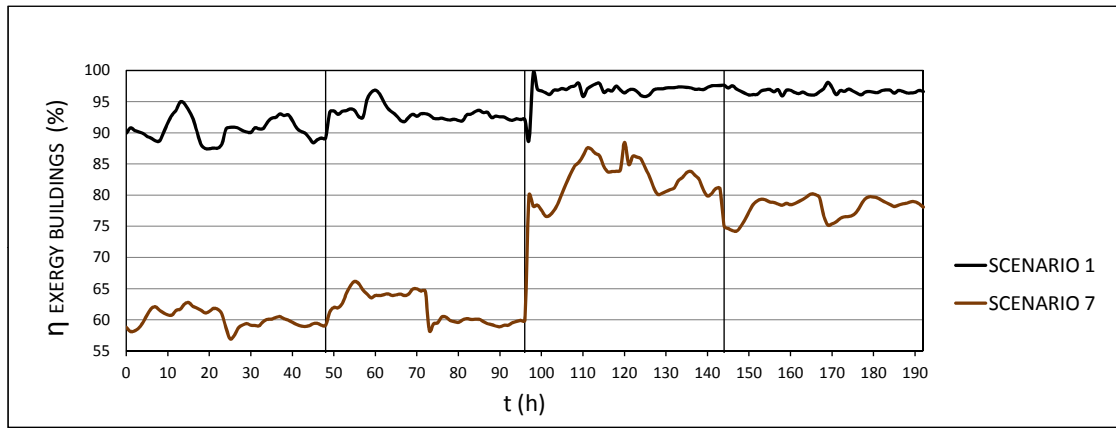
Figure 6.103: Exergy efficiency for all buildings. Comparison scenarios 1 and 7

Looking at the figure 6.102 it is possible to see how the exergy losses are again increasing dramatically. The highest increase is produced in winter periods, when the heat pumps are switched on, following a similar behaviour as scenario 5. There are also exergy losses in mid-season and summer, both associated to the heating branch, as it will be analysed later.
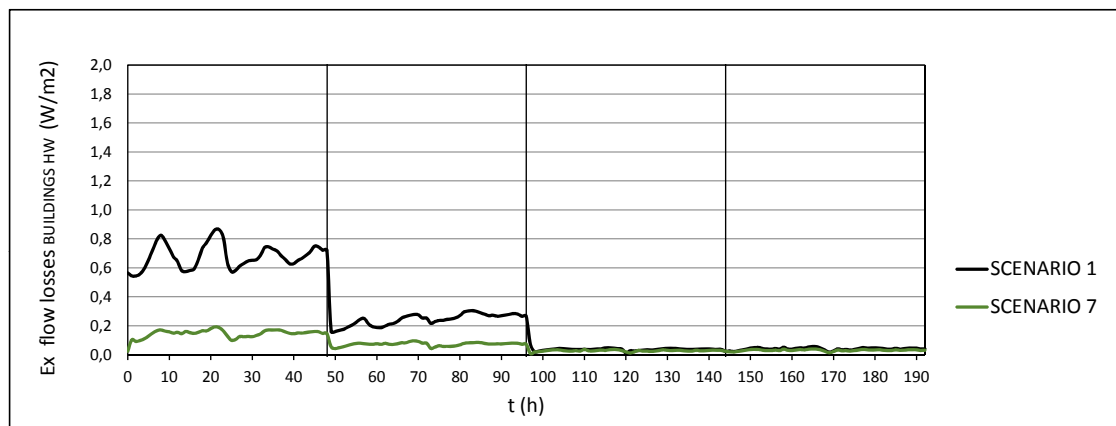
Figure 6.104: Exergy flow losses for all buildings, DHW branch. Comparison scenarios 1 and 7
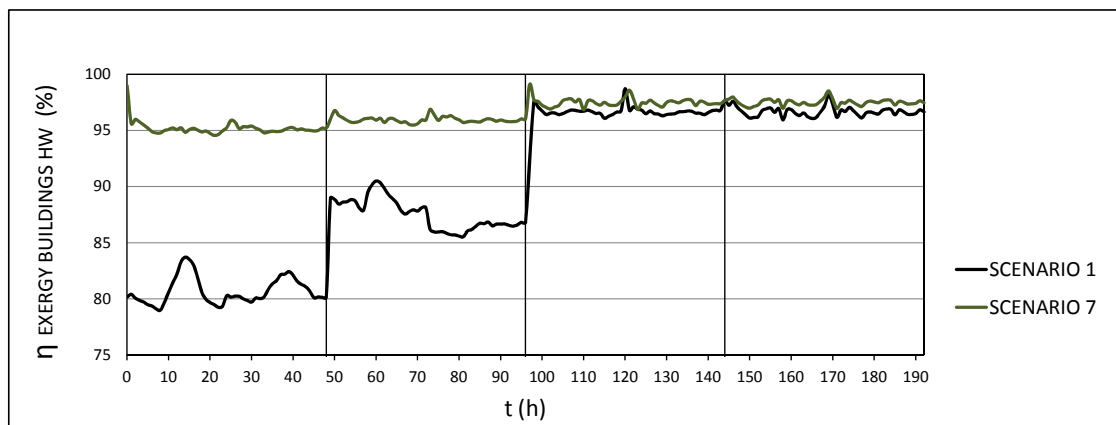
Figure 6.105: Exergy efficiency for all buildings, DHW branch. Comparison scenarios 1 and 7

In this case, the exergy efficiency (figure 6.103) moves from 90 to 60% in extreme winter, and from 93 to 65/60% in normal winter. Both drops involve a decrease of the efficiency of about 35% for both periods, respectively.

As shown in the figures 6.104 and 6.105, the DHW branch performs in the same way as scenarios 2, 4 and 5. In all those scenarios the DHW branches are operating in a very similar way, including the configuration of the branch and the temperature levels.

Ultimately, the exergy efficiency of this branch will remain high. The values will oscillate between 95% and 97% in the winter periods, and approx. 98% in mid-season and summer.

In the heating branch, the situation is somewhat similar to hypothesis 5, in which the heat pump operation determines the exergetic performance of the whole group of buildings. However, there are important differences to be considered. In scenario 5, the heat pump worked only under need, while here it works along all seasons (figure 6.106). In winter, the system heats radiant floors' water and consumes electric power. In summer, the same device cools the water by exchanging the heat directly with the anergy network water, without any power consumption (see figure 6.93).
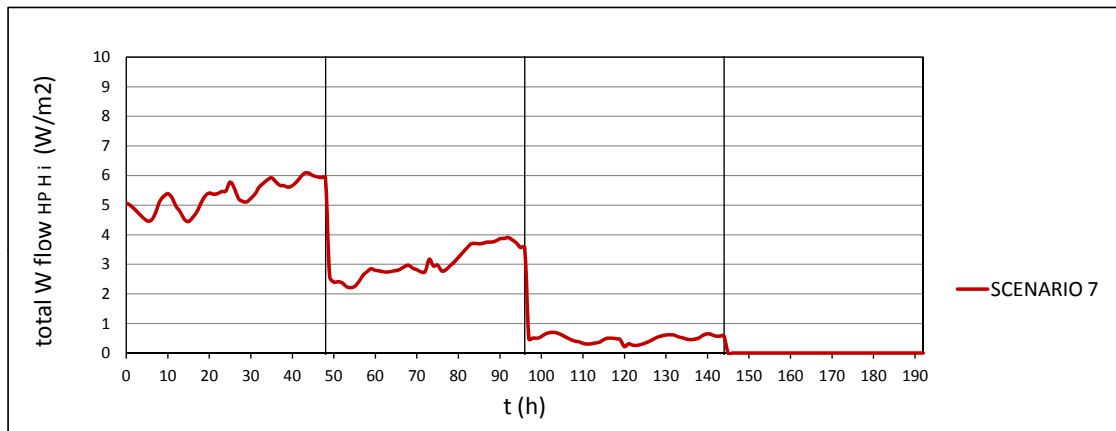
Figure 6.106: Heat pump's electric consumption, heating branch
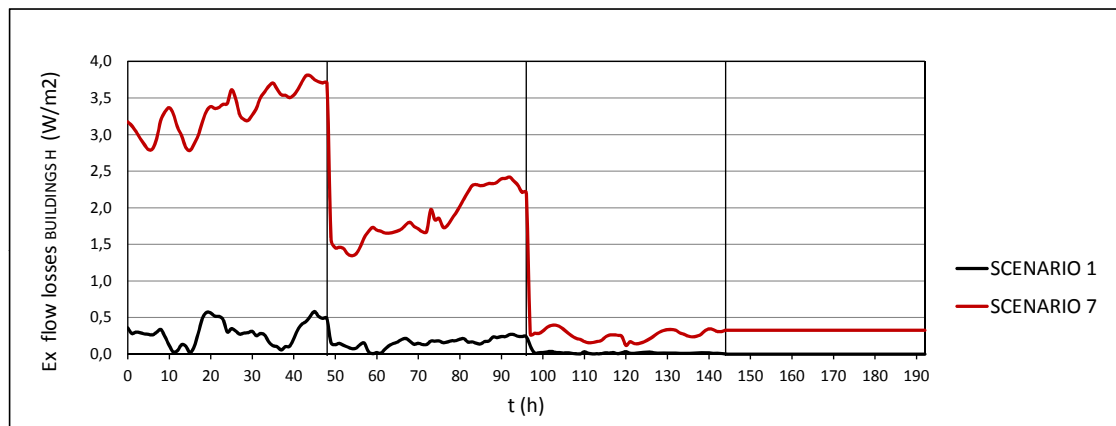
Figure 6.107: Exergy flow losses for all buildings, heating branch. Comparison scenarios 1 and 7
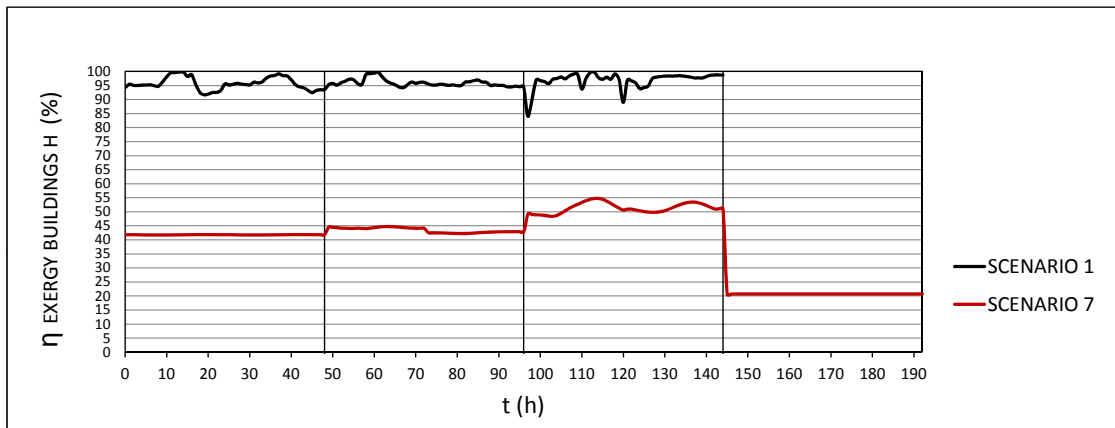
Figure 6.108: Exergy efficiency for all buildings, heating branch. Comparison scenarios 1 and 7

As a comment to the figure 6.106, it is interesting to note how the electric power consumption is not excessively high, especially if we compare it with the consumption of figure 6.83. The explanation lies in the low temperature levels at which the heat pump has to work (generally from 25 to 35°C, radiant floor's temperatures), compared to those in scenario 5 (approx from 65 to 90°C, radiator's temperatures).

In such a way, the exergy balance defined in the figure 6.107 shows values from the hour 144 onwards (beginning of summer). This is a constant value because the cooling demand ($\dot{Q}_{CD\,i}$), the inlet ($T_{CS\,C}$) and the outlet temperatures ($T_{r\,CS\,C}$) have been estimated constant for this period as well. In conclusion, there will be also exergy efficiency values, although those values will not be so high (see figure 6.108).

6.5.7   Scenario 8 vs scenario 1 (see section 3.3.8)

The main feature that rules this configuration is that the DHN has been completely removed from the system. Both branches - DHW and heating - are powered by heat pumps. Therefore, the power grid and the anergy network are the only option to keep these systems in operation.
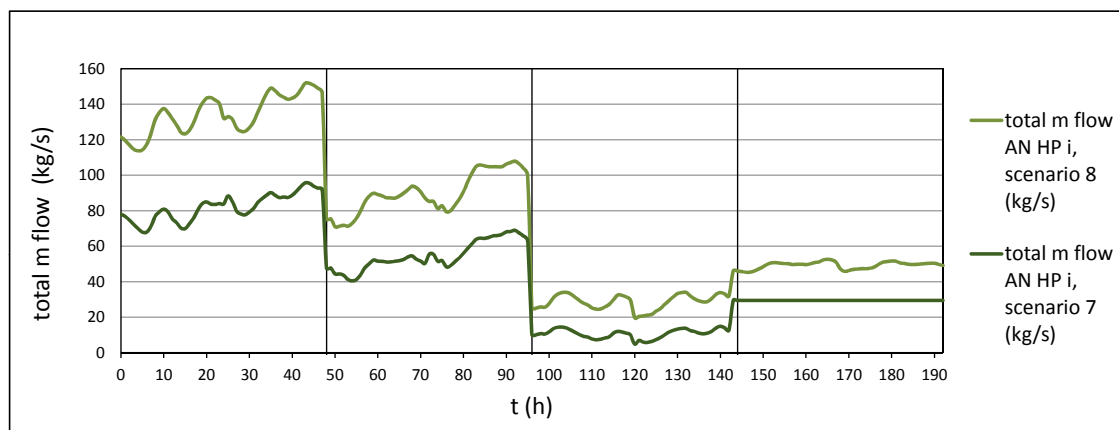
Figure 6.109: Mass flow of water supplied to the anergy network

The heat pumps are the only heat suppliers from both branches, forcing a greater anergy flow to be extracted from the anergy source. That means a higher water mass flow in comparison with the previous scenario. As shown in figure 6.109, approximately between 40 and 55 kg/s have to be used in extreme winter, between 35 and 30 kg/s for normal winter, and approximately 10 kg/s during mid-season and summer periods. These values are respectively implying an increase of 50, 66, 142 and 70 % compared with scenario 7.

6.5.7.1   Exergy Balance

Here, the following expressions are used:

- Buildings: equations 4.61 and 4.62

- Buildings, DHW branch: equations 4.63 and 4.64

- Buildings, Heating branch: equations 4.65 and 4.66

After removing the DHN, the exergy flow is not supplied any more from that source. Hence, for all these equations, the terms $\sum_i^n \dot{Ex}_{DHS\ HW\ i}$ and $\sum_i^n \dot{Ex}_{DHS\ HW\ i}$ are equal to zero.

All those equations can be found in section 4.2.5, obtained from figure 4.4. Results are displayed along the following graphs:
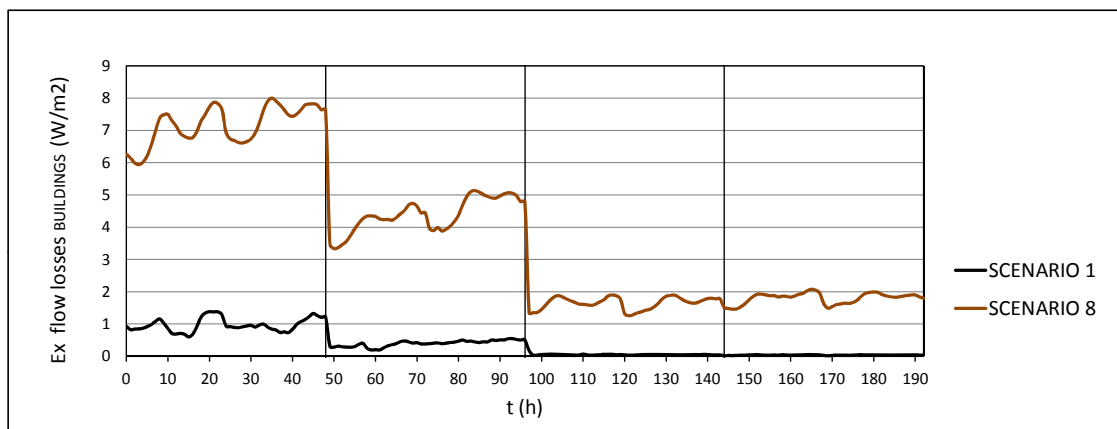
Figure 6.110: Exergy flow losses for all buildings. Comparison scenarios 1 and 8

Instead of one, this time there are two heat pump devices operating inside each building, resulting in an increase in the exergy losses of approximately 100 % for all the period (Figure 6.110). The exergy performance falls again, leading to smaller values that do not reach the 43 % in winter and summer periods, as well as 46 % in mid-season (Figure 6.111). These values are significantly lower than those in scenario 7, demonstrating again how the installation of heat pumps into the system influences negatively on the exergy efficiency, as it has been referred previously.
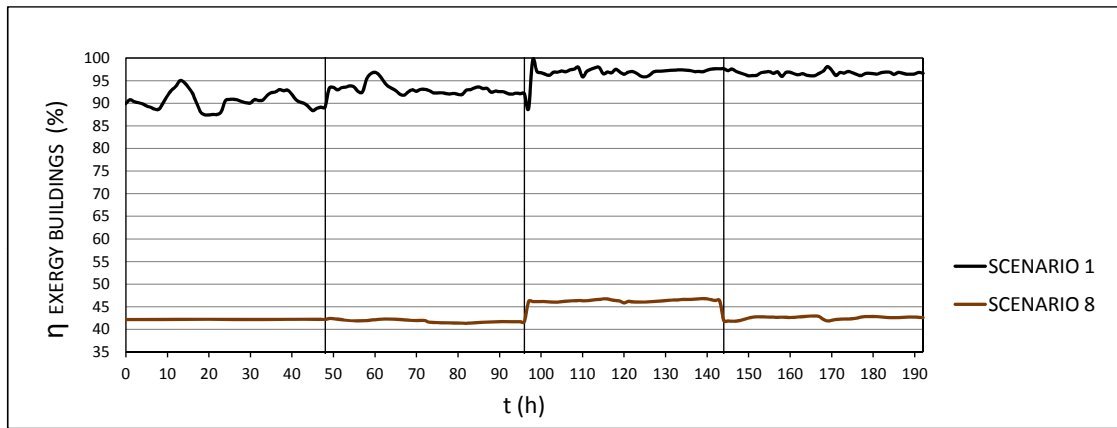
Figure 6.111: Exergy efficiency for all buildings. Comparison scenarios 1 and 8

Likewise, figure 6.112 helps to understand about how the systems are functioning in this configuration. Obviously, the heating branch works exactly in the same way as the previous scenario. However, the DHW branch's heat pump operates continuously, working accordingly to the heat demand required throughout the year.

It is observed how the range of values for the DHW production branch $\left(\sum_{i=1}^{n} \dot{W}_{HP\ HW\ i)}\right)$ is always higher than the heating branch $\left(\sum_{i=1}^{n} \dot{W}_{HP\ H\ i)}\right)$, which is logical due to the higher temperature level required for the DHW branch in comparison with the heating branch.

Ultimately, these calculations are showing us how the power consumption is an affordable magnitude, in comparison with the high anergy network's mass flow. This is the controlling factor for the viability of this hypothesis.
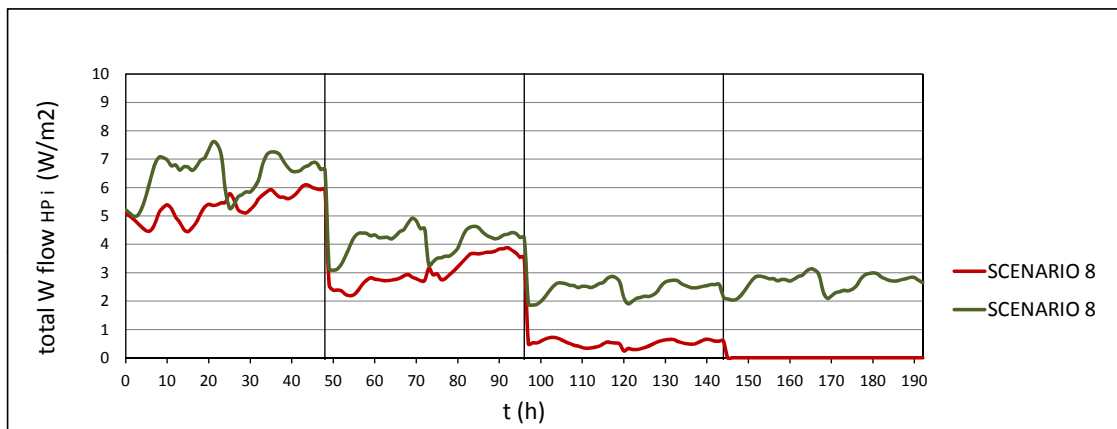
Figure 6.112: Heat pump's electric consumption, heating and DHW branches

The power supplied to the new added heat pump generates a considerable increase of the exergy losses of the DHW production branch (Figure 6.113), which influences a strong decrease of the exergy performance. These new exergy efficiency values oscillate between 40 and 45 % for the entire period studied (Figure 6.114). On the other side, the heating branch performs in the same way as scenario 7.
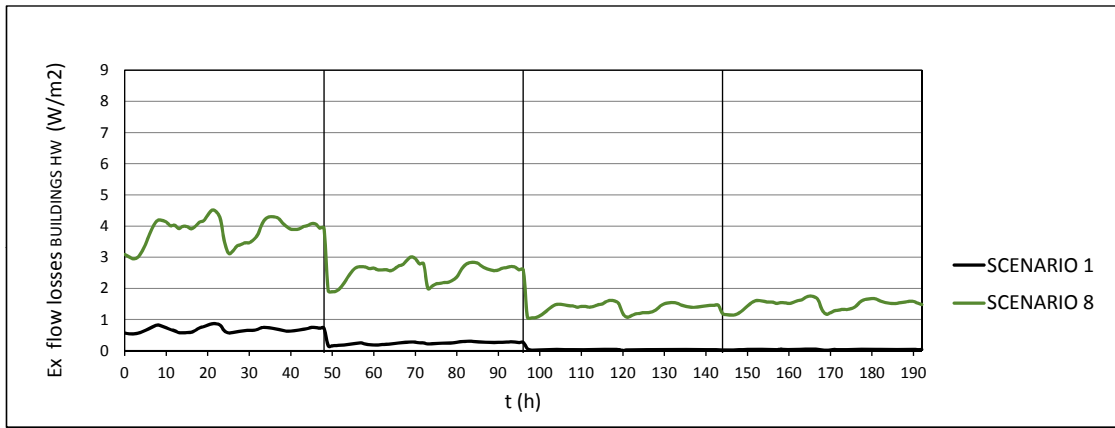
Figure 6.113: Exergy flow losses for all buildings, DHW branch. Comparison scenarios 1 and 8
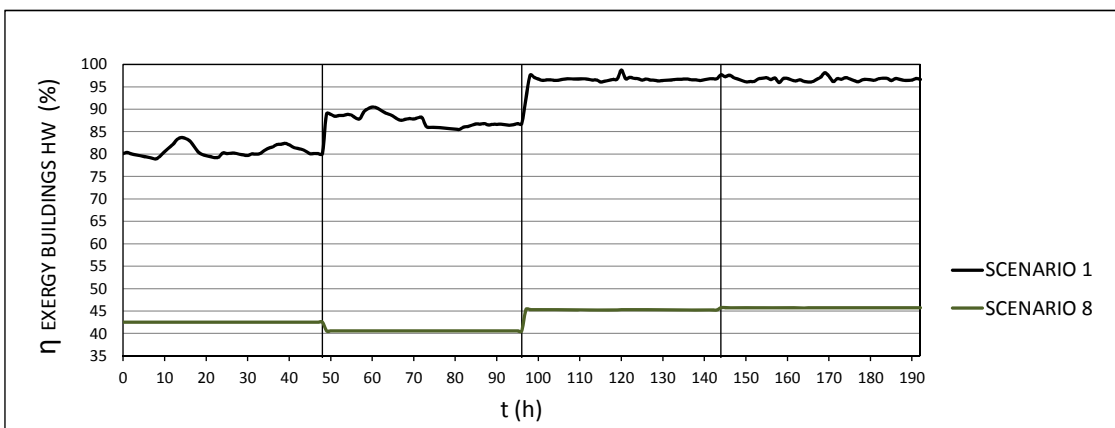
Figure 6.114: Exergy efficiency for all buildings, DHW branch. Comparison scenarios 1 and 8
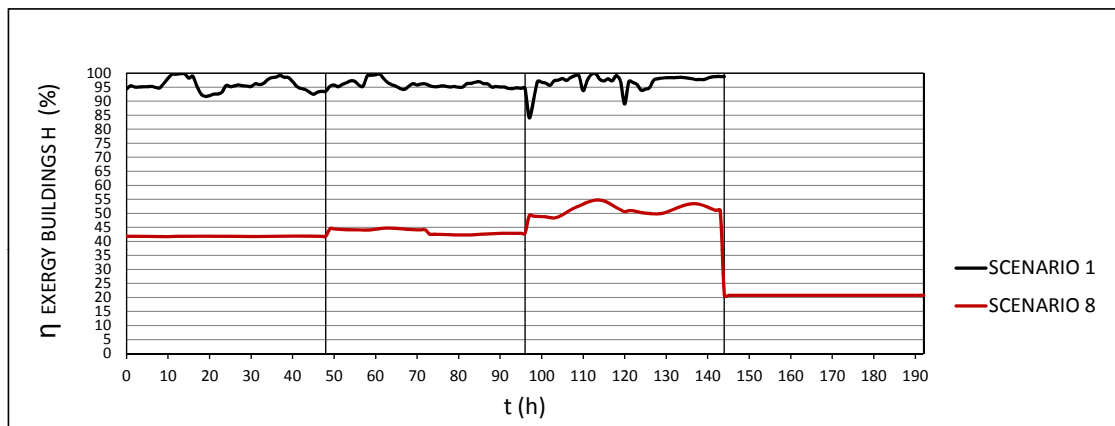
Figure 6.115: Exergy efficiency for all buildings, heating branch. Comparison scenarios 1 and 8

6.6   Discussion

A comparative overview for each of the 8 scenarios regarding to scenario 1 is shown below. All variables chosen correspond to the coldest hour of the year, in which the value of external temperature is minimum ($t = 6h \rightarrow T_{ext} = -12.31°C$). This is the chosen value, since it is considered as the most exigent moment for the network, and therefore, it will be used to elaborate the following diagrams and analysis.

The radar graphs are used along this section, in order to easily visualize multivariate data in a two-dimensional chart. All numbers represented there are normalized values extracted from several of the previous profiles. Fixed costs values are qualitatively assigned to each scenario using a scale from 0 to 7, with 0 as the current situation and 7 the situation associated to a higher fixed costs (installing, replacing or removing equipments, public works, etc).
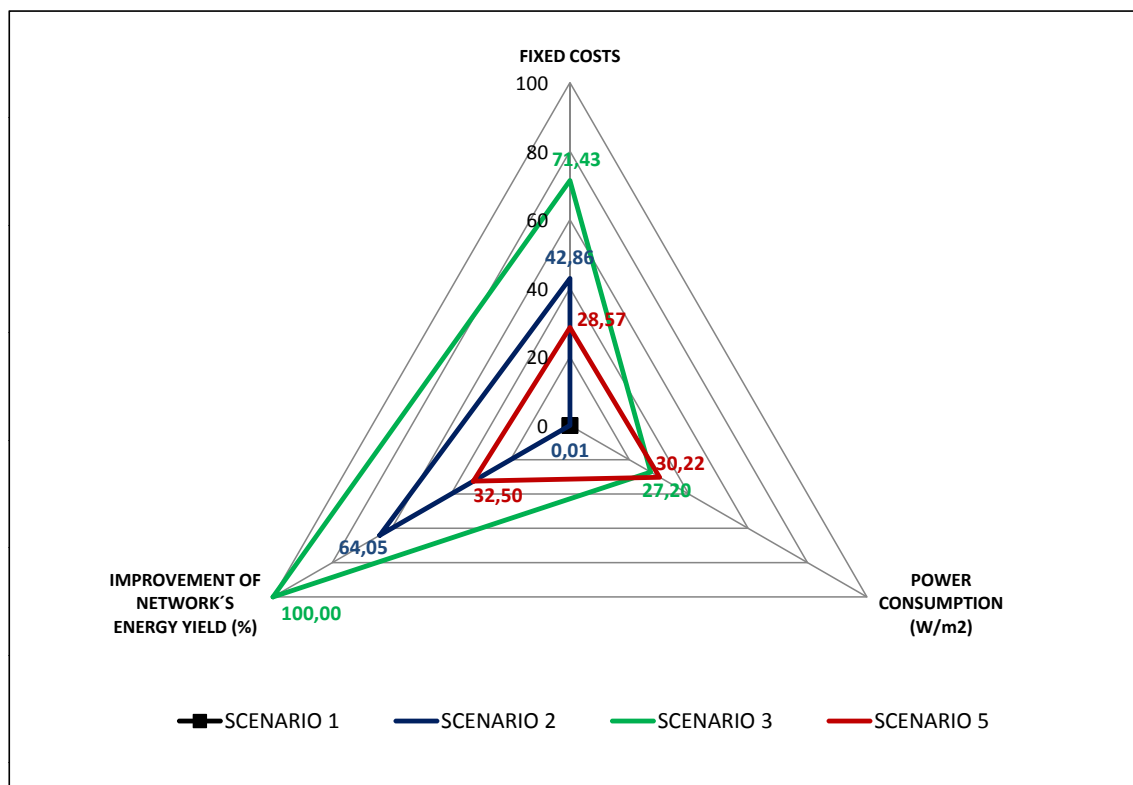
Figure 6.116: Radar chart comparison between scenarios 1, 2, 3 and 5

The figure 6.116 shows a gradual optimization of the current thermal network towards the minimum possible temperature level and involving the installation of the new technologies available: heated floors and heat pumps.

Replacing radiators by heated floors contributes to reduce the temperature levels, decreasing the energy and exergy losses through the network, and therefore, increasing the efficiency.

Adding heat pumps to the system allows the introduction of electricity into the heating sector, diversifying to other possible (renewable) energy sources. Among other aspects, exergy balances warn and inform about the power consumption and all possible inefficiencies produced by the heat

pumps. Even so, these devices are the best possible option to feed the thermal network using Power to Heat technology.

If the only purpose is decreasing and stabilizing network's temperature without the costs associated to the heat pumps, scenario 2 is a good option. Together with scenario 4, it is the second best option in terms of network's energy efficiency. The counterpart is the replacement of radiators and the execution of works inside the buildings in order to install the radiant floors.

It can be affirmed that scenario 3 is the natural evolution of scenario 2, and it is revealed as the best hypothesis for the energy savings and the energy efficiency as was documented in previous works [97] [96]. In addition, this option brings the highest exergy efficiency at network level and contemplates the adaptation of the current Viennese DHN to a LTDHN as a real possibility, advancing towards the fourth generation of DH networks [2].

However, this configuration implies high fixed costs associated with the elimination of radiators, the adaptation of buildings, the subsequent installation of radiant floor systems and the installation of heat pumps connected to the DHN. In addition, there are other operational costs associated with the electrical energy consumption (pure exergy), resulting in a significant decrease of the exergetic performance at building level.

Scenario 5 still allows the reduction of network's temperature and entails an electricity consumption similar to scenario 3. In this case, fixed costs much lower than scenarios 2 and 3, keeping radiators in place and saving considerable refurbishment works inside the buildings. However, the energy efficiency improvement obtained here is approx. a third compared to the previous scenarios.
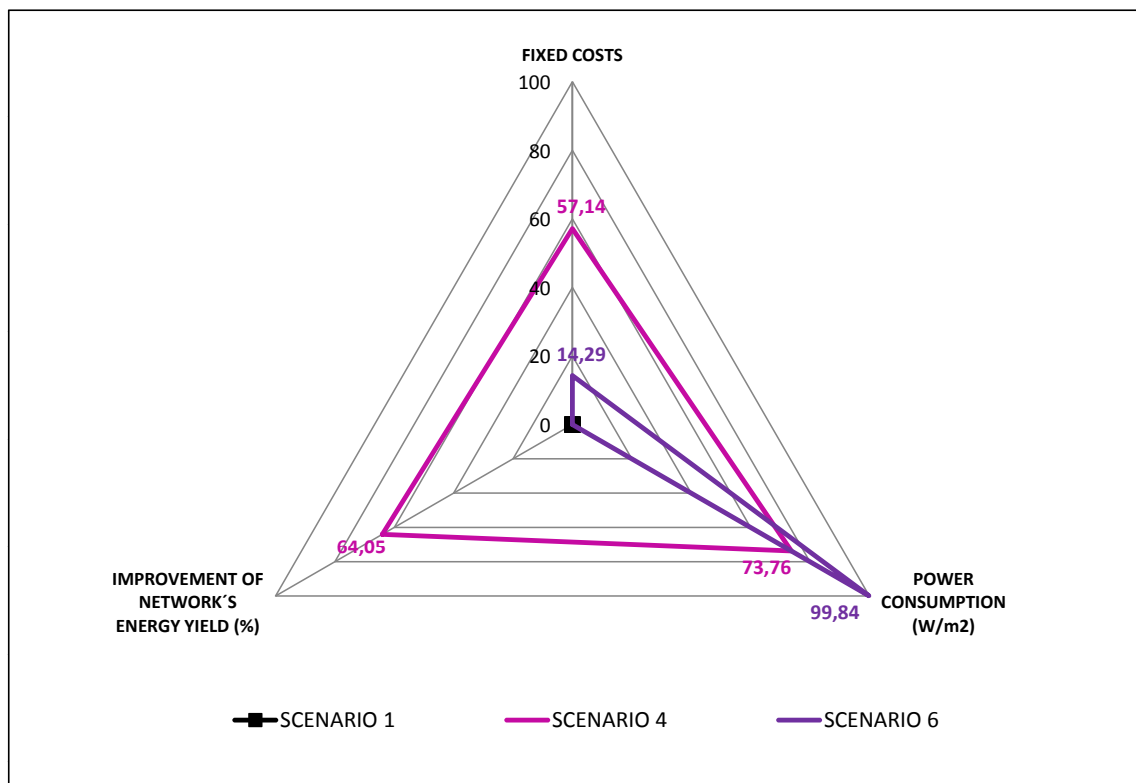
Figure 6.117: Radar chart comparison between scenarios 1, 4 and 6

Both scenarios 4 and 6 use central heat pumps in the substation without any heat extraction from

any primary network. These options are especially useful for urban areas located far away from the principal thermal network, and they would also be valuable in those cases in which industrial effluents or wastewater are available to be used by the general heat pump as an anergy source, which is still thermally viable (25/30 °C). Thereby, they work as an energetic link between industrial and urban areas.

Scenario 6 is even more feasible since it does not require any refurbishment or installation work inside the buildings, allowing the radiators to remain. Therefore, this option would be the cheapest in terms of fixed and installation costs.

The main disadvantage are the high power consumptions attached to the general heat pumps. As shown in the figure 6.117, these 2 configurations are the largest power consumers among all the scenarios studied. In consequence, it is possible here to do without the thermal network, but not without a reliable electrical network able to guarantee a continuous power supply.
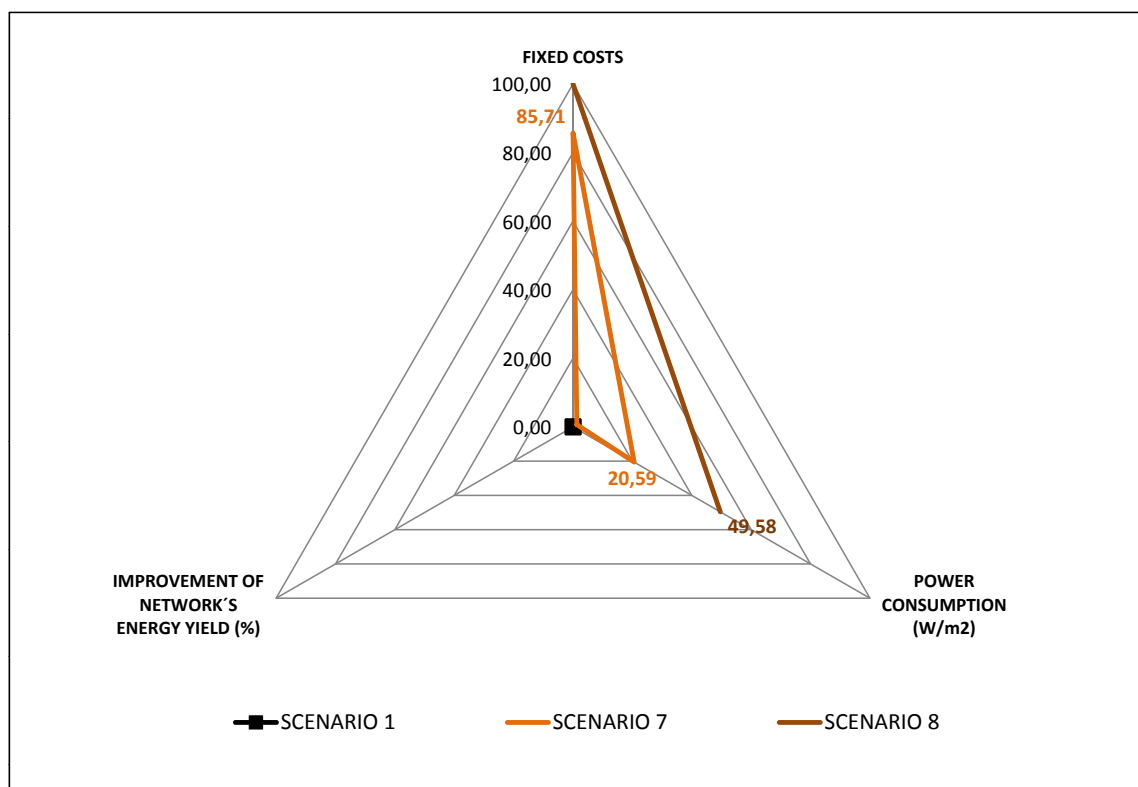
Figure 6.118: Radar chart comparison between scenarios 1, 7 and 8

Scenario 7 is the typical case in which the heating systems are located in a decentralised way, but, at the same time, a connection to the DHN must be available. In contrast, scenario 8 no longer has a network; only a hydraulic network remains at moderate or ambient temperature, providing anergy to the individual heat pumps installed in the buildings. The consequence would be a total reconversion of the system, moving into an anergy network [104], advancing towards the fifth generation of DH networks.

Both configurations generate the highest fixed costs among all the scenarios studied. These costs are generated by the installation of radiant floors, the installation of individual heat pumps and, in addition, the construction of the anergy network.

Chapter 7

Conclusions

This research work is based, first of all, on the development of a representative model of a part of the Viennese district heating network and a simulator capable to integrate all these models and use them to predict and calculate the different variables associated to this network. This model can be used not only for the current situation but also for other possible hypotheses that lead to transformations either in the substation, in the network or inside the buildings.

The followed work methodology has been useful to organize the large amount of initial data and information, classify the necessary parameters, define the different thermodynamic systems, raise and feed the physical and mathematical models, and finally run the simulation. The simulator worked correctly and without failures for the 8 studied scenarios, being able to resolve with acceptable accuracy all pressure, mass, energy, and exergy balances. The obtained results are considered realistic and coherent.

The second main goal is the thermodynamic analysis of the 8 purposed configurations. This objective has been achieved successfully as well. The product of this work is expected to be used as a help or reference for urban planners, technicians, and decision makers concerning all possible actions that might increase the efficiency of the thermal networks, in combination with urban energy systems.

Thirdly, although this is a detailed study and focuses on a small local network, all the models and the simulator have been designed to work also for networks with a greater number of buildings or even superior networks. It would also be possible to simulate the primary network as a link between several secondary networks, or even create new models associated with other systems, such as electrical networks, renewable energy generation systems, or thermal plants themselves. The block methodology and the association Matlab-Simulink are flexible enough to allow all these possibilities.

Finally, serves this project as a first step that may lead in the future to an extension, or even other similar projects, with the final goal of improving the energy and exergy efficiency of the urban energy systems.

<div align="right">Ing. Mario Potente Prieto</div>

Appendix A

Tables of buildings and pipes

Buildings					
Name	Id.	Type	Services	History (∗)	HS with DH (m^2)
GA	104	Primary, last building	H/HW	12.12.1994	8320
GB	98	Primary	H	22.09.1994	704
GC	74	Primary	H/HW	22.07.1994	883.11
GD	86	Primary	H/HW	21.06.1994	1239.56
GD1		Secondary of 86	H/HW	19.07.1994	2440.21
GD2		Secondary of 86	H/HW	12.09.1994	6693.99
GE	68	Primary	H/HW	09.06.1994	1505.19
GF	92	Primary	H/HW	27.06.1994	3330.99
GF1		Secondary of 92	H/HW	04.07.1994	3335.42
GG	62	Primary	H/HW	19.07.1994	1203.75
GH	80	Primary	H/HW	09.06.1994	2597.72
GI	32	Primary	H/HW	31.08.1992	7808.45
GI_1		Slave of 32	H/HW	31.08.1992	
GI_2		Slave of 32	H/HW	31.08.1992	
GI_3		Slave of 32	H/HW	31.08.1992	
GJ	26	Primary	H/HW	31.08.1992	1699.84
GJ_1		Slave of 26	H/HW	31.08.1992	
GK	14	Primary	H/HW	31.08.1992	3033.82
GL	50	Primary	H/HW	31.08.1992	2871.58
GM	44	Primary	H/HW	31.08.1992	1651.30
GM1	38	Primary	H/HW	31.08.1992	2716.69
GM2	56	Primary	H/HW	13.09.1993	2568.75
GN	20	Primary	H/HW	31.08.1992	3691.04
GN1	8	Primary	H/HW	31.08.1992	2575.18
GN2	2	Primary	H/HW	31.08.1992	1086.94
GN2_1		Slave of 2	H/HW	31.08.1992	

Table A.1: Table of Buildings. Id = Identification (∗) Start-up of the measuring devices of the District Heating system in the building, THS with DH = Total Heating Surface by District Heating

Pipes				
Id.	Type	ND (mm)	L (m)	Observations
PH		NDA	NDA	Primary Network, feed line
PC		NDA	NDA	Primary Network, return line
FBC	Main	250	Neg.	Secondary Network
FH	Main	250	Neg.	Secondary Network, feed line
FC	Main	250	Neg.	Secondary Network, return line
1H	Lateral	80	6.18	
1C	Lateral	80	6.18	
2H	Lateral	100	69.56	
2C	Lateral	100	69.56	
2H_in	Lateral	100	Neg.	
2C_out	Lateral	100	Neg.	
3H	Lateral	100	28.68	
3C	Lateral	100	28.68	
4H	Lateral	80	15.75	
4C	Lateral	80	15.75	
5H	Lateral	80	20.62	
5C	Lateral	80	20.62	
6H	Lateral	65	24.44	
6C	Lateral	65	24.44	
7H	Lateral	125	6.09	
7C	Lateral	125	6.09	
7H_in	Lateral	125	Neg.	
7C_out	Lateral	125	Neg.	
8H	Lateral	100	28.05	
8C	Lateral	100	28.05	
9H	Lateral	80	27	
9C	Lateral	80	27	
9H_in	Lateral	80	Neg.	
9C_out	Lateral	80	Neg.	
9B_H	Lateral	NDA	NDA	
9B_C	Lateral	NDA	NDA	
10H	Lateral	65	20.83	
10C	Lateral	65	20.83	
11H	Main	250	107.84	
11C	Main	250	107.84	
12H	Lateral	125	17.82	
12C	Lateral	125	17.82	
12H_in	Lateral	125	Neg.	
12C_out	Lateral	125	Neg.	
12B_H	Lateral	NDA	NDA	
12B_C	Lateral	NDA	NDA	

Table A.2: Table of Pipes. ND = Nominal Diameter, L = Length , NDA = No Data Available, Neg. = Negligible

Pipes				
Id.	Type	ND (mm)	L (m)	Observations
12C_H	Lateral	NDA	NDA	
12C_C	Lateral	NDA	NDA	
12D_H	Lateral	NDA	NDA	
12D_C	Lateral	NDA	NDA	
12E_H	Lateral	NDA	NDA	
12E_C	Lateral	NDA	NDA	
12F_H	Lateral	NDA	NDA	
12F_C	Lateral	NDA	NDA	
13H	Lateral	80	30.3	
13C	Lateral	80	30.3	
14H	Lateral	80	17.5	
14C	Lateral	80	17.5	
14H_in	Lateral	80	Neg.	
14C_out	Lateral	80	Neg.	
14B_H	Lateral	NDA	NDA	
14B_C	Lateral	NDA	NDA	
15H	Lateral	80	28.28	
15C	Lateral	80	28.28	
16H	Main	250	153.24	
16C	Main	250	153.24	
17H	Lateral	65	16.02	
17C	Lateral	65	16.02	
18H	Main	250	21.79	
18C	Main	250	21.79	
19H	Lateral	50	13.74	
19C	Lateral	50	13.74	
20H	Main	250	13.74	
20C	Main	250	13.74	
21H	Lateral	100	7.58	
21C	Lateral	100	7.58	
21H_in	Lateral	100	Neg.	
21C_out	Lateral	100	Neg.	
21B_H	Lateral	NDA	NDA	
21B_C	Lateral	NDA	NDA	
22H	Main	250	6.9	
22C	Main	250	6.9	
23H	Lateral	65	24.54	
23C	Lateral	65	24.54	
24H	Main	200	65.36	
24C	Main	200	65.36	

Table A.3: Table of Pipes 2

Pipes				
Id.	Type	ND (mm)	L (m)	Observations
25H	Lateral	125	6.95	
25C	Lateral	125	6.95	
25H_in	Lateral	125	Neg.	
25C_out	Lateral	125	Neg.	
25B_H	Lateral	NDA	NDA	
25B_C	Lateral	NDA	NDA	
25C_H	Lateral	NDA	NDA	
25C_C	Lateral	NDA	NDA	
25D_H	Lateral	NDA	NDA	
25D_C	Lateral	NDA	NDA	
26H	Main	200	25.06	
26C	Main	200	25.06	
27H	Lateral	50	4.77	
27C	Lateral	50	4.77	
28H	Main	150	198.22	
28C	Main	150	198.22	
29H	Lateral	65	28.37	
29C	Lateral	65	28.37	
30H	Main	125	269.67	Last pipe
30C	Main	125	269.67	Last pipe

Table A.4: Table of Pipes 3

Appendix B

Calculation of pressure drop
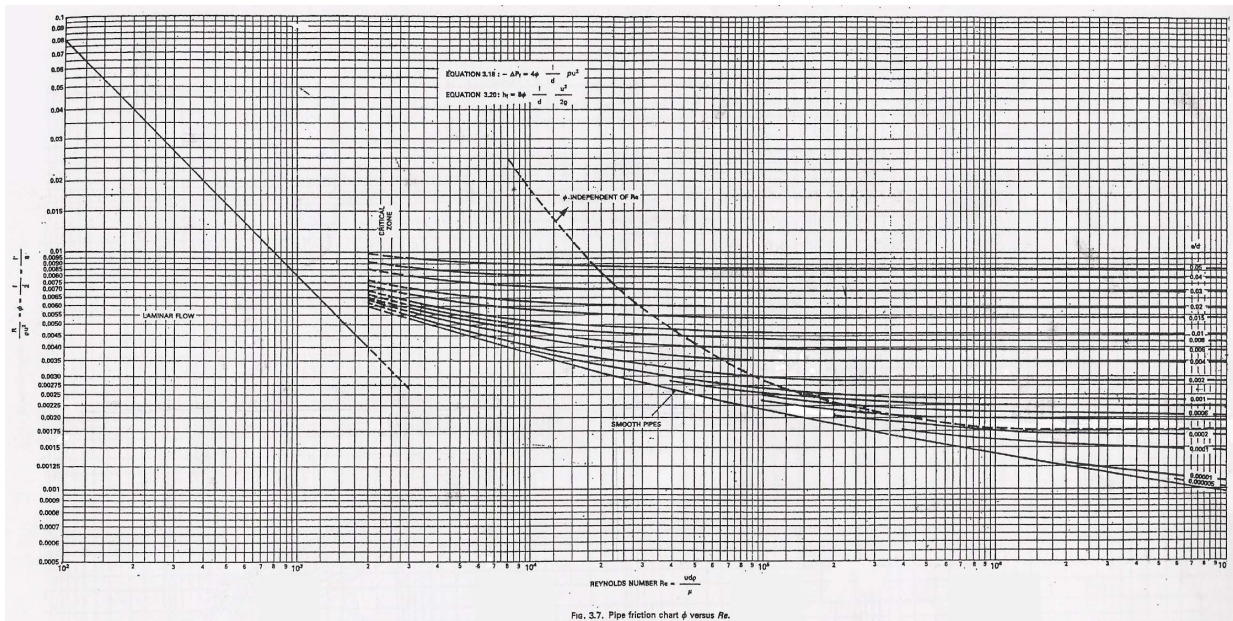
Figure B.1: Moody diagram

φ (y)	Re (x)
0.006	2000
0.00525	3000
0.0048	4000
0.0045	5500
0.0042	7000
0.00375	10000
0.0033	15000
0.0031	20000
0.0028	30000
0.0025	50000
0.0023	70000
0.00225	85000
0.00215	100000
0.002	150000
0.00175	300000
0.0016	500000
0.0015	700000
0.0014	850000
0.00135	1000000
0.0013	1500000
0.00125	2000000
0.0012	3000000
0.0011	5000000
0.00105	7000000
0.001	10000000

Table B.1: φ vs Reynolds table, obtained from Moody's diagram

List of Tables

List of Figures

Bibliography

[1] EUROPEAN COMMISSION, *Energy Roadmap 2050*. Publications Office of the European Union, Luxembourg, 2012. Available from: https://ec.europa.eu/energy/sites/ener/files/documents/2012_energy_roadmap_2050_en_0.pdf. Last time consulted, 24-09-2019.

[2] H. LUND, S. WERNER, R. WILTSHIRE, S. SVENDSEN, J. E. THORSEN, *4th Generation District Heating (4GDH) Integrating smart thermal grids into future sustainable energy systems*. Energy 68, 1-11, 2014.

[3] B. REZAIE, M.A. ROSEN, *District Heating and Cooling: Review of technology and potential enhancements*. Applied Energy 93 (2012) 2-10.

[4] P. A. TIPLER, *Modern Physics*. Worth Publishers, Inc., New York, U.S.A. (1978)

[5] M. VESTERLUND, J. SANDBERG, B. LINDBLOM, J. DAHL, *Evaluation of Losses in a District Heating System, a case study*. Proceedings of ECOS 2013 - The 26th International Conference on Efficiency, Cost, Optimization, Simulation and Environmental Impact of Energy Systems. July 16-19, 2013, Guilin, China.

[6] WIKIPEDIA: THERMAL PLANT OF CEUTA, https://es.wikipedia.org/wiki/Central_diesel_de_Ceuta. Last time consulted, 10-12-2018. (In Spanish)

[7] SPANISH GOVERMENT, MINISTRY OF ECOLOGICAL TRANSITION: THERMAL PLANT OF CEUTA, http://www.prtr-es.es. Last time consulted, 24-09-2019. (In Spanish)

[8] WIKIPEDIA: THERMAL PLANT OF VELILLA, https://es.wikipedia.org/wiki/Central_termica_de_Velilla. Last time consulted, 24-09-2019. (In Spanish)

[9] S.P. FILIPPOV, *Development of centralized district heating in Russia*. Thermal Engineering, 2009, vol. 56, nr. 12, pp 985-997.

[10] A. FICHERA, R. VOLPE, M. FRASCA, *The centralized energy supply in a network of distributed energy systems: A cost-based mathematical approach*. International Journal of Heat and Technology, vol. 35, Special Issue 1, September 2017, pp s191-s195.

[11] M. RÄMÄ, M. WAHLROOS, *Introduction of new decentralized renewable heat supply in an existing district heating system*. Energy 154 (2018) 68-79.

[12] M. VESTERLUND, A. TOFFOLO, J. DAHL, *Optimization of multi-source complex district heating network, a case study*. Energy 126 (2017), 53-63.

[13] P. A. OSTERGAARD, B. V. MATHIESEN, B. MÖLLER, H. LUND, *A renewable energy scenario for Aalborg Municipality based on low-temperature geothermal heat, wind power and biomass*. Energy 35 (2010), 4892-4901.

[14] B. HOWARD, A. SABA, M. GERRARD, V. MODI, *Combined heat and power's potential to meet New York City's sustainability goals*. Energy Policy 65 pp 444-454, 2004.

[15] A. M. HENDRICKS, J. E. WAGNER, T. A. VOLK, D. H. NEWMAN, T. R. BROWN, *A cost-effective evaluation of biomass district heating in rural communities*. Applied Energy 162 (2016) 561-569.

[16] R. MADLENER, *Innovation diffusion, public policy, and local initiative: The case of wood-fuelled district heating systems in Austria*. Energy Policy 35 (2007) 1992-2008.

[17] P. A. OSTERGAARD, H. LUND, *A renewable energy system in Frederikshavn using low-temperature geothermal energy for district heating*. Applied Energy 88 (2011) 479-487.

[18] M. MARINOVA, C. BEAUDRY, A. TAOUSSI, M. TRÉPANIER, J. PARIS, *Economic Assessment of Rural District Heating by Bio-Steam Supplied by a Paper Mill in Canada*. Bulletin of Science, Technology and Society, Volume 28, issue 2, 159-173, April 1, 2008.

[19] F. AHAMMED, D. A. TAUFIQ, *Case Study: Applications of Solar PV On Rural Development in Bangladesh*. Journal of Rural Community Development 3 (2008) 93-103.

[20] H. A. KAZEM, M.H. ALBADI, A.H.A. AL-WAELI, A. H. AL-BUSAIDI, M. T. CHAICHAN, *Techno-economic feasibility analysis of 1 MW photovoltaic grid connected system in Oman*. Case Studies in Thermal Engineering 10 (2017) 131-141.

[21] A. AL MALIKI, M. AL AMRI, H. AL JABRI, *Experimental Study of Using Renewable Energy in the Rural Areas of Oman*. Renewable Energy, Vol. 14, Nos. 1-4, pp. 319-324, 1998.

[22] ASHRAE, *Handbook HVAC Systems and Equipment*. ASHRAE; Inc. 2000, USA.

[23] H.I. ONOVWIONA, V.I. UGURSAL, *Residential cogeneration systems: review of the current technology*. Renewable & Sustainable Energy Reviews, 10 (2006) 389-431.

[24] EUROPEAN COMMISSION, *Directive 2012/27/EU of the European Parliament and of the Council of 25 October 2012 on energy efficiency, amending Directives 2009/125/EC and 2010/30/EU and repealing Directives 2004/8/EC and 2006/32/EC*.
Available from: https://eur-lex.europa.eu/legal-content/EN/TXT/PDF/?uri=CELEX:32012L0027&from=EN. Last time consulted: 24-09-2019.

[25] EUROPEAN COMMISSION, *European Commission, Policies, Information and Services*.
Available from: https://ec.europa.eu/energy/en/topics/energy-efficiency/targets-directive-and-rules/energy-efficiency-directive. Last time consulted: 24-09-2019.

[26] EUROPEAN COMMISSION, *European Commission, Cogeneration of heat and power, promoting cogeneration in Europe*. Available from: https://ec.europa.eu/energy/en/topics/energy-efficiency/cogeneration-heat-and-power. Last time consulted: 24-09-2019.

[27] R. BÜCHELE, R. HAAS, M. HARTNER, R. HIRNER, M. HUMMEL, L. KRANZL, A. MÜLLER, K. PONWEISER, M. BONS, K. GRAVE, E. SLINGERLAND, Y. DENG, K. BLOK, *Assessment of the potential for application of high-efficiency cogeneration and efficient district heating and cooling. Final Report*. Technical University of Vienna and ECO-FYS 2015 commisioned by: Austrian Federal Ministry of Science, Research and the Economy (BMWFW). Available from: https://ec.europa.eu/energy/sites/ener/files/documents/at_report_en.pdf. Last time consulted: 24-09-2019.

[28] C. KITTEL, H. KROEMER, *Thermal Physics (2nd edition)*. San Francisco: W.H. Freeman (1980).

[29] EUROPEAN COMMISSION, *Small-scale cogeneration, why? In which case? A guide for decision makers*. Directorate General for Energy DGXVII, July 1999.

[30] G. MAJOR, *Small scale cogeneration. The Netherlands: Centre for the Analysis and Dissemination of Demonstrated Energy Technologies*. CADDET Energy Efficiency Analysis Series 1. IEA/OECD; 1995.

[31] M. POTENTE PRIETO, J. M. PENYA-ROJA OLTRA, *Viability study of the implementation of a cogeneration system for the optimization of the biogas use produced in the anaerobic digestion of the Alacant-Monte Orgeria WWTP*. Master Thesis, Research Group on Environmental Engineering belonging to the Department of Chemical Engineering in the University of Valencia, 2012. (In Spanish). Publications list of the University of Valencia are available from: http://giam.blogs.uv.es/que-hacemos/thesis

[32] U. EICKER, S. CAJOT, N. SCHULER, J-L. ROBINEAU, P. WATE, P. RODRIGUES, K. WANG, G. AGUGIARO, G. KAZAS, S. GOY, A. SANCHO TOMAS, M. POTENTE PRIETO, N. SOLOMAKHINA, G. TARDIOLI, P. MONSALVETE ALVAREZ DE URIBARRI, *Urban Energy Systems for Low-Carbon Cities*. Academic Press, Elsevier, 2019. (Chapter 5)

[33] RENOVETEC, *Renovetec, Ciclos Combinados* Available from: http://www.cicloscombinados.com. Last time consulted: 19-12-2018. (In Spanish)

[34] J. GIL MARTINEZ, J. R. BERTOMEU, *Proposal for Biogas Recovery from the WWTP of the Heineken Factory of Valencia*. Master Thesis, University of Valencia, Polytechnic University of Valencia, 2017. Available from: https://riunet.upv.es. Last time consulted: 19-12-2018. (In Spanish)

[35] S. E. HOSSEINI, M. A. WAHID, *Development of biogas combustion in combined heat and power generation*. Renewable and Sustainable Energy Reviews 40 (2014) 868-875.

[36] A. ROUBAUD, D. FAVRAT, *Improving performances of a lean burn cogeneration biogas engine equipped with combustion prechambers*. Fuel 84 (2005) 2001-2007.

[37] I. D. BEDOYA, S. SAXENA, F. J. CADAVID, R. W. DIBBLE, M. WISSINK, *Experimental study of biogas combustion in an HCCI engine for power generation with high indicated efficiency and ultra-low NOx emissions*. Energy Conversion and Management 53 (2012) 154-162.

[38] K. R. VOORSPOOLS, WILLIAM D. D'HAESELEER, *The evaluation of small cogeneration for residential heating*. International Journal of Energy Research. 2002; 26: 1175-1190.

[39] R. CLAUSIUS, *Über die bewegende Kraft der Wärme*. Annalen der Physik 79: 368-397, 500-524, 1850. (In German)

[40] W. THOMSON, *On the Dynamical Theory of Heat, with Numerical Results Deduced from Mr. Joule's Equivalent of a Thermal Unit, and M. Regnault's Observations on Steam*. Transactions of the Royal Society of Edinburgh 20: 261-268, 289-298.

[41] C.Y. CHENG, C.K. CHENG, *Performance optimization of an irreversible heat pump*. Journal of Physics D: Applied Physics 28, 2451, August 1995.

[42] J. CHEN, *The maximum power output and maximum efficiency of an irreversible Carnot heat engine*. Journal of Physics D: Applied Physics 27, 1144, February 1994.

[43] D. LAUKA, J. GUSCA, D. BLUMBERGA, *Heat Pumps Integration Trends in District Heating Networks of the Baltic States*. The 5th International Conference on Sustainable Energy Information Technology (SEIT 2015). Procedia Computer Science 52 (2015) 835-842.

[44] T. OMMEN, W. B. MARKUSSEN, B. ELMEGAARD, *Heat pumps in combined heat and power systems*. Energy 76 (2014) 989-1000.

[45] K. HOFFMANN, D. FORBES PEARSON, *Ammonia Heat Pumps for District Heating in Norway - a case study*. Star Refrigeration Ltd. The institute of refrigeration, April 2011. To be presented before the Institute of Refrigeration at London Chamber of Commerce and Industry, 33 Queen Street, London. Available from: http://ior.org.uk

[46] R. PETITJEAN, *L'Equilibrage hydraulique global : Un manuel traitant du contrôle efficace du confort thermique, page 379*. Feuillets mobiles, Diff. TA Control France, France, 1989, ISBN-10: 2906955043, ISBN-13: 978-2906955042

[47] H. RECKNAGEL, E. SPRENGER, *Manual Técnico de Calefacción y Aire Acondicionado, page 868 (Tecnical Handbook for Heating and Hot Water)*. Editorial Belisco, 1993, ISBN: 8485198611 (In Spanish)

[48] IDAE, *Comentarios al RITE-2007, IT 1.2.1 Exigencia de eficiencia energética (Comments to RITE-2007, IT 1.2.1 Energy Efficiency Requirement)*. Available from: http://www.idae.es/file/9050/download?token=Cuj6NCWm. Last time consulted: 24-09-2019. (In Spanish)

[49] MEINERTZ WEB PAGE, http://meinertz.com. Last time consulted: 24-09-2019.

[50] MATERIALES CALEFACCIÓN (HEATING MATERIALS) WEB PAGE, http://www.materialescalefaccion.com. Last time consulted: 24-09-2019. (In Spanish)

[51] FABRICANTES DE GENERADORES Y EMISORES DE CALOR (FEGECA), FUNDACIÓN DE LA ENERGÍA DE LA COMUNIDAD DE MADRID (FENERCOM)(MANUFACTURERS OF HEAT GENERATORS, ENERGY FOUNDATION OF THE REGION OF MADRID), *Guía del suelo radiante (Radiant floors guide), page 75*. Available from: https://www.fegeca.com/docs/fegeca-guia-suelo-radiante.pdf. Last time consulted: 24-09-2019. (In Spanish)

[52] FABRICANTES DE GENERADORES Y EMISORES DE CALOR (FEGECA), FUNDACIÓN DE LA ENERGÍA DE LA COMUNIDAD DE MADRID (FENERCOM)(MANUFACTURERS OF HEAT GENERATORS, ENERGY FOUNDATION OF THE REGION OF MADRID), *Guía del*

suelo radiante (Radiant floors guide). Available from: https://www.fegeca.com/docs/fegeca-guia-suelo-radiante.pdf. Last time consulted: 24-09-2019. (In Spanish)

[53] ALB SISTEMAS, *Sistema de climatización radiante. Manual Técnico 1/2017 (Radiant climatization systems. Technical Manual 1/2017)*. Available from: https://www.alb.es/arxius/descarregues/mte/ALBManualSCR.pdf. Last time consulted: 24-09-2019. (In Spanish)

[54] UPONOR, *Manual Técnico de Climatización Invisible (Technical Manual for Invisible Climatization)*. Available from: http://www.solarcondicionado.pt. Last time consulted: 24-09-2019. (In Spanish)

[55] EN 1264-1:2011, *Water based surface embedded heating and cooling systems - Part 1: Definitions and symbols*. Available from: https://www.une.org/encuentra-tu-norma/busca-tu-norma/norma?c=N0049641. Last time consulted: 24-09-2019. (In Spanish)

[56] EN 1264-2:2008 + A1:2012, *Water based surface embedded heating and cooling systems - Part 2: Floor heating: Prove methods for the determination of the thermal output using calculation and test methods*. Available from: https://www.une.org/encuentra-tu-norma/busca-tu-norma/norma?c=N0051332. Last time consulted: 24-09-2019. (In Spanish)

[57] FABRICANTES DE GENERADORES Y EMISORES DE CALOR (FEGECA), FUNDACIÓN DE LA ENERGÍA DE LA COMUNIDAD DE MADRID (FENERCOM)(MANUFACTURERS OF HEAT GENERATORS, ENERGY FOUNDATION OF THE REGION OF MADRID), *Guía del suelo radiante (Radiant Floors Guide), page 44*. Available from: https://www.fegeca.com/docs/fegeca-guia-suelo-radiante.pdf. Last time consulted: 24-09-2019. (In Spanish)

[58] NOVELEC WEB PAGE, https://blog.gruponovelec.com/. Last time consulted: 24-01-2019. (In Spanish)

[59] FABRICANTES DE GENERADORES Y EMISORES DE CALOR (FEGECA), FUNDACIÓN DE LA ENERGÍA DE LA COMUNIDAD DE MADRID (FENERCOM)(MANUFACTURERS OF HEAT GENERATORS, ENERGY FOUNDATION OF THE REGION OF MADRID), *Guía del suelo radiante (Radiant Floors Guide), page 46* Available from: https://www.fegeca.com/docs/fegeca-guia-suelo-radiante.pdf. Last time consulted: 24-09-2019. (In Spanish)

[60] CONSTRUMATICA WEB PAGE, https://www.construmatica.com/. Last time consulted: 24-09-2019. (In Spanish)

[61] FABRICANTES DE GENERADORES Y EMISORES DE CALOR (FEGECA), FUNDACIÓN DE LA ENERGÍA DE LA COMUNIDAD DE MADRID (FENERCOM)(MANUFACTURERS OF HEAT GENERATORS, ENERGY FOUNDATION OF THE REGION OF MADRID), *Guía del suelo radiante (Radiant Floors Guide), page 30* Available from: https://www.fegeca.com/docs/fegeca-guia-suelo-radiante.pdf Last time consulted: 24-09-2019. (In Spanish)

[62] D.K. BAKER, S.A. SHERIF, *Heat transfer optimization of a district heating system using search methods*. Int. J.Energy Res. 21 233-252, 1997.

[63] S. WERNER, *District heating and cooling in Sweden*. Energy 126 pp 419-429, 2017.

[64] HISTORY OF THE DANISH DISTRICT HEATING NETWORK, WEBSITE. http://www.dbdh.dk/. Last time consulted: 03-12-2018.

[65] S. PAIHO, H. SAASTAMOINEN, E. HAKKARAINEN, L. SIMILA, R. PASONEN, J.KÄHEIMO, M. RÄMÄ, M. TUOVINEN, S. HORSMANHEIMO, *Increasing flexibility of Finnish energy systems, a review of potential technologies and means*. Sustainable Cities and Society, Volume 43, 509-523, 2018.

[66] H. LUND, B. MÖLLER, B.V. MATHIESEN, A. DYRELUND, *The role of district heating in future renewable energy systems*. Energy 35, 1381-1390, 2010.

[67] M. MORANDIN, R. HACKL, S. HARVEY, *Economic feasibility of district heating delivery from industrial excess heat: A case study of a Swedish petrochemical cluster*. Energy 65, 209-220, 2014.

[68] H. LUND, *Renewable Energy Systems: A Smart Energy Systems approach to the choice and Modelling of 100% Renewable Solutions*. 2nd edition. Academic Press, Burlington, USA, 2014, ISBN: 9780124095953.

[69] H. LUND, B.V. MATHIESEN, D. CONNOLLY, P.A. OSTERGAARD, *Renewable Energy Systems - A Smart Energy Systems Approach to the choice and modelling of 100% renewable solutions*. CET, Chemical Engineering Transactions, vol 39, 2014.

[70] A. COLMENAR-SANTOS, D. BORGE-DIAZ, E. ROSALES-ASENSIO, *District Heating and Cooling Networks in the European Union*. Springer International Publishing AG 2017, ISBN: 978-3-919-57951-1

[71] A. COLMENAR-SANTOS, D. BORGE-DIAZ, E. ROSALES-ASENSIO, J.J. BLANES-PEIRO, *District Heating and Cogeneration in the EU-28: Current situation, potential and proposed energy strategy for its generalisation*. Renewable and Sustainable Energy, Reviews 62 (2016) 621-639, ISBN: 978-3-919-57951-1

[72] D. CONNOLLY, B.V. MATHIESEN, P.A. OSTERGAARD, B. MÖLLER, S. NIELSEN, H. LUND, U. PERSSON, D. NILSSON, S. WERNER, D. TRIER, *Heat Roadmap Europe 2050, First Pre-study for the EU 27*. Department of Development and Planning, Aalborg University, 2012.

[73] D. CONNOLLY, B.V. MATHIESEN, P.A. OSTERGAARD, B. MÖLLER, S. NIELSEN, H. LUND, U. PERSSON, D. NILSSON, S. WERNER, D. TRIER, *Heat Roadmap Europe 2, Second Pre-study for the EU 27*. Department of Development and Planning, Aalborg University, 2013.

[74] D. OLSTHOORN, F. HAGHIGHAT, P.A. MIRZAEI, *Integration of storage and renewable energy into district heating systems: A review of modelling and optimization*. Solar Energy 136 (2016) 49-64.

[75] B. AKKAYA, D. ROMANCHENKO, *Modelling and analysis of a district heating system containing thermal storage. Case study of the district heating system of Boras*. Chalmers University of Technology, pp 9-51. Göteborg, Sweden, 2013.

[76] D. SCHMIDT, *Low exergy systems for high performance buildings and communities*. Energy and Buildings 41 pp 331-336, 2009.

[77] R. MARX, D. BAUER, H. DRUECK, *Energy efficiency integration of heat pumps into solar district heating system with seasonal thermal energy storage*. Energy Procedia 57, pp 2706-2715, Stuttgart, 2014.

[78] S. MASSOUD AMIN, B. F. WOLLENBERG, *Toward a Smart Grid*. IEEE Power & Energy Magazine 3 (5): 34-41. October 2005.

[79] S. BLUMSACK, A. FERNANDEZ, *Ready or not, here comes the smart grid!*. Energy 37 (2012) 61-68.

[80] H. LUND, A.N. ANDERSEN, P.A. OSTERGAARD, B.V. MATHIESEN, D. CONNOLLY, *From electricity smart grids to smart energy systems- A market operation, based approach and understanding*. Energy 42 (2012) 96-102.

[81] F. ORECCHINI, A. SANTIANGELI, *Beyond smart grids - the need of intelligent energy networks for a higher global efficiency through energy vectors integration*. International Journal of Hydrogen Energy 2011; 36(13): 81, 26-33

[82] R.R. SCHMIDT, *Smart Cities: Challenges and Opportunities for Geothermal, District Heating and Cooling Systems*. 9. Internationale Geothermiekonferenz, Freiburg, 15-17 May 2013.

[83] ENERGY EFFICIENT BUILDINGS WEB PAGE, http://ectp.ectp.org/cws/params/ectp/download_files/36D2981v1_Eeb_cPPP_Roadmap_under.pdf. Last time consulted: 04-12-2018.

[84] A. DÉNARIÉ, M. MUSCHERÁ, M. CALDERONI, M. MOTTA, *Industrial excess heat recovery in district heating: Data assessment methodology and application to a real case study in Milano, Italy*. Energy 166(2019) 170-182, 2019.

[85] D. DJURIC ILIC, L. TRYGG, *Economic and environmental benefits of converting industrial processes to district heating*. Energy Conversion and Management 87 (2014) 305-317

[86] J. IVNER, S. BROBERG VIKLUND, *Effect of the use of industrial excess heat in district heating or greenhouse gas emissions: a systems perspective*. International Refrigeration and Air Conditioning Conference. Paper 734. 2004.

[87] W. ZHOU, J. LI, *Sewage heat source pump system's application examples and prospect analysis in China*. International Refrigeration and Air Conditioning Conference. Paper 734. 2004.

[88] M. KOFINGER, D. BASCIOTTI, R.R. SCHMIDT, *Reduction of return temperatures in urban district heating systems by the implementation of energy-cascades*. The 15th International Symposium on District Heating and Cooling, Energy Procedia 116 438-451 (2017).

[89] 4GDH WEB PAGE, https://www.4dh.eu. Last time consulted: 24-09-2019.

[90] X. LI, W. WU, X. ZHANG , W. SHI, B. WANG, *Energy saving potential of low temperature hot water system based on air source absorption heat pump*. Applied Thermal Engineering 48 (2012) 317-324.

[91] O. CULHA, H. GUNERHAN, E. BIYIK, O. EKREN, A. HEPBASLI, *Heat Exchanger applications in wastewater source heat pumps for buildings: a key review*. Energy and Buildings 104 (2015) 215-232.

[92] A. HEPBASLI, O. AKDEMIR, E. HANCIOGLU, *Experimental study of a closed loop vertical ground source heat pump system*. Energy Conversion and Management 44 (2003) 527-548.

[93] O. OZGENER, A. HEPBASLI, *Experimental performance analysis of a solar assisted ground-source heat pump greenhouse heating system*. Energy and Buildings 37 (2005) 101-110.

[94] M.A. SAYEGH, J.DANIELEWICZ, T.NANNOU, M.MINIEWICZ, P.JADWISZCZAK, K.PIEKARSKA, H. JOUHARA, *Trends of European research and development in district heating technologies*. Renewable and Sustainable Energy Reviews 68 (2017) 1183-1192.

[95] M. S. AL-HOMOUD, *Performance characteristics and practical applications of common building thermal insulation materials*. Building and Environment 40 (2005) 353-366.

[96] O. GUDMUNDSSON, M. BRAND, J. E. THORSEN, *Ultra-low temperature district heating and micro heat pump application-economic analysis*. The 14th International Symposium on District Heating and Cooling, Stockholm, Sweden, September 7-9th 2014.

[97] E. ZVINGILAITE, T. OMMEN, B. ELMEGAARD, M.L. FRANCK, *Low temperature district heating consumer unit with micro heat pump for domestic hot water preparation*. The 13th International Symposium on District Heating and Cooling, Copenhagen, Denmark, 3rd-4th September 2012.

[98] O. KWON, D. CHA, C. PARK, *Performance evaluation of a two-stage compression heat pump system for district heating using waste energy*. Energy Volume 57, 1 August 2013, Pages 375-381.

[99] M. RÄMÄ, K. SIPILÄ, *Transition to low temperature distribution in existing systems*. The 15th International Symposium on District Heating and Cooling, Energy Procedia 116 (2017) 58-68.

[100] B. ELMEGAARD, T. SCHMIDT OMMEN, M. MARKUSSEN, J. IVERSEN, *Integration of space heating and hot water supply in low temperature district heating*. Energy and Buildings 124 (2016) 255-264.

[101] ÖNORM EN 806, *Technical regulation for drinking water installations (Technische Regeln für Trinkwasser Installationen), 2011*. (In german)

[102] ÖNORM B 5019, *Hygienerelevante Planung, Ausführung, Betrieb, Überwachung und Sanierung von zentralen Trinkwasser-Erwärmungsanlagen, 2011*. (In german)

[103] D. BOTHE, *Modellierung und Simulation von weit verzweigten, vermaschten Netzen für thermische Energie und Gas*. Dissertation TU Wien, Wien, 2006.

[104] J. NAGLER, *Design Criteria for GCHP-Systems with Seasonal Storage (Anergienetze)*. Dissertation TU Wien, Wien, 2006.

[105] R. D. GRIGORIEFF ET AL., *Modelling and Numerical Simulation of District Heating Networks with Time-Saving Solution Methods*. Mathematics - Key Technology for the Future: Joint Projects between Universities and Industry. Ed. by Willi Jäger et al. Berlin, Heidelberg: Springer Berlin Heidelberg, 2003, pp. 252-262. ISBN: 978-3-642-55753-8.

[106] D. BAUER, *Zur Thermischen Modellierung von Erdwärmesonden und Erdsondenwärmespeichern*. Doctor Thesis. Institut fur Thermodynamik und Warmetechnik, Universitat Stuttgart, 2011.

[107] I. DEL HOYO ARCE, S. HERRERO LÓPEZ, M. RÄMÄ, K. KLOBUT. J. A. FEBRES, *Models for fast modelling of district heating and cooling networks*. Renewable and Sustainable Energy Reviews 82 (2018) 1863-1873.

[108] M. VESTERLUND, J. DAHL, *A Method for the simulation and optimization of district heating systems with meshed networks*. Energy Conversion and Management 89 (2015), 555-567.

[109] M. VESTERLUND, A. TOFFOLO, J. DAHL, *Simulation and analysis of a meshed district heating network*. Energy Conversion and Management 122 (2016), 63-73.

[110] P. JIE, Z. TIAN, S. YUAN, N. ZHU, *Modeling the dynamic characteristics of a district heating network*. Energy 39 (2012), 126-134.

[111] J. ZHENG, Z. ZHOU, J. ZHAO, J. WANG, *Function method for dynamic temperature simulation of district heating network*. Applied Thermal Engineering 123 (2017), 682-688.

[112] H.V. LARSEN, H. PÁLSSON, B. BøHM, H. F. RAUN, *Aggregated dynamic simulation model of district heating networks*. Energy Conversion and Management 43 (2002) 995-1019.

[113] G. SCHWEIGER, P. LARSSON, F. MAGNUSSON, P. LAUENBURG, S. VELUT, *District heating and cooling systemys - Framework for Modelica - based simulation and dynamic optimization*. Energy 137 (2017), 566-578.

[114] B. VAN DER HEIJDE, M. FUCHS, C. RIBAS TUGORES, G. SCHWEIGER, K. SARTOR, D. BASCIOTTI, D. MÜLLER, C. NYTSCH-GEUSEN, M. WETTER, L. HELSEN, *Dynamic equation-based thermo-hydraulic pipe model for district heating and cooling systems*. Energy Conversion and Management 151 (2017), 158-169.

[115] B. VAN DER HEIJDE, A. AERTGEERTS, L. HELSEN, *Modelling steady-state thermal behaviour of double thermal network pipes*, International Journal of Thermal Sciences 117 (2017), 316-327.

[116] A. DÉNARIÉ, M. APRILE, M. MOTTA, *Heat transmission over long pipes: New model for fast and accurate district heating simulations*. Energy 166 (2019) 267-276.

[117] V. D. STEVANOVIC, B. ZIVKOVIC, S. PRICA, B. MASLOVARIK, V. KARAMARKOVIC, V. TRKULJA, *Prediction of thermal transients in district heating systems*, Energy Conversion and Management 50 (2009), 2167-2173.

[118] M. LEŚKO, W. BUJALSKI, *Modelling of district heating networks for the purpose of operational optimization with thermal energy storage*, Archives of Thermodynamics, Vol. 38 (2017), No 4, 139-163.

[119] S. FALKNER, *Modellierung und Simulation von thermischen Speichern*, Diplomarbeit TU Wien, Wien, 2014.

[120] L. OZGENER, A. HEPBASLI, I. DINCER, *Energy and Exergy analysis of geothermal district heating systems: an application*. Building and Environment, Volume 40, Issue 10 (2005), pp 1309-1322.

[121] H. LI, S. SVENDSEN, *Energy and Exergy analysis of low temperature district heating network*. Energy 45 (2012) 237-246.

[122] M. GONG, S. WERNER, *Exergy analysis of network temperature levels in Swedish and Danish district heating systems*. Renewable Energy 84 (2015) 106-113.

[123] K. ÇOMAKLI, B. YÜKSEL, Ö. ÇOMAKLI, *Evaluation of energy and exergy losses in district heating network*. Applied Thermal Engineering 24 (2004) 1009-1017

[124] E. HÖCKNER, *Wien Energie - District Heating, Presentation for the 2nd training module of the CI-NERGY European Project*. Vienna, October 2014.

[125] FERNWÄRME WIEN GMBH. DEPARTMENT OF RESEARCH AND DEVELOPMENT, *Technical documentation TR-SZT, FERNWÄRME WIEN GmbH*. Available from: `https://www.wienenergie.at/media/files/2015/technischerichtlinietr-sztschemen,zeichnungen,tabellen_140556.pdf` Last time consulted: 24-09-2019. (In German)

[126] FERNWÄRME WIEN GMBH. DEPARTMENT OF RESEARCH AND DEVELOPMENT, *Technical documentation TR-TAB, FERNWÄRME WIEN GmbH*. Available from: `https://www.wienenergie.at/media/files/2015/technischerichtlinietr-tabtechnischeauslegungsbedingungen_140557.pdf` Last time consulted: 24-09-2019. (In German)

[127] I. MARTÍNEZ, *Termodinámica Básica y Aplicada (Basic Applied Thermodynamics)*. Editorial Dossat (1992), ISBN: 978-8-423-70810-9 (In Spanish).

[128] Z. RANT, *Exergie, Ein neues Wort für technische Arbeitsfähigkeit (Exergy, a new concept for the useful work)*. Forschung auf dem Gebiete des Ingenieurwesens 22: 36-37. (1956) (In German).

[129] M. J. MORAN, H. N. SHAPIRO, *Fundamentos de Termodinámica Técnica (Notions of Technical Thermodynamics)*. Editorial Reverté, S.A. (2004), ISBN: 84-291-4313-0 (In Spanish).

[130] T. J. KOTAS, *The exergy method of thermal plant analysis*. Krieger publishing company, Malabar (1995), pp 113-137, 197-204.

[131] M. HOLMGREN, *X STEAM FOR MATLAB, *. Technical documentation of X Steam Software implemented in Matlab. Available from: `http://www.x-eng.com` (2016) Last time consulted: 29-04-2019.

[132] UNE-EN 1264-2:2009+A1:2013, *Water based surface embedded heating and cooling systems - Part 2: Floor heating: Prove methods for the determination of the thermal output using calculation and test methods), 2013*. (In Spanish and English)

[133] INDUSTRIAL HEAT PUMPS WEBSITE. DE KLEIJN ENERGY CONSULTANTS & ENGINEERS, `http://industrialheatpumps.nl`. Last time consulted: 26-04-2019.

[134] J. M. COULSON, J. F. RICHARDSON, J. R. BACKHURST, J.H. HARKER, *Chemical Engineering, Volume 1. Fluid Flow, Heat Transfer and Mass Transfer*. Butterworth Heinemann-Elsevier Group (1999), ISBN: 978-0-7506-4444-0.

[135] ASHRAE, *Thermodynamic Properties of Dry Air and Water and S.I. Psychrometric Charts*. ASHRAE; Inc. 1983, USA.

[136] WIKIPEDIA: CHLORINATED POLYVINYL CHLORIDE, https://en.wikipedia.org/wiki/Chlorinated_polyvinyl_chloride. Last time consulted, 24-05-2019.

[137] PLASTICBAGES INDUSTRIAL,S.L., https://plasticbages.com/caracteristicaspvc.html. Last time consulted: 24-05-2019. (In Spanish)

[138] WIKIPEDIA: AISLANTE TÉRMICO (WIKIPEDIA: THERMAL INSULATION), https://es.wikipedia.org/wiki/Aislante_termico. Last time consulted: 24-05-2019.

[139] CONDUCTIVIDAD TÉRMICA Y AISLAMIENTO DE TUBERÍAS (THERMAL CONDUCTIVITY AND PIPES INSULATION): https://instalacionesyeficienciaenergetica.com. Last time consulted, 24-05-2019. (In Spanish)

[140] INSTITUTO PARA LA DIVERSIFICACIÓN Y AHORRO DE LA ENERGÍA, MINISTERIO DE INDUSTRIA, TURISMO Y COMERCIO (INSTITUTE FOR THE ENERGY SAVINGS AND DIVERSIFICATION, MINISTRY OF INDUSTRY, TOURISM AND TRADE), *Guía Técnica. Diseño y cálculo del aislamiento térmico de conducciones, aparatos y equipos (Technical Guide for the design and calculation of thermal insulations for equipments, devices and pipes)*. Available from: https://www.idae.es/publicaciones (2007), ISBN: 978-84-96680-08-1. Last time consulted: 24-05-2019. (In Spanish)

[141] O. REYNOLDS, *An Experimental investigation of the circumstances which determine whether the motion of water shall be direct or sinuous, and of the law of resistance in parallel channels*. Philosofical Transactions of the Royal Society 174 (1883) 935-982.

[142] H. H. S. CHU, *Correlating Equations for Laminar and Turbulent Free convection from a Horizontal Cylinder*. Int. J. Heat Mass Transfer, 18, 1049 (1975)

[143] R. H. PERRY, D. W. GREEN, *Perry's Chemical Engineer's Handbook*. McGraw-Hill, 7th Edition (1997), ISBN: 0-07-049841-5.

[144] CRANE CO., *Flow of Fluids through valves, fittings and pipe. Metric EDITION*. Technical Paper No. 410M (1982), Crane Co.

[145] TUTORIALS POINT. http://www.tutorialspoint.com/matlab/matlab_quick_guide.htm. Last time consulted: 03-05-2019. (In Spanish)

CV Mario Potente Prieto

MARIO POTENTE PRIETO
+43 6507523603
mpotente@hotmail.com
Porzellangase 47/2/6, 1090, Wien (Austria)
Date and place of birth: Valladolid (Spain), 31/07/1985.
Driving licence B1.

WORK EXPERIENCE

- Researcher in WienEnergie and TU Wien (Vienna, Austria). *Feb 2014-Feb 2018*

  Marie Curie European ITN Project CI-NERGY

  - Exergy assessment of urban energy systems, focusing on design, modelling and simulation of district heating networks.

  - Improving grids towards 4th generation systems working on the following factors:

    1- Reconfiguration of internal hydraulic networks in buildings: replacement of radiators by radiant floors, improvement of thermal insulation, etc

    2- Heat pumps connection supporting the district heating network

    3- Adaptation to Low Temperature district heating networks

  - Development of physical models and simulations related to hydraulic transport and heat transmission in district heating networks

  - Teamwork and coordination with other CI-NERGY areas, related to urban energy planning, heat demand estimation in buildings, combination between heating and power grids and integration of renewable energies

  - Participation in conferences, seminars, workshops, debates and other events

- Leonardo Internship in **Wetsus**, **centre of excelence for sustainable water technology** (Leewarden, The Netherlands). *Mar-Ago 2013*

  Proyect: "Biological H_2S and thiols removal from sour gas streams"

  - Performing a mathematical model to know the evolution of the various key compounds present in the process

  - Experiment plan for methanethiol and DMDS removal.

  - Diverse methods and analysis (Cuvette tests method, refractometer, GIC-FID and MICRO – GC)

  Proyect: "Pitzer´s model study in salt recovery from brines by eutectic crystallization process"

  - Development of Pitzer´s parameter database

  - Pitzer´s algorithm calculation with different compounds and conditions.

- Training internship as assistant plant manager at the wastewater treatment plant of Fuente del Jarro (Paterna, Valencian Community, Spain), *Apr-Aug 2012*

  - Taking decisions, operation and control of the purification biological process.

  - Analytical data supervision and process evaluation.

  - Administrative tasks, report and process simulation through DESASS software.

OTHER OCCUPATIONS

- Shop assistant in drugstore-perfumery business. Contact with suppliers, management and customer service. (2001-2005)

- Assistant in upholstery workshop (family business)

EDUCATION

- **PHd-Studium** in TU Wien (Wien, Österreich). *Feb 2014-Aktuell.*

  "Modelling, Simulation and Energy-Exergy Assessment of a local District Heating Network in Vienna"

- **MSc Master Environmental Engineer**, University of Valencia. *Sept 2010-Jul 2012*.

  - Waste water purification: Physical, chemical and biological treatment, modelling, optimization, disinfection and water quality

  - Contaminated soils, Waste Management

  - Environmental Law

  End MSc proyect, "Technical and Economical Study of Cogeneration in a Water Treatment Plant in Monte Orgegia" (Alicante, Valencian Community, Spain).

  - Energy extraction from biogas (Data ascertainment, design of the Biotrickling filters and cogeneration system, Adaptation of the entire design as a function of the WTP, Economical study)

- **BSc Chemical Engineer**, University of Valladolid (Valladolid, Spain). *Sept 2003-Jun 2010*. University of Valencia, (Valencia, Spain). SICUE-Séneca program.

  End MSc proyect, "Design of a catalist reactor for dehydration of Butanol to Butenes''

  - Design of the entire process of transformation of natural butanol obtained from biological processes to the corresponding products.
  - Piping and Instrumentation diagrams, process simulation with HYSYS software (ASPENTECH), including security and environmental topics and economic study

PUBLICATIONS

- U. Eicker, S. Cajot, N. Schuler, J-L. Robineau, P. Wate, P. Rodrigues, K.Wang, G. Agugiaro, G. Kazas, S. Goy, A. Sancho Tomas, M. Potente Prieto, N. Solomakhina, G. Tardioli, P. Monsalvete Alvarez de Uribarri, *Urban Energy Systems for Low-Carbon Cities*. Academic Press, Elsevier, 2019. eBook ISBN: 9780128115541, Paperback ISBN: 9780128115534.

- M. Potente Prieto, K. Ponweiser, *"Simulation of a district heating network for a case study in the city of Vienna considering Energy and Exergy losses",* TU WIEN, The 15th International Symposium on District Heating and Cooling, Sept. 4-7, 2016, South Korea.

- M. Potente Prieto, J. M. Penya-Roja Oltra, *Viability study of the implementation of a cogeneration system for the optimization of the biogas use produced in the anaerobic digestión of the Alacant-Monte Orgeria WWTP*. Master Thesis, University of Valencia, 2012. (In Spanish) Publications list is available from: giam.blogs.uv.es/que-hacemos/thesis/

SOCIAL AND ORGANIZATION SKILLS

- University theatre group "Ingenieros Cómicos". Theatrical performances and monologues. Communication and exposition skills to the audience.

- Language exchange workshop in Valladolid. Organization of meetings, activities and events for learning and improvement of languages (English, French, German and Spanish).

- Competences for Management, Teamwork and Coordination.

- Competence for Design and graphic expression (process diagrams, drafts, P&I, images, etc)

SOFTWARE SKILLS

- Microsoft Office Pack, Visual Basic & Visio (High level).

- High graphic design knowledge: Visio, Autocad, Photosop.

- High programming level on Matlab, Matlab-Simulink and Visual Basic.

- Chemical processes Simulators: (Hysys & Aspen) and biological (DESASS)

- Other Control and Instrumentation softwares: LabView, C-Station, Java regula, GAMS, EcosimPro

COMPLEMENTARY TRAINING

- Photoshop and Graphic Design course (NEWTON centre, Valladolid, Spain) (2002)

- Autocad 2D y 3D course (Polythechnic University of Valencia) (2011)

- Course of Design of Solar photovoltaic installations (General Foundation, University of Valladolid, LACECAL) (2012)

LANGUAGES

- Spanish: Mother language

- English: Fluid

- German: Fluid

- Italian: Medium level